UNIVERSITAT POLITÈCNICA DE CATALUNYA BARCELONATECH

Levels and behaviour of radionuclides in water treatment plants: the case of the Barcelona metropolitan area urban water cycle

Dani Mulas

UNIVERSITAT POLITÈCNICA DE CATALUNYA
BARCELONATECH
Institut de Tècniques Energètiques

Levels and behaviour of radionuclides in water treatment plants: The case of the Barcelona metropolitan area urban water cycle

The present document corresponds to
the Ph.D. dissertation submitted to the
Unviersitat Politècnica de Catalunya
following the requirements of the
Nuclear and Ionizing Radiation
Engineering program.

Dani Mulas (Ph.D. candidate)

Dr. Maria Amor Duch (Director)

Dr. Antonia Camacho (Co-director)

December 2019

The present Ph.D. has been done in the *Laboratori d'Analisi de Radioactivitat* from the *Institut de Tècniques Energètiques* at the *Universitat Politècnica de Catalunya*

Dedicated to all the people who have suffered the harmful effects of ionizing radiation and those who work to reduce the radiological risk as low as reasonably achievable.

Family walking in the starlight: Drawing done by a testimony of the Hiroshima bomb where three victims walk with difficulties in front of him. The location was at 23.6 km from the hypocenter (Hiro-Machi, Kure City) on 6th August from 1945 at night.

Reference: Hiroshima Peace Memorial Museum. *A-bomb drawing survivors*. 2007.

Abstract

The Barcelona metropolitan area (BMA; 3.2 M inhabitants) has an integrated urban water cycle management. Different type of treatment plants are located along the drinking, sewerage and reuse networks where specific treatments are applied to guarantee a good enough standard of the water quality.

The presence of radionuclides in treatment plants and in the aquatic environment is well known. Primordial and daughters, cosmogenic, global fall-out and nuclear-legacy radionuclides can be found in the urban water cycle. Moreover in nuclear medicine (NM), short-lived radionuclides are administered to patients, excreting part directly into the sewage network and entering into the urban water cycle.

Thus, the levels of radionuclides in waters and materials from water treatment plants were experimentally checked in the BMA in order to understand the behaviour during the water treatment and to perform a risk assessment. An integrated study focused on the study of the radionuclides levels at different three types of water treatment plants from the same network was carried out. A total of 233 samples were taken at 1 drinking water treatment plant (DWTP), 7 wastewater treatment plants (WWTPs) and 1 reclaimed water treatment plant (RWTP). The concentrations were determined by gamma-spectroscopy techniques after acquisitions performed by high-purity germanium detectors.

Primordial and daughters radionuclides were found in materials from the DWTP studied and the highest specific activities found for sludge, sand and reverse osmosis brine corresponded to ^{40}K. Nevertheless, the maximum concentration in the case of granular activated carbon was found for ^{238}U. Moreover cosmogenic ^{7}Be and fall-out ^{137}Cs were found in sludges.

A total of 5 different NM radionuclides were found in the analysis carried out in the samples from the 7 WWTPs. In the case of water and sewage sludge the highest maximum values and detection frequencies corresponded to ^{99m}Tc and ^{131}I. Moreover ^{67}Ga, ^{111}In and ^{123}I were found but showing significantly lower levels. The detection frequencies and the mean levels found at the WWTPs of ^{67}Ga, ^{99m}Tc, ^{111}In and ^{131}I agreed with the NM radionuclides total activity administered in the region studied. Furthermore the concentrations and detection frequencies were significantly

higher in the sewage sludge samples taken at the very large-sized WWTP-1 (325,000 m3/d), partially explained by their low sludge age. Medically-derived ^{131}I was also found in reclaimed water for reuse from the RWTP and materials from DWTP, which represent novel contributions to the current knowledge in this field.

Taking into account the present findings some considerations from the radiological protection point of view can be done. Despite the presence of radionuclides in the DWTP materials, they do not pose a radiological risk. In the case of the WWTPs and the RWTP studied, the levels found in waters and materials do not represent a significant risk, however, ^{131}I concentrations were pointed out as the most significant.

With the aim to achieve a better understanding of ^{131}I behaviour in WWTPs and predict the ^{131}I levels novel methods of ^{131}I partitioning analysis as well as prognosis models were adapted successfully to a WWTP. ^{131}I partitioning results pointed out that the settling fraction predominates in the reactor while in the rest of the WWTP samples dissolved iodide fraction was the most significant. Furthermore the activated sludge reactors from WWTPs were revealed as the key step for ^{131}I removal from wastewater. Specifically, reactors with the highest total nitrogen kjeldahl removal were also the most effective for ^{131}I reduction. Regarding the ^{131}I modelling a total of 82 % of simulated data fit with the experimental results in the sewage effluent within uncertainties.

Resumen

El Área Metropolitana de Barcelona (AMB; 3.2 M de habitantes) posee un sistema integrado para la gestión del ciclo urbano del agua con diferentes tipos de plantas de tratamiento. En las redes de agua potable, residual y regenerada se aplican tratamientos específicos para garantizar los estándares de calidad requeridos en cada caso.

Estudios previos en plantas de tratamiento de aguas y en ecosistemas acuáticos revelan la presencia de radionúclidos primordiales y de su cadena de desintegración, cosmogénicos y procedentes de accidentes y del legado nuclear. Además en medicina nuclear (MN) radionúclidos artificiales de vida corta son administrados a pacientes, dichos isótopos son posteriormente excretados entrando en el ciclo urbano del agua a través del agua residual.

En el presente estudio en el AMB las concentraciones de radionúclidos en aguas y materiales de las plantas de tratamiento se han estudiado de forma integrada con el objetivo de determinar su comportamiento durante el tratamiento y realizar una evaluación radiológica de los niveles. El estudio ha incluido 233 muestras tomadas en tres tipos diferentes de plantas de tratamiento, 7 estaciones depuradoras de agua residual (EDARs), 1 estación de regeneración de agua (ERA) y de 1 estación de tratamiento de agua potable (ETAP). Las concentraciones de radionúclidos se han determinado con detectores de germanio de alta pureza mediante la aplicación de técnicas de espectrometría gamma.

Radionúclidos primordiales y de su cadena de desintegración fueron detectados en los materiales sólidos de la ETAP estudiada. Las actividades más altas en el caso de los fangos, las arenas y el rechazo de la osmosis inversa correspondieron al ^{40}K mientras que en el caso de carbón activo granulado al ^{238}U. Además se confirmó la presencia de ^{7}Be y ^{137}Cs.

Un total de 5 radionúclidos relacionados con la MN fueron detectados en los análisis de las muestras de las 7 EDARs. Respecto a las aguas y los fangos analizados las máximas concentraciones y los más detectados fueron el ^{99m}Tc y el ^{131}I. Además fueron detectados en concentraciones más bajas el ^{67}Ga, ^{111}In y el ^{123}I. Las frecuencias de detección y niveles concordaron con la actividad total administrada en

la zona de estudio. Especial mención merecen los resultados de la EDAR-1 (325,000 m3/d), de grandes dimensiones, ya que los valores y frecuencia de detección fueron mayores que en el resto lo que se explica en parte por la reducida edad del fango que genera. El ^{131}I se encontró también en agua regenerada de la ERA y los materiales de EDAR estudiadas, lo que representa una nueva aportación por a lo que ^{131}I de origen médico se refiere.

Con los presentes resultados se pueden realizar las siguientes consideraciones desde el punto de vista de la protección radiológica. A pesar de la presencia de radionúclidos en aguas y materiales de las plantas estudiadas, las concentraciones de actividad determinadas no suponen un riesgo radiológico significativo. Sin embargo puede afirmarse que las concentraciones de ^{131}I fueron las más relevantes.

Con el objetivo de avanzar en el conocimiento del comportamiento de ^{131}I en EDARs y predecir sus concentraciones nuevas metodologías de análisis del ^{131}I así como modelos predictivos se adaptaron satisfactoriamente a una de las EDAR estudiadas. La distribución fisicoquímica del ^{131}I resultó en que la fracción precipitable predominó en las muestras tomadas en el reactor ya que es un tratamiento clave para su eliminación, mientras que en el resto de muestras analizadas el yodo inorgánico disuelto fue mayoritario. Otro descubrimiento relevante fue constatar que los reactores que presentaban una mayor disminución de la concentración del nitrógeno kjeldahl mostraron también una reducción significativa del ^{131}I. Respecto al modelo, un total del 82 % de las concentraciones de ^{131}I simuladas para los efluentes de planta se ajustaron satisfactoriamente a los resultados experimentales considerando las incertidumbres.

Contents

Chapter 1

The BMA urban water cycle and presence of radionuclides

1.1 Description of the BMA urban water cycle

The Barcelona metropolitan area (BMA) has 3.2 M inhabitants and is divided into 36 different municipalities, including the city of Barcelona, occupying an area of 636 km^2. The 42 % of the population of the Catalonia region live in the BMA which represents only 2 % of the territory (AMB 2018). The BMA is located in the Llobregat and Besòs River lower basins and in terms of population is the 7th most important European metropolitan area in Europe. Moreover the economic activity in the metropolitan area represents the 51 % of the gross domestic product of Catalonia and primary, secondary and tertiary sectors are present in the territory (Fig. 1.1).

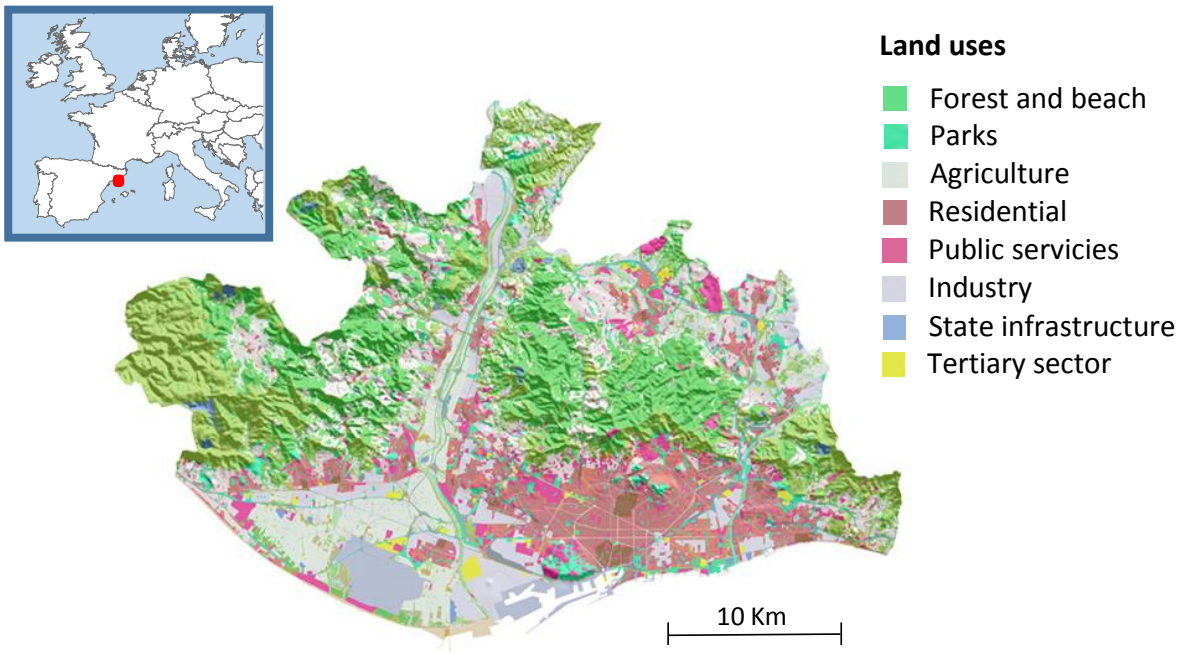

Figure 1.1: Boundaries and land uses in the BMA (AMB 2018).

All BMA municipalities share the management of the urban water cycle (Fig. 1.2) in an interconnected network of pipes, tanks and treatment plants. Water usually needs treatments prior to human consumption, release to the environment or reuse as it may contain contaminants. Specific treatments are applied to improve water quality and different technologies are currently used in order to guarantee the water quality demands from each urban water cycle step.

The management in the BMA includes the catchment of the raw water (river surface, well or marine), purification and supply followed by collection of wastewater (domestic, hospital, industrial and storm water) and its treatment previously to the sewage effluent release into the environment. In some cases sewage effluents receive an additional treatment for reclaimed water production (Fig. 1.2) to be reused in different applications.

According to the water quality demands for drinking water, sewage effluent and reclaimed water specific depuration techniques are applied at drinking water treatment plants (DWTPs), wastewater treatment plants (WWTPs) and reclaimed water treatment plants (RWTPs) facilities, respectively. The location of the different water treatment from the BMA urban cycle are detailed in (Fig. 1.3).

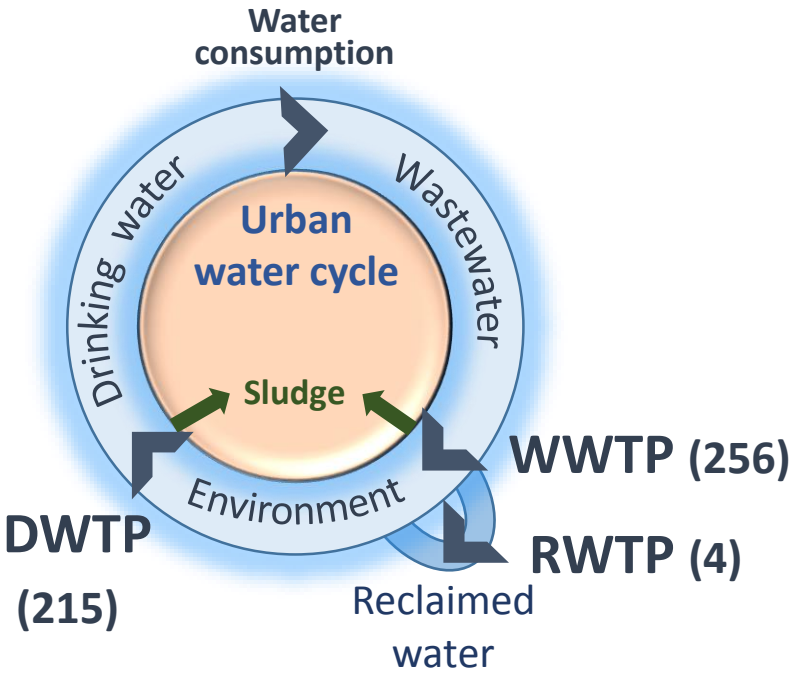

Figure 1.2: BMA urban water cycle scheme and water volumes treated in the year 2014 in $Hm^3 \cdot y^{-1}$ within brackets.

Figure 1.3: Location in the BMA of the treatment plants studied. Some of the DWTPs which supply the BMA with water for human consumption are located out of the boundaries (triangle symbol).

1.1.1 DWTPs

In the case of raw water from the aquatic environment, it usually needs treatment at DWTPs prior to human consumption as it may contain suspended solids, chemical substances dissolved or pathogens that can make it unsafe. Specific treatments are applied to improve water quality and different technologies are currently used in order to guarantee a good enough standard of the drinking water supply.

According to the BMA (AMB 2018) a total of 215-225 $Hm^3 \cdot y^{-1}$ raw water from different origins has been treated for the period 2014-2017 for water supply in the BMA and 13 out of the 15 DWTP that treats the raw water are located in the BMA territory. The main sources have been the surface captations located in Ter and Llobregat rivers (82-87 %) while other sources as groundwater (12-15 %) and seawater (1-5 %) have been complementary sources. A total number of 15 DWTPs are connected to the supply network (Table 1.1). However, most of the treated water corresponded to the DWTP-1 and DWTP-3, which represented the 78 % of the volume treated in the year 2014. Both treatment plants combine a first physical treatment in order to reduce significantly the total suspended solids (TSS) concentration present in surface catchments while a dissolved contaminants removal and disinfection treatments are applied in a secondary and tertiary steps respectively. DWTP-2 is treating most of the water form the River Llobregat surface while DWTP-4 treats seawater by applying desalination procedures to adapt seawater to the human consumption. Furthermore 11 independent facilities treat groundwater from the Besòs and Llobregat lower basins aquifers (Table 1.1).

Table 1.1: Details of the DWTPs that supply the BMA with water for human consumption (AMB 2018).

Treatment plant	Raw water source	Main treatment steps[b]
DWTP-1	Ter River	1) Particle decanters 2) GAC filter
DWTP-2	Llobregat River	1) Particle decanters 2) pH adjustment 3) Sand filter 4) Electrodyalisis reversal
DWTP-3	Llobregat river basin (river and aquifers)	1) Particle decanters 2) Sand filter 3) GAC filter 4) Reverse osmosis
DWTP-4	Mediterranean Sea	1) Particle decanters 2) Sand and anthracite filter 3) Reverse osmosis
Other DWTPs[a]	Besòs and Llobregat river basins aquifers	Stripping, filtration, reverse osmosis, nanofiltration, oxidation[c]

a) Besòs, Sant Feliu de Llobregat, El Papiol, Sant Joan Despí–Cornellà, Sant Vicenç dels Horts, Mas Blau, Monturiol, La Llagosta, Sagnier, Nicolàs, Camí del Repeu
b) All the treatments include a chlorination step
c) Different type of treatments found in the 11 DWTPs
GAC: Granular activated carbon

1.1.2 WWTPs

The urban wastewater treatment network includes collection via sewerage network, the treatment in a WWTP and the discharge of sewage effluent into the environment. The BMA wastewater treatment network has 7 urban WWTPs (Table 1.2). Dimensioning, design and location of the WWTPs depend on different factors such as the volume treated per day, the physicochemical characteristics of the inflow water, the quality standards required in the sewage effluent or the morphology of the territory. Pretreatment steps are necessary to remove grifts, sand and oil which can affect to the normal operation of the treatment plant. A total of 5 out of 7 WWTPs have primary treatment, which is focused in decrease the TSS, separated from the activated sludge treatment. In contrast, both small-sized WWTP-6 and WWTP-7 do not have primary treatment before the activated sludge step (Table 1.2). Heterogeneous activated sludge reactors designs can be found in the BMA as conventional activated sludge reactors, membrane bioreactors or integrated fixed-film sludge reactors. Some of the reactors work under special operational regimes where the nitrogen cycle is carried out (Che et al., 2017), showing significant removals in the sewage effluent (Table 1.2). The most relevant WWTPs are the WWTP-1 and WWTP-2 facilities which treat the 81 % of the total wastewater collected by the sewerage

network (ACA 2014). The BMA system has combined sewers where storm and wastewater share the same catchment network.

Table 1.2: Urban WWTPs characteristics in the BMA and description of the reclaimed water treatment lines.

	Mean volume treated[a] **$m^3 \cdot d^{-1}$**	**Primary settling tank**	**High nitrogen removal efficiency in the activated sludge line**	**Sewage effluent release point**	**Energy cogeneration**	**Reclaimed water facility treatments**[b]
WWTP-1	325.000	Yes	No	Mediterranean Sea	No	-
WWTP-2	240.000	Yes	Yes (5/11 reactors)	Mediterranean Sea	Yes	**RWTP-2:** Particles removal, ultrafiltration reverse osmosis, UV-rays
WWTP-3	48.000	Yes	No	Besòs River	Yes	**RWTP-3:** Wetland
WWTP-4	50.000	Yes	Yes	Llobregat River	Yes	**RWTP-4:** Particles removal
WWTP-5	37.000	Yes	Yes (2/4 reactors)	Mediterranean Sea	Yes	**RWTP-5:** Particles removal, ultrafiltration
WWTP-6	800	No	Yes	Vallvidrera Brook	No	-
WWTP-7	900	No	Yes	Begues Brook	No	-

a) Data from ACA (2014)
b) All receive chlorination treatments

1.1.3 RWTPs

Reclaimed water is obtained after the application of a tertiary treatment in RWTPs to sewage effluents from the WWTPs that adapt the water quality to the requirements of the final application (RD 1620/2007). The diversity and the total number of human activities with water demand as industry or agriculture in the BMA, a reduced area of territory, opens up the possibility of reuse applications of reclaimed water. Other factors that are favourable for the reclaimed water use are the existence of the important volumes of depurated water and the lower Besòs and Llobregat river basins wetlands, agriculture and industrial areas. After a directly application of a tertiary treatment to the sewage effluent in 4 out of 7 WWTPs the reclaimed water is obtained and several reuse applications are planned (AMB 2018). The water treatment applied in 3 out 4 RWTPs takes place in a tertiary line from the WWTP, however, in the case of the RWTP-3 part of the sewage effluent is transferred to a wetland area from Besòs River Basin which becomes the tertiary treatment before flow into the Besòs River. The total volume of wastewater regenerated in RWTPs was 2 % at 2014 (Fig 1.2) and the reuse applications are urban parks and agriculture irrigation and the regulation of the hydrological systems of Llobregat and Besòs rivers lower basins. Furthermore, the network supply of RWTP-2 is connected with

industrial areas with the potentiality to implement reuse projects in near future (AMB 2014).

1.1.4 Sludges

The main by-product obtained due to the urban water cycle management processes is the sludge from the DWTPs and WWTPs (Fig 1.2). The intrinsic characteristics of sludge allows to reuse it in different applications (AMB 2014). On one hand, the sludge from the DWTPs is mainly recycled as additive in the cement industry (Rodríguez et al., 2010). On the other hand during the period 2014-2017 (AMB 2018) between 55,000-60,000 t dry weight per year were produced in the WWTPs and recovered as compost (70-71 %), direct application in agriculture (20-24 %) as combustible in the cement industry (2-5 %) as well as other uses (3-6 %). Apart from the direct management, mesophilic bacteria previously digest sewage sludge in 4 WWTPs (Table 1.2) sludge lines during some weeks in order to produce biogas (Lu et al., 2013; Achermann et al., 2018). The energy recovery per year (40,605-47,801 $MW{\cdot}h^{-1}$; AMB 2014) were between the 38-47 % of the electricity consumption on the WWTPs from the BMA per year for the period 2014-2017.

1.1.5 Water treatments applied

Several water treatment technologies are implemented in the three types of the water treatment plants at the BMA (Tables 1.1 and 1.2). Processes of particles settling take place in all the treatment plants usually as primary treatment as well as before the sewage effluent obtention at WWTPs. Sands filtration is applied in DWTPs and RWTPs with the aim to refine the particle removal processes as well as granulated activated carbon to remove dissolved contaminants. In order to reduce dissolved compounds from the flow in WWTPs activated sludge is applied as secondary treatment at all the BMA WWTPs. Most exhaustive techniques processes as nanofiltration, ultrafiltration and reverse osmosis are also implemented in particular at DWTPs and RWTPs. Moreover a wetland area specially designed for this objective is also applied as a water treatment in RWTP-3. Some pictures from treatment steps located at the water treatment plants from the BMA can be found at Fig 1.4.

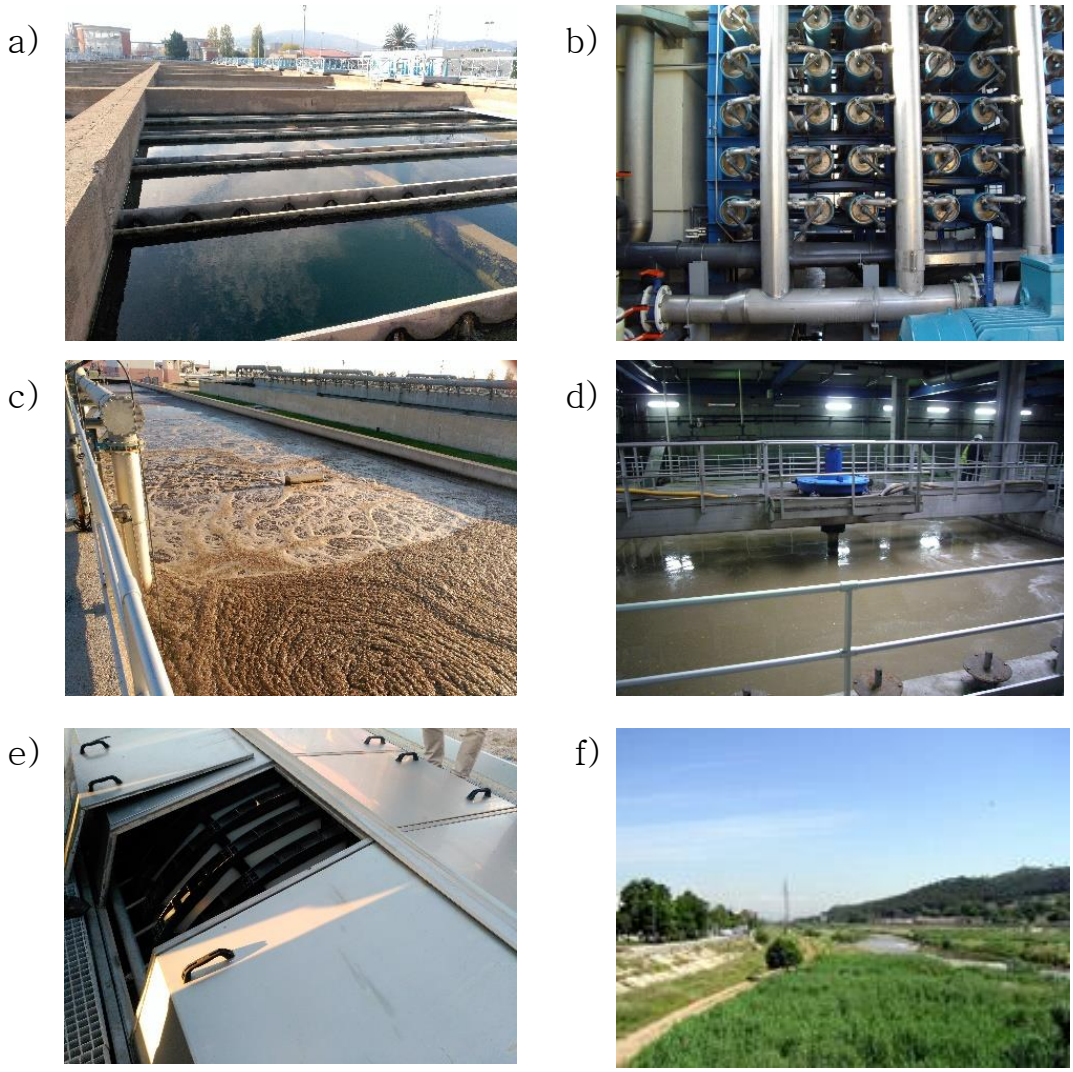

Figure 1.4: Examples of treatments applied in the BMA urban water cycle management:
a) Particles decanters from the DWTP-3
b) Reverse osmosis line from medium-sized DWTP facility
c) Activated sludge reactor from WWTP-2
d) Entrance to the primary treatment in WWTP-1
e) Ultrafiltration discs from the RWTP-2
f) Wetland area from the RWTP-3

1.2 Radionuclides in the urban water cycle

The existence of radioactivity at detectable levels in the environment is well known and the presence of radionuclides with natural and artificial origins has been documented in the atmosphere, lithosphere and consequently at the hydrosphere (UNSCEAR 2000).

The presence and concentrations of radionuclides in an urban water cycle depend on the environmental characteristics in the case of the natural radionuclides and the presence of human activities with radionuclides emissions. Furthermore, the type of treatments applied during the water management can also concentrate radionuclides in the by-products and filtering materials. As of today, the concentrations of radionuclides at water treatment plants are not predictable with precision without any experimental determination.

Materials and waters with radionuclides can represent a risk from the radiological protection point of view. It is necessary to perform levels evaluation of the radionuclides found (Beyermann et al., 2010; Baeza et al., 2016) as well as in some cases dosimetric evaluations in order to discard any significant radiological risk in the activities performed with water or materials from water treatment plants (Al-Jaseem et al., 2016; Baeza et al., 2016; Beyermann et al., 2010).

One previous relevant study on this field is Bastian et al. (2005) giving information about 311 sewage sludge samples from WWTPs located in the United States and 35 sewage sludge ash samples, where 44 different radionuclides from diverse origins (natural and artificial) were found. In the review from Fonollosa et al. (2015) a total of 28 radionuclides were found in the sludges from the different DWTPs studied. In spite of the diversity of applications of reclaimed water, the radionuclides levels in RWTPs have not been significantly studied.

Nonetheless, there is a lack of information of the presence of radionuclides in different type of treatment plants from the same urban water cycle and its dynamics along the different steps of the treatment processes. This kind of studies allow an integrated discussion on the radionuclides concentrations as well as to determine the most relevant issues to address from the radiological protection point of view. Despite their tendency to concentrate contaminants, other materials from treatment plants different than sludge have been not studied enough. Details about the different sources of the most significant radionuclides found in previous studies in the urban water cycle are described as follows.

1.2.1 Primordial and daugthers

The existence of primordial radionuclides since the earth formation have given rise to, for example, the presence of ^{40}K or daughters from the decay chains of ^{238}U, ^{235}U and ^{232}Th. The accumulation of natural radionuclides in materials during industrial processes can give rise to natural occurring radioactive materials (NORM) with special indications from the radiological protection point of view (UNSCEAR 2000).

A Previous study has determined the presence in the Llobregat River lower basin surface water ^{nat}U and ^{40}K as major sources of radioactivity concentrations in the order of 0.1 Bq·L^{-1} and 1 Bq·L^{-1}, respectively (Camacho et al., 2010). Although be potential sources of accumulations of radionuclides, data of primordial and daughters on different materials that can concentrate contaminants as filtering materials and reverse osmosis brine have not been reported more than in single previous study in Australian DWTPs (Kleinschmidt and Akber 2008). Furthermore no previous studies have been carried out in the BMA focused on primordial and daughters radionuclides accumulation in filtering materials from DWTPs.

1.2.2 Cosmogenic

Other type of natural radionuclides present in the environment with a natural origin are cosmogenic radionuclides. The interactions between the cosmic rays and the upper layers of the atmosphere give rise to the production of ^{7}Be, ^{10}Be, ^{14}C, ^{3}H, ^{22}Na and ^{36}Cl among other radionuclides (Poluanov et al., 2016; Webber et al., 2007). In the BMA ^{7}Be is associated to stormwater and is usually detected in atmospheric samples (Grossi et al., 2016).

Apart from the presence of the radionuclides in aquatic environments and water treatments plants some studies use its presence in detectable amounts to trace environmental process. These are the cases of Rose et al. (2015), Fischer et al. (2009) and Grossi et al. (2016) studies which use ^{7}Be to trace sedimentary dynamics of particles in aquatic systems or atmospheric processes.

1.2.3 Global fall-out and nuclear-legacy

Nowadays, the nuclear industry is a source of anthropogenic radionuclides such as ^{3}H, ^{14}C, ^{60}Co, ^{90}Sr, ^{131}I, ^{137}Cs, ^{239}Pu, ^{240}Pu, ^{241}Am, ^{129}I, ^{236}U and ^{99}Tc among other radionuclides, which have been released into the environment due to nuclear power plants operation, nuclear weapons tests, nuclear fuel reprocessing and nuclear waste management (Zerquera et al., 2017; Steinhauser et al,. 2014; Prâvâlie 2014; Casacuberta et al,. 2017; Fréchou and Calmet 2003). Other novel applications of

fall-out radionuclides are to trace marine flows with ^{129}I and ^{236}U (Casacuberta et al., 2017) or sediments datation with $^{239/240}$Pu (Garcia-Orellana et al., 2009).

1.2.4 Medically-derived

Medical uses of radionuclides in nuclear medicine (NM) represent an additional source of anthropogenic radionuclides to the environment. Radionuclides as ^{123}I, ^{125}I, ^{131}I, ^{99m}Tc, ^{111}In, ^{67}Ga, ^{201}Tl and ^{177}Lu are the most administered for diagnosis procedures or treatments in the order of MBq-GBq per patient in Europe (EC 2014; IAEA 2014).

Radionuclides applied in NM procedures are administrated into patients which can release through excretions part of the activity. Medically-derived radionuclides enter into the urban water cycle through wastewater as well as effluents from industries. Furthermore NM facilities present in the catchment area can release radionuclides through urban wastewater. Direct determinations are necessary to know the levels of ^{131}I and in general from NM radionuclides, which have shown until now an independent behaviour as regards other contaminants and wastewater quality indicators (Souti et al., 2014; Barredo 2010). Apart from their presence in the wastewater treated the activities can be concentrated in sludges and also be present in the sewage effluent released to the environment. A relevant study about the presence of radionuclides in WWTPs is Fischer et al. (2009) which reported the presence of medically-derived ^{99m}Tc and ^{131}I in wastewater, sludges, sewage effluent and in sediments. Although some studies reported levels of medically-derived radionuclides in WWTPs (Barci-Funnel et al., 1993; Dalmasso et al., 1997; Bastian et al., 2005; Rose et al., 2012; 2013; Rose and Swanson 2013; Punt et al., 2007; Fenner and Martin 1997; Montaña et al., 2013a; Barredo 2010; Chang et al., 2011; Mc Gowan et al., 2014; Martínez et al., 2018), very few studies have gone one step beyond and identify relationships of the levels found with other factors (Zannonni et al., 2018; Hormann and Fischer 2018).

Even though reclaimed water was pointed out as prone to carry ^{131}I and ^{99m}Tc due its presence in sewage effluents (WHO 2017), there is a lack of information about it, and levels were only checked in one RWTP for environmental uses (Rose et al., 2013). The interest of go further in the present knowledge of contaminants in reclaimed water is in agreement with water scarcity which is a factor to take into account in future climate scenarios, in special for South Europe countries where reclaimed water is an expanding option to satisfy water demands (DEMOWARE 2017). Furthemore medically-derived ^{131}I can be applied to trace nitrogen emitted through the sewage effluent to the environment (Rose et al., 2015).

The BMA is a medical centre with 15 radionuclides administration facilities which in some cases give service to all the population of the Catalonia region. Pa-

tients excrete the medically-derived isotopes into the sewerage network over a variable period lasting hours or days after administration depending on the effective half-life of the radiopharmaceutical supplied to the patient, which is a combination of the biological half-life of the radiopharmaceutical and the physical half-life of the radionuclide (ICRP, 1988, 1998, 2004, 2008). The number of NM procedures has experienced an increase in the past decade and there is a high variation of the total number of NM procedures among different countries, ranging from about 500 to 3,800 per 1.0 M of population according to the latest available study on Medical Radiation Exposure of the European Population (EC 2014). In Spain, the 6 most applied radionuclides for diagnosis are detailed in Table 1.3 with an administered activity of the order of MBq (CSN SEPR SEFM SEMNIM 2014) and with relatively short physical half-lives.

Table 1.3: Details of top-6 diagnosis radionuclides administered in NM in Spain and administration ratio estimations of ^{131}I treatment procedures.

Radionuclide / radiopharmaceutical	Physical half-life	Different types of diagnostic procedures	Ratio administrations 1M inhabitants / year	Mean activity / Activity range (GBq)
Diagnosis[a]				
^{99m}Tc	6.0 h	12	11,172	0.63
^{18}F	109 m	1	1,360	0.34
^{123}I	13.3 h	3	340	0.20
^{67}Ga	3.3 d	1	219	0.23
^{131}I	8.0 d	2	158	0.18
^{111}In	2.8 d	1	128	0.16
Treatment with ^{131}I				
Na^{131}I	8.0 d	Thyroid cancer	40[b]	1.1-7.4[c]
Na^{131}I	8.0 d	Hyperthyroidism	150[d]	0.19-0.80[c]
^{131}I-MIBG	8.0 d	Neural-crest tumors	N.D.	3.1-7.5[e]
^{131}I-lipiodol	8.0 d	Hepatic tumors	N.D.	0.9-3.6[f]

a) CSN SEPR SEFM SEMNIM (2014)
b) Zafon et al. (2015)
c) CSN SEPR SEFM (2011)
d) UNSCEAR (2000)
e) Wafelman et al. (1997)
f) Furtado et al. (2015)
N.D.= No data

1.2.4.1 Management of patients treated with ^{131}I

For therapy purposes, high amounts of ^{131}I of the order of MBq−GBq are administered to patients (Table 1.3) and some comments from the radiological protection point of view must be made due to the activity carried by the patient (IAEA 2009). In some countries as Denmark, Finland, the United Kingdom or the United States of America the ^{131}I present in the excreta from inpatients flows also directly into the sewerage network without the use of any abatement system (EC 1999; Fenner and Martin, 1997; McGowan et al., 2014; Rose et al., 2012). While in other coun-

tries, such as Germany or France high−activity therapy ^{131}I treatments (>0.25 and >0.74 GBq respectively) are performed at specialized departments equipped with a sewage collection system (EC 1999; Fischer et al., 2009; IAEA 2009). In Spain, patients treated with an activity >0.8 GBq need hospitalization in a confined area as required by Spanish criteria on the management of patients treated with ^{131}I compounds (CSN SEPR SEFM 2011) which is based on ICRP (2004) recommendations.

^{131}I is mainly excreted through urine and is collected in specific abatement systems usually consisting of several sewage holding tanks (Fig 1.6) where ^{131}I is allowed to decay before being discharged to the hospital main sewer. Discharges from facilities must remain below a limit of 75 Bq·L^{-1} at the point of discharge into the public sewerage network (CSN 2002). Although there are no available national data about the total number of ^{131}I−MIBG and ^{131}I-lipiodol treatments, is significantly lower than the number of Na^{131}I treatments (Yeong et al., 2014) (Table 1.3). The inpatients are discharged from the facilities when their retained activity falls below 0.8 GBq, which means the patients' external dose rate is no higher than 40 μSv·h^{-1} at 1 m (CSN SEPR SEFM 2011), thus they continue to excrete residual activity when they return home. ^{131}I effective life in the human body is different depending on the radiopharmaceutical used and the treated illness, and ranges from 3–6 days for thyroid cancer up to 7–10 days for hyperthyroidism (CSN SEPR SEFM 2011).

Figure 1.5: Holding tanks for urine storing from confined patients' treated with ^{131}I located in the basement from one BMA hospital.

The administration of ^{131}I for therapy and diagnosis procedures to patients in NM has direct relationship with its presence in WWTPs. Concentrations in previous studies in other urban WWTP abroad form the BMA ranged between 0.1-148,000 $Bq{\cdot}kg^{-1}$ dry weight in sewage sludge (Fischer et al., 2009; Rose and Swanson 2013). Furthermore, ^{131}I has been found in the sewage effluent from WWTPs with activities between 0.04-115 $Bq{\cdot}L^{-1}$ (Punt et al., 2007; Mc Gowan et al., 2014; Fischer et al., 2009; Rose et al., 2012; Carvalho et al., 2013), in river water (<0.003-18 $Bq{\cdot}L^{-1}$; Punt et al., 2007; Rose et al., 2013) and in air after sewage sludge incineration (<0.1-6.0 $mBq{\cdot}m^{-3}$; Kitto et al., 2006).

Thus, the concentration in the BMA of NM radionuclides, specially in WWTP sewage sludge depends on the specific operational conditions of the treatment plants, health system total administration of radionuclides and treatment patient management. Although the thousands of patients treated per year in the BMA (Table 1.3), the levels of medically-derived radionuclides in WWTPs have not been checked before. In order to determine the radionuclides levels accurately specific sampling campaigns and experimental procedures are necessary. Furthermore a comparison between the levels of ^{131}I at WWTPs in different countries with different models of patients‘ management has not been performed before.

1.3 Radionuclides partitioning methods for water samples

In water samples radionuclides can be found attached to particles or colloids as well as dissolved as different chemical species. The partitioning in the water column and the water treatments applied have a direct influence on the radionuclide behaviour along the different steps of the treatment plants and its accumulation in filtering materials and by-products. The chemical species of the radionuclides has influence for example in the precipitation processes from the water column for experimental determinations (Hou et al., 2009) as well as in radionuclides removal in drinking water treatment plants (Baeza et al., 2006). Specific radichemical techniques have been developed to determine the presence of a radionuclide in one or some of previously defined fractions of water samples (Saari et al., 2010; Maringer et al., 2015; Hormann and Fischer 2017; Chabaux et al., 2008 review). Furthermore, some techniques have been applied to completely extract and concentrate a radionuclide present in several fractions in a water sample in order to perform a low-level measurement in terms of total concentration (Rodríguez el al., 2018).

Radioiodine and specifically environmental ^{129}I from nuclear reprocessing processes and fall-out (Li et al., 2014; Casacuberta et al., 2017) and ^{131}I from NM procedures and NPPs (Hormann and Fischer 2017) have been matter of interest due to their mobility and diversity of species in environmental samples and also the potential harmful effects of human body incorporation of radioiodine (IAEA 2014). Apart from the total concentrations of ^{131}I partitioning determinations can give extra information about the chemical behaviour and removal of ^{131}I along the water treatment (Cosenza et al., 2015; Hormann and Fischer 2017). Works about the radioiodine partitioning have been carried out with specific developed techniques for water samples (Hou et al,. 2009; Rose et al., 2013). Moreover a special technique has been developed in Hormann and Fischer (2017) in order to determine the behaviour of medically-derived ^{131}I in the different treatment steps from a WWTPs, differentiating between settled, dissolved inorganic and dissolved residual fractions. Nevertheless, the analytic techniques proposed need from more validation tests with the aim to be accurate in the activity reported for the different fractions analysed.

1.4 NM radionuclides and modelling at WWTPs

Some works have published models of NM radionuclides in WWTPs for different proposals (Table 1.4). A risk evaluation of the release of medically-derived radionuclides by patients after NM procedures to the sewage network has been performed in Sundell-Bergman et al. (2008) while in Nakamura et al. (2005) the experimental proportional fractions after known amounts administered to patients have been determined.

The implementation of models in order to predict the levels of ^{131}I in treatment plants is an interesting tool from the radiological protection point of view. However, the present knowledge about NM radionuclides modelling at WWTPs is scarce.

In Hormann and Fischer (2018) a previous study of ^{131}I partititiong in the different steps of a WWTP (Hormann and Fischer 2017) opens up the possibility to develop a prognosis model taking into account the behaviour of ^{131}I along the process and validated with experimental concentration. Furthermore in Chang et al. (2011) the statistical paths from the patient to the WWTP sewage effluent determined in Punt et al. (2007) for ^{131}I were directly applied in order to predict the sewage effluent levels. Experimental data is shown to compare simulated results and experimental levels, however, both differ significantly.

Table 1.4: Previous models of prediction of NM radionuclides levels in WWTPs.

Type of model	**Radionuclides**	**Values reported**	**Reference**
Compartimental and probabilistic	^{99m}Tc, ^{111}In, ^{123}I, ^{131}I and ^{201}Tl	Dose to WWTPs workers μSv·y^{-1}	Sundell-Bergman et al. (2008)
Compartimental	^{99m}Tc, ^{123}I, ^{67}Ga, and ^{201}Tl	Proportions of the dose injected to a patient in the sewage treatment system	Nakamura et al. (2005)
Statistical	^{131}I	Sewage effluent levels	Chang et al. (2011)
Compartimental	^{131}I	Sewage effluent levels	Hormann and Fischer (2017)

1.5 Aim of the PhD thesis

During the research period, the main goal of the present work has been to advance in the present knowledge of levels and behaviour of radionuclides in the BMA treatment plants. Furthermore, in the most relevant case a model implementation of the radionuclide behaviour in the treatment plant has been carried out. The main activities of the present work were:

i) To determine the medically-derived radionuclides concentrations and variabilities in liquid samples and sludges from the 7 WWTPs and in one RWTP

ii) To adapt and apply an existing ^{131}I partitioning analysis methodology to the WWTP-2 liquid samples and to model the levels in the sewage effluent

iii) To study the concentrations dynamics and to evaluate the natural and artificial radionuclides presence in materials from the DWTP-3

Chapter 2

Materials and methods

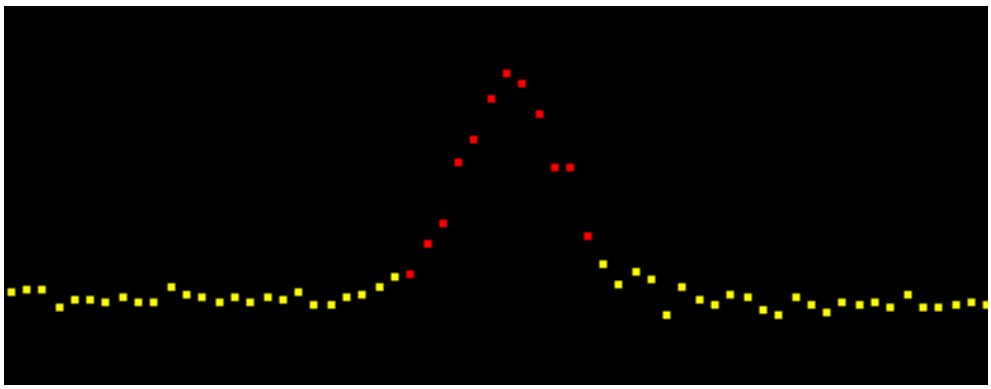

2.1 Introduction

In order to accomplish with the objectives set for the present work, the radionuclides concentrations in samples taken in the Barcelona metropolitan area (BMA) water treatment plants have been determined.

Most of the radionuclides which are expected to be found in the urban water cycle are gamma-emitters and gamma-spectroscopy has been considered the most appropriate technique to carry out the activity determinations. The chosen technique allows a non-destructive multi-nuclide activity quantification with the same spectra acquisition. The use of high-purity germanium (HPGe) detectors for the quantification of radionuclide activities is a well-known technology which offers high accuracy in environmental samples. Moreover intercomparison exercises are available for the method validation. The measurements have been taken place in the *Laboratori d'Anàlisi de Radioactivitat* (LARA) facilities from the *Institut de Tècniques Energètiques* at the *Universitat Politècnica de Catalunya* with continuous experience in this type of determinations since 1986.

Apart from the radionuclides concentrations, determination of the physicochemical parameters were carried out in several samples in the *Laboratori d'Anàlisi de Paràmetres Fisicoquímics* (LAPF) from the *Societat General d'Aigües de Barcelona*. These analysis leads to a better understanding of the radionuclides levels found in waters and materials from the water treatment plants.

Details about the sampling, activity determination and physicochemical parameters methods can be found in the following sections of the present chapter.

2.2 Sampling

The samples analysed in the present compilation were taken at water treatment plants from the BMA urban water cycle network between the years 2012 and 2018. The campaign details as the volume, the total number of samplings in a treatment plant and the total number of samples taken in a treatment step can be found in the experimental chapters of the present document (Chapter 3-6) while the sampling dates are detailed in the *Appendix D.1.*

Samplings were carried out by the staff from the company at charge of the management of the facilities (AGBAR). In order to maintain uniformity of sampling points during the campaigns the company staff followed the same internal procedures than those for obtain daily information from the physiochemical properties.

All sewage sludge and materials from the WWTPs correspond to spot samples while the liquid samples combine spot and pooled samples, in the latter case by using ISCO® 3700 samplers (Fig. 2.1) which takes one sample per hour along 24-hour period.

Then, the samples were sent to the LARA and to the LAPF in polyethylene containers with a volume between 1-25 L in order to perform the programed analysis.

Figure 2.1: ISCO ® 3700 sampler in the WWTP-1 inflow wastewater sampling point.

2.3 Radionuclides activity determinations

Radionuclides concentrations (liquids and materials from water treatment plants) or total activity (^{131}I partitioning methodology) have been determined by applying gamma-ray spectrometry.

The present work focused in a total of 13 medically-derived radionuclides, 6 primordial and daughters radionuclides, 1 cosmogenic radionuclide and 1 fall-out radionuclide. However, different pre-treatments were necessary to optimize the measurements of radionuclides depending of the targeted radionuclides and the type of samples.

Sample pre-treatment, decay data of the radionuclides studied, detectors characteristics and details of the procedures implemented to report the final specific activities are described in the present section.

2.3.1 Radioactive decay basics

The physical instability of radioactive nuclides leads to the decay of the number of nucleus following the fundamental law of radioactive disintegration. Several types of physical disintegration processes which involve alpha particles emission (helium nucleus) or beta particles emission (electron and positron) through by beta minus, beta plus and electronic capture disintegrations occur can during the radioactive nuclide decay (Knoll 2010). After the disintegration, an immediate emission of photons due to an excess of excitation energy in daughters can take place. The presence of a radionuclide in sample can be quantified through the activity (A) that is defined in eq. 2.1:

$$A = -\frac{dN}{dt} = \lambda N = A_{(t=0)} \cdot e^{-\lambda \cdot t} \tag{2.1}$$

where N is the number of radioactive nucleus and λ the radionuclide decay constant which is related to the radionuclide half-life ($t_{1/2}$) (eq. 2.2):

$$\lambda = \frac{ln(2)}{t_{1/2}} \tag{2.2}$$

Radionuclides with low decay constants have long half-lives and a higher permanence in a sample. In the present work the activity (A) for each radionuclide in a measured sample has been reported as disintegrations per second; bequerels (Bq; according to the International System of Units).

2.3.2 Sample pre-treatment

Depending on the sample and the aim of the radioactivity determination, a sample pre-treatment before the measurement was performed while other samples were directly poured into the geometry and measured in the high-purity germanium (HPGe) detector.

In the case of the nuclear medicine short-lived radionuclides determinations, sample pre-treatment and measurement, began as soon as the sample arrived at the LARA in order to minimize the influence of the radionuclides decay before the start of the spectra obtention. In the case of samples where the primordial and daughters were measured, a minimum of 21 days of elapsed time between the sample pre-treatment and measurement was established in order to achieve secular equilibriums necessary for the concentration determination. In Table 2.1 intrinsic characteristics of the different samples in the present work at the measurement time, the radionuclides studied, the geometry chosen and the acquisition time are detailed.

The material of interest (samples) is poured into containers (named as geometries) with the aim to place a sample with a known mass and density onto the HPGe detector and carry out the gamma-spectra acquisition. Marinelli (400 mL) and cylindrical (45 and 100 mL) containers were used in the present work (Fig. 2.2). After the sample addition the geometry is sealed by inner and outer covers. Adhesive tape was used to fix the covers.

Regarding the samples from the water treatment plants studied the activity measured in liquid samples was divided by the volume measured, nevertheless, in solid samples was divided by mass and was corrected by the humidity content before reporting the final specific activity in dry weight (eq. 2.1):

$$Bq \cdot kg^{-1}\ d.w. = \frac{Activity\ (Bq)}{Wet\ weight\ (kg)} \cdot \frac{Wet\ weight\ (kg)}{Dry\ weight\ (kg)} \tag{2.3}$$

The activities were expressed in Bq·L^{-1} or Bq·kg^{-1} dry weight (d.w.), respectively (Table 2.1). In the case of the ^{131}I partitioning analysis the total activity was reported in Bq.

More specific details about the sample pre-treatment and the activity reported for the different type of samples from the water treatment plants as well as for the ^{131}I partitioning methodology are specified as follows.

Table 2.1: Details of the samples intrinsec propierties, pre-treatment and measurement.

Samples	Radionuclides	Type of sample	Density g·cm^{-3}	Geometry	Adquisition time	Reported data
WWTP (Chapters 3 and 5)						
Waters	Nuclear medicine	Liquid	1.0	Marinelli (400 mL)	7,886-220,327 s	Bq·L^{-1}
Primary and activated	Nuclear medicine	Wet solid	0.9-1.0	Marinelli (400 mL)	7,467-105,142 s	Bq·kg^{-1} d.w.
Dehydrated	Nuclear medicine and ^{7}Be	Wet solid	0.7-1.3	Cylindrical (100 mL)	7,253-86,376 s	Bq·kg^{-1} d.w.
RWTP (Chapter 5)						
Waters	Nuclear medicine	Liquid	1.0	Marinelli (400 mL)	10,756-129,235 s	Bq·L^{-1}
DWTP (Chapter 6)						
Sludge	Primordial and daughters, ^{7}Be and ^{137}Cs	Dry solid	0.5-1.0	Cylindrical (50-100 mL)	56,684-108,941 s	Bq·kg^{-1} d.w.
Sand	Primordial and daughters, ^{7}Be and ^{137}Cs	Dry solid	1.3-1.4	Cylindrical (100 mL)	85,231-429,596 s	Bq·kg^{-1} d.w.
GAC	Primordial and daughters, ^{7}Be and ^{137}Cs	Dry solid	0.8-1.0	Cylindrical (100 mL)	69,159-108,932 s	Bq·kg^{-1} d.w.
RO Brine	Primordial and daughters, ^{7}Be and ^{137}Cs	Dry solid	1.0	Marinelli (400 mL)	70,000-158,000 s	Bq·L^{-1}
Sludge	^{131}I	Wet solid	1.0-1.5	Cylindrical (100 mL)	18,667-64,244 s	Bq·kg^{-1} d.w.
Sand	^{131}I	Wet solid	1.5-2.1	Cylindrical (100 mL)	21,850-74,078 s	Bq·kg^{-1} d.w.
GAC	^{131}I	Wet solid	1.2-1.6	Cylindrical (100 mL)	20,089-330,116 s	Bq·kg^{-1} d.w.
^{131}I Partitioning method validation (Chapter 4)						
Reference dissolution	^{131}I	Liquid	1.0	Cylindrical (100 mL)	2,485-58,662 s	Bq
Precipitates AEI BEI	^{131}I	Wet solid	1.0	Cylindrical (100 mL) Marinelli (400 mL)	2,822-60,423 s	Bq
Supernatant RI	^{131}I	Liquid	1.0	Marinelli (400 mL)	10,393-46,362 s	Bq
^{131}I Partitioning method application (Chapter 5)						
Precipitates AEI BEI	^{131}I	Wet solid	1.0	Cylindrical (100 mL) Marinelli (400 mL)	4,691-234,726 s	Bq
Supernatant RI	^{131}I	Liquid	1.0	Marinelli (400 mL)	17,351-112,770 s	Bq

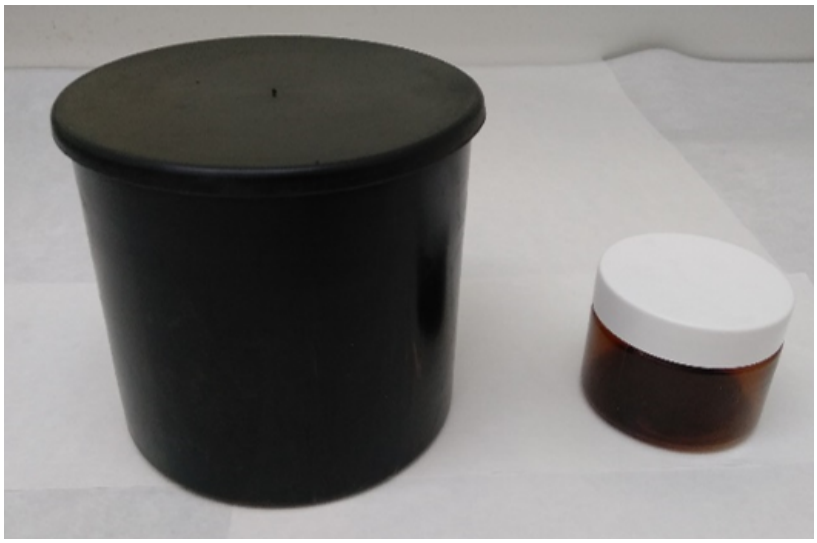

Figure 2.2: Marinelli (left) and cylindrical (right) geometries.

2.3.2.1 WWTPs and RWTP samples

Medically-derived radionuclides concentrations in liquid and sewage sludge and ^{7}Be in dehydrated sludge samples from the WWTPs have been determined. In 14 % of the samples from WWTPs two spectra were obtained for the same sample. Firstly, one short and immediate measurement for the relative short-lived ^{99m}Tc in order to maintain a measurable activity (7,200-89,000 s). Secondly, a longer measurement focused on the rest of radionuclides studied (14,000-235,000 s). Depending on the treatment step of the plant the sewage sludge is more concentrated showing different properties significant for the sample preparation for the measurement.

Liquid samples: The samples were homogenized by shacking in the sampling container and a 400 mL aliquot measured in a graduated cylinder was transferred into the Marinelli beaker for the gamma analysis and sealed with adhesive tape. In order to prevent settling of total suspended solids and maintain the sample homogeneity during counting in the general recirculation and activate sludge reactor samples from WWTP (Chapter 5) a mass between 13-32 g·L^{-1} of dust of paper paste Ceys© was added and mixed. The radionuclides activity concentrations and MDA were reported as Bq·L^{-1}.

Primary and activated sludge: Behave as a fluid and were homogenized by shacking and a 400 mL aliquot measured in a graduated cylinder poured into Marinelli geometry and the containt weighted. The specific activity and minimum detectable activity of the studied medically-derived radionuclides were reported following the eq. 2.3 in dry weight.

Dehydrated sludge: No solids settling occurred during the measurement due to the homogeneity of the sample and the activity was determined in wet weight and after corrected and expressed in dry weight (eq. 2.3).

2.3.2.2 ^{131}I partitioning method

After applying the radiochemical procedures (Chapter 4) two precipitates; Aluminium chlorohydrate extractable iodine (AEI) and bentonite extractable iodine (BEI) and a final supernatant as residual iodine (RI) were obtained. The total amount of Bq was determined in each fraction and the percentage present in each partitioning fraction was determined by following Chapter 4 equations (*4.3.3 Experiment description and recovery determinations*).

Precipitates: Depending on the final precipitated volume 100 mL polyethylene or 400 mL Marinelli geometries were filled with the wet precipitate and distilled water until the container was fully filled. In order to avoid settling at the geometry bottom during the gamma-acquisition dust of wallpaper paste Ceys© was added (17-40 $g{\cdot}L^{-1}$), mixed until became an homogenized paste where the precipitate is homogenically suspended.

Supernatant: The liquid was homogenized by shacking and poured into a 400 mL Marinelli geometry and sealed with adhesive tape. The proportion of the liquid measured in relation with the total amount obtained in this step was determined by weight.

2.3.2.3 DWTP materials

Three different protocols were fixed to analyse the DWTP samples depending on the radionuclides determined and the material studied.

^{137}Cs, ^{7}Be, primordial and daughters radionuclides in solid samples: were measured after being homogenized and dried in an oven at 105 °C for 48 hours until constant weight. A graduated cylinder measured the total amount of sample poured into the cylindrical geometries (45 mL or 100 mL). The sample weight was determined by the difference between the geometry full and empty. The geometries were wrapped with polytetrafluoroethylene thread seal tape (0.2 mm) to avoid ^{222}Rn and ^{220}Rn leak for at least 21 days and reach the secular equilibrium between the ^{226}Ra daughters and between the ^{228}Th daughters, respectively.

RO brine samples: 400 mL were measured in a graduated cylinder poured into Marinelli beaker and sealed for at least 21 days to allow the secular equilibrium between ^{226}Ra and ^{214}Pb daughter for ^{226}Ra determination (Table 2.1).

^{131}I in solid samples: were measured in wet weight in a 45 or 100mL polyethylene jar after a short period of time between 1-10 days after sampling. With a graduated cylinder the total amount of sample was measured and poured intor the cylindrical geometries (45 mL or 100 mL) and the sample weight controlled. The activities were deterimined followiwng the eq. 2.1 (reported as Bq·kg^{-1} d.w.).

2.3.3 Gamma-ray spectroscopy techniques

2.3.3.1 Radionuclides physical decay data

During the disintegration, some radionuclides give rise to short-lived gamma-emitters and the unique decay properties of each radionuclide (Fig. 2.3) allows identifying it through energy (keV) in a gamma-spectrum. Furthermore, other properties well known as the half-life and the gamma-ray emission yields (proportion of emission in relation with the total radionuclide disintegrations) must be taken into account for determine quantitatively the radionuclide concentration. The decay data from the National Laboratory Henry Bequerel (LNHB 2016) has been considered for the activity determinations (Table 2.2).

In contrast with gamma monoenergetic radionuclides as ^{210}Pb or ^{7}Be, other radionuclides like ^{131}I (Fig. 2.3), ^{67}Ga or ^{212}Pb have more than one decay gamma-ray energy line (LNHB 2016). The most favourable energy line for the activity determination (absence or capability to correct interferences from other radionuclides present during counting and higher detection efficiency) was chosen (Table 2.2). Most of the radionuclides studied were determined by direct detection of the gamma-ray emitted due to its radioactive decay. Nevertheless, the activities of some radionuclides from the ^{238}U and ^{232}Th decay chains (Fig 2.4) were determined through the daughter indicated within brackets (Table 2.2).

2.3.3.2 HPGe coaxial detectors and geometries placement

HPGe coaxial detectors were used. The semi-conductor properties of germanium, working in vacuum and at 77 K with liquid N_2 refrigeration, reduce the number of electrons in the germanium conduction band making easier the detection of the interaction of gamma-rays due to an extra excitation of electrons (Gilmore 2008). Furthermore, exists a direct relationship of the electron-hole pairs produced in the germanium crystal with the gamma-ray energy absorbed by the detector (Gilmore 2008). A detailed description of its operation and electronics can be found at Knoll (2010) and Gilmore (2008). In Table 2.3 the specific characteristics of HPGe detectors and activity determination information are detailed.

In Fig. 2.5 a picture of one of the HPGe from LARA is shown. Two types of containers were used in the present work with the help of a specific fixation piece for each geometry and detector.

Cylindrical (45 and 100 mL): The polyethylene geometry is placed on top of the germanium crystal to perform the gamma-spectra obtention.

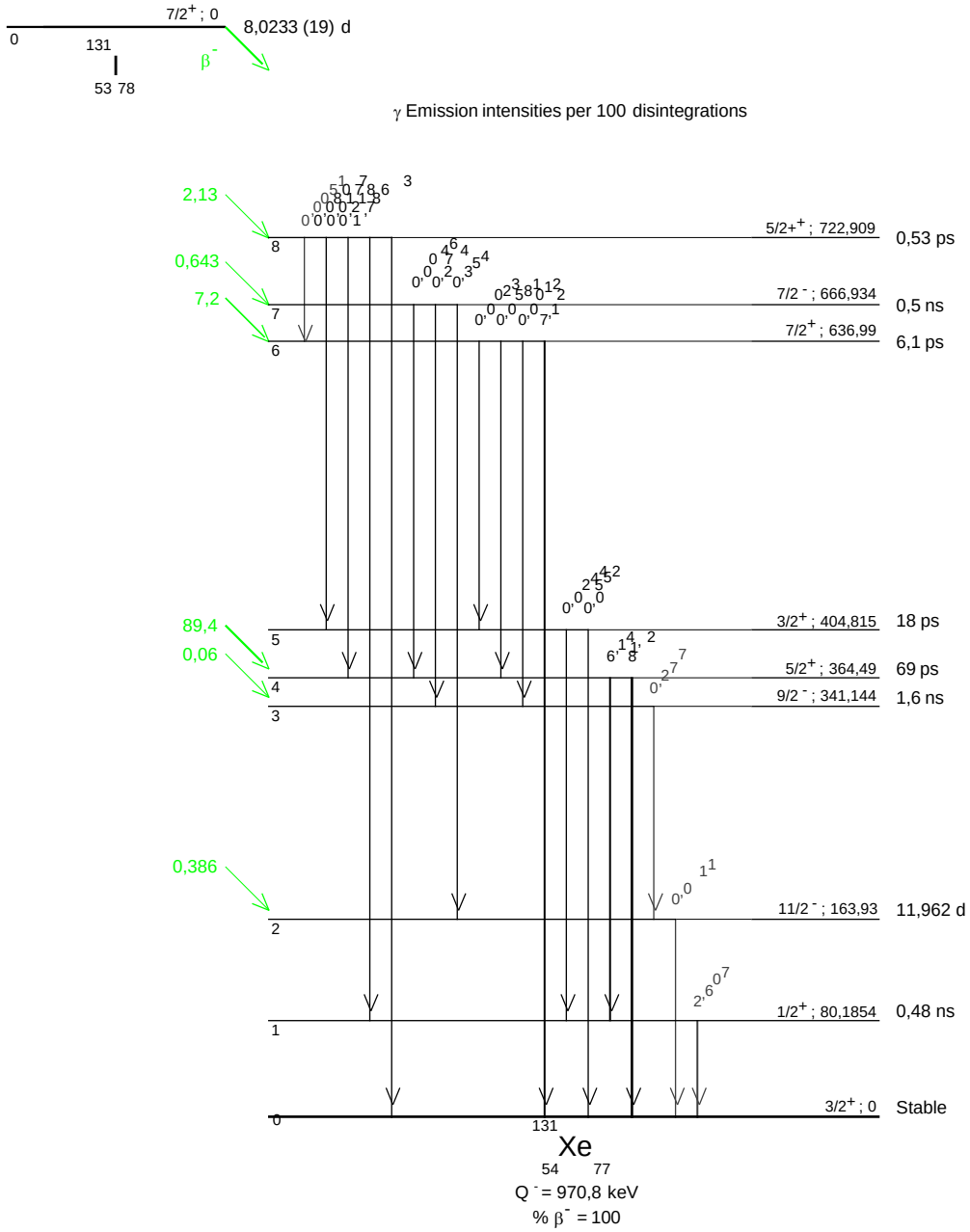

Figure 2.3: Radioactive decay scheme of the ^{131}I beta minus disintegration including subsequently gamma-ray emissions (LNHB 2016).

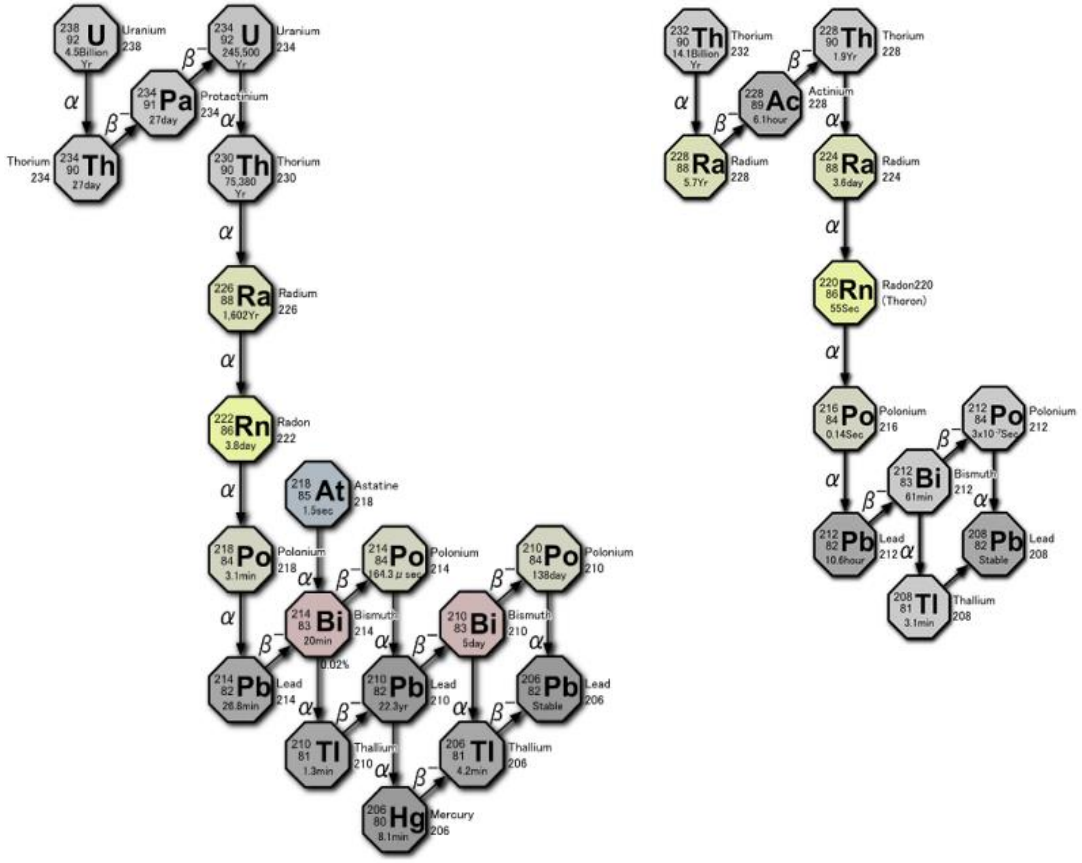

Figure 2.4: Radioactive decay chains of ^{238}U and ^{232}Th.

Marinelli (400 mL): This type of polyethylene geometry reduces the sample self-absorption effect expected in a cylindrical geometry of the same volume placed on the detector (De Felice et al., 2000). The cylindrical hole at the bottom allows to place the geometry at the top at the same time than surrounding the detector.

2.3.3.3 HPGe detector calibration

In activity determination methodology with HPGe the voltage of each pulse is obtained after the charge collection in the detector. After a pre-amplification process the pulses are sorted by the multichannel analyser as counts in different intervals (channels) depending on the pulse height (Gilmore 2008). The different channels of the HPGe detectors are calibrated at energy and efficiency experimentally by using known sources of gamma-emitter radionuclides. Regarding energy calibration, a multinuclide reference solution is measured and a relationship between the number of spectra channel and the gamma energy line defined.

Table 2.2: Radioactive decay data applied in the radionuclides determination.

Radionuclides	$t_{1/2}$ [b]	**Energy (keV)** [b]	**Yield (%)** [b]
Medically-derived			
^{51}Cr	27.704 (4) d	320.083 (4)	9.89 (2)
^{54}Mn	312.19 (3) d	834.848 (3)	99.9752 (5)
^{67}Ga	3.2613 (5) d	300.232 (2)	16.6 (4)
^{99}Mo	2.7479 (6) d	739.50 (2)	12.12 (2)
^{99m}Tc	6.007 (1) h	140.511 (1)	88.5 (2)
^{111}In	2.8049 (4) d	245.35 (4)	94.12 (6)
^{123}I	13.223 (4) h	158.97 (5)	83.3 (2)
^{131}I	8.023 (2) d	364.489 (5)	81.2 (5)
^{153}Sm	1.92855 (5) d	103.18012 (2)	29.2 (2)
^{177}Lu	6.647 (4) d	208.3662 (4)	10.38 (7)
^{186}Re	3.719 (2) d	137.157 (8)	9.42 (6)
^{198}Au	2.6843 (3) d	411.8021 (2)	95.62 (6)
^{201}Tl	3.042 (2) d	135.31 (4)	2.604 (2)
Primordial and daughters			
^{238}U (^{234}Th)[a]	4468 (5) My	63.30 (2)	3.75 (8)
^{226}Ra (^{214}Pb)[a]	1600 (7) y	351.963 (2)	35.60 (7)
^{210}Pb	22.2 (1) y	46.539 (1)	4.25 (4)
^{228}Ra (^{228}Ac)[a]	5.75 (4) y	911.196 (6)	26.2 (8)
^{228}Th (^{212}Pb)[a]	1.9126 (9) y	238.632 (2)	43.6 (5)
^{40}K	1250.4 (3) My	1460.822 (6)	10.55(1)
Cosmogenic			
^{7}Be	53.22 (6) d	447.603 (2)	10.44 (4)
Fall-out			
^{137}Cs	30.05 (8) y	661.657 (3)	84.0 (2)

a) Half-life data correspond to the parent while energy line and yield to the daughter(#)
b) Uncertainties are shown as k=1

Experimental efficiency calibration at different densities (0.66; 1.02; 1.26; 1.60 g·cm^{-3}) for the 100 mL, at 0.56 g·cm^{-3} in the 45 mL geometry and at 1.02 g·cm^{-3} density for the 400 mL geometry have been carried out in the three HPGe detectors. In the case of 1.02 g·cm^{-3} calibration density a known amount of multinuclide reference solution containing ^{51}Cr ,^{57}Co, ^{60}Co, ^{85}Sr, ^{88}Y, ^{109}Cd, ^{113}Sn, ^{123m}Te, ^{137}Cs and ^{210}Pb was added into 1.02 g·cm^{-3} distilled water with salts including stable elements from the radionuclides added. For the rest of 100 mL geometry densities and 0.56 g·cm^{-3} density in the 45 mL geometry a known amount of multinuclide reference dissolution (^{57}Co, ^{60}Co, ^{88}Y, ^{109}Cd, ^{113}Sn, ^{137}Cs, ^{139}Ce and ^{241}Am or ^{57}Co, ^{60}Co, ^{85}Sr, ^{88}Y, ^{109}Cd, ^{113}Sn, ^{137}Cs, ^{139}Ce, ^{203}Hg, ^{210}Pb and ^{241}Am) was dissolved in water with salts including the stable elements from the radionuclides present. The solution was added to solid materials with different densities (granular activated carbon, soil and ash), dried, poured into the cylindrical geometry and measured for performing the calibration.

Table 2.3: HPGe detectors and activity determinations details.

	Canberra-GR2020	**Canberra-GX3020**	**Canberra-GX4020**
HPGe characteristics			
Description	Reverse coaxial, n-type	Coaxial, very thin contact window, Be cryostat window, p-type	Coaxial, very thin contact window, C epoxi cryostat window, p-type
Relative efficiency[a b]	23.2 %	33.0 %	40.9 %
Ge crystal volume (cm^3)	98	137	171
FWHM[a]	1.73	1.77	1.86
Peak to Compton ratio[a]	57:01	65:01	61:01
Primary shielding	Lead (10 cm)	Iron (14.4 cm)	Lead (10.5 cm)
Secondary shielding	Copper (2 mm)	-	Copper(2 mm)
Activity determinations			
Software	Genie 2000© 2.1v	Genie2000© 3.1v	Genie2000© 2.1v
Number of channels	4096	4096	4096
Energy range	1-1761 keV	1-1880 keV	1-1768 keV

a) ^{60}Co at 1332.5 keV
b) To 3 inch NaI(Tl) crystal

After being poured into Marinelli (400 mL) or cylindrical geometry (45 or 100 mL) the solution is measured in the three HPGe detectors. The resulting efficiency points along the energy spectra are taken to generate a dual efficiency curve (Fig. 2.6; pages 288-299; Genie 2000©, Customization tools manual) establishing the 122 keV energy line from ^{57}Co as cross-over (Fig 2.6).

2.3.3.4 Activity determination

After the sample measurement some peaks found in the spectra (Fig. 2.7) can correspond to the radionuclides of interest. The Genie 2000© software was employed for spectral analysis, and physical decay corrections of the activity during sampling (only pooled samples), between sampling and analysis and during counting. The initial peak area is corrected taking into account background contribution if any. The determination of the radionuclides activity in Bq found in the measured sample is performed by applying the eq. 2.4:

$$A(Bq) = \frac{S}{\varepsilon \cdot Y \cdot t \cdot Kc \cdot Kw \cdot Ks} \tag{2.4}$$

Figure 2.5: HPGe detector model GX4020 with the shielding door open ready to introduce a sample for a gamma-spectra obtention.

where S correspond to the net peak area of counts in the spectra, ε the efficiency experimentally determined for the geometry used, sample density and energy, Y the decay yield of the radionuclide energy chosen for the determination, t the effective counting time in seconds. Moreover, Kc and Kw factors from the eq. 2.4 are included to correct the radionuclide decay during the measurement and between sampling and measurement respectively. The factor Ks was considered 1 in the case that a punctual sample was analysed while for a pooled sampled is between 1 and 0. Equations of Kc, Kw and Ks factors are defined in the technical document from Genie 2000© and are sensible in the case of relative short-lived radionuclides (pages 368-370; Genie 2000©, Customization tools manual). Some traces of primordial and daughters radionuclides are present in the HPGe materials giving rise to a background detection, nevertheless, its contribution to the gamma-spectra is subtracted from the total counts of the peak in order to obtain the net peak area (S) from the sample measured.

In spite of direct measurement of the radionuclide studied, activities of some primordial and its daughters radionuclides were determined through a daughter from the radioactive decay chain (Fig 2.4) (Gilmore 2008). After the sample preparation for the measurement they have the same activity because secular equilibrium is achieved (eq. 2.5). The equilibrium takes place some days after if the half-life of the parent is significantly longer than the daughter ($t_{1/2}$parent>>>$t_{1/2}$daughter).

$$A_{daughter} = A_{parent} = A_{(t=t0)parent} \cdot e^{-\lambda_{parent} \cdot t} \tag{2.5}$$

A total of 4 radionuclides were measured after this assumption. ^{238}U was determined through ^{234}Th, ^{226}Ra through ^{214}Pb, ^{228}Ra through ^{228}Ac and ^{228}Th through

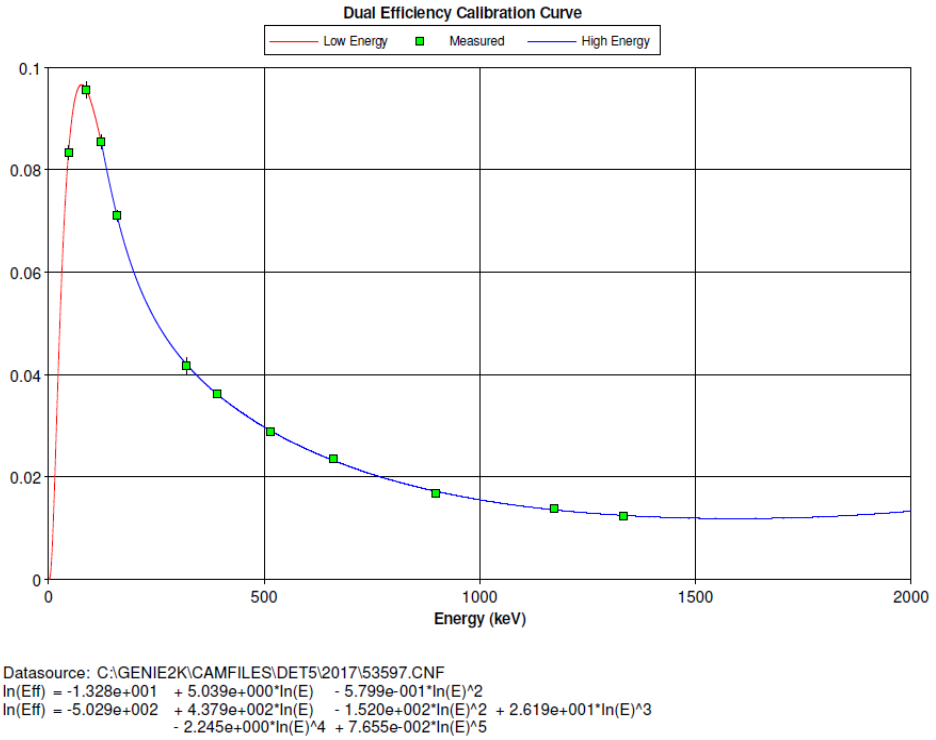

Figure 2.6: Report from Genie 2000© after the calibration procedure including the efficiency curve determined at the Canberra-GX4020 for a 100mL polyetilene geometry with 1.03 g·cm^{-3} denstity.

^{212}Pb assuming the half-life of the parent and the decay energy and yield from the daughter (Table 2.2).

Regarding ^{67}Ga quantifications, an interference of ^{212}Pb from natural origin due to its presence in the sample and background must be considered. Both radionuclides have a similar energy line in their gamma emissions with of 300.23 and 300.08 keV for ^{67}Ga and ^{212}Pb respectively (LNHB 2016). The S (eq. 2.4) value for the ^{67}Ga activity determination needs a correction following the eq. 2.6. determining the contribution of ^{212}Pb to the 300 keV ^{67}Ga peak through the registered activity in the 239 keV ^{212}Pb peak.

$$S\ ^{67}Ga_{300keV} = S^{*}\ ^{67}Ga_{300keV} - S\ ^{212}Pb_{239keV} * \frac{Y^{212}Pb_{300keV} \cdot \varepsilon^{212}Pb_{300keV}}{Y^{212}Pb_{239keV} \cdot \varepsilon^{212}Pb_{239keV}} \quad (2.6)$$

Moreover, the medically-derived radionuclide ^{99m}Tc ($t_{1/2}$=6.0 h) is the daughter of ^{99}Mo ($t_{1/2}$=2.7 d). The presence of ^{99}Mo in the sample can give rise to ^{99m}Tc

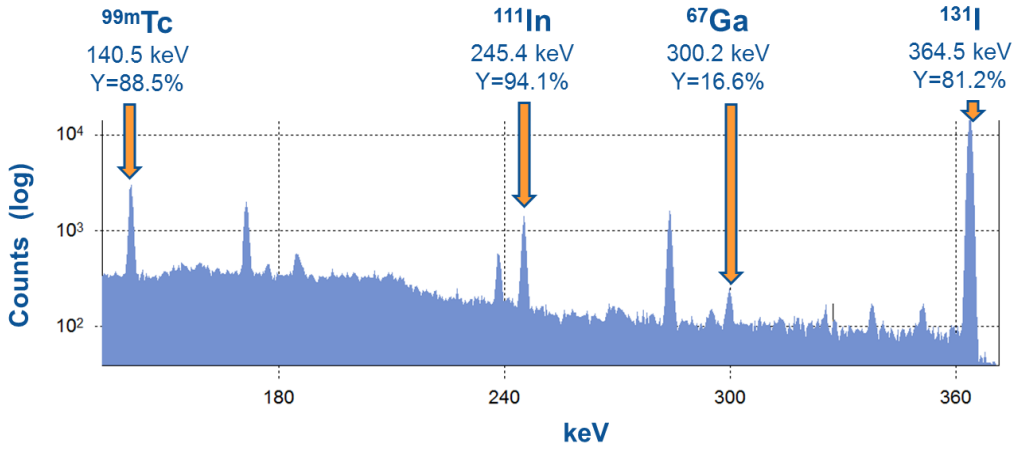

Figure 2.7: 120-380 keV gamma-spectra range from a WWTP sample measured in the HPGe. Peaks for some medically-derived radionuclides are pointed out.

affecting the determination at the sampling time. Nevertheless, ^{99}Mo presence has been controlled by the 739.50 keV energy and no peak has been quantified, ruling out the influence of ^{99}Mo in the ^{99m}Tc activity determinations.

2.3.3.5 Uncertainties reported

Uncertainties reported in the present work correspond to the combined uncertainty (u), where the net peak area quantification (S) and the efficiency (ε) are the significant sources of uncertainty considered in the radionuclide concentration determinations.

The uncertainties associated to each activity reported consider the contribution of the total amount of counts determination in the net peak area due to the adjustment of the peak to a normal distribution (σ_S). Furthermore, the determination of the calibration uncertainties (σ_{ε}) was also taken into account. In the eq. 2.7 the u determination is detailed an expressed in the present work with a coverage factor of k=2 ($U_{(k=2)}$). The combined expanded uncertainty determination by applying the main uncertainty sources is performed with the Genie 2000© software.

$$U_{(k=2)} = A \cdot \sqrt{\frac{\sigma_S}{S} + \frac{\sigma_\varepsilon}{\varepsilon}} \tag{2.7}$$

2.3.3.6 MDA

All the radionuclide determinations have an associated minimum detectable activity (MDA) which has been determined with the Genie 2000© software. The determination has been done following the eq. 2.8:

$$A(Bq) = \frac{Ld}{\varepsilon \cdot Y \cdot t \cdot Kc \cdot Kw \cdot Ks} \tag{2.8}$$

where all the paramaters included correspond to those defined in eq. 2.4 while the Ld is determined following the traditional Currie determination for gamma-spectroscopy techniques (Kirkpatrick et al., 2013) by Genie 2000© (pages 391-396; Genie 2000©, Customization tools manual).

Along the present study a total of 13 medically-derived radionuclides have been included in the gamma-spectra analysis of the wastewater treatment plant samples. The corresponding mean MDAs for samples from WWTPs and RWTP are detailed in the Table 2.4. However, the MDAs for primordial and daughters, ^{7}Be and ^{137}Cs from the DWTP samples analysis is detailed with the experimental results in case no concentration above the MDA was found.

Table 2.4: HPGe detectors and data from activity determinations.

Radionuclide	**Mean MDAs**[a]		
	Waters	**Primary and activated sludge**	**Dehydrated sludge**
	Bq·L^{-1}	**Bq·kg^{-1} d.w.**	**Bq·kg^{-1}d.w.**
^{51}Cr	2.0	95	28
^{54}Mn	0.3	12	3.1
^{67}Ga	1.5	72	19
^{99}Mo	2.8	120	35
^{99m}Tc	5.7	110	100
^{111}In	0.3	12	3.7
^{123}I	0.9	39	15
^{131}I	0.3	12	3.5
^{153}Sm	6.5	270	59
^{117}Lu	2.1	100	32
^{186}Re	2.2	130	31
^{198}Au	0.3	12	3.7
^{201}Tl	8.4	430	110

a) Currie MDA (Kirkpatrick et al., 2013)

2.3.3.7 Threshold

The threshold factor is applied in gamma-spectroscopy with the aim to fix criteria which allows to differentiate between the existence of a peak in the gamma-spectra

or the absence of it (Korun et al., 2019). In the present work the threshold value fixed in Genie 2000© software analysis (pages 238-240; Genie 2000©, Customization tools manual) was 2.5 for artificial and cosmogenic ^{7}Be and 3.0 for the primordial and daughters radionuclides studied. Some radionuclides from the ^{238}U and ^{232}Th series (Fig. 2.8) have presence in the detectors background and a more strict criteria was assumed in order to avoid false positive error (type I).

2.3.3.8 Quality control

With the aim to verify the calibration, sample pre-treatment and measurements procedures from the gamma-spectroscopy technique to quantify radionuclides reference materials has been measured (2012-2018) in the geometries used in the present work. Moreover on the HPGe detectors energy calibration and background are checked once per month by the technical staff from LARA.

$$z_{score} = \frac{Value_{LARA} - Value_{Intercomparison}}{Value_{Intercomparison}} \tag{2.9}$$

Regarding the 45 mL and 100 mL cylindrical geometries calibrations at different densities were applied for the measurement of 20 samples on open proficiency test exercises from international and national organisms (IAEA, EC and CSN). A total of 61 results (Fig 2.8) including radionuclides determined in the present work (^{7}Be ,^{40}K ,^{99}Mo ,^{131}I, ^{137}Cs,^{210}Pb ,^{226}Ra,^{228}Th ,^{228}Ra and ^{238}U) were reported. For most of the determinations have been qualified as "satisfactory" values (Fig 2.8) which means a z_{score}<2 (eq. 2.9). In contrast 2 were quantified <MDA and can not be evaluated.

In the case of Marinelli geometry (400 mL) a quality control was performed by measuring a reference material (1.00 g·cm^{-3}) from the IAEA-TEL-2017-03 worldwide open proficiency test exercise with ^{133}Ba and ^{60}Co. In this geometry both radionuclides sum-peak effect is minimized with a maximum of 10% of deviation (De Felice et al., 2000; Ababneh and Eyadeh 2015). All the results for all the detectors were qualified under the IAEA proficiency test criteria (eq. 2.9) as "accepted" with a mean deviation of 5% from the reference values and z_{score}<2.

Regarding the ^{238}U measurement through the daughter ^{234}Th a period of 120 days is necessary in order to achive the same activities by secular equilibrium (eq. 2.5). However, in the solid materials from the DWTP studied in the present work no significant differences were found between the ^{234}Th activities when the spectra acquisitions were performed after 1-10 days than the sampling date and those after 27-84 days (n=11). Thus, both radionuclides were almost near the secular equilib-

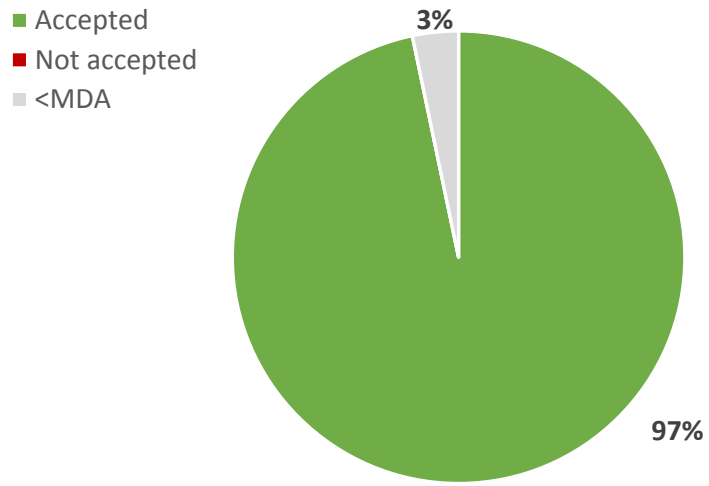

Figure 2.8: Quality control results for the cylindrical geometries.

rium at the sampling time and the ^{238}U determination trough ^{234}Th were correct.

As has been noted previously in some WWTP liquid samples glue was added with the aim to prevent TSS settling during the spectra acquisition. Nevertheless, TSS settling effect in primary inflow samples during counting was evaluated and both datasets resulted undistinguishable (1.48 ± 0.33 and 1.45 ± 0.17 for ^{131}I and 14.7 ± 2.2 and 17.0 ± 2.2 for ^{99m}Tc, respectively). Thus, glue was not added.

Quality control was also performed for WWTP samples after apply the ^{131}I partitioning method (Chapter 5). The radiochemical method gives rise to the three fractions (aluminium chlorohydrate extractable iodine, AEI; bentonite extractable iodine, BEI; residual iodine, RI). In some cases a previous measurement of the total ^{131}I concentration were carried out. If the sums of the concentrations in the three fractions (eq. 2.10) are compared with the total concentration undistinguishable results were found (Table 2.5).

$$AEI + BEI + RI = Total\ ^{131}I \tag{2.10}$$

Table 2.5: Data of the samples available with ^{131}I direct measurement concentration and sum of the three phases from the partitioning method.

	Direct measurement $\mathbf{Bq{\cdot}L^{-1}}$	**Eq. 2.10** $\mathbf{Bq{\cdot}L^{-1}}$
Sewage effluent A	2.50 ± 0.21	2.36 ± 0.15
Reclaimed water	0.77 ± 0.10	0.56 ± 0.11
General recirculation	1.51 ± 0.22	1.60 ± 0.14
Primary inflow	1.48 ± 0.33	1.24 ± 0.10

Furthermore, this quality control (Table 2.5) confirms no lack of ^{131}I by volatilization after the method implementation as well as than that sum of the results obtained with different geometries match with the total concentration experimental results.

2.4 Physicochemical parameters determination

Some physicochemical parameters in water, sewage sludge and solid materials were determined on the samples taken for the radioactive content determination. The analysis were carried out in the LAPF. Furthermore periodically along the different steps of the water treatment plant samples are taken as quality control of the treatment process and some of the data were used along the discussion of the experimental results from the present document. In Table 2.6 the parameters, a brief description of the standardized technique and references of the methodologies implemented in the LAPF are detailed.

The applied techniques for the analysis (Table 2.6) correspond to consolidate methodologies from standardization organisms as the International Organization of Standardization (ISO), the American Public Health Association (APHA), the American Water Works Association (AWA), the Water Environment Federation (WEF), American Society for Testing and Materials (ASTM) the *Asociación Española de Normalización* (UNE). The analysis were under the quality control requirements of the ISO 17025®, which specify the general requirements for the competence to perform calibrations and tests.

Table 2.6: Physicochemical parameters determined in samples from water treatment plants.

Physicochemical parameters	**Units**	**Description of the method**	**Reference**
Liquid samples from WWTPs			
Conductivity at 25°C	$\mu S \cdot cm^{-1}$	Electrometry	APHA AWA WEF (2005)
pH	-	Electrometry	APHA AWA WEF (2012)
Turbidity	NTU	Nephelometry	APHA AWA WEF (1998)
TSS: Total suspended solids	$mg \cdot L^{-1}$	Filtration and driying at 105°C	UNE (2006)
BOD5: Biological oxigen demand	$mg \cdot L^{-1}$	Manometer OXI TOP(c)	APHA AWA WEF (2005)
COD: Chemical oxigen demand	$mg \cdot L^{-1}$	Colour kit measurement LOVIBOND (c)	ISO (2002)
DOC: Dissolved organic carbon	$mg \cdot L^{-1}$	Filtered and measured by diference TC- TIC with ifrared detector	APHA AWA WEF (2005)
N-NH4: Ammonical Nitrogen	$mg \cdot L^{-1}$	Destilation recovered with H_3BO_3. The borate formed is valorated with H_2SO_4.	APHA AWA WEF (2005)
N-Kjedahl	$mg \cdot L^{-1}$	H_2SO_4 and K_2SO_4 digestion. The borate formed is valorated with H_2SO_4.	APHA AWA WEF (2012)
N-NO2: Nitrogen dioxide	$mg \cdot L^{-1}$	Ion-exchange cromathography	APHA AWA WEF (2017)
N-NO3: Nitrate	$mg \cdot L^{-1}$	Ion-exchange cromathography	APHA AWA WEF (2017)
TP: Total Phosphorus	$mg \cdot L^{-1}$	Segmented flow analysis and colorimetry	APHA AWA WEF (2005)
Cl-: Clorurs	$mg \cdot L^{-1}$	Mörh method: valoration with $AgNO_3$	APHA AWA WEF (2012)
Sewage sludge			
Dry weight (105°C)	%	Dried in an oven at 105°C until constant weight	APHA AWA WEF (2012)
VSS= Volatile suspened solids	%	Filtered and dried in an oven at 550°C until constant weight	APHA AWA WEF (2005)
Activated sludge reactor samples			
MLSS	$mg \cdot L^{-1}$	Filtration and driying at 105°C	UNE (2006)
V30	$ml \cdot L^{-1}$	Solids decanted in 30 minutes in a Imhoff cone	APHA AWA WEF (2012)
SVI: Sludge volume index	$ml \cdot g^{-1}$	(V30 / MLSS) 10^6	-
Granulated activated carbon			
Iodine index	mg $I_2 \cdot g^{-1}$ GAC	Absorbed I_2 at 0.01 $mol \cdot L^{-1}$ by GAC	ASTM (2014)

Chapter 3

Medically-derived radionuclides levels in seven heterogeneous urban WWTPs: The role of operating conditions and catchment area

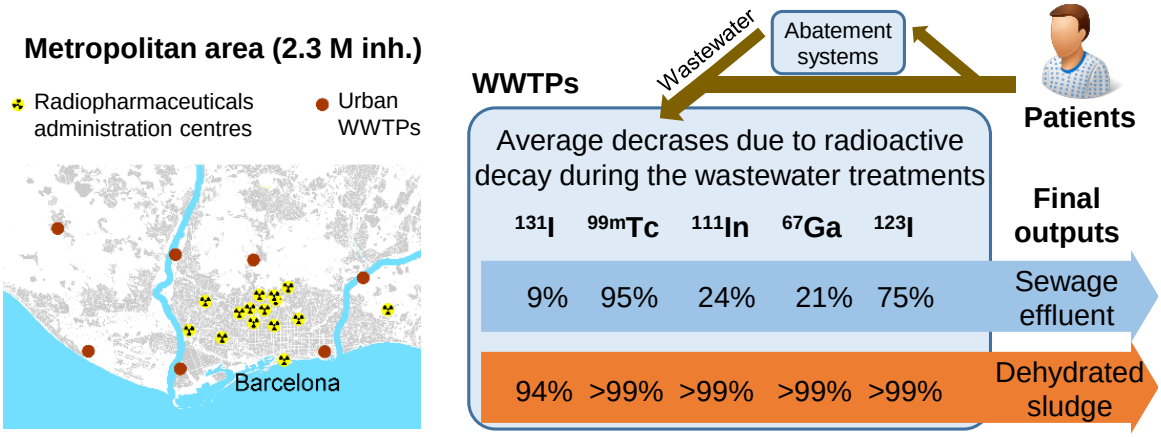

***Chapter published as:** Mulas, D., Camacho, A., Garbayo, A., Devesa, R., Duch, M.A., (2019). Medically-derived radionuclides levels in seven heterogeneous urban wastewater treatment plants: The role of operating conditions and catchment area. *Sci. Total Environ.*
doi:10.1016/J.Scitotenv.2019.01.349

3.1 Introduction: nuclear medicine radionuclides and levels in WWTPs

Many articles have been devoted to the analysis of the nuclear medicine (NM) radionuclides content of sewage effluent and its discharge into the environment (Carvalho et al., 2013; Fischer et al., 2009; Rose et al., 2013). However, very few articles provide an integral picture of the behaviour and fate of medically-derived radionuclides in a wastewater treatment plant (WWTP), since, in most cases, the presence of such isotopes is based on only one kind of samples: sewage sludge (Bastian et al., 2005) or sewage effluent (McGowan et al., 2014; Rose et al., 2012). In Europe the most recent and comprehensive studies have been published by Fischer et al.(2009) for a single German WWTP, and Cosenza et al. (2015) with results from medium-sized (20,000–153,000 $m^3 \cdot d^{-1}$) WWTPs located on the northwestern Sicilian coast. Very recently (Martínez et al., 2018) published a work on two medium-sized WWTPs (25,000–35,000 $m^3 \cdot d^{-1}$) in the south of Catalonia (Spain). At a worldwide level can be cited the studies of (Rose et al., 2012) in the USA and (Chang et al., 2011) in Korea for different sized plants (3,000–1,400,000 $m^3 \cdot d^{-1}$), however, they provide results mainly on sewage effluent. Among several conclusions, in these previous studies, it was pointed out that it is of the utmost importance to sampling the inflow, the effluent and sewage sludges of the WWTPs in order to determine their radioactivity content, and consequently, to know the behaviour of the medically-derived isotopes in the different stages of the treatment. This knowledge opens up the possibility to design and apply prognostic models to foresee effluent activity concentrations (Hormann and Fischer, 2018; Nakamura et al., 2005), and to carry out environmental impact studies (Carvalho et al., 2013; Fischer et al., 2009; Rose et al., 2013). Furthermore, the role of the WWTP operating conditions can contribute to the understanding of radioactivity concentration levels in waters and sewage sludges.

Specifically, there is no available published information on the influence of sewage sludge age (hours, days, or even weeks depending on the plant operating conditions). This parameter can greatly affect the activity concentration of the sewage sludge, since administered radiopharmaceuticals in NM procedures usually have relatively short half-lives (hours and days).

Furthermore NM services have been revealed as a source of diagnosis radionuclides in urban wastewater (Krawczyk et al., 2013; Martínez et al., 2018) and its presence in the catchment area may vary the final levels in the WWTP. Differences in the patient's management treated with ^{131}I and in the type of activated sludge treatment applied makes difficult to predict NM radionuclide concentrations in sewage sludge and effluent in a specific country and for a specific WWTP, which is essential for the evaluation of the radiological implications of patients' excreta

(Petrucci and Traino, 2015). Furthermore, rain events are studied since have been identified as an influence factor that can induce high variability of the radionuclide levels found in a WWTP (Fischer et al., 2009). Finally, it is worth mentioning that most of the published studies have been focused on ^{131}I (Fenner and Martin, 1997; McGowan et al., 2014; Rose et al., 2012), since it has a relatively mid half-life (8 days) and was easily found in the different treatment stages. However, very few studies reported data for other radionuclides (Dalmasso et al., 1997; Fischer et al., 2009).

3.2 Objective

The aim of this section is to characterize the 7 urban WWTPs located in the Barcelona metropolitan area (BMA)(Fig 3.1) in order to study the role of the operating conditions and their influence on activity concentrations of medically-derived radionuclides in sewage effluent and sludges from different treatment stages. The selected network allows to study the influence of:

i) Sewage sludge age

ii) Wastewater flow treated per day

iii) Different activated sludge treatments

iv) The presence of anaerobic sewage sludge digestion for biogas production

This study provides results for 5 out of 7 most used NM radionuclides in Europe (^{67}Ga, ^{99m}Tc, ^{111}In, ^{123}I and ^{131}I; EC 2014) in inflow wastewater, sewage effluent and sewage sludges, with a special emphasis for the largest studied plant (WWTP-1) which operate with significantly lower sewage sludge ages. Therefore, this work contributes to the current knowledge of accumulation tendencies of medically-derived radionuclides in the different types of sludges studied.

3.3 Details of the BMA wastewater depuration network

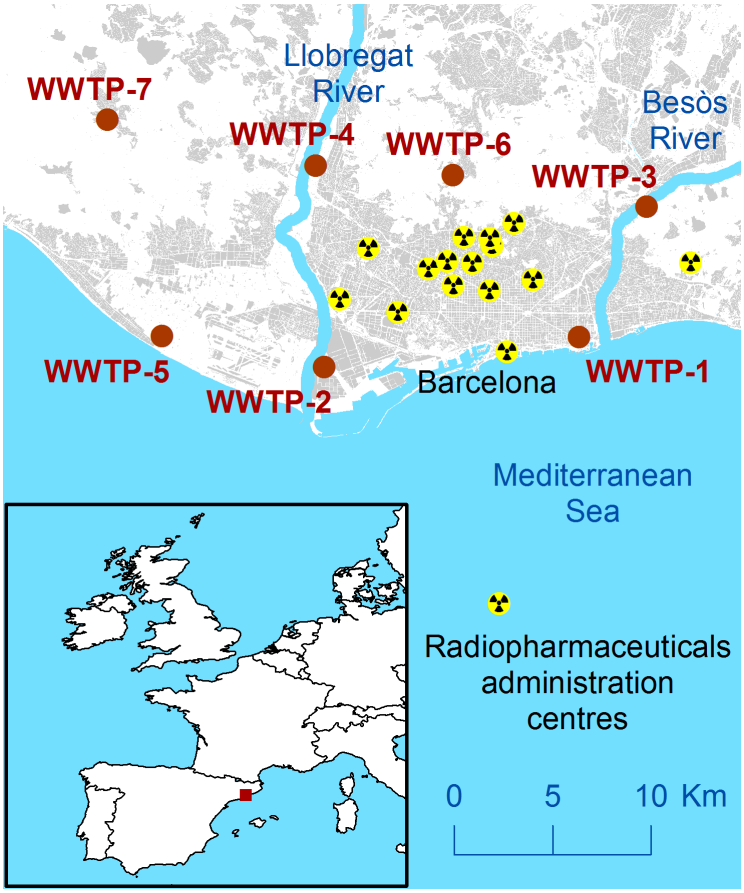

Figure 3.1: BMA map with the locations of the 7 WWTPs included in the present study and the distribution of the radiopharmaceuticals administration centres.

The seven WWTPs locations are detailed in Fig. 3.1. The WWTPs can be classified by the total amount of urban wastewater treated ($m^3 \cdot d^{-1}$). Three main groups are defined in the present study:

i) Very large-sized (>200,000 $m^3 \cdot d^{-1}$; WWTP-1 and 2)

ii) Medium-sized (40,000–80,000 $m^3 \cdot d^{-1}$; WWTP-3, 4 and 5)

iii) Very small-sized plants (<1,000 $m^3 \cdot d^{-1}$; WWTP-6 and 7)

The urban wastewater from around 2 million inhabitants is treated in the two large-sized plants (WWTP-1 and 2) while the rest of the wastewater flow is treated in the other five facilities. Very large-sized and medium WWTPs have a primary treatment which removes most of the total suspended solids by settling giving rise

to the primary sludge (Fig. 3.2). All the plants have activated sludge treatment lines for nutrient removal carried out by microorganisms suspended in the reactor which mainly interact with the chemical compounds dissolved in the treated inflow (Fig. 3.2). Three different types of activated sludge reactors described in de la Torre et al. (2015) can be found in the BMA urban wastewater depuration network (Fig. 3.2):

i) Conventional activated sludge system (CAS)

ii) Membrane bioreactor (MBR)

iii) Integrated fixed-film activated sludge system (IFAS)

In the CAS and MBR the activated sludge is suspended in the reactor while in the IFAS reactors activated sludge suspended and attached to a carrier is combined. Particle removal takes place after activated sludge treatment in the CAS and IFAS systems where the suspended solids are settled in a tank, while in the case of MBR the suspended solids are ultrafiltered (<0.04 μm).

The sludge generated in primary step and in the activated sludge reactor is thickened or centrifuged and mixed before a dehydration process in order to obtain the final solid outcome. Not all the plants have facilities for the final sewage sludge step. The medium-sized WWTP-3 and small-sized WWTP-6 and 7 send the thickened sludge to be dehydrated at other plants (Fig. 3.2). In the case of WWTP-2, WWTP-4 and WWTP-5 anaerobic digestion between thickening and dehydration is carried out to generate biogas for energy recovery, thus increasing significantly sludge hydraulic retention time inside the digesters to several weeks (Fig. 3.2). However, in WWTP-1, which is an underground facility integrated into the urban landscape and handles huge wastewater volumes (Fig. 3.2), two significant operational differences should be emphasised. Firstly, in the activated sludge reactor the operational conditions lead to a significantly faster renewal of the suspended activated sludge than in the other WWTPs. Secondly, dehydrated sludge digestion does not take place, which significantly accelerates the dehydrated sludge outcome. A mix of effluents and particles generated in the sewage sludge line, corresponding to a mean percentage in each WWTP between 2 % and 9 % of the total treated flow per day, are discharged into the primary treatment in both the very large and medium-sized WWTPs or in the activated sludge treatment in small-sized plants. The BMA sewerage system has combined sewers where storm water enters the same sewerage network as wastewater.

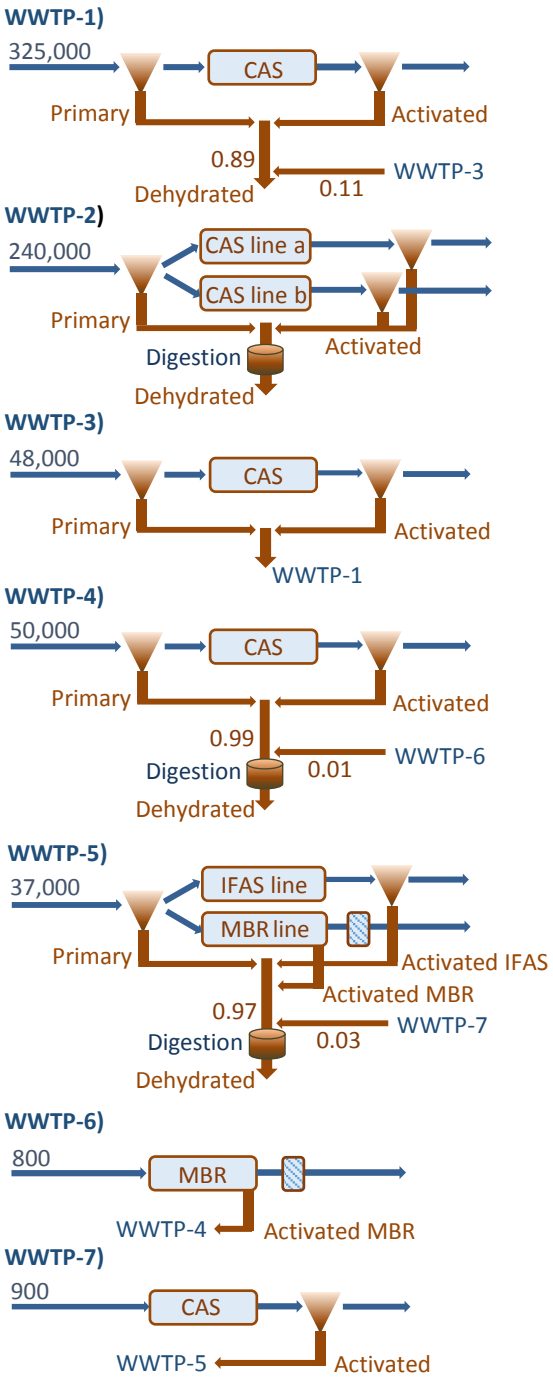

Figure 3.2: Basic schematics of the 7 WWTPs studied. The mean inflow wastewater treated is detailed above the inflow wastewater arrow ($m^3 \cdot d^{-1}$). The different primary, activated and dehydrated sludges if any are indicated for each plant and the type of activated sludge treatment are detailed.

3.4 Sampling and water samples properties

A total of 17 campaigns were carried out during the period 2014–17 (Appendix D.1; Tables A and B) in the WWTPs and 10 inflow wastewater, 12 sewage effluent, 17 primary sludge, 23 activated sludge and 14 dehydrated sludge samples were collected (Table 3.1).

Table 3.1: Total number and type of samples taken in the studied WWTPs

	WWTP-1	WWTP-2	WWTP-3	WWTP-4	WWTP-5	WWTP-6	WWTP-7
Waters							
Inflow wastewater	4	1	1	1	1	1	1
Sewage effluent	4	2[a]	1	1	2[a]	1	1
Sludges							
Primary	9	2	2	2	2	NA	NA
Activated	9	2	2	2	4	2	2
Dehydrated	8	2	NA	2	2	NA	NA

a) WWTP with two sewage effluent lines
NA: Not available (this type of sludge was not produced in the studied WWTP)

Firstly, one simultaneous first sampling of waters and sludges was performed in each plant. Secondly, one extra sampling of each type of sludge was carried out in all the studied WWTPs. Pooled samples (5 L taken along 24 h) were taken in the inflow water at the same time as the water effluent using ISCO® 3700 samplers, however, they should be considered independent samples not directly comparable as a single wastewater pulse. Results of the physicochemical properties of the water samples taken are detailed in Table 3.2. Spot sludge samples (primary, activated and dehydrated, depending on existence at each facility; Fig. 3.2 and Table 3.1) using 2 L polyethylene containers were taken just before water sampling had finished. Sampling days corresponded to weekdays, from Tuesdays to Wednesdays in the case of the 24-h pooled water samples and on Wednesday in the case of sludge spot samples. Nevertheless, the first complete sampling of waters and sludge in the WWTP-7 was carried out from Monday to Tuesday and the second extra sampling of MBR activated sludge in WWTP-5 on Thursday. The specific sampling points in each plant were after the grit removal for the inflow wastewater and the final effluent released into the environment for the sewage effluent. In the case of sludges the thickening tanks sludge or centrifuges output for the primary and activated and the dehydrated sludge obtained in the centrifuge facilities after the primary and activated sludges mixing and the anaerobic digestion (in 3 out of 4 plants) were the sampling points.

Sampling at WWTP-1 was expanded with three more complete simultaneous characterizations of inflow wastewater, sewage effluent and sludges in different months

as well as daily consecutive samplings of all sludges (primary, activated and dehydrated) for five days from Monday to Friday.

Table 3.2: Physicochemical properties of the inflow wastewater and sewage effluent samples.

	Conductivity at 25 °C μS·cm^{-1}	pH	Turbidity NTU	COD mg·L^{-1}	BOD_5 mg·L^{-1}	Total suspended solids mg·L^{-1}	N-Ammoniacal mg·L^{-1}	N-Kjeldahl mg·L^{-1}	Total Phosporus mg·L^{-1}
Inflow wastewater									
WWTP-1 (n=4)	2329 - 3527	7.5 - 7.6	130 - 270	411 - 680	490 - 276	210 - 420	25 - 56	41 - 76	2 - 5.1
WWTP-2	3238	7.4	390	945	-	500	48	69	13
WWTP-3	1652	7.6	170	732	600	280	45	64	8
WWTP-4	2351	7.8	110	429	220	140	35	46	4
WWTP-5	3061	7.5	440	1850	1000	960	53	91	18
WWTP-6	1664	7.5	160	532	400	220	37	48	8
WWTP-7	2451	7.9	110	420	280	140	48	59	6
Sewage effluent									
WWTP-1 (n=4)	1885 - 2950	7.5 - 7.7	3.8 - 8.3	55 - 77	-	12 - 21	25.1 - 53.5	27.2 - 57.2	2 - 5.1
WWTP-2a	2185	8	2.7	35	-	5.2	4.4	5.1	4.8
WWTP-2b	2440	7.8	8.2	60	-	23	30.7	30.7	4.9
WWTP-3	1652	7.5	9.5	54	6	15	45.1	47.8	<1
WWTP-4	1785	7.5	3	-	35	4	1.6	2.7	<1
WWTP-5 IFAS	2673	7.9	18	92	29	27	59.6	63.9	6.1
WWTP-5 MBR	2351	7.8	0.94	33	<5	<2	7.4	9.3	1.1
WWTP-6	1320	7.8	0.56	<30	<5	<2	<1	<2	3.6
WWTP-7	1675	7.5	9.1	34	12	20	6.8	8.8	<1

3.5 Results and discussion

In Fig. 3.3 the data for NM radionuclides in waters are presented. The results regarding activity content in primary and dehydrated sludges are presented in Fig. 3.4 and results on activated sludge are shown in Fig. 3.6. In Figs. 3.4 and 3.6 the sludges samples from the first sampling are above and the extra sampling is located below. WWTP-1 sludge results are presented in Fig. 3.5 because temporal studies were made. Based on this data a discussion regarding the influence of different features of the study can be made.

Moreover in the *Appendix D.1* all data of the present chapter represented in figures can be found in Tables A and B as raw data. All the NM radionuclides data from the present section has been obtained under the procedures detailed in *2. Materials and methods* chapter.

3.5.1 Medically-derived radionuclide levels and influence of HRT and sewage sludge age

In this section the activities of the NM radionuclides found in the studied WWTPs are discussed by type of sample (waters, primary, activated and dehydrated sludge) and subsequently taking into account the operational characteristics of the WWTPs.

3.5.1.1 Inflow wastewater and sewage effluent

The presence of ^{131}I and ^{99m}Tc from NM procedures was detected in 63 % and 41 % of the samples analysed (Fig. 3.3), respectively. The activity concentrations showed an important diversity of results both in inflow and effluent waters with values ranging from <0.2–4.4 Bq·L^{-1} for ^{131}I and between <5–50 Bq·L^{-1} for ^{99m}Tc.

^{131}I was detected in the medium-sized WWTP-3 and WWTP-4 with values one degree of magnitude below those found in the very large-sized WWTP-1 and WWTP-2 plants. The maximum detected value corresponded to WWTP-1 (4.43 ± 0.29 Bq·L^{-1}). The presence of ^{131}I in the effluent is in agreement with its incomplete removal, a value between 1 % and 75 %, in wastewater treatment plants reported by previous studies (Ham al., 2003; Hormann and Fischer, 2017; Punt et al., 2007; Rose et al., 2012). This is in contrast to the drastic reduction due to the treatment of other parameters such as total suspended particles, N-Ammoniacal, COD or BOD_5 (Table 3.2) which reach mean removals of around 90–95 % in the studied plants (ACA, 2018). In fact, more specific techniques, different than particle settling and activated sludge, are necessary to remove iodine effectively (Lee et al., 2016). In addition, higher activities of ^{131}I in the sewage effluents than in the inflow wastewater were observed in samples from WWTP-2 and in one case of WWTP-1 for sampling

done the same day. This phenomenon may be explained by high variabilities in the inflow wastewater found in previous studies with factors within 10:1 to 5:1 (Fischer et al., 2009; Punt et al., 2007) where a higher activity in the previous days could give rise to a one-off higher concentration in the WWTP sewage effluent.

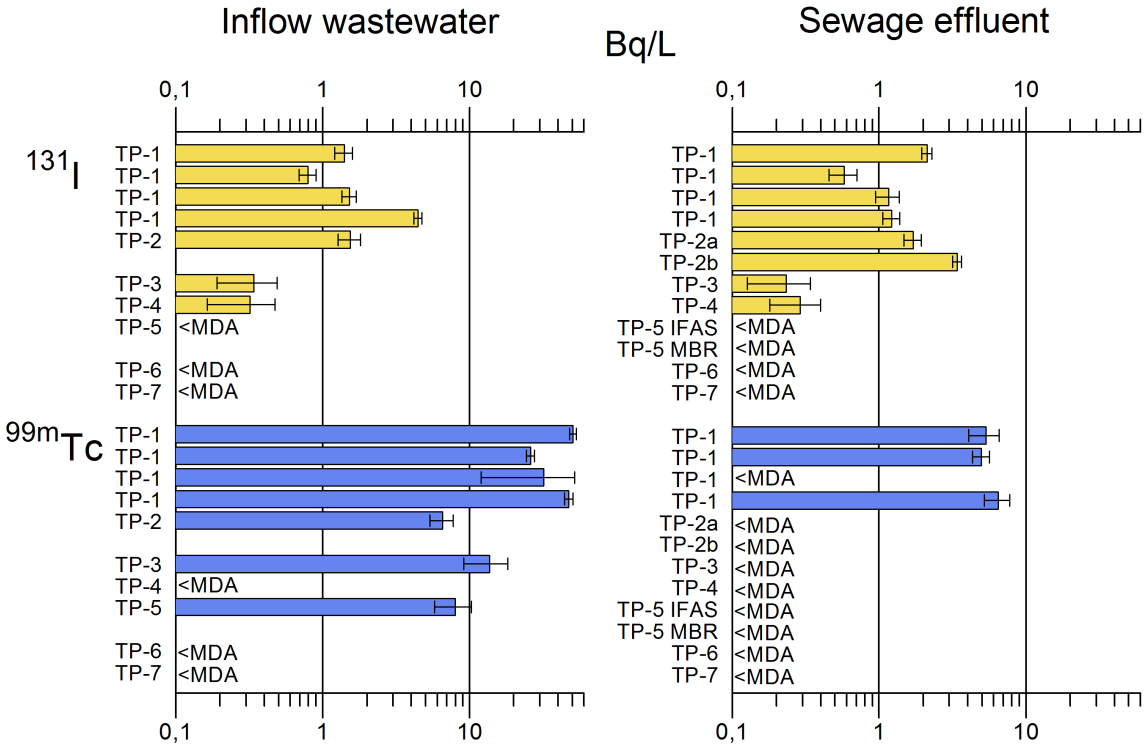

Figure 3.3: Specific activities of ^{131}I and ^{99m}Tc (Bq·L^{-1}) found in the influent wastewater and the sewage effluent waters in the 7 studied plants.

The presence of ^{99m}Tc was determined in inflow wastewaters at four out of seven WWTPs with a maximum of 50.4 ± 2.7 Bq·L^{-1} in WWTP-1 where was also found three times in the sewage effluent. As regards ^{111}In, traces were detected once in the inflow wastewater, twice in the WWTP-1 effluent and once in the WWTP-4 effluent (0.18–0.28 Bq·L^{-1}). There are no previous reported values of this radionuclide in any sewage effluent and the presence in samples can be explained by its overuse in the BMA healthcare system compared with other European countries (CSN SEPR SEFM SEMNIM, 2014). In addition, traces of ^{123}I were quantified once at the inflow from WWTP-1 (0.64 ± 0.44 Bq·L^{-1}), while ^{67}Ga was not detected >MDA in the analysed waters.

3.5.1.2 Primary sludge

Medically-derived ^{131}I was detected in all the plants with primary sludge and the large-sized WWTP-1 and WWTP-2 showed the ^{131}I highest activities (Figs. 3.4 and 3.5). High diversity of results were found for ^{99m}Tc, with a maximum (9,530 ± 340 Bq·kg^{-1} d.w.) reached in WWTP-1. This value for ^{99m}Tc is slightly higher than that obtained in one previous study at a German plant (Fischer et al., 2009; 6,040 Bq·kg^{-1} d.w.). The concentrations in primary sludge ranged between <154–3,350 Bq·kg^{-1} d.w. in the other plants from the present study. With reference to ^{67}Ga, ^{111}In and ^{123}I have been shown significantly lower specific activities than those obtained for ^{131}I and ^{99m}Tc if the results for the same WWTP are compared (Figs. 3.4 and 3.5).

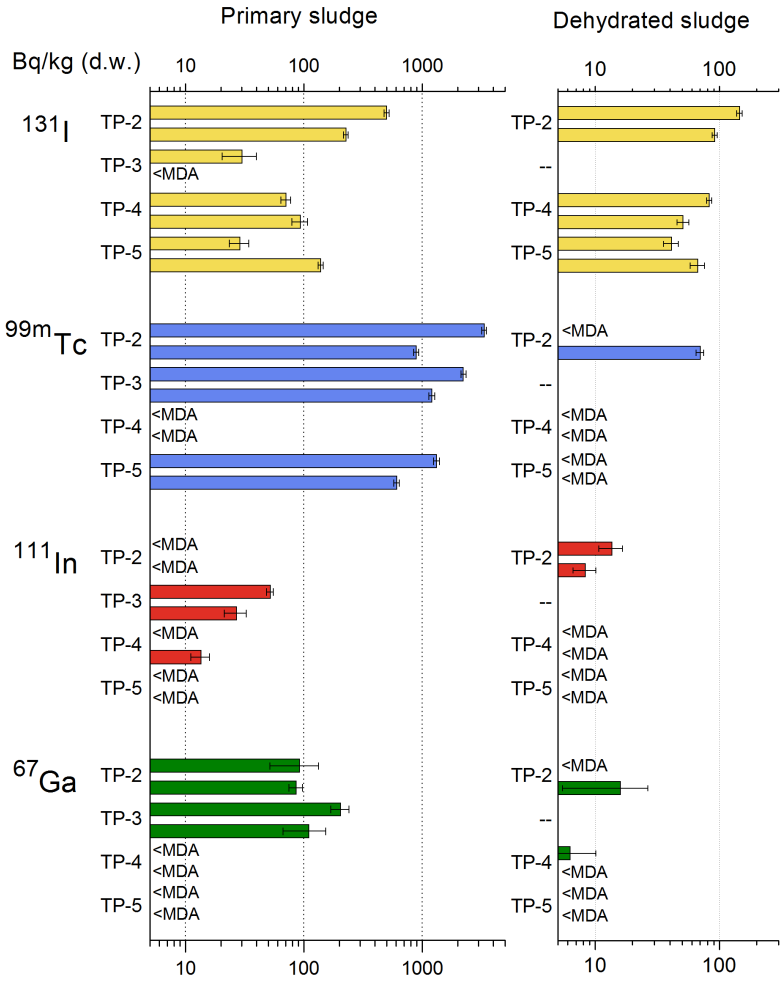

Figure 3.4: Specific activities (Bq·kg^{-1}d.w.) of medically-derived radionuclides found in the primary and dehydrated sludges in WWTP-2, 3, 4 and 5. Two samples from different sampling days for each plant and sludge were analysed.

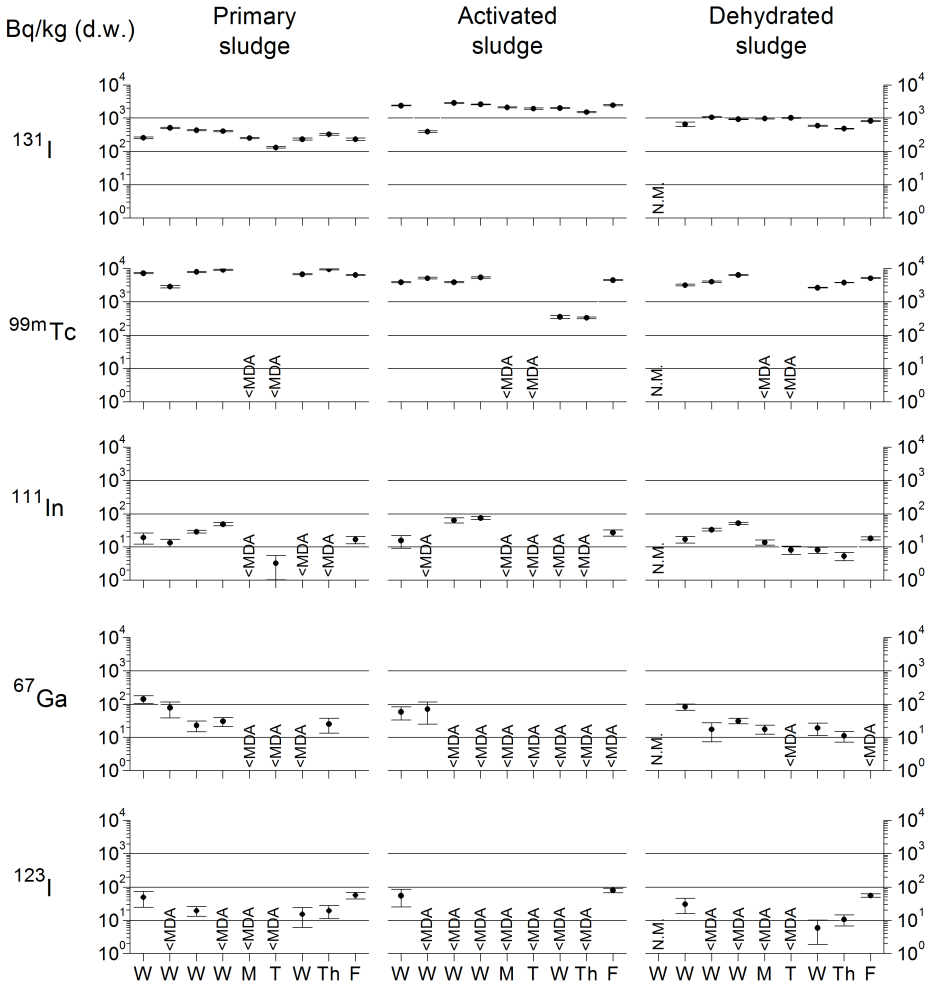

Figure 3.5: Specific activities (Bq·kg^{-1}d.w.) for primary, activated and dehydrated sludges from WWTP-1. Four one-off samplings and the daily sampling for one week (from Monday to Friday) are shown. N.M: Not measured.

3.5.1.3 Activated sludge

^{131}I was found in all the WWTPs at least once (Figs. 3.5 and 3.6) in agreement with previous studies, which reported accumulations of medically-derived ^{131}I in this by-product (Fischer et al., 2009; Punt et al., 2007). The reason is that some of the ^{131}I is fixed on the activated sludge particles by microorganisms during biological treatment (Cosenza et al., 2015; Hormann and Fischer, 2017), and this step plays a key role in partial ^{131}I removal. As regards ^{99m}Tc was found in 4 out of 7 plants studied with a maximum in WWTP-1 of 5,450 ± 280 Bq·kg^{-1} d.w., one order of magnitude higher than the activities found in the other WWTPs from the study and also than the maximum in activated sludge from another study (252 Bq·kg^{-1} d.w.; Fischer et al., 2009). Another radionuclide found in the same number of WWTPs

was ^{111}In, but at a significantly lower range of activities (Fig. 3.6), while ^{123}I and ^{67}Ga were detected twice in WWTP-1 (Fig. 3.5).

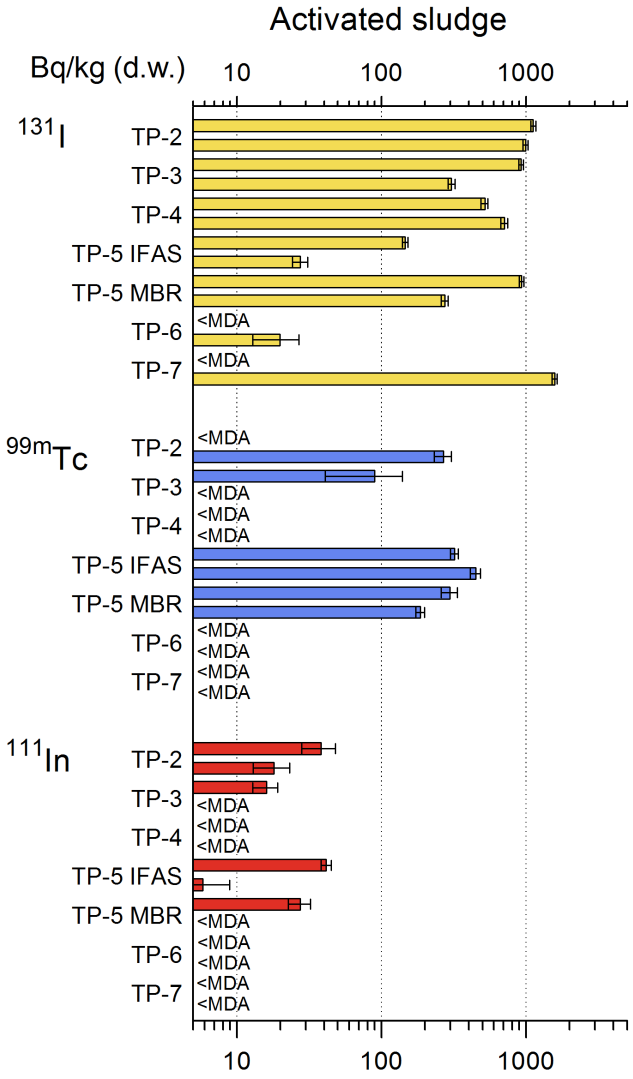

Figure 3.6: Specific activities (Bq·kg^{-1} d.w.) from medically-derived radionuclides found in activated sludge for 6 out of 7 WWTPs studied. Two samples taken in different days for each WWTP are shown.

3.5.1.4 Dehydrated sludge

The results for the four plants with dehydration sludge facilities are shown in Figs. 3.4 and 3.5. ^{131}I, ^{99m}Tc, ^{111}In, ^{67}Ga and ^{123}I were determined in a total of 4, 2, 2, 3 and 1 out of 4 WWTPs, respectively, the maximum concentrations corresponded to WWTP-1 in all cases. Furthermore, the number of determinations above the MDA of different radionuclides other than ^{131}I in WWTP-2, WWTP-4 and WWTP-5 is

very limited. Only ^{111}In and ^{99m}Tc in WWTP-2 were determined, which could be explained mainly due to the primary sludge that had recently entered into the digester tanks. ^{123}I was not detected in WWTP-2, 4 and 5 plants above the MDA.

3.5.1.5 Intensive study in WWTP-1 sewage sludges

A total of four complete samplings and five daily consecutive samplings of the sewage sludges (Fig. 3.5) were carried out. The present findings allowed us to look deeper into the WWTP-1 case and observe some tendencies on the presence of radionuclides in the different types of sludges during weekdays. As regards results in sludges, it is worth mentioning the second sampling (Fig. 3.5), where ^{131}I in activated sludge and ^{99m}Tc in primary sludge together with ^{111}In in both sludges has shown lower values compared with the other 4 samplings on Wednesday. The lower levels in both sludges can be explained by an important rain event during the three days before the sewage sludges sampling with an increase of the inflow wastewater of 90 %, 50 % and 100 %, respectively from the mean yearly flow (AGBAR 2018) which has some operational implications in the WWTP-1. The dilution of the urban wastewater and consequently of medically-derived radionuclides (dissolved and contained in particles) with the incorporation of the storm water could explain the observed reduction of the activity concentrations in primary sludge. Furthermore, a part than the dilution effect, in the specific case of the activated sludge reactor the lower residence times due to the flow increase could also reduce the contaminants removal due to a lower wastewater residence time. Excluding the lowest level obatined during the rain event (395 $\pm$ 22 Bq·kg^{-1} d.w.), ^{131}I shows concentrations in activated sludge in a range of 1,530–2,890 Bq·kg^{-1} d.w. (Fig. 3.5) without any remarkable tendency during weekdays. Nevertheless, ^{99m}Tc shows a strong increase from a value <MDA for the one-off sampling on Monday for all the sewage analysed sludges. The meteoric increase is within 3–4 orders of magnitude higher than the following weekdays (Fig. 3.5) could be related with the pattern administrations and the relative low half-life of ^{99m}Tc. In a previous study this phenomena has been used as internal tracer of the WWTP establishing a division within the weekend and weekdays sludge (Fischer et al., 2009). The data obtained from ^{67}Ga, ^{111}In and ^{123}I showed relatively low concentrations in comparison to ^{131}I and ^{99m}Tc (Fig. 3.5). ^{67}Ga was generally detected in primary and dehydrated sludges, ^{111}In was present in some samples of all types of sludges, while the ^{123}I appeared in detectable amounts in the daily consecutive samplings by the end of the weekdays (from Wednesday to Friday).

3.5.1.6 WWTPs working as abatement systems: the role of the HRT and sewage sludge age

The hydraulic retention times (HRTs) and sewage sludge ages reported in the present study for each WWTP correspond to an average of the daily HRT and sludge age

data determined by Eqs. (3.1), (3.2), (3.3) and (3.4). HRT and sludge ages were determined for one day with operational monitoring daily data (Personal communication) from the sampling year (several years in some cases). The daily HRT and sludge ages that were averaged in order to obtain the mean age reported in the present study was n = 323.

Daily hydraulic retention time (HRT) determination :

The operational daily HRT (days) for each plant was determined following formula (3.1):

$$HRT = \frac{\text{Total volume of settling tanks and reactors m}^3}{\text{wastewater inflow m}^3/\text{d}} \tag{3.1}$$

Daily sewage sludge ages determination :

Determinations of the solid retention time for each type of sludge were carried out to determine the daily sludge ages (days) on the sampling day for all the analysed sludges. The significant steps considered for the age determinations in the primary sludge line were settling and thickening tanks (Eq. (3.2)). For the activated sludge line the main steps were reactors and settling tanks (Eq. (3.3)); and in the dehydrated sludge line were digester tanks (Eq. (3.4)). Nevertheless, in the case of dehydrated sludge first the ages of the primary and activated sludges, which come into the digester tanks mixed, are weighted (Eq. (3.4)) in order to give an initial age to the resulting mass.

$$Primary\,sludge(PS)\,age = \frac{\text{PS ST}_{vol}\cdot\text{PS ST}_{TSSC} + \text{PS TT}_{vol}\cdot\text{PS TT}_{TSSC}}{\text{TSS}_{flowPS}} \tag{3.2}$$

$$Activated\,sludge(AS)\,age = \frac{\text{R}_{vol}\cdot\text{R}_{TSSC} + \text{AS TT}_{vol}\cdot\text{AS TT}_{TSSC}}{\text{TSS}_{flowAS}} \tag{3.3}$$

$$Dehydrated\,sludge(DS)\,age = \frac{\text{PS}\cdot\text{TSS}_{flowPS} + \text{AS TSS}_{flowAS}\cdot\text{AS TT}_{TSSC}}{\text{TSS}_{flowPS} + \text{TSS}_{flowAS}} + \frac{\text{DG}_{vol}\cdot\text{DG}_{TTSC}}{\text{TSS}_{flowDS}\cdot(\text{1-Vf})} \tag{3.4}$$

$$Volatilization\,factor(Vf) = \frac{\text{VSS}_{initial}\text{-VSS}_{final}}{\text{VSS}_{initial}} \tag{3.5}$$

where; TSSC=total suspended solids concentration, ST=settling tank, TT= thickening tank, R=Reactor, DG=digester tank (or storage tank in WWTP-1) and TSSflowX is equal to the concentration of total suspended solids multiplied with the m3 of sludge generated in one day. In Eq. (3.5) the parameter Vf is defined where; VSS = volatile suspended solids.

Three exceptions should be mentioned, the WWTP-2 activated sludge age Eq. (3.3) data is reported as a weighted mean by mass because the two activated sludges lines are mixed before the activated sludge sampling point (Fig. 3.2). Furthermore, the two different activated sludge ages (IFAS and MBR) in WWTP-5 were weighted in order to obtain a mean activated sludge age, required in Eq. (3.4) for DS age determination and the MBR lines in WWTP-5 and WWTP-6 do not have settling tank (Fig. 3.2).

Physical decay as a function of HRT and sludge age determination: The percentage of the initial activity, which would remain at a certain moment of time (HRT or sludge age) due to physical decay, has been determined for each radionuclide following the physical decay equations from *Materials and methods* chapter (Chapter 2; eq. 2.1 and 2.2). The percentage of decay at a certain time is obtained subtracting A(t) value to the initial 100 % of activity.

NM radionuclides levels in WWTPs and retention times relationship: Some factors are involved in total removal of NM radionuclides by the seven WWTPs studied. Firstly, there is direct removal through particle settling or absorption by the activated sludge treatment. Secondly, NM radionuclides have a physical half-life comparable to or even much shorter than operational characteristics of the WWTPs as the hydraulic retention time (HRT) and the solid retention times, expressed in the present study as sewage sludge age. The combination of both factors definitely contributes to decrease the specific activities either of the sewage effluent or the different sludge types (Fig. 3.7). In Fig. 3.7a HRT and sewage sludge age data of the seven WWTPs are presented (determined with eqs. 3.1, 3.2, 3.3 and 3.4), while Fig. 3.7b shows the times necessary for the initial activity to decay by 90 % and 99 % for each radionuclide. If data from both figures are compared, the results in the previous section can be partially explained. The average decreases expected due to radioactive decay during wastewater treatments in the sewage effluents due to the HRT (1–2 days) were 9 %, 95 %, 24 %, 21 % and 75 % for ^{131}I, ^{99m}Tc, ^{111}In ^{67}Ga and ^{123}I, respectively. In the case of the final solid output of the BMA urban wastewater depuration system network (dehydrated sludge) the mean decrease for ^{131}I, ^{99m}Tc, ^{111}In ^{67}Ga and ^{123}I in WWTP-1, taking into account 4 days of sewage sludge age, were 28 %, >99 %, 62 %, 56 % and >99 %, respectively. In contrast, in the rest of the WWTPs with dehydrated sludge ages between 37 and 49 days ^{131}I is expected to decrease by a mean of 97 % during the treatment, while for

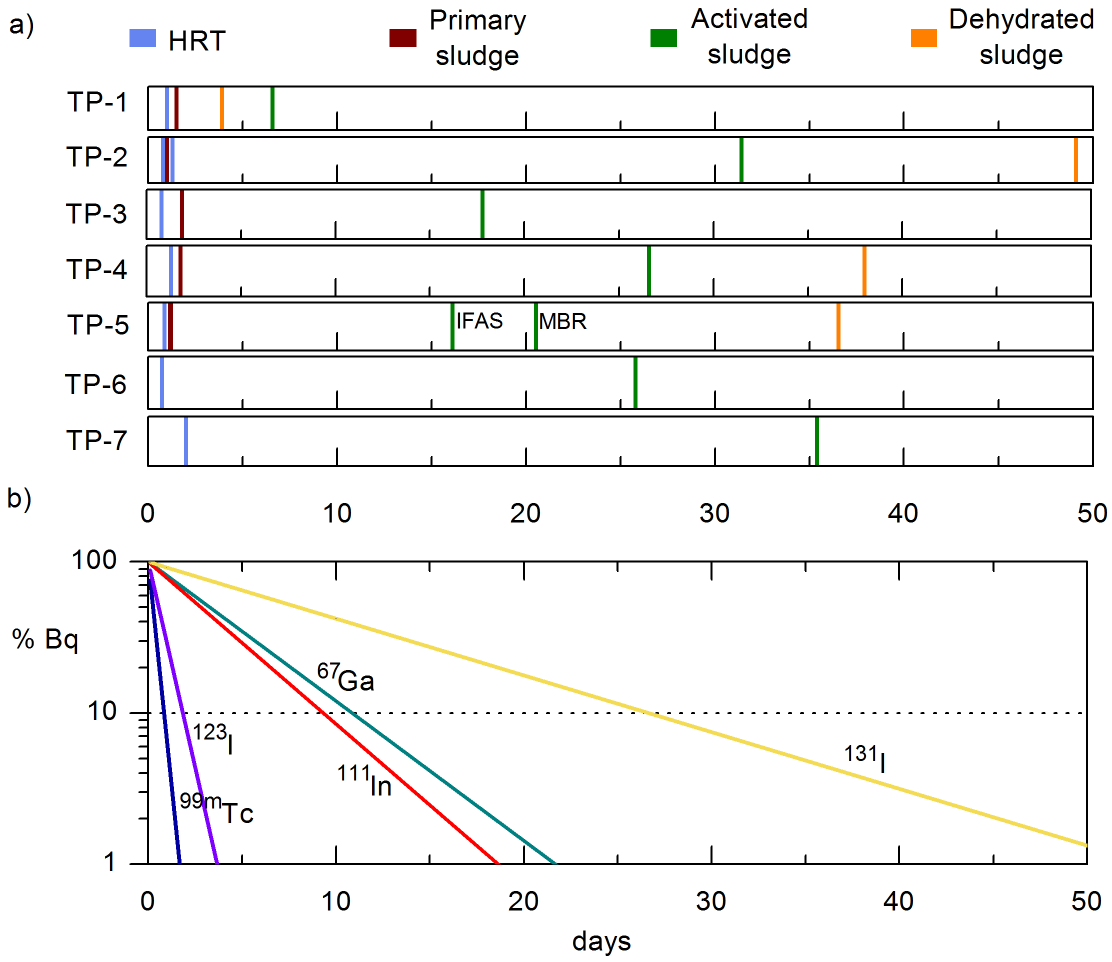

Figure 3.7: Panel a: Mean WWTP operational data (HRT of the inflow wastewater and sludge ages). WWTP-2 and WWTP-5 show 2 HRTs due to the two differentiated effluents (Fig. 3.2). The mean RSD from the reported means of HRT and sludge age results was 23 %. Panel b: Physical decay lines of the studied medically-derived radionuclides.

the other radionuclides studied it is >99 %. The radionuclide that showed the greatest sensitivity to elimination by physical decay during the wastewater treatment process was ^{99m}Tc ($t_{1/2}$ = 6.0 h) and Fig. 7b shows that ^{99m}Tc activities decayed by approximately 99 % in 2 days, while the calculated HRTs are of 1–2 days. On the other hand, HRTs are significantly shorter than the physical half-life of ^{131}I ($t_{1/2}$=8.0 d), thus producing a total decrease of 5–17 % (Fig. 3.7) similar to an estimation of 7 % in a large-sized plant in the United Kingdom (Punt et al., 2007).

Consequently, the primary sludge is the by-product that has a relatively low age between 1 and 2 days (Fig. 3.7a) and has the highest levels of ^{99m}Tc for all the plants (Figs. 3.4 and 3.5). In addition, other radionuclides such as ^{67}Ga and ^{123}I have also shown higher detection frequencies in primary sludge than in the other sludges (Figs. 3.4, 3.5 and 3.6). In contrast, activated and dehydrated sludges, showed lower activity concentrations due to their significantly higher age and associated physical decay (Fig. 3.7a and b). In terms of concentrations, WWTP-1 has the most relevant medically-derived radionuclides specific activities in the BMA urban wastewater depuration system network, both activated and dehydrated sludge ages are factors that definitely contribute to the relatively high levels found.

Furthermore, the sewage sludge age in activated sludge can be used as a tool in WWTP-5 to compare the ^{131}I concentration capacities in the two differentiated activated sludge treatment lines (IFAS and MBR Fig. 3.2), which treat the same wastewater. In this case, the ^{131}I MBR/^{131}I IFAS activities ratio for both sampling days are 9.1 ± 1.2 and 6.4 ± 1.2 (Fig. 3.6), respectively, while the sewage sludge age ratio is 1.3 (Fig. 3.7a), which means that if both treatment lines had the same ^{131}I concentration capacity, activities should be similar. However, the ^{131}I-MBR/^{131}I-IFAS ratios reveal a relatively higher absorption by the MBR per sludge kg in dry weight than in the IFAS.

3.5.2 Integral analysis of the activities detected in the BMA depuration system

In this section, the range of ^{131}I results in inflow wastewater is compared to other studies. In addition, there is a discussion of the relationship between the amounts of medically-derived radionuclides detected in the 7 WWTPs with the total flow treated in the plant and the characteristics of the wastewater catchment area.

3.5.2.1 ^{131}I therapy abatement systems and influence on inflow wastewater levels

Despite the diferences in the sewerage networks and catchment area, the ^{131}I levels in inflow wastewaters in the BMA and in other studies can be listed in order to evaluate whether there are differences due to systematics of NM services. Concentrations

Table 3.3: Comparison between the results of ^{131}I concentrations in the inflow wastewater of the present study with data available of urban wastewater before comes into the treatment from other studies.

	^{131}I activites (Bq·L^{-1})			
	Min.	$\bar{x}$	Max.	Reference
With ^{131}I abatement systems				
Barcelona Metropoltian Area - Spain	<0.2	1.1[a]	4.4	Present study
Valladolid - Spain	0.3	1.2	2.7	Jiménez (2010)
Bremen - Germany	0.2	0.6	0.9	Fischer et al. (2009)
Without ^{131}I abatement systems				
London - United Kingdom	<1.5	24[a]	50	Punt et al. (2007)
Daejon - South Korea	0.3	1.3	3.5	Chang et al. (2011)

a) Concentrations under the MDA were considered as 2/3*MDA.

of ^{131}I in previous metropolitan studies for inflow wastewater and values of the present study are shown in Table 3.3, classified by whether or not abatement systems were used for the excreta from inpatients treated with GBq of ^{131}I. The activities found in the studies carried out in urban areas, where the hospitals were equipped with abatement systems, showed a one-order-of magnitude lower range than those obtained from the United Kingdom, where abatement systems are not used. In contrast, the data from the Korean study are discussed by the potential for growth of patients treated per year with ^{131}I (Chang et al., 2011). The present findings are also useful to find out the baseline levels of medically-derived ^{131}I in BMA urban wastewater treatment system outputs (sewage sludge and sewage effluents) with the use of abatement systems for inpatients and a patient release criteria of 0.8 GBq (CSN SEPR SEFM, 2011). The reduction of ^{131}I levels in the inflow wastewater due to the use of abatement systems has also an influence on the levels in sewage sludges and the total amount that enters the environment (Fischer et al., 2009).

3.5.2.2 Relationships between variabilities in concentrations, detection frequencies and WWTP sizes

In a preliminary plant-by-plant analysis, results from large-sized WWTP-1 and 2 not only showed most of the highest activity concentrations of the medically-derived radionuclides in sludges, also different statistical characteristics compared to the other plants. The differences were significant in the case of the relative standard deviation (RSD) of ^{131}I in activated sludge (Fig. 3.8) and ^{67}Ga, ^{111}In and ^{123}I detection frequencies (Figs. 3.4, 3.5 and 3.6). In the largest plants were found the lower RSD variabilities of ^{131}I concentrations in activated sludge (in the case of WWTP-1 only Wednesday samplings were considered in order to maintain the same sampling day as in the other plants studied with the exception of one due to

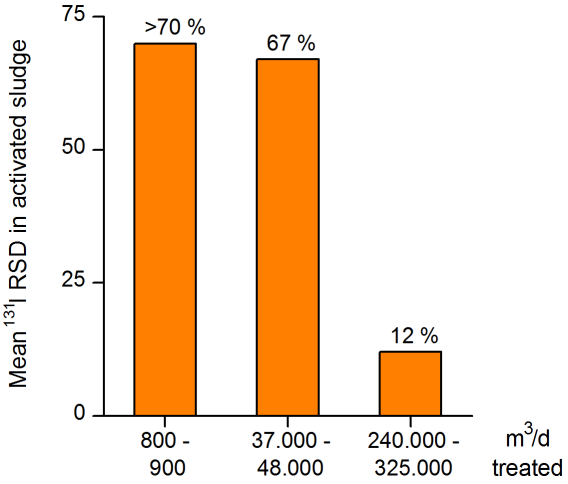

Figure 3.8: Mean RSDs for the ^{131}I levels found in activated sludges for the different WWTP influent wastewater flows. Data from MBR and IFAS activated sludge lines in WWTP-5 are considered as individual sources.

an important rain event) and higher total detection frequencies of ^{67}Ga, ^{111}In and ^{123}I in sewage sludges with 55 % and 56 % (WWTP-1 and 2, respectively) than in the sewage sludges from the other five plants (0–25 %). In order to explain the present trends in the seven WWTPs three main hypothesis should be mentioned:

i) The presence of NM services in the catchment area (Fig. 3.2). The BMA and especially the city of Barcelona is an important regional healthcare service centre. WWTP-1 and 2 receive all the radiopharmaceuticals administration centres effluents (10 and 5 respectively). This fact could justify an increase in WWTP levels and detection frequencies compared to the other studied plants.

ii) The total number of outpatients and diagnostic inpatients excreting directly in the wastewater catchment area in the very large-sized WWTP-1 and 2 could be behind the statistically stable ^{131}I levels in activated sludge (Fig. 3.8) as well as the higher detection frequencies for ^{67}Ga, ^{111}In and ^{123}I in sewage sludges (Figs. 3.4, 3.5 and 3.6). In contrast, significantly different results were obtained for the small-sized WWTP-6 and 7. These plants treat a relatively low daily wastewater flow (Fig. 3.2) from smaller communities (4,000–7,000 inhabitants registered), where the presence of patients excreting radiopharmaceuticals in the catchment area is probabilistically sporadic for ^{131}I, ^{67}Ga, ^{111}In and ^{123}I with a few people per year (Table 3.3).

iii) The WWTP size and sludge type sampled due to dilution dynamics in the large-sized WWTPs could have also an influence on the stable ^{131}I levels in activated sludge (Fig. 3.8) and also increase the detection frequencies of ^{67}Ga, ^{111}In and ^{123}I.

3.5.3 Radiological risk assessment

Although it was not the aim of this work, since the dataset is limited for an accurate evaluation from the radiological protection point of view, some comments can be made in order to contextualize the present findings.

As regards the activity concentrations found in the sewage effluents, a comparison with derived activity concentrations for water consumption was done (Table 3.4). In all the cases, the concentrations were lower than the reference levels. In the case of sewage sludge, the exemption levels indicated in the Council Directive 2013/59/Euratom (EC 2013a) were used for this assessment, these values were compared with the sewage sludge activity concentrations in $Bq{\cdot}kg^{-1}$ d.w. as a conservative scenario, and all results were always well below the existing reference levels. It means that the radiological risks to individuals caused by the practice are sufficiently low, as to be of no regulatory concern, in particular the effective dose expected to be incurred by a member of the public due to the artificial radionuclides is of the order of 10 μSv or less in a year (EC 2013a).

Table 3.4: Maximum concentrations found for each radionuclide in sewage effluents and sewage sludges with and derived activity concentrations and exemption levels, respectively.

	Sewage effluent $Bq{\cdot}L^{-1}$		**Sewage sludge ($Bq{\cdot}kg^{-1}$)**	
NM Radionlucides	Maximum in the BMA	Derived activity concentrations from a committed effective dose for water ingestion <100 $\mu Sv{\cdot}y^{-1}$ for adults (>17 years)[a]	Maximum in the BMA	Exemption level for solid materials (Dose <10 $\mu Sv{\cdot}y^{-1}$)[b]
^{131}I	3.4	6.2	2,460	10,000
^{99m}Tc	6.5	6,200	9,200	100,000
^{111}In	0.26	470	155	10,000
^{67}Ga	<1.3	720	210	100,000[c]
^{123}I	<0.9	650	80	100,000

a) Values determined by Grande and Risica (2015) taking into account the indicative dose limit from EC (2013b)
b) EC 2013a
c) No specific value in the directive and Spanish national reference value was assumed (CSN 2003)

3.6 Conclusions

In the 7 urban WWTPs from the BMA a total of 5 different radionuclides applied in NM procedures have been found. The highest levels have corresponded to the ^{99m}Tc, which is used in diagnosis procedures, and to ^{131}I, which is used in both diagnosis and treatment procedures. The other radionuclides found (^{67}Ga, ^{111}In, ^{123}I) have shown lower activities and detection frequencies.

Regarding ^{99m}Tc level the maximum concentrations in waters and sewage sludge were found in inflow waters (50.4 ± 2.7 Bq·L^{-1}) and primary sludge (9,530 ± 340 Bq·kg^{-1} d.w.) while the maximums of ^{131}I corresponded to inflow water (4.43 ± 0.29 Bq·L^{-1}) and activated sludge (2,890 ± 110 Bq·kg^{-1} d.w.). All maximums listed corresponded to samples from the WWTP-1. Furthermore, the highest values in dehydrated sludge, which is the final solid output, for the radionuclides studied are 2-3 orders of magnitude higher in WWTP-1 than in the rest of the WWTPs.

HRTs and sewage sludge ages were found and considered as significant factors in order to explain the role of decay during the treatment in the final activities found. All the radionuclides studied have half-lives between 6 hours and 8 days while the HRTs 1-2 days and sewage sludge ages 1-49 days.

It is noteworthy that operating conditions with lower sewage sludge ages in the WWTP-1 (2-7 days) are a key factor to reduce physical decay during the sewage sludge line steps and show higher concentrations and detection frequencies in the final solid outcome. Regarding waters, the higher concentrations of ^{99m}Tc can be explained the high concentration of NM services in the catchment area of WWTP-1.

The present study in the BMA, which include simultaneous samplings in the different steps of the sewage sludge line, enables discussion of the main pathways of the different medically-derived radionuclides studied to sewage sludge line. The maximums of ^{99m}Tc in primary sludge and ^{131}I in activated sludge were explained by the sludge age and the absorption by microorganisms respectively. Furthermore, the prevalence of detectable ^{131}I in dehydrated sludge, the final solid output of the sludges line, despite digestion over weeks has been demonstrated.

The levels found in the inflow wastewaters were compared with other systems where the treated patients with ^{131}I include abatement systems. The range of results found are within those from other countries but are one order of magnitude lower than the UK results where abatement systems are not currently used.

Chapter 4

Adaptation and experimental validation of a ^{131}I partitioning methodology for wastewater

4.1 Introduction: Physicochemical dynamics of ^{131}I in wastewater and analytical methods

Low levels of medically-derived ^{131}I can be found at detectable concentrations in WWTPs water samples and have been shown in Chapter 3 (<0.2-3.4 Bq·L^{-1}). Thus, specific methods are needed to determine low-level of ^{131}I in liquid environmental samples with the aim to concentrate it and optimize the measurement (Rodríguez et al. 2018; Souti et al., 2014). Some of the existing methods are based in the extraction of iodide (I^-) or iodate ($I0_3{}^-$), one of the most favourable inorganic species in environmental aqueous media (Hou et al., 2009), by adding $AgNO_3$ to the solution in order to bound the inorganic iodine species to the Ag^+ and conform insoluble species (Hou et al. 2009). However the ^{131}I mobility and complex partitioning in environmental liquid samples, with presence in particles, colloids and dissolved organic substances (Rodríguez et al. 2018; Rädlinger and Heumann 2000; Hormann and Fischer 2017), restricts a complete captation in the concentrate. With the addition of some reagents and the application of separation techniques iodine bounded to particulate and dissolved organic fractions can be completely dissociated and transformed to inorganic iodine and extracted from the sample. Several methods have been proposed to concentrate the different fractions of ^{131}I from aqueous samples in a unique precipitate before the measurement:

i) To dissociate the iodine fraction contained as organic species and retain all the iodine in a strong anion exchange resin (Rodríguez et al. 2018)

ii) To precipitate organic iodine fraction after $CaCl_2{\cdot}2H_20$ addition together with the inorganic iodine through AgI formation (Souti et al., 2014)

iii) To digest the dissolved organic fraction with H_20_2 in order to take all the dissolved iodine with the AgI formation (Rodríguez et al. 2018)

In addition to determine the ^{131}I levels, a partitioning analysis can give extra information about the percentages in different fractions of the water column and can help in the present knowledge of ^{131}I behaviour along a WWTP (Hormann and Fischer 2017). Furthermore a better understanding of the interactions of ^{131}I along a WWTP can give enough information to develop and implement ^{131}I prognosis models (Hormann and Fischer 2018).

In Table 4.1 a list of the possible forms of medically-derived ^{131}I in wastewater can be found. Regarding the most administered radiopharmaceuticals to patients ($Na^{131}I$ and ^{131}I-MIBG), they are mostly excreted via urine in the same compounds than those administered (Wafelmann et al., 1997; Legget 2010) whereas a small fraction is excreted through feces (Legget 2010). After entering into the sewerage network via the excreta from patients, ^{131}I can interact in the wastewater media with organic materia from suspended solids (Hormann and Fischer 2014) and absorbed

into organic molecules as humic acids (Rädlinger and Heumann 2000). Along the WWTP the main expected process is to be partially fixed to suspended organic matter in the activated sludge reactor (Hormann and Fischer 2017) before be released into the environment through the sewage effluent and to interact with the ecosystem (Lee et al., 2018). Despite the iodine interactions with particles or organic molecules, iodide has been revealed as the most expected form of ^{131}I in WWTPs (Hormann and Fischer 2017).

Table 4.1: Differentiated ^{131}I fractions and compounds expected in a WWTP sample.

Fractions	**References**
Particulate phase	
Organic materia	Hormann and Fischer (2014)
Inorganic phase	
I^-	Legget (2010); Hormann and Fischer (2017)
Dissolved organic phase	
T3 and T4 hormones	Legget (2010)
MIBG	Waffelman et al. (1997)
Humic acids	Rädlinger and Heumann (2000)

An specific analysis method where ^{131}I can be separated in three different fractions has been developed in Hormann and Fischer (2017) based on the method from Souti et al., (2014) with the aim to study the ^{131}I partitioning in WWTP samples. The method differentiates between: aluminum chlorohydrate (ACH) extractable iodine (AEI), bentonite extractable iodine (BEI) and residual iodine (RI). Total suspended solids (TSS), colloids and large and hydrophobic molecules are expected to be concentrated in the AEI precipitate while in through the BEI precipitate all the iodide (I^-) is expected to be removed. In the final supernatant (RI) hydrophilic and/or small organic molecules with ^{131}I remain in the dissolution.

However, this method has not been yet validated and it is of utmost importance that the fractions will be determined accurately in order to avoid biases in the discussion about ^{131}I behaviour in WWTP.

4.2 Objective

The main objective of the present chapter is to study the recovery of the ^{131}I partitioning method developed by Hormann and Fischer (2017) in the BEI step, specifically, after the addition of known amounts of a $^{131}I^-$. The experiments have been carried out in the following water media:

i) $NaHCO_3$ 2 mM water

ii) WWTP samples

The variables studied in the present work were:

i) To change the reagents dosage

ii) To apply different timings on some phases of the method in the case of WWTP samples

These experiments will allow to evaluate the effect of the sample matrix, the differences in the concentrations of the reagents applied, and the time of settling during the ^{131}I uptake process in the BEI settling phase.

4.3 Description of the experiments

Known amounts of $^{131}I^-$ were added to WWTP and distilled water samples artificially carbonated ($NaHCO_3$ 2 mM). After the application of the ^{131}I partitioning method the BEI fraction was measured in order to evaluate the the dissolved iodide recovery capacity under different experimental conditions. ^{131}I concentration at some AEI and RI phases of WWTP samples were also measured. The details of the experiment are given as follows.

4.3.1 Radiochemical method description

In Fig. 4.1 is depicted the ^{131}I partitioning method applied which is based in the previous work from Hormann and Fischer (2017). The details of the radiochemical procedures that give rise to two differentiate precipitates (AEI and BEI) and a final supernatant (RI) are described as follows.

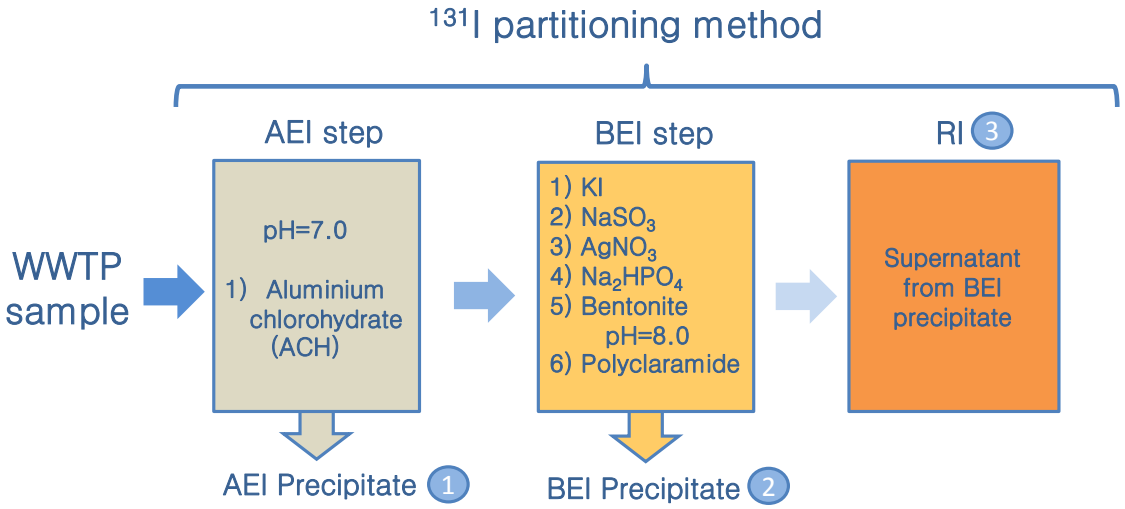

Figure 4.1: Graphical description of the ^{131}I partitioning method with three differentiated fractions.

ACH extractable ^{131}I (AEI): The precipitate generation (Fig 4.2) is performed by the addition of ACH solution (ACH 10-15 ml·L^{-1}) and CH_3OOH 10 M or NH_4^+ 6 M in order to adjust pH to 7.0 in case it is necessary.

It is worth mentioning that CH_3COOH was added into most of our WWTP samples in order to drive the pH from slightly alkaline samples (pH 7.1-8.1) to 7.0, whilst in the WWTP samples analysed by in Hormann and Fisher (2017) were always driven from acid solution to pH 7.0 with NH_4^+. Although this fact points

out that our WWTP samples had a different initial pH, the method itself is not affected by this fact, since CH_3COOH and I^- do not interact (Raihle et al,. 1972).

The total amount of ACH added depends on the TSS concentration in the different WWTP sampling points (Hormann and Fisher 2017). The dosages are 10, 6 and 1.5 $mL{\cdot}L^{-1}$ for inflow wastewater (IW), primary effluent (PE) and sewage effluent (SE) respectively and always in excess giving rise to a white layer above the precipitate (Fig.4.2a). In the case of $NaHCO_3$ 2 mM samples ACH was added although any particle extraction had to be performed. The samples were decanted between 3 and 22 h and subsequently the supernatant extracted and centrifuged at 2000 r.p.m. for 15 minutes. After the centrifugation, the second supernatant is separated again from the precipitated and mixed with the first supernatant for the next step of the radiochemical method.

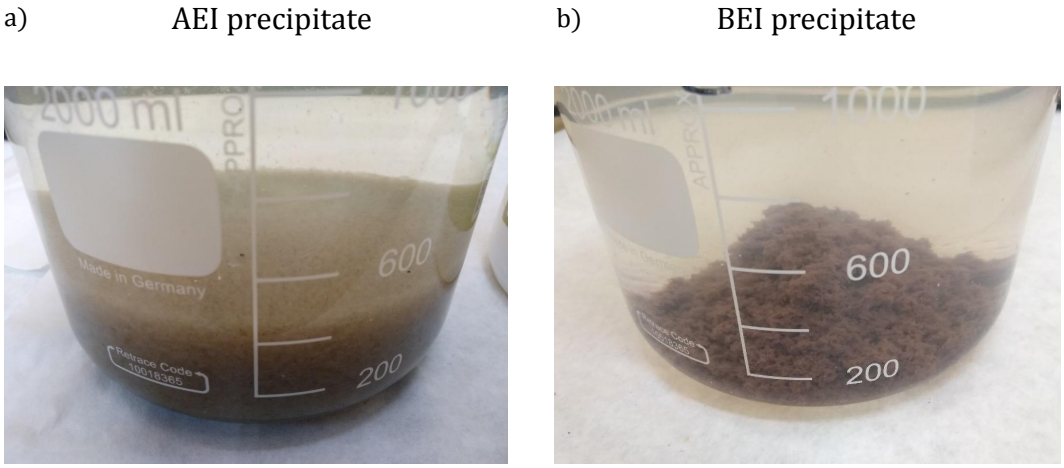

Figure 4.2: Precipitates obtained in a urban wastewater sample after D5 reagents dosage. N.M. = Not measured.

Bentonite extractable ^{131}I (BEI): in this step the first four reagents are added under stirring in the order listed in the Fig 4.1 with the aim to capture the $^{131}I^-$ present in the sample and precipitate it. $NaSO_3$ avoid the oxidation from I^- to $IO_3{}^-$, KI and $AgNO_3$ generate the insoluble and positive charged AgI compound (eq. 4.1) and Na_2HPO_4 trace the dissolution with a net positive charge with Na^+. After the four reagents addition the stirring is stopped and the dissolved bentonite is added in order to capture the AgI, the pH adjusted to 8 with $NH_4{}^+$ and stirred for 45 minutes. Bentonite is extracted with the addition of polyclaramide compound giving rise to the final precipitate and leaved settling between 3 hours and overnight

(Souti et al., 2014). After the settling time the supernatant (Fig 4.2) is extracted and the precipitated centrifuged (2000 r.p.m. fo 15 minutes) in order to obtain the final precipitate to perform the BEI fraction measurement.

$$Ag^{+}(aq) + I^{-}(aq) \mapsto AgI(s) \quad (Kps = 8.52 \cdot 10^{-17}) \tag{4.1}$$

Residual ^{131}I (RI): both supernatants from the BEI radiochemical procedure are mixed conforming the residual phase where all the ^{131}I not extracted in both previous steps still remains in the sample.

Apart from the concentrations proposed by Hormann and Fischer (2017) (D1; Table 4.2) other reagents dosages were tested at the BEI step (D2-5; Table 4.2). The KI and $AgNO_3$ reagents dosage proposed for D3-5 had the same Ag/I molar ratio than the method proposed by Baeza et al. (2004) while in order to maintain the role of the reagents added (Hormann and Fischer; 2017) Na_2SO_3 and $Na_2HPO_42H_2O$ dosages were increased at D5 and bentonite at D4 and D5 progressively. Nevertheless, polyclaramide concentration was maintained stable because the concentration was enough to agglomerate the primary flocs conformed and to precipitate larger flocs as described in Souti et al. (2014).

Table 4.2: Different reagents concentrations tested in the BEI step.

Dosage	**Ag/I**	**KI**	**Na_2SO_3**	**$AgNO_3$**	**$Na_2HPO_42H_2O$**	**Bentonite**	**Polyclaramide**
	molar ratio	**mg/L**	**mg·L^{-1}**	**mg·L^{-1}**	**mg·L^{-1}**	**mg·L^{-1}**	**mg·L^{-1}**
D1	1.2	2.7	20	3.2	1000	160	6
D2	-	-	20	3.2	1000	160	6
D3	2.3	1.3	20	3.2	1000	160	6
D4	2.3	26.5	20	64	1000	530	6
D5	2.3	100	500	236	2000	2000	6

4.3.2 ^{131}I reference dissolution preparation

In order to prepare the $^{131}I^{-}$ dissolution one radiopharmaceutical capsule was opened and the $Na^{131}I(s)$ added into a distilled water with $NaHCO_3$ 2 mM to stabilize pH and prevent from iodine volatilization as I_2 (Hou et al., 2009). The high solubility of NaI(s) (184 g·100 mL^{-1} at 25 °C) allows dissolving quickly the compound under stirring, giving rise to the presence of iodide (eq. 4.2).

$$Na^{131}I(s) \mapsto Na^{+}(aq) +^{131} I^{-}(aq) \tag{4.2}$$

After the preparation, an aliquot of the dissolution was measured and the activity concentration of ^{131}I determined in order to add to the samples a known amount of $^{131}I^-$. Two preparations with two different $Na^{131}I$ capsules were carried out with specific activities of 1,355 ± 41 (I-1) and 433 ± 21 (I-2) Bq·L^{-1} respectively.

4.3.3 Experiment description and recovery determinations

Known amounts of $^{131}I^-$ were added to 15 samples, the volumes of the initial samples were between 0.4-1.8 L and the total activity added to each sample ranged between 3-205 Bq. Subsequently the ^{131}I partitioning method described in the *4.3.1 section* was applied to the samples taken from different treatment steps of the WWTP-2 (Chapter 1) as well as to dissolutions of distilled water at pH=8.0 artificially carbonated with $NaHCO_3$ 2 mM. The samples from the WWTP corresponded to inflow wastewater (IW#), primary treatment effluent (PE#) and sewage effluent (SE#).

The variables controlled during the experiment were:

i) The reactive concentrations in the dissolution

ii) The matrix

iii) The AEI settling time

Due to the presence of a background level of ^{131}I in WWTPs samples an aliquot of each WWTP sample was measured to determine the concentration of ^{131}I (<0.4 – 1.2 Bq·L^{-1}). The background concentrations found give rise to a maximum deviation of 3 % of the BEI activities.

Since it was expected that the $^{131}I^-$ added will be mainly present in the BEI precipitates and a very small activity in the other phases in most of the samples only BEI precipitate was measured. Only in two IW# and two SE# samples the direct determination of the AEI and RI was carried out as a quality control of the results. In order to know the % of recovery in the different fractions of the method the following equations (4.3-5) were considered:

$$AEI\ \% = \frac{Bq\ AEI}{Total\ Bq\ added} \cdot 100 \tag{4.3}$$

$$BEI\ \% = \frac{Bq\ BEI}{Total\ Bq\ added} \cdot 100 \tag{4.4}$$

$$RI\ \% = \frac{Bq\ RI}{Total\ Bq\ added\ \cdot\ Fmeasurement} \cdot 100 \tag{4.5}$$

The total amount of Bq measured in each sample fraction is detailed in the thesis appendix (Appendix D.1; Table C). In some cases the Bq RI was not equal to the total RI activity because the volume of the sample exceed the Marinelli 0.4 L volume and an aliquout of 0.4 L was taken. Thus, a correction factor was used in the eq. 4.5 (eq. 4.6):

$$Fmeasurement = \frac{RI\ volume\ obtained}{RI\ volume\ measured} \tag{4.6}$$

4.4 Results and discussion

In the present section the experimental ^{131}I partitioning method tests are shown. All the ^{131}I activity measurements were performed following the procedures indicated in the *2. Materials and methods* chapter. The raw data of the experiments can be found in the *Appendix D.1* (Table C).

4.4.1 Recovery test in $NaHCO_3$ 2 mM water

The percentages of ^{131}I recovery in the BEI step from the total activity by applying different dosages of reagents are detailed in Fig. 4.3. The present findings show different recovery efficiencies of $^{131}I^-$ from the dissolution depending on the total amount of reagents dosed (D1-5).

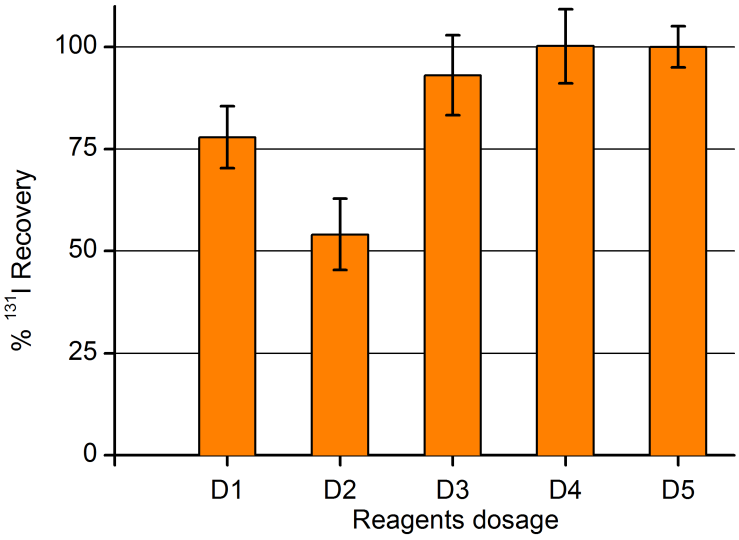

Figure 4.3: Recovery in $NaHCO_3$ 2 mM water in the BEI step.

The lowest recovery (54 ± 9 %) corresponds to the dosage D2 in which KI was not added and the only iodide available in the dissolution is the radioactive ^{131}I. The ^{131}I Bq added represent a very low chemical concentration of iodide $6{\cdot}10^{-16}$ M in contrast with the reagents dosage D1 where the expected iodide was $1.63{\cdot}10^{-5}$ M and the recovery was 78 ± 8 %. Thus, the role of the stable I^- added as KI has been found significant at helping to concentrate the $^{131}I^-$ in the BEI precipitate. For D3 the reagents concentrations were the same than for D1 but with a slight reduction of the KI addition in order to achieve a 2.3 Ag/I ratio in the dissolution similar to the proposed in Baeza et al. (2004). The recovery was higher for the the sample D3, which has the highest ratio, than for D1 reagents concentrations.

Moreover, in D4 and D5 the ^{131}I recovery in the BEI step by applying an overdose of reagents in comparison to Hormann and Fischer (2018) (D1) have been tested (Table 4.2). The results show for both dosages the highest recoveries found in $NaHCO_3$ 2 mM water, where around 100 % of the ^{131}I Bq added was measured in the BEI precipitate (Fig. 4.3). Thus, the present findings point out D4 and D5 reagents dosages as the most effective in the $^{131}I^-$ recovery in the artificially carbonated water samples.

To sum up, the BEI step has shown better recoveries with higher reactives dosages and Ag/I ratio in agreement with the dosages from a inorganic iodine recovery existing method for water samples (Baeza et al., 2004).

4.4.2 Recovery test in WWTP samples

The percentage of recoveries for IW#, PE# and SE# WWTP samples in the AEI and BEI precipitates and in the final supernatant (RI) are detailed in Table 4.3. Apart from the test of different reagents concentrations IW# and SE# samples were analysed in parallel with different settling times of the AEI phase.

Table 4.3: Recovery percentages from WWTP samples in the different phases analysed.

	Method variables		**Measurements**		
Sample code	**Reagents in the BEI step**	**Time between AEI and BEI steps**	**AEI (%)**	**BEI (%)**	**RI (%)**
Inflow wastewater					
IW8	D1	3 h	NM	2.4 ± 0.4	NM
IW9	D4	3 h	NM	101 ± 6	NM
IW1	D5	3 h	1.8 ± 0.2	97 ± 5	2.2 ± 0.7
IW2	D5	22 h	1.8 ± 0.1	103 ± 5	0.9 ± 0.3
Primary effluent					
PE1	D1	3 h	NM	91 ± 6	NM
PE2	D4	3 h	NM	94 ± 6	NM
PE3	D5	3 h	NM	101 ± 5	NM
Sewage effluent					
SE8	D1	3 h	NM	47 ± 4	NM
SE9	D4	3 h	NM	93 ± 6	NM
SE1	D5	3 h	1.4 ± 0.1	100 ± 5	0.9 ± 0.3
SE2	D5	22 h	2.0 ± 0.1	99 ± 5	1.1 ± 0.4

N.M.= Not measured

In the BEI precipitate after the ^{131}I addition the recovery had been found around 100 % (Table 4.3) when the reagents dosages were D4 or D5 in agreement with the results in $NaHCO_3$ 2 mM water. In particular, D5 seems to show a tendency of slightly higher recovery percentages in PE and SE samples than D4. Nonetheless, the samples with D1 have shown ^{131}I recoveries significantly lower in IW# (2.4 ± 0.4 %) and SE# (47 ± 4 %) samples and slightly lower than 100 % in PE# samples (Table 4.3) similar than in artificially carbonated water (Fig. 4.3). Thus, a matrix effect has been confirmed for WWTPs samples analysed with D1. Regarding different settling times and results found in the samples analysed no significant differences have been found in the BEI fraction determined after 3 and 22 h of settling times at the AEI step for D5.

In some cases (Table 4.3) the AEI and RI phases were also analysed and ^{131}I found at detectable amounts. However, the recovery percentages represent a very reduced part of the total amount added (0.9-2.0 %; Table 4.3). Regarding the AEI fraction the activities can be attributed to the water that remains in the wet AEI precipitated and in the case of RI to a little amount of $^{131}I^-$ not removed in the BEI phase. Regarding AEI fraction residual ^{131}I presence in particulate or dissolved organic materia which settle with the AEI precipitate (Hormann and Fischer 2014; Hormann and Fischer 2017) have revealed as not significant pathways for the added $^{131}I^-$ at WWTP samples. Moreover the testimonial presence of $^{131}I^-$ at RI fraction can be explained by the absorption by dissolved organic compounds that would remain in RI phase (Rädlinger and Heumann 2000).

4.5 Conclusions

In the present chapter the reagents concentration that allows a total recovery of $^{131}I^-$ in the BEI step in distilled water and in WWTP samples has been found. The most indicated reagents combination for the WWTP analysis was D5 which showed a recovery around 100 % in WWTP samples. The present validation opens up the possibility to implement the ^{131}I partitioning analysis to samples from a WWTP in order to determine changes in the proportion of the different phases along the different steps of the treatment.

Nevertheless, the diversity of compounds with ^{131}I that could be present in wastewater leads to continue studying the behaviour of substances different than I^- in the partitioning analysis studied in the present chapter. Specifically, is matter of interest test how the reagents interacts with the three different types of organic compounds expected in the residual iodine fraction from a WWTP sample.

Chapter 5

Intensive study of ^{131}I levels and partitioning in the WWTP-2 and in the reclaimed water line. Flows determination and modelling adaptation.

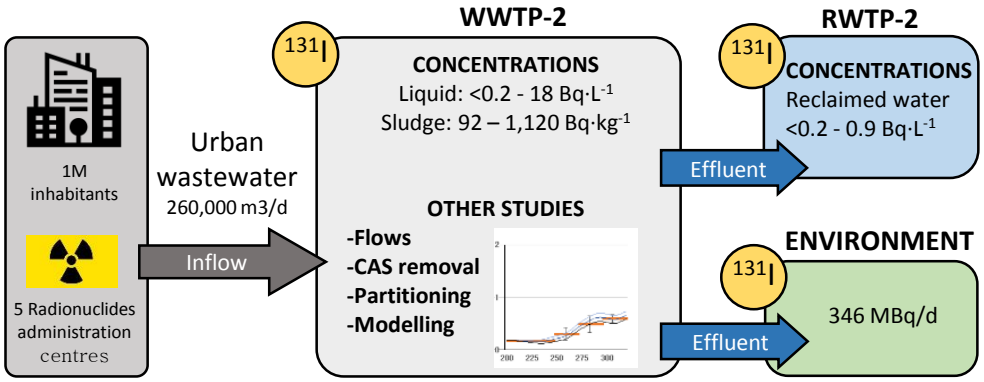

***Chapter partially published as:** Mulas, D., Camacho, A., Hierro, A., S., Garbayo, A., S. Devesa, R., Duch, M.A., (2020). Levels and chemical behaviour of ^{131}I in a large-sized WWTP with conventional activated sludge reactors (In progress).

5.1 Introduction: Physicochemical dynamics of ^{131}I in WWTPs

Levels of nuclear medicine (NM) radionuclides in the Barcelona metropolitan area (BMA) were determined in the 7 urban wastewater treatment plants (WWTPs) as described in Chapter 3. The study highlighted a higher stability of ^{131}I levels in activated sludge apart from higher detections frequencies in sewage sludge of medically-derived radionuclides in the very large-sized treatment plants (>200,000 $m^3 \cdot d^{-1}$) WWTP-1 and 2. Thus, the results open up the possibility to explain, after a deeper characterization at some points of the water treatment process, and in combination with water quality parameters the behaviour of ^{131}I along the treatment. The levels found in BMA point out ^{131}I as the most relevant radionuclide from the radiological protection point of view (Chapter 3) and its presence in the sewage effluent from WWTP-2 might carry some ^{131}I to the adjacent reclaimed water treatment plant (RWTP-2) with multiple direct applications. In view of the above, in the present section the NM radionuclides levels at WWTP-2 and RWTP-2 from the BMA have been studied exhaustively.

The presence at WWTP-2 of two differentiated lines of conventional activated sludge (CAS) reactors working at different configurations can give information about the better operational conditions to remove ^{131}I. Furthermore with a greater number of samplings the mean daily flow of ^{131}I released to the environment through the sewage effluents can be estimated.

After a previous validation work, the application of a ^{131}I partitioning analysis methodology (Chapter 4) to samples from different stages of the treatment process can be performed. Finally, go further in the ^{131}I dynamics in the WWTP opens up the possibility to test a novel prognosis model (Hormann and Fischer 2018) that simulates the levels in both WWTP sewage effluents. The model works by dividing the interactions of ^{131}I along the treatment steps in three different stages, the primary treatment, the activated sludge reactors and the sewage effluent decanting tanks (WWTP scheme; Fig. 5.1). The modelling of the treatment process is based in concentrations changes during the treatment in the dissolved ^{131}I fraction and in the AEI phase. The model simulate the pathway of the particles along the process and the transference from the dissolved to the AEI phase in the activated sludge reactor. Moreover, the decay of the short-lived ^{131}I during the treatment is considered.

Intensive study of ^{131}I levels and partitioning in the WWTP-2 and in the reclaimed water line. Flows determination and modelling adaptation.

5.2 Objective

The aim of the present chapter is to determine the medically-derived radionuclides concentrations and dynamics in the different treatment steps of the integrated WWTP+RWTP facility chosen, reporting novel information of the presence of medically-derived radionuclides in reclaimed water. Further objectives are:

i) To advance in the present knowledge of the ^{131}I removal during the treatment

ii) To establish the ^{131}I levels in the reclaimed water

iii) To study the ^{131}I partitioning in a WWTP+RWTP facility by applying the methodology validated in Chapter 4

iv) To apply and assess the accuracy of the model proposed by Hormann and Fischer (2018) in order to predict the presence of ^{131}I in both sewage effluents of the WWTP-2

5.3 Water treatment plants description and samplings

5.3.1 WWTP-2 and RWTP-2 description

The integrated facility (Fig. 5.1) is located at the South of the Barcelona city and included in the BMA (41.312505 N; 2.126327 E) wastewater depuration network. The WWTP facility is a very large-sized treatment plant, which processes a total of 35 % of the urban wastewater produced in the Barcelona city and in other 8 municipalities (248,000 $m^3 \cdot d^{-1}$). The WWTP studied (WWTP-2) is the second largest in the BMA and the third in Spain per mean volume treated, where 1.0 M of inhabitants are registered as residents in the urban wastewater catchment area. Part of the sewage effluent is sent to a second facility (Fig. 5.1), the RWTP-2 where reclaimed water for reuse is obtained. A detailed scheme of both treatment processes can be found in Fig. 5.1 and explained in the following subsections.

WWTP:

The inflow wastewater (93 %) after the grift removals receive the effluents generated in the sludges line (general recirculation; 6 %) and the mix of both flows (primary inflow) comes into the wastewater treatment line for the primary and secondary treatments. The addition of the general recirculation flow gives rise to an increase of the presence of contaminants in the primary inflow in comparison with inflow wastewater values (Table 5.1).

Primary treatment (Settling tank): most of the suspended materials from the primary inflow are removed in the settling tank giving rise to the primary sludge. The mean value of TSS of the primary effluent represents only the 19 % of the concentration in the primary inflow showing a significant reduction in this treatment step. The mean hydraulic residence time of treated water in the primary treatment is 4 hours and the primary effluent is sent to the secondary treatment (Fig. 5.1).

Secondary treatment (CAS reactors and settling tank): the second stage of the treatment takes place into the reactors where flocs of microorganisms are suspended, known as mixed liquor suspended solids (MLSS). The treated flow is split into two lines (Fig. 5.1) with different operational characteristics. Both lines work with CAS treatments where the reactors are divided in 3 compartments, anaerobic, anoxic and aerobic taking the 8 %, 28 % and 64 % of the total operational reactor volume. Mean values of chemical oxygen demand (COD) and biological oxygen demand (BOD_5) show a significant decrease after the activate sludge reactors treatment, however, total nitrogen kjeldahl (TNK) levels show significantly differences between both activated sludge treatment lines (Table 5.1). After the final clarifica-

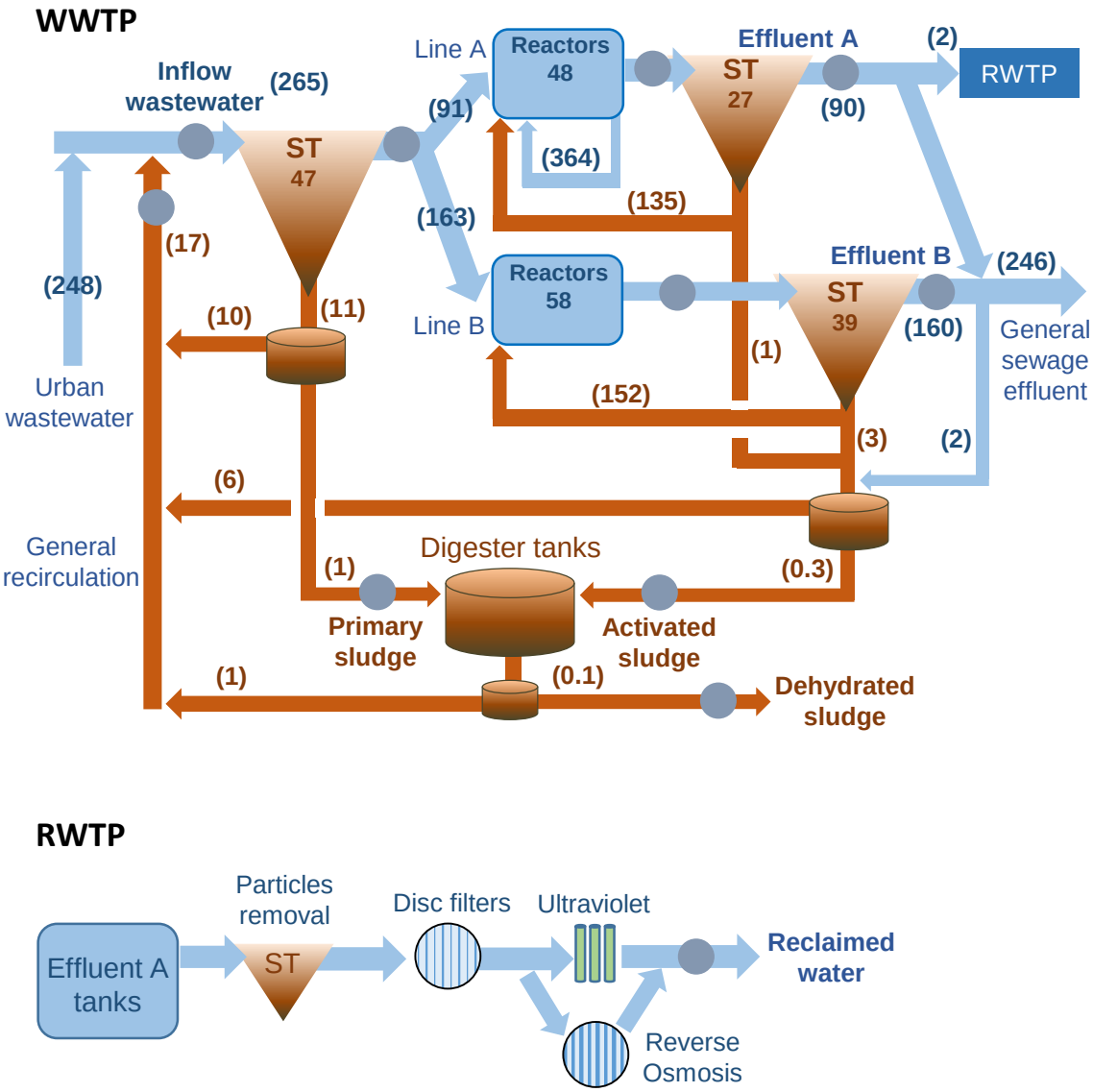

Figure 5.1: Design schemes of the treatment plants studied and sampling points marked with grey dots. Mean flow rates ($dam^3 \cdot d^{-1}$) above lines and dimensioning in dam^3 inside the settling tanks and reactors are detailed within brackets (AGBAR 2018). ST= Settling tank.

Table 5.1: Averages of the physicochemical parameters at different steps of the treatment process for the period 2014-2018 (AGBAR 2018).

	WWTP						**RWTP**
Physicochemical parameters	**Inflow wastewater**	**General recirculation**	**Primary inflow**	**Primary effluent**	**Sewage effluent A**	**Sewage effluent B**	**Reclaimed water**
pH	7.6	7.4	7.3	7.8	7.8	7.9	7.8
Conductivity (μS·cm^{-1})	2532	2914	2533	2340	1980	2205	1999
Turbidity (NTU)	211	1718	276	140	4	12	1
TSS (mg·L^{-1})	379	2600	750	139	10	26	5
TSS Organic materia	81 %	72 %	81 %	75 %	94 %	91 %	78 %
BOD_5 (mg·L^{-1})	318	720	565	165	4	11	2
COD (mg·L^{-1})	681	3201	1007	404	36	65	25
DOC (mg·L^{-1})	51	55	51	50	4	7	6
TNK (mg·L^{-1})	69	166	81	61	5	43	4
N-NH4+ (mg·L^{-1})	50	71	57	52	3	39	3
P-total (mg·L^{-1})	10	39	16	9	4	3	2

tion process in the decanter tanks, which reduces significantly the TSS (Table 5.1), the sewage effluent is partially sent to the RWTP tank in the case of the line A. The rest of the sewage effluent A together with the sewage effluent B is released 3.2 km into the Mediterranean Sea by undersea outfall 60 m depth as general sewage effluent. The activated sludge precipitated in the settling tanks is mainly carried to the reactors again, however, a reduced part is purged periodically in order to balance out the microorganism growing and maintain stable the MLSS concentration in the reactors.

Sludges line: the primary sludge decanted in the primary treatment (0.5% d.w.) is thickened in tanks generating a more concentrated by-product (3.7 % d.w.) and sent to sludge digester tanks for 3-4 weeks for biogas production. Similar process is carried out with the purged activated sludge (0.6 % d.w.) where the sewage sludge from the two lines is accumulated in a tank previously concentrated by centrifugation (3.9 % d.w.) and send it to the digester tank. Following the digestion of the mix of primary and activated sludge during weeks the total water content is decreased by centrifugation giving rise to the dehydrated sludge (24 % d.w.). The thickening and centrifugation processes in the sludges line, a part than progressively concentrate sludges around 150 times from the settling tanks to dehydrated sludge output, produce liquid effluents enriched in TSS that are mixed and carried to the beginning of the treatment as a general recirculation, amounting up to the 6 % flow of the primary inflow.

RWTP:

Tertiary treatment: Part of the sewage effluent A accumulated in tanks is treated in the RWTP. The treatment process in order to obtain the reclaimed water begin with the particles removal by the addition of coagulants, polyelectrolytes and powdered sand, and followed by disc filters (compounds <10 μm), disinfection with ultraviolet light and chlorination and a water re-oxygenation. Moreover a reverse osmosis line is sometimes used which include ultrafiltration and reverse osmosis treatments and a re-mineralization.

By comparing sewage effluent A and reclaimed water physicochemical parameters of turbidity and TSS values show a significant reduction, adjusting the water quality to the demands of reuse. A mean of 2,070 $m^3 \cdot d^{-1}$ are processed by the RWTP but in most cases is just for maintenance reasons. Main reuse applications of the RWTP effluent during the 2014-18 period were aquifer recharge (36 %), river flow increase (27 %) and wetland areas recovery (37 %). In the case of the Llobregat River the reclaimed water is released before the surfacte catchment point of a drinking water treatment plant (Chapter 6) with a maximum operational release achieved of 27,540 $m^3 \cdot d^{-1}$ for the period 2014-18 and a maximum capacity of 280,800 $m^3 \cdot d^{-1}$ ready

for working during intense drought periods. Furthermore, the RWTP distribution network is ready for industrial and irrigation uses.

5.3.2 Samples analysed

Between years 2014 and 2018 (Sampling dates; Appendix D.1 Tables D-G) multiple campaigns of radioactivity determination of water and sludges were carried out (Table 5.2). Furthermore, the primary inflow and both sewage effluents were sampled simultaneously in two periods along 5 and 8 consecutive days respectively while in the 5-days sampling primary sludge was also taken once per day and dehydrated sludge on Friday. Apart from study the daily variabilities, the continuous 24-h samplings along 5 and 8 days at the inflow and both effluents of the treatment, will be crucial for the validation of the ^{131}I prognosis model.

Table 5.2: Type, total number of samplings and analysis performed at the different steps of the treatment.

Sampling point	**General NM radionuclides determinations**		**Number of ^{131}I partitioning samples and analysis details**		
	Total samples analysed and type of sampling (punctual/pooled)	**Weekly samplings**	**AEI (sample volume)**	**ACH addition mL/L**	**BEI and RI (sample volume)**
WWTP					
Waters	**19/79**				
Primary treatment					
General recirculation	2/3	-	5 (2-7 L)	10	1 (4 L)
Primary inflow	1/24	2	2 (3-8 L)	10	1 (4 L)
Primary effluent	6/1	-	4 (0.6-6 L)	6	1 (4 L)
Activated sludge Line A					
Sewage effluent	5/27	2	2 (7-25 L)	1.5	1 (25 L)
Reactor	1/-	-	1 (4 L)	15	
Activated sludge Line B					
Sewage effluent	3/24	2	2 (7-25 L)	1.5	1 (25 L)
Reactor	1/-	-	1 (4 L)	15	
Sludges	**20/-**				
Primary	10/-	1	-		-
Activated	5/-	-	-		-
Dehydrated	5/-	-	-		-
RWTP					
Reclaimed water	11/-	-	2 (25 L)	1.5	1 (25 L)
TOTAL	**50/79**		**19**		**6**

The ACH dosage may vary for the AEI step depending on the TSS concentration in the sample (Hormann and Fischer 2017), which are detailed in Table 5.2, while the reagents dosages applied in the BEI step equals to those which have demonstrated a complete removal of ^{131}I as iodide (Dosage 5; Chapter 4). Moreover the

total concentration of ^{131}I was determined in most cases by direct measurement. However, in some cases when the ^{131}I partitioning method was performed and the total concentration has not been measured or the value has more uncertainty than those obtained by sum of the three fractions, the used total concentration was the sum of the ^{131}I fractions (Hormann and Fischer 2017).

5.4 Results and discussion

In the samples of waters and sludges analysed from the WWTP ^{131}I, ^{99m}Tc, ^{111}In, ^{67}Ga and ^{123}I radionuclides applied in nuclear medicine (NM) procedures were found. In contrast, ^{51}Cr, ^{54}Mn, ^{99}Mo, ^{153}Sm, ^{177}Lu, ^{186}Re, ^{198}Au, ^{201}Tl medically-derived radionuclides were not quantified above the MDA.

Firstly, the activity concentrations of ^{99m}Tc, ^{111}In, ^{67}Ga and ^{123}I in the studied water treatment facility are shown. Secondly, the results for ^{131}I total activity in water and sludge samples are presented while removal differences between line A and B, balances along the treatment process, ^{131}I partitioning results and model adjustment are discussed.

All the NM radidonuclides determinations were carried out following the procedures indicated in the *2. Materials and methods* section (Chapter 2) while the ^{131}I partitioning method is detailed in Chapter 4. Furthemore The experimental raw data from the present section is available in the *Appendix D.1* (Tables D-G) and the results from the WWTP-2 ^{131}I modelling tests in both sewage effluents with different factors can be found in the *Appendix D.2* (Tables J-W).

5.4.1 Presence of ^{99m}Tc, ^{111}In, ^{67}Ga and ^{123}I

Medically-derived ^{99m}Tc has been often found in the WWTP-2 waters (detection frequency of 29 %). Maximums for ^{99m}Tc and ^{111}In for all the waters of the WWTP analysed have been found in the general recirculation samples. ^{99m}Tc in water samples previous to the activated sludge treatment (general recirculation, primary inflow and primary effluent) has shown a relatively high percentage of detections >MDA of 70 % while in both sewage effluent lines was only 2 % (Table 5.3) which is partially explained for its faster physical decay during the treatment due to the hydraulic retention time as pointed out in Chapter 3.

In the daily sampling results of waters ^{99m}Tc (Fig. 5.2) was not found on Saturday and Sunday which is in agreement with the lower values and detection frequencies in a previous study including weekend samples (Fischer et al., 2009). Although ^{99m}Tc is one of the most administrated in NM, its short half-life (6.0 h) and the reduction of diagnosis procedures at weekends leads to lower values. In contrast, ^{111}In was detected in the 8 % of the total samples (Table 5.3). With reference to ^{67}Ga was found only twice in the sewage effluent A (0.73 ± 0.36 and 0.61 ± 0.28 Bq·L^{-1}) while ^{123}I once in the primary inflow (0.44 ± 0.29 Bq·L-1) and once in the primary effluent (0.74 ± 0.41 Bq·L^{-1}). Regarding reclaimed water any of those radionuclides were determined above MDA.

Table 5.3: Type, total number of samplings and analysis performed at the different steps of the treatment.

Sampling point	**^{99m}Tc (Bq·L^{-1})**				**^{111}In (Bq·L^{-1})**			
	n>MDA / n	**Min.**	**-**	**Max.**	**n>MDA / n**	**Min.**	**-**	**Max.**
General recirculation	2/5	3.3	-	17.3	1/5			0.39
Primary inflow	20/25	3.0	-	17.0	3/25	0.19	-	0.32
Primary effluent	3/7	1.0	-	5.9	0/7			
Reactors	2/2	2.0	-	3.4	0/2			
Sewage effluent A	2/31	0.7	-	10.9	2/31	0.12	-	0.26
Sewage effluent B	0/27				3/27	0.14	-	0.33
Reclaimed water	0/11				0/11			

In Fig. 5.3 sewage sludge results can be shown. The most frequently detected radionuclides in sewage sludges were ^{99m}Tc and ^{111}In (70 % and 75 % detection frequencies respectively). For the three types of sewage sludges studied primary sludge showed the highest activities for all the medically-derived ^{99m}Tc, ^{111}In, ^{67}Ga and ^{123}I, which is explained in part by significant differences of the radioactive decay associated to the sewage sludge age (Chapter 3). ^{67}Ga was detected >MDA three times in primary sludge and two in dehydrated sludge while ^{123}I once in primary sludge (Fig. 5.3). When the results from the weekly samplings in sewage sludges

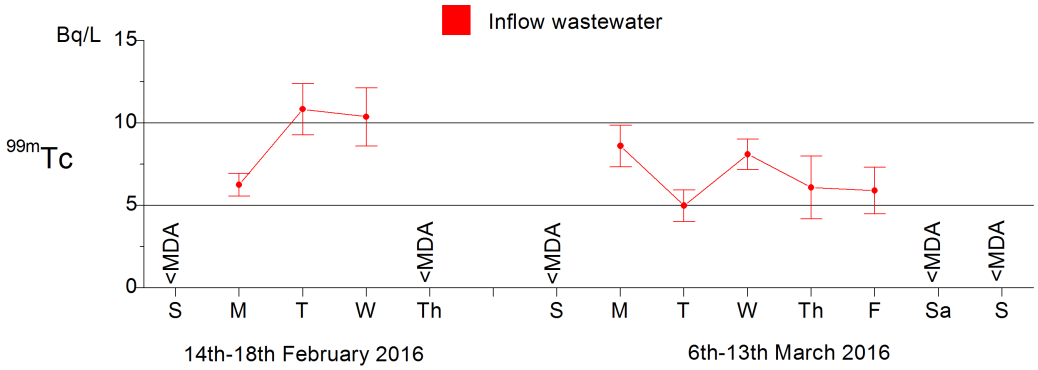

Figure 5.2: Results of ^{99m}Tc in weekly samplings at primary inflow.

(Fig. 5.3) are compared with those from another very large-sized plant of the same depuration system (WWTP-1; Chapter 3) two shared trends should be mentioned:

i) No presence of ^{99m}Tc at the beginning of the week in sewage sludge

ii) The effect of an increase of the $m^3 \cdot d^{-1}$ of primary inflow due to a rain event (47 % increase 2 days before the sampling; AGBAR 2018)), which gave rise to the minimum observed concentrations of ^{131}I, ^{99m}Tc and ^{111}In in primary sludge

Furthermore an evaluation from the radiological protection point of view of the levels found in the WWTP+RWTP can be performed. Although in sewage effluent ^{99m}Tc and ^{111}In exceed the levels reported in Chapter 3 and ^{67}Ga and ^{123}I were found above the MDA, the values in sewage effluent and sewage sludges were well below the very conservative levels taken as reference (Table 3.4; Chapter 3).

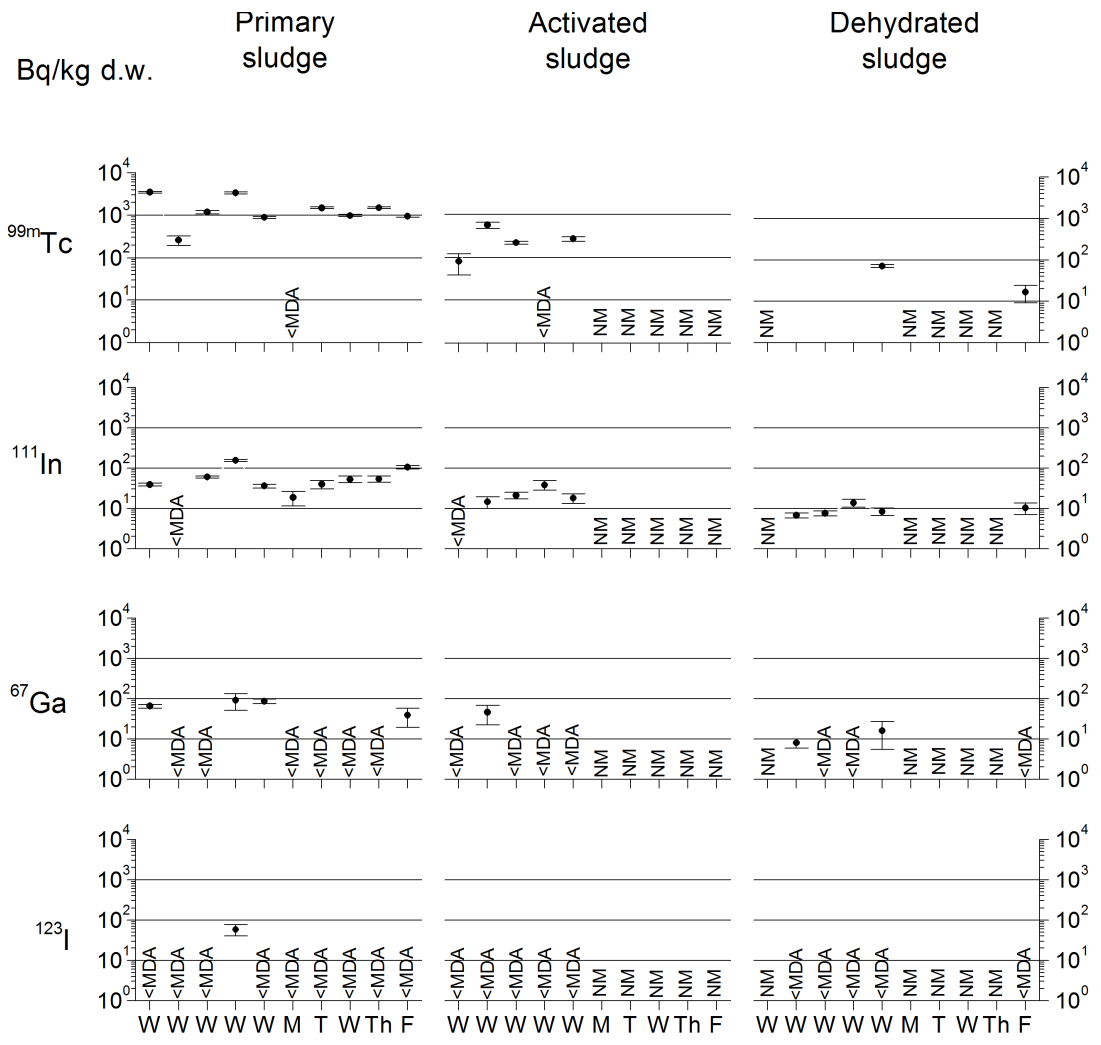

Figure 5.3: Specific activities of ^{99m}Tc, ^{111}In, ^{67}Ga and ^{123}I in sewage sludges. Five one-off samplings, the daily sampling of primary sludge for one week and the extra sampling for dehydrated sludge on Friday are shown. N.M.= Not measured.

5.4.2 ^{131}I levels in the WWTP+RWTP facility

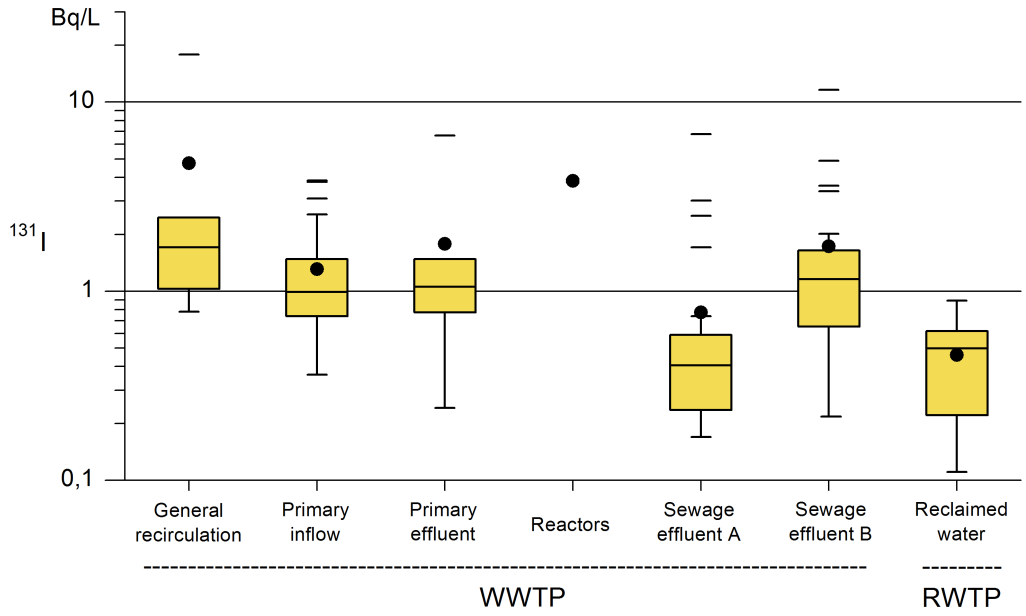

Figure 5.4: Boxplots of ^{131}I activities at the different sampling points of the treatment process. The line in the box and the circle correspond to the median and the mean respectively. Extreme cases outside the box (-) correspond to values lower than Q1-1.5*IQR or greater than Q3+1.5IQR.

In most of WWTP water samples taken at different stages of the facility ^{131}I has been determined >MDA (97 % detection frequency) which allows to point out a constant presence of ^{131}I. Only two samples of sewage effluent A, one of primary inflow and one of reclaimed water were <MDA and introduced in the Fig. 5.4 and 5.5 as 2/3·MDA. Primary inflow and the sewage effluents were sampled more times than the other points of the treatment and histograms with all the results are shown in Fig. 5.5. Specifically, the weekly samplings are shown at Fig. 5.6. Considering only the concentrations >MDA, ^{131}I punctually has achieved ratios from 19:1 to 58:1 from the highest to the lowest value in the different water sampling points analysed (Fig. 5.4) showing a wide range of values. The variability mentioned in waters can be remarked taking into account that a percentage between 11-20 % of the data in the sampling points are represented in the boxplot figure as outliers (Fig. 5.4). Regarding general recirculation 4 out of 5 samples showed ^{131}I concentrations between 0.78-2.4 Bq·L^{-1}, however, a punctual sample gave a ^{131}I maximum of 17.8 Bq·L^{-1}. Moreover, both line A and B reactors were sampled once reporting 3.8 and 3.9 Bq·L^{-1} respectively. After the analysis of reclaimed water samples medically-derived ^{131}I was found in the 91 % of the samples with a median value of 0.5 Bq·L^{-1}.

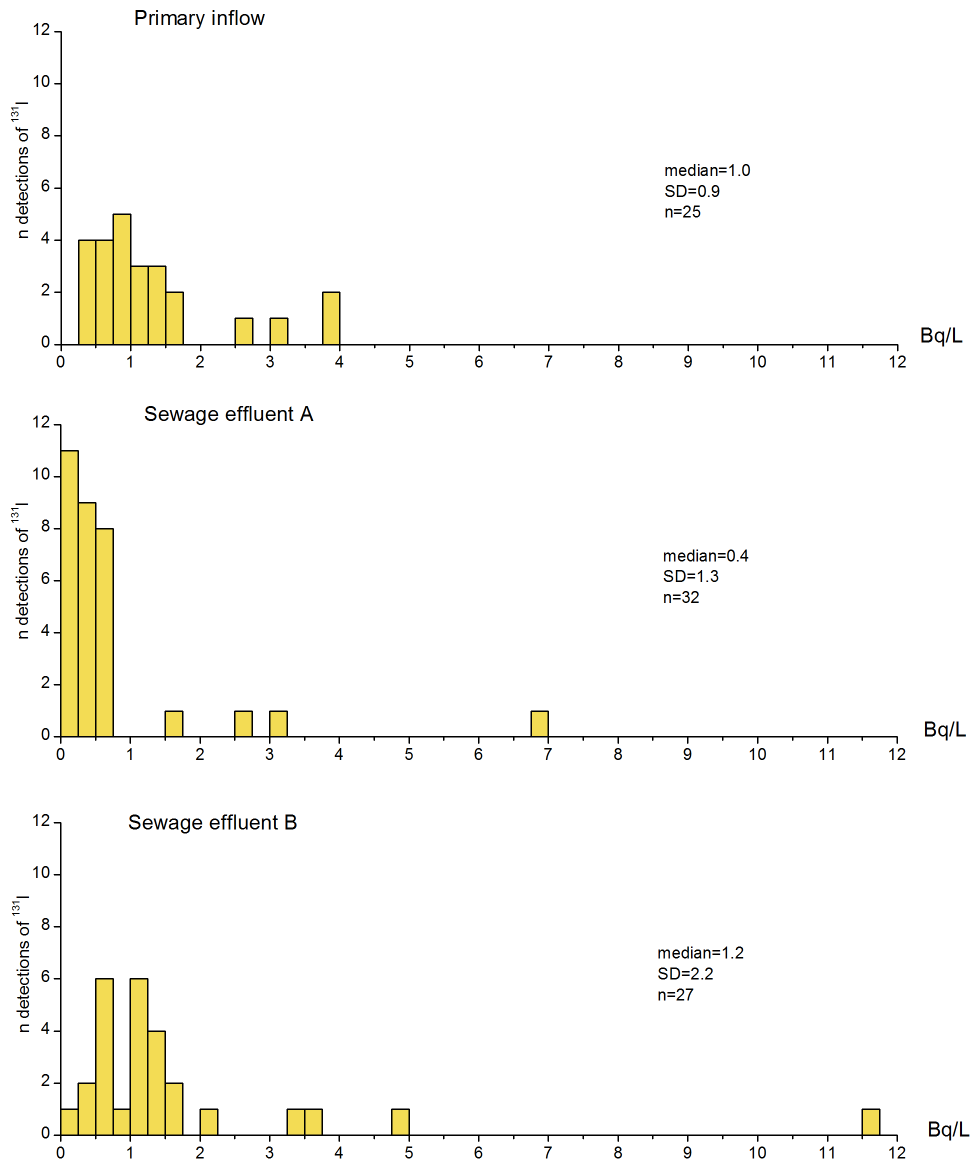

Figure 5.5: Histograms of ^{131}I activity concentrations found in primary inflow and both sewage effluents.

Taking into account the results from Fig. 5.4 the role of the treatment in the different concentrations of ^{131}I can be discussed. There is a intake process by the activated sludge supended in the line A reactors, reducing the concentrations in the following sampling points, the effluent A and reclaimed water. Thus, the removed ^{131}I is absorbed by the activated sludge of the reactors showing a higher mean than the other sampling points as in previous studies in WWTPs (Cosenza et al., 2015; Hormann and Fischer 2017).

In contrast, the median ^{131}I levels in primary effluent and in effluent B are not significantly influenced by the treatment. Furthermore the general recirculation flow have a median concentration above all the others studied, which is explained because contains TSS from the sewage sludge line which can contribute significantly to enrich primary inflow concentrations.

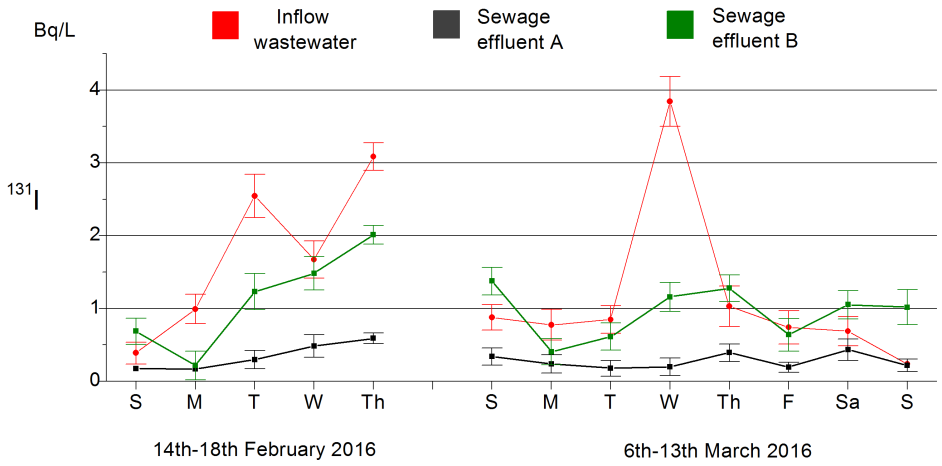

Figure 5.6: Results of ^{131}I in weekly samplings at primary inflow and both sewage effluents.

In contrast with water samples, sewage sludge ^{131}I activity ratios of 3:1, 2:1 and 3:1 in primary, activated and dehydrated sludge respectively showing the lowest ratios range (Fig. 5.7). Results were in agreement with the hypothesis that dilution effect and the catchment area characteristics stabilize the ^{131}I concentrations in sludges from the large-sized WWTPs (Chapter 3). Furthermore, a relationship in the dehydrated sludge were found between the cosmogenic ^{7}Be, medically-dervied ^{131}I and accumulated storm water in wastewater the last 30 days (Fig. 5.8). ^{7}Be increases its concentrations in sewage sludge during rain events due to the runoff in the catchment area (Fischer et al., 2014; Fischer et al., 2009) while medically-derived radionuclides including ^{131}I can decrease its concentrations due to the dilution of contaminants (Chapter 3). Thus, ^{7}Be/^{131}I ratio explains the variabilities of ^{131}I in dehydrated sludge and the dilution of ^{131}I in sewage sludge during rainfall events.

With the aim to contextualize the radiological risk of the levels found some reference levels can be taken in consideration. It is important to highlight that the mean ^{131}I concentrations found in the WWTP-2 effluents and sewage sludges are below the levels fixed in the very conservative risk scenarios of direct water ingestion by public and external irradiation by workers (Table 3.4; Chapter 3). Nevertheless, ^{131}I was the most significant NM radionuclide found in terms of radiological protection point of view.

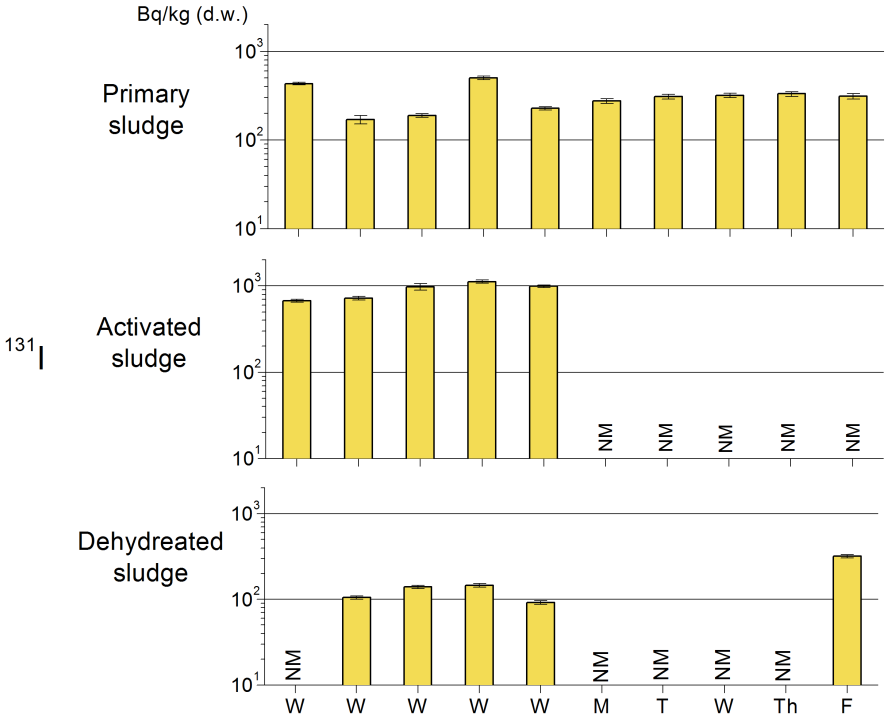

Figure 5.7: Specific activities of ^{131}I in sewage sludges. Five one-off samplings, the daily sampling of primary sludge for one week and the extra sampling for dehydrated sludge on Friday are shown. N.M.= Not measured.

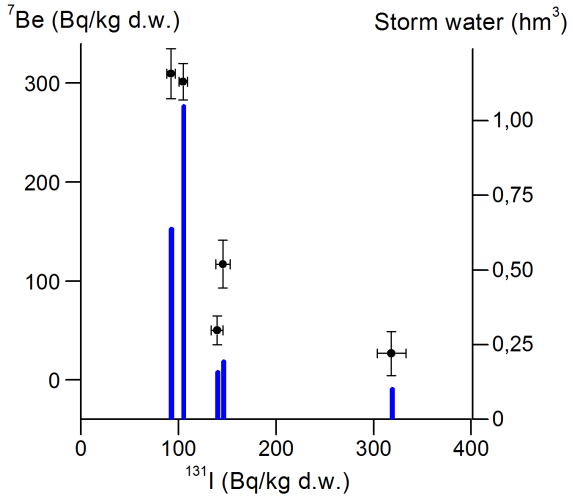

Figure 5.8: Relationship between ^{7}Be and ^{131}I concentrations in dehydrated sludge and total storm water treated in the WWTP along the 30 days before the sampling.

5.4.3 Removal analysis at both activated sludge lines

The ^{131}I values observed in the sewage effluents were systematically lower than the mean in the line A (Fig. 5.4) as well as the samples taken in the same day (Fig. 5.9) after comparison with line B results. The different operational conditions between activated sludge line A and B (Table 5.4) are behind the lower mean levels of contaminants in line A (Table 5.1). The most significant difference is the internal recirculation of the treated water in the line A reactors (Fig. 5.1; Table 5.4) which allows to increase significantly TNK removal (Table 5.1) in the anoxic compartment as N_2 (g) after nitrification and denitrification processes (Che et al., 2017). Other operational differences between line A in comparison with B (Table 5.4) consist in higher MLSS concentration of 19 %, sludge age (41 %), hydraulic retention time (83 %) and SVI (20 %).

Table 5.4: Operational characteristics in both line A and B CAS reactors.

Operational characteristics	**Line A reactors**	**Line B reactors**
Flow treated	34 %	66 %
Number of reactors x Volume (m^3)	5 x 10400	6 x 10400
Number of settling tanks x Volume (m^3)	5 x 5542	7 x 5542
MLSS (mg/l)	3503	2934
V30 (ml/l)[a]	212	223
SVI (ml/g)[b]	91	76
Hydraulic retention time (days)[c]	1.1	0.6
Sludge age (days)[c]	41	29
Sludge recirculation	Yes	Yes
Advanced TNK removal	Yes	No
Internal pumping	Yes	No

a) Solids decanted in 30 minutes in a Imhoff cone
b) V30 / MLSS
c) Data determined following the Chapter 3 (section 3.5.1.6) for the period 2014-2017

Line B works under operational conditions (Table 5.4) that allow to reduce significantly quality parameters as COD, BOD_5 and DOC but not TNK in contrast with line A that either reduce significantly TNK. Considering the TNK concentrations in the primary effluent and both sewage effluents the line A designed working conditions leads to a significantly higher TNK removal than B (a mean of 92 % and 25 % respectively; Table 5.1). Furthermore, the results also show that has significant influence also in ^{131}I removal by activated sludge and an influence of this kind of CAS operational conditions must be point out.

In line B the removal estimation by the primary and secondary treatments in the first and second sampled weeks is 31 % and 19 % taking into account mean values

from both sampling periods (Fig. 5.6). However, showed a mean reduction along the treatment in the effluent A of 76 % and 75 % (Fig. 5.2), significantly higher than most of the medically-derived ^{131}I removal of 1-28 % in WWTPs found before (Line B; Ham et al., 2002; Punt et al., 2007) and above the range of 50-75 % from WWTP given in Hormann and Fischer (2017).

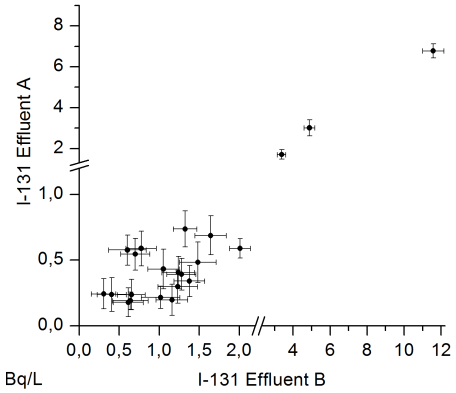

Figure 5.9: ^{131}I concentrations in both sewage effluents at the same sampling time.

5.4.4 ^{131}I partitioning in water samples

In Fig. 5.10 the results of the application of the ^{131}I partitioning metohd (Chapter 4) in samples taken in the different steps of the treatment process are shown. The results are divided in two differentiated bar-charts. Firstly, the total concentration is divided in the precipitable (AEI fraction which is defined as the extractable fraction after ACH addition and centrifugation) and the non-precipitable fractions. The non-precipitable ^{131}I value for each sample is obtained by subtracting the AEI fraction to the total ^{131}I activity. Secondly, in Fig. 5.10 the results of the second step of the ^{131}I partitioning method application to the non-precipitable fraction shows the BEI fraction, which corresponds to the ^{131}I expected to be found as iodide extracted through AgI formation. Moreover the RI fraction is shown, which corresponds to ^{131}I bounded to organic compounds and other no removed in the previous precipitates (Hormann and Fischer 2017). The percentages given for the BEI and RI are always relative to the non-precipitable ^{131}I fraction.

The percentage of AEI fraction in the analyzed samples allows discussing the pathway of ^{131}I along the WWTP (Fig. 5.10). The treatment can be divided by type of particles in two sides, first the primary treatment particles (primary treatment) and the activated sludge particles (reactors, effluents). The general recirculation receive mainly the sludges line effluents from primary and activated sludge steps. The AEI fraction has shown results between 17-29 % of precipitable ^{131}I in 4 out of 5 samples with a mean TSS concentration of 750 mg·L^{-1} (Table 5.1). However, in the GR2 sample has been found a significantly higher percentage (61 %) in the AEI fraction at the same time than a higher concentration of TSS (5,200 mg·L^{-1}). In the case of the primary treatment the non-precipitable ^{131}I fraction was predominant and a relative higher AEI fraction was observed in the inflow (10 and 24 %) than in the effluent (2-5 %) explained by the TSS significant removal in the primary treatment (Table 5.1). In the activated sludge reactor the AEI fraction has been revealed as the predominant in both A and B lines due to the ^{131}I absorption by the suspended microorganisms (Hormann and Fischer 2017), being the AEI/non-precipitable ^{131}I ratio higher in line A (1.1 $\pm$ 0.1 and 2.9 $\pm$ 0.7 respectively). In the case of the sewage effluents and reclaimed water the AEI fraction is lower than in the previous steps of the treatment due to the significantly TSS reduction (Fig. 5.1; settling) and reclaimed water obtention (Fig. 5.1; settling and filtration). The effluent A showed relatively higher results (3 and 5 %) than in the effluent B (0.8 and 1.0 %), that can be explained by the higher capacity of absorption of ^{131}I by the activated sludge in line A.

Regarding the non-precipitable phase, the BEI and RI fractions have been determined. After the analysis, significant differences between the WWTP and RWTP samples have been found. The BEI fraction has shown significantly higher percentage (86-95%) than the RI in all the samples of the WWTP due to predominance

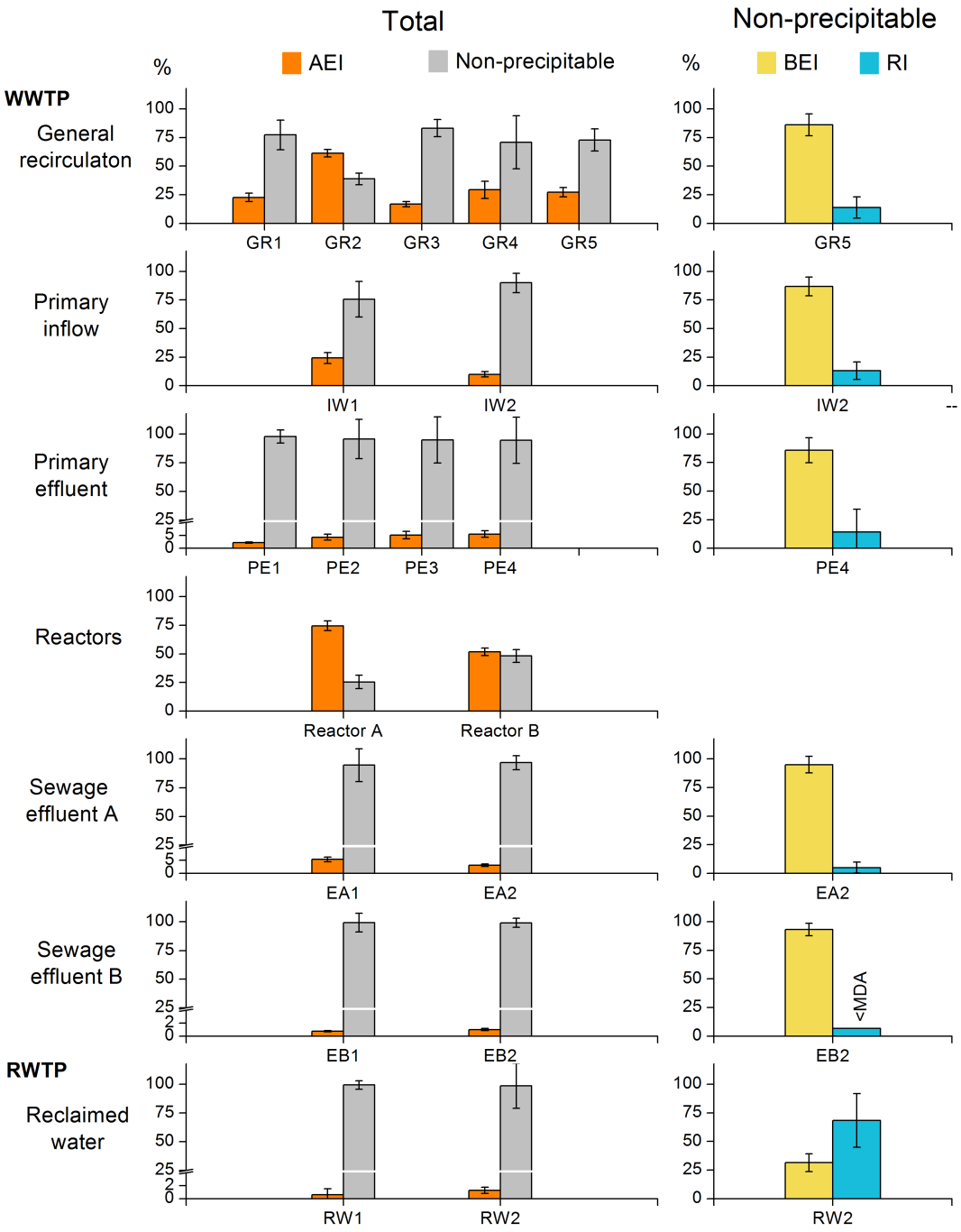

Figure 5.10: Sample codes and results for the ^{131}I partitioning analysis of different samples from the WWTP.

of ^{131}I as iodide in the sample. The prevalence of inorganic iodine in the WWTP samples is in agreement with the higher activity administered as Na^{131}I (Chapter 1; Table 1.3) and the excretion as $^{131}I^-$ (Legget 2010). In contrast, in the case of the results in the reclaimed water the percentage of the BEI fraction (32 %) is significantly lower than in the RI (68 %). The relative high presence of ^{131}I in the RI fraction can be attributed to a process of transformation of the iodide from the WWTP into forms present in the RI fraction. The most plausible hypothesis is the progressively incorporation of the radioactive iodide into DOC ($\bar{x} = 6.3$ mg·L^{-1}), especially to humic acids expected in the wastewater media (Rädlinger and Heumann 2000). The sewage effluent A is stored in a tank for a mean of 10 days during which can partially incorporate the ^{131}I as iodide into humic acids or colloids (Rädlinger and Heumann 2000; Rose et al., 2013).

In the case of the reduced percentage of ^{131}I that has been found in the RI fraction from the WWTP samples, several possible pathways can be taking into account to explain the presence of ^{131}I in the RI fraction:

i) Iodide (I^-) absortion by humic acids (Rädlinger and Heumann 2000)

ii) Despite a few treatments per year, the presence of organic compounds with ^{131}I is expected in wastewater due to excretions after radiopharmaceuticals administration (Chapter 1; Waffelman et al., 1997)

iii) Thyroid hormones from hyperthyroidism patients excretions (Legget 2010)

5.4.5 Flows of ^{131}I along the treatment steps

After the characterization of the concentrations of ^{131}I in the different steps of the wastewater treatment line and sewage sludge line and taking into account the WWTP+RWTP flows ^{131}I MBq·d^{-1} were determined (Table 5.5). The general sewage effluent ^{131}I flow was determined by summing the sewage effluent A and B as well as reclaimed water effluent. ^{131}I mean flow results are presented with a mean uncertainty by assuming a normal distribution of the dataset determined as MBq·d^{-1} ± standard deviation of the mean with a level of confidence k=2 (Table 5.5). The sum of the primary and activated sludges mean mass flows is far from the mean final sludge output (dehydrated sludge). The mass lost during the biogas obtention in the digestion tanks (20-30 %) as well as the recirculation of part of the sludge after the centrifugation process which generate the final dehydrated sludge (30-40 %) are behind the mass lost along the sewage sludge line.

Table 5.5: Flows of ^{131}I in the WWTP+RWTP.

Treatment Step	Flow[a]	Mean activity concentration	MBq/d	Unc. (k=2)
Water flow data	m^3·d^{-1}	Bq·L^{-1}		
General recirculation	17,000	4.7	61	± 83
Primary inflow	265,000	1.3	348	± 98
Sewage effluent A	90,000	0.8	70	± 40
Sewage effluent B	160,000	1.7	276	± 138
Reclaimed water	2,000	0.5	0.9	± 0.3
General effluent	ND	ND	346	± 143
Sewage sludge data	Tn d.w.·d^{-1}	Bq d.w.·kg^{-1}		
Primary sludge	45	307	14	± 3
Activated sludge	16	898	15	± 3
Dehydrated sludge	23	160	4	± 2

a) Mean operational data for the period 2014-2018

For the studied period (2014-2018), the ^{131}I released through the general effluent to the Mediterranean Sea was point out as the most relevant output source of ^{131}I from the WWTP+RWTP facility (Table 5.5). In contrast, for the dehydrated sludge the mean flow determined in the final solid outcome represents only the 1.2 ± 0.8 % of the ^{131}I released through the general effluent (Table 5.5).

Moreover regarding the internal ^{131}I flows at the WWTP+RWTP facility (Table 5.5) the following observations can be highlighted:

i) Most of the wastewater is treated in the line B where the ^{131}I removal is significantly lower than in line A giving rise to similar ^{131}I flows in the primary inflow and the general effluent (Chapter 5; section 5.4.3)

ii) In reclaimed water the relative lower mean volume and mean ^{131}I concentration than in the sewage effluents gives rise to a significantly lower ^{131}I flow

iii) In the case of the sewage sludge line internal flows, the influence in the reduction of the ^{131}I flow by radioactive decay was found significant during the anaerobic digestion of primary and activated sludges (Chapter 3)

iv) The ^{131}I flow from the general recirculation coming from the sludge line to the primary inflow can be significant

5.5 Model implementation in the WWTP

The compartmental model proposed by Hormann and Fischer (2018) has been implemented in the WWTP-2 and the simulated effluent activities confronted with the experimental results. A description of the model has been included as follows.

5.5.1 Modeling of the treatment steps and parameterization

The prognosis model input data and algorithms interacts in a specific design built with the Simulink® toolbox from the software package MATLAB® as well as a MATLAB® script file. Eventually the model reports the sewage effluent ^{131}I levels.

In the present implementation the conventional activated sludge branch of the model has been taken in agreement with the working conditions and design of the activated sludge reactors from lines A and B of the studied WWTP (Fig. 5.1). The input data correspond to:

Operational and dimensioning data of the WWTP:

i) The primary inflow flow ($m^3 \cdot h^{-1}$)

ii) Flow splitting factors along the treatment

iii) TSS concentrations along the treatment ($g \cdot L^{-1}$)

iv) Hydraulic retention time (h)

v) Dimensioning (m^3) of the compartments of the process

^{131}I concentrations and AEI fraction:

vi) Activity concentrations ($Bq \cdot L^{-1}$) determined experimentally in 24-hour pooled primary inflow samples along 5 or 8 consecutive days (Fig. 5.6)

vii) AEI fraction in primary inflow

Adjustable parameters:

viii) Kr transference constant in the activated sludge reactor (h^{-1})

ix) α parameter in primary(α_{pe}) and sewage effluent (α_{se}) settling tanks

The modelling basis of the most relevant steps of the implemented model are divided in three main steps and explained as follows:

(i) Primary treatment: The behaviour of ^{131}I concentrations in the primary treatment settling tank has been modelled following a phenomenological model (Fig.

5.11) in the step where the primary sludge (*ps*; Fig. 5.11) is obtained. In Fig. 5.11 blue arrows represent the flows of the dissolved activity (A_D) and the brown arrows of particulate activity (A_P). The parameters λ_{ini} and λ_{pe} in Fig. 5.11 equals to the AEI fraction in the primary inflow and effluent respectively can be determined experimentally or taken from bibliography. F_{pe} value is equal to the Q_{pi}/Q_{ps} flows ratio (Fig. 5.11). After the determination of the previous parameters α_{pe} factor can be determined (eq. 5.1) in order to perform the ^{131}I balances of AEI and dissolved fractions in the settling tank (Hormann and Fischer 2018).

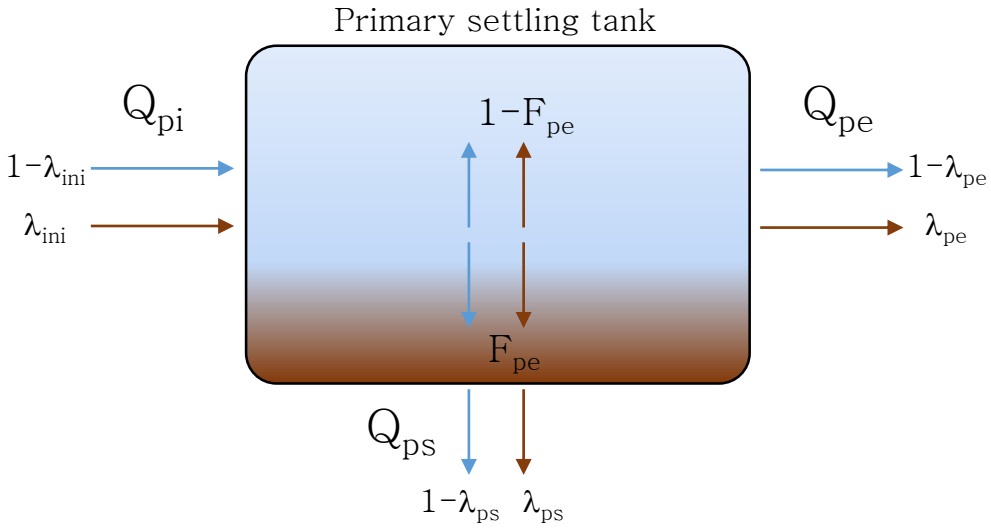

Figure 5.11: Scheme of the parameters associated to the primary settling tank modeling.

$$\alpha_{pe} = \frac{1}{F_{pe}} + \frac{1 - F_{pe}}{F_{pe}} \cdot \frac{\lambda_{pe}(1 - \lambda_{ini})}{\lambda_{ini}(1 - \lambda_{pe})} \tag{5.1}$$

(ii) Activated sludge reactors: The ^{131}I incorporation from the dissolved (A_D) to the AEI fraction (A_P) that takes place in the aerobic compartments of the CAS reactors is also modelled. Two coupled ordinary differential equations (eq. 5.2) are considered to model the ^{131}I behaviour concentrations in this stage of the treatment.

$$\begin{aligned} \frac{dA_D}{dt} &= -(\frac{Q(t)}{V} + \frac{ln2}{t_{1/2}}) \cdot A_D - Kr \cdot A_D + q_{D,in}(t) \\ \frac{dA_P}{dt} &= -(\frac{Q(t)}{V} + \frac{ln2}{t_{1/2}}) \cdot A_P + Kr \cdot A_D + q_{P,in}(t) \end{aligned} \tag{5.2}$$

The equations take into account the ^{131}I physical decay along this step where Q is the flow rate ($m^3 \cdot h^{-1}$) calculated by the model considering the input data and V the volume of the aerobic part of the reactor (m^3) and $t_{1/2}$ the half-life of ^{131}I. The $q_{D,in}$ and $q_{P,in}$ correspond to initial activity flows in dissolved and AEI fractions respectively determined by the model in function of the previous stages. Furthermore, the Kr constant parameter is defined in the preadjustment of the simulation (5.5.2 Preadjustment of the simulation).

(iii) Sewage effluent settling tank: The activated sludge reactor effluent is lead to the settling tanks with the aim to reduce significantly the TSS concentration (Table 5.1) removing most of the activated sludge suspended. The settling tank model considered for the primary treatment (Fig. 5.11) is also applied in the sewage effluent settling tank (Fig. 5.12). In Fig. 5.12 blue arrows represent the flows of the dissolved activity (A_D) and the brown arrows of particulate activity (A_P). In eq. 5.3 the α_{se} factor for the sewage effluent settling tank, which will define the particles removal in the settling tank, has been determined. The parameters λ_{rc} and λ_{se} are equal to the reactor effluent and sewage effluent AEI fractions respectively. The F_{se} parameter (eq. 5.3) has been obtained by the Q_{rc}/Q_{as} flows ratio obtention (Fig. 5.12).

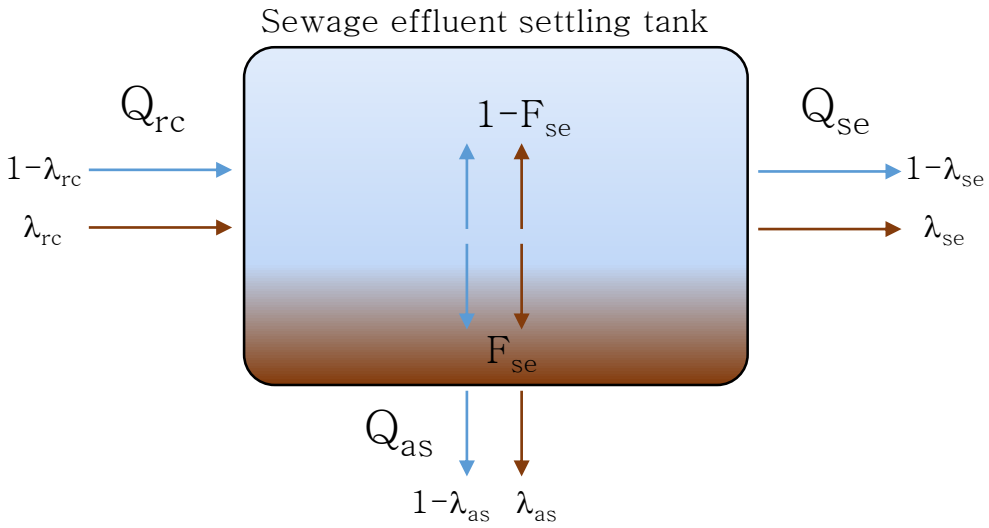

Figure 5.12: Scheme of the parameters associated to the sewage effluent settling tank modelling.

$$\alpha_{se} = \frac{1}{F_{se}} + \frac{1 - F_{se}}{F_{se}} \cdot \frac{\lambda_{se}(1 - \lambda_{rc})}{\lambda_{rc}(1 - \lambda_{se})} \tag{5.3}$$

5.5.2 Pre-adjustment of the simulation

The Kr parameter equals to the constant that regulate the transference of ^{131}I from the A_D fraction to the A_P fraction (eq 5.2). It is considered an intrinsic property of each conventional activate sludge reactor line and is determined by adjusting the simulated concentrations to the experimental values in the sewage effluent.

The two weekly datasets available of primary inflow concentrations (Fig. 5.3) were used as input concentrations. Specifically, the first ^{131}I experimental data of the sewage effluent activity concentration set is used for the adjustment of the estimated initial level of ^{131}I in the primary inflow. The reported concentration of the model should be within the limits of the first experimental value. The data obtained in the simulation is dividied in two steps:

t= 0 - 200 (h): During the first 200 h of simulation the WWTP fluxes are adjusted by introducing the inflow concentration that has been determined for the estimated initial level of ^{131}I in the primary inflow

t= 201 - end of the sampling in the sewage effluent (h): The results reported in this stage of the simulation equals to the simulated sewage effluents concentrations influenced by experimental ^{131}I primary inflow concentrations

5.5.3 Data validation method

In order to asses the goodness of the model, experimental concentrations from 24-hour samples in weekly campaigns were taken as reference. The figure of merit (FOM) methodology (eq 5.4) has been used to do it. The 24-h mean concentration reported by the model (x_i) and the 24-h pooled sample experimental value (y_i) are used.

$$FOM(\%) = \frac{\sum_{i=1}^{n} |x_i - y_i|}{\sum_{i=1}^{n} y_i} \cdot 100 \tag{5.4}$$

5.5.4 Model parameters adjustments and results

In the first step of the model adjustment Kr parameter has to be fixed for both lines (Fig. 11a and 12a) and figure of merit (FOM) value has been used for both cases in the adjustment evaluation (eq 5.4). The λ_{rc} and λ_{se} parameters which are necessary for the α_{pe} were determined experimentally as AEI fraction in the ^{131}I partitioning analysis for line A (Fig. 5.10; λ_{rc}=0.75 and λ_{se}=0.04) and line B (Fig. 5.10; λ_{rc}=0.52 and λ_{se}=0.01).

The data available for the two AEI fraction in the primary effluent (Fig. 5.10) are used in the λ_{ini} parameter definition, nonetheless, differ significantly. At this

stage of the process wastewater homogenization have not taken place yet and representativeness of two samples could not be enough. Thus, λ_{ini} value which has implications for the α_{pe} determination in the primary treatment was fixed bibliographically (Hormann and Fischer 2018) by assuming that the removal (eq. 5.5 ; R) of ^{131}I in the primary treatment is 1.5% (eq. 5.5; R=0.015). In contrast λ_{pe} has been determined as the mean of the AEI fraction values (n=4) obtained experimentally in the primary effluent (Fig. 5.10; λ_{pe}=0.042). Thus, in eq. 5.5 λ_{ini}=0.057 was determined for the primary settling tank.

$$\lambda_{ini} = \lambda_{pe} + R \tag{5.5}$$

Three different Kr have been tested in line A and B for the February 2016 and March 2016 datasets (green lines in Fig. 5.13a and Fig. 5.14a). Regarding both lines there are no expected significant differences in the Kr value between both dates due to proximity in time and working conditions. In the case of February 0.140 and 0.005 have been found as the Kr parameters with the lowest FOMs for line A and B respectively (Table 5.6). Nevertheless, significant differences in FOM values and consequently in the most favourable adjustment for the Kr value has been found between the February and March datasets (Table 5.6).

Table 5.6: FOM for the different datasets and parameters studied.

	Sewage effluent A			**Sewage effluent B**		
February 2016						
Kr (λ_{ini}=0.06)	0.120	0.140	0.160	0.005	0.015	0.025
FOM (%)	13	6	7	23	24	27
March 2016						
Kr (λ_{ini}=0.06)	0.120	0.140	0.160	0.005	0.015	0.025
FOM (%)	23	24	27	50	48	43
$\lambda_{ini}{}^{a}$	0.06	0.10	0.24	0.06	0.10	0.24
FOM (%)	39	34	28	50	48	43

a) The Kr was fixed as 0.140 and 0.005 for line A and B respectively

Specifically, in the case of March dataset the day 5 and 6 of simulation show the highest deviations from the experimental values with overestimations for the most favourable Kr parameters on February of 51 % and 71 % in line A and 58 % and 131 % in line B, respectively. These punctual deviations contrast with the rest of the March datasets. Since this behaviour appeared in both sewage effluent lines

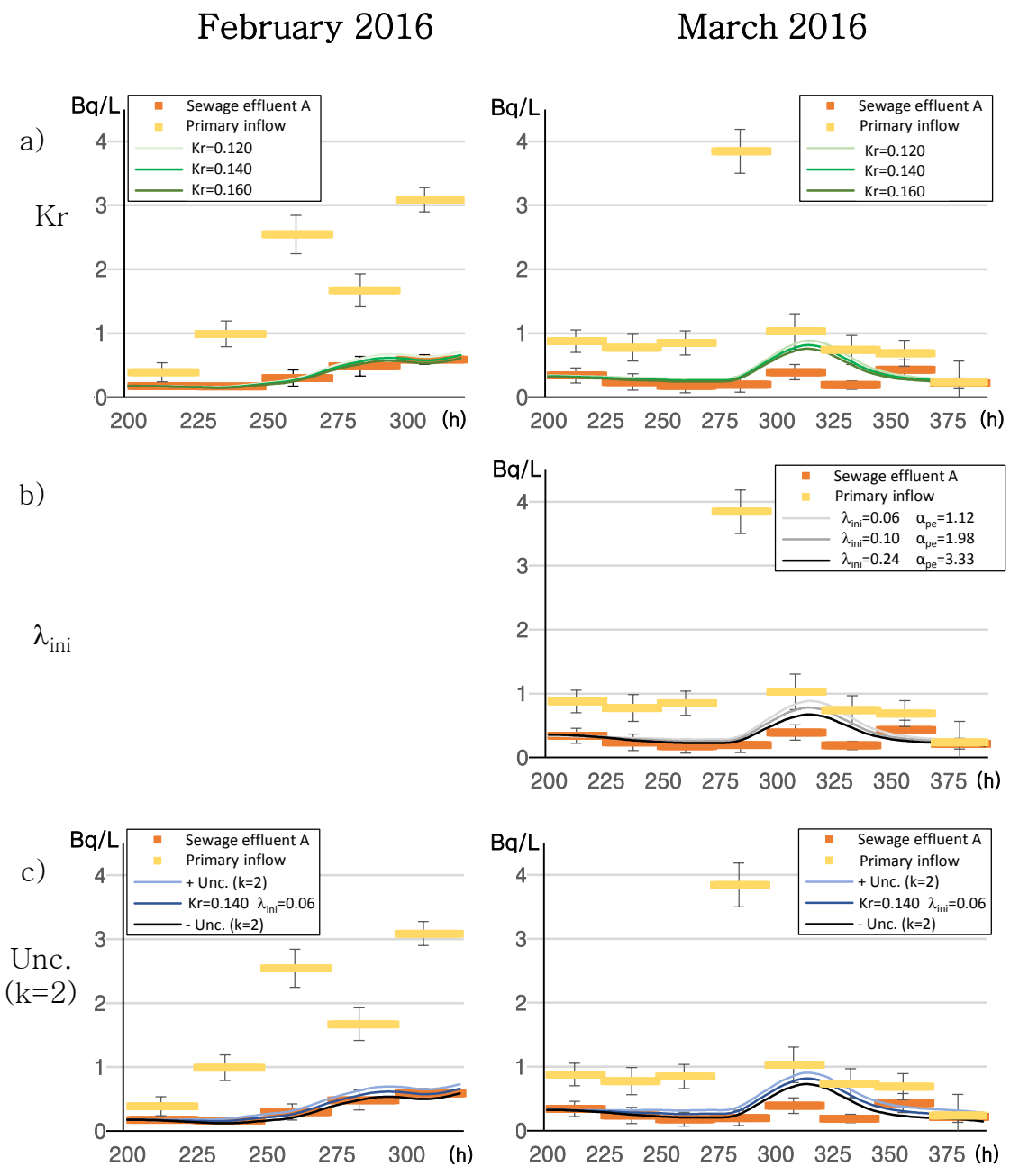

Figure 5.13: Adjustment of the simulation with experimental results with different **(a)** Kr and **(b)** λ_{ini} at sewage effluent A. The primary inflow input data for the model is also represented as well as **(c)** the final simulation with uncertainties.

one hypothesis is that a punctual recirculation with higher activity and percentage of ^{131}I in TSS (Fig. 5.8) affected the primary inflow λ_{ini} parameter assumed as constant.

With the Kr constant previously fixed for both lines, other λ_{ini} values were tested with the aim to find a better adjustment for the 5th and 6th days from the March 2016 dataset. The two experimental AEI fractions determined in the primary inflow (Fig. 5.10) were taken as λ_{ini} (Table 5.6; 0.10 and 0.24). Consequently the ^{131}I particulate fraction were higher, the removal were increased to 6 % and 20 % in the primary treatment and the R factor change (eq. 5.5; R=0.06 and R=0.10 respectively). In the new simulations the overestimation of the simulate data significantly decreases showing the most favourable FOM for 5th and 6th day of effluents simulated when the highest λ_{ini} were tested (grey lines in Fig. 5.13b and Fig. 5.14b).

Eventually the simulation has been represented including the uncertainties of the primary inflow ^{131}I data and the Kr most favourable parameters for February (blue lines in Fig. 5.13c and Fig. 5.14c). Taken into account the experimental uncertainties simulated values were between the experimental ones with the exception of the already discussed 5th and 6th days of simulation on March 2016 dataset.

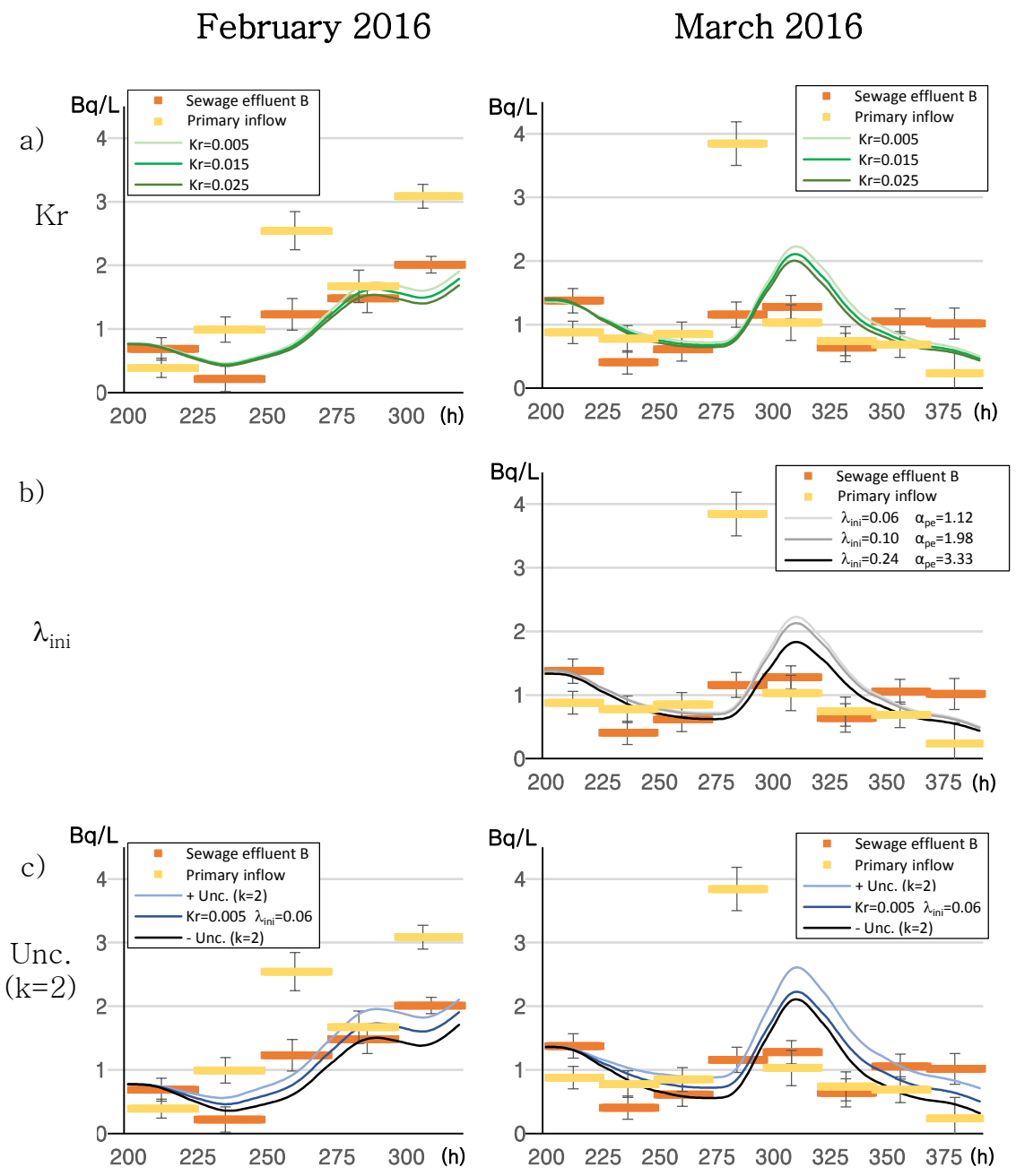

Figure 5.14: Adjustment of the simulation with experimental results with different **(a)** Kr and **(b)** λ_{ini} at sewage effluent B. The primary inflow input data for the model is also represented as well as **(c)** the final simulation with uncertainties.

5.6 Conclusions

The ^{131}I, ^{99m}Tc, ^{111}In, ^{67}Ga, and ^{123}I NM radionuclides were found in WWTP-2 waters and sludges. The exhaustive campaigns of measurements allowed to study the presence, detection frequencies and variabilities of NM radionuclides. The most frequently detected radionuclide was ^{131}I. Moreover ^{99m}Tc in the primary process samples and ^{111}In corresponding the highest levels to ^{99m}Tc at primary sludge. Specifically, ^{131}I variabilities were significantly higher in waters while values at sludges showed a relative higher stability.

In the case of the RWTP-2 it was confirmed that ^{131}I is still present in reclaimed water after the treatment. Taking into account the present findings, to perform risk assessment scenarios, ^{131}I should be considered in water reuse projects from large-sized WWTPs.

The most relevant radionuclide from the radiological point of view found in the WWTP-2 was ^{131}I. Study in detail the path of ^{131}I along the treatment has been also useful for a better understanding of the factors involved in the ^{131}I decrease levels in the treated flow. The present intensive study shows that the most favourable operational conditions in a conventional activate sludge for TNK removal also lead to a significantly relevant ^{131}I reduction in the studied plant.

Moreover, the partitioning methodology applied in the present section has revealed that during the WWTP treatment the ^{131}I precipitable and non-precipitable phases proportions are in agreement with the different procedures along the treatment plant. In the case of the non-precipitable part, iodine is mostly present as iodide. In contrast, in reclaimed water the dissolved ^{131}I predominates in the residual fraction of the analysis.

The model from Hormann and Fischer (2018) has been adapted to the WWTP-2 with a satisfactory data adjustment in most of the cases of the both sewage effluent lines. However, overestimation of simulated effluent concentrations have been occurred after a sudden increase of ^{131}I concentration, explained by the addition particles enriched in ^{131}I form the general recirculation to the treated flow in the primary treatment (λ_{ini} parameter).

Both methodologies, only previously tested in another WWTP before the present work, can be adapted to other WWTP as tools in order to improve future radiological risk assessment scenarios:

i) To establish the ^{131}I partitioning in the sewage effluent released or reclaimed water for reuse respectively

ii) To predict the ^{131}I concentration release through the sewage effluent

Chapter 6

Natural and artificial radionuclides in materials from a metropolitan DWTP

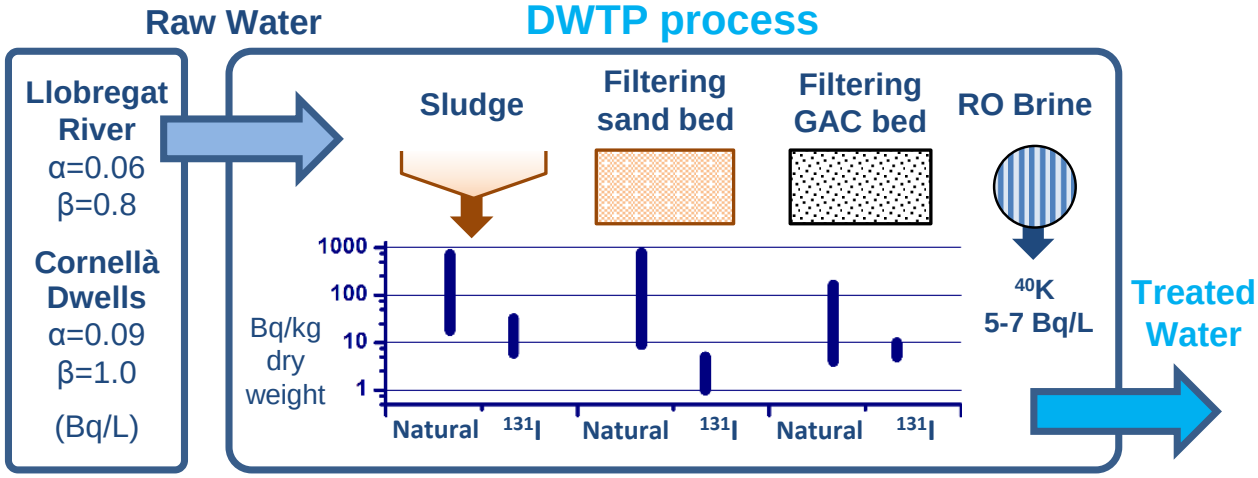

***Chapter published as:** Mulas, D., Camacho, A., Serrano, I., Montes, S., Devesa, R., Duch, M.A., 2017. Natural and artificial radionuclides in sludge, sand, granular activated carbon and reverse osmosis brine from a metropolitan drinking water treatment plant. *J. Environ. Radioact.* 177, 233–240. doi:10.1016/j.jenvrad.2017.07.001

6.1 Introduction: accumulation of radionuclides in DWTPs

Depending on water flow characteristics and water treatment technology, radionuclides will be removed from the water and will accumulate in by-products and other materials (Chapter 1). Extensive research has been devoted to radioactivity content in water, as in (Desideri et al., 2007; Karamanis et al., 2008), and how to reduce it (Baeza et al., 2006; Montaña et al., 2013b). Conventional drinking water treatment plants (DWTPs) have a fairly standard sequence of processes which essentially consist of solid separation using physical processes such as coagulation, flocculation, filtration and settling, together with chemical processes such as oxidation and final disinfection. In the review (Fonollosa et al., 2014), the authors highlighted the fact that the radioactivity content in sludge, mainly of a natural origin, is highly variable from plant to plant, depending on the characteristics of the raw water and also on the treatment followed by the plant. Consequently, the radiological risk of such sludge also depends on these factors. In addition, it should be pointed out that most of the previous studies do not provide information on the variability of the radioactivity content in DWTP sludges generated by the plants.

Despite the studies done in this field, at present information available on the radioactivity content in filtering materials and other byproducts routinely generated in the purification process in fullscale DWTPs is still scarce and studies have been done on plants with low-medium water treatment capacity (<1,000-94,043 population)(Kleinschmidt and Akber, 2008). Furthermore, there is no available prior published information which deals with the presence of medically-derived radionuclides in DWTP by-products and materials. Therefore, this study aims to provide novel information on the radioactivity content in by-products and different filtering materials from a large-scale metropolitan DWTP that treats both surface water and groundwater.

Evaluation of risk management of wastes containing natural and/or man-made radionuclides and their disposal is a matter of interest, since when the predicted exposure is not certain to be trivial, their disposal or re-use should be authorized depending on the regulatory requirements of each country. As regards naturally occurring radioactive materials (known as NORM), there are some studies related to different industries including water treatment e.g. the petroleum or mineral industry (Mora et al., 2016; Pontedeiro et al., 2007; Smith et al., 2003; Mulas et al., 2016). As regards artificial radionuclides in DWTPs, available studies are focused on postaccident scenarios (Jeong et al., 2014; Park et al., 2015) and do not deal with operational routines.

6.2 Objective

This work will contribute to the current knowledge in the field of presence and variability of radionuclides under real working conditions in materials from the DWTP-3:

i) Sludge

ii) Sand

iii) Granular activated carbon (GAC)

iv) Reverse osmosis (RO) brine

Furthermore, from a mid-term sampling campaign over six years, the radiological risk of the studied materials will be assessed by applying current international recommendations (EC 2013a; IAEA 2004).

6.3 Raw water and DWTP-3 characteristics

The plant under investigation supplies the Barcelona metropolitan area (more than 3.2 M inhabitants) with a maximum capacity of 5.3 $m^3 \cdot s^{-1}$. For the period 2007-2014 the plant supplied the distribution network with 74-100 $\cdot$ $10^6 \cdot m^3 \cdot y^{-1}$, which represents 30-50 % of the annual basis of the water for human consumption in the metropolitan area. The Llobregat River (LR) is the main source of raw water for the plant; however, sometimes the plant is supplied with wells.

Table 6.1: Raw water characteristics (2007-14).

	Min.	Median	Max.	SD	n
Llobregat River					
Flow treated per year[a] ($m^3 \cdot s^{-1}$)	1.9	2.7	3.7	0.88	8
$HC0_3{}^{-a}$ ($mg \cdot L^{-1}$)	174	402	581	71	88
Conductivity[a] ($\mu S \cdot cm^{-1}$)	624	1493	3046	381	88
K[a] ($mg \cdot L^{-1}$)	11	30	86	16	88
pH[a]	6.6	8.1	8.8	0.4	170
Suspended particles[b] ($mg \cdot L^{-1}$)	15	106	248	78	17
Gross Alpha Activity[c] ($Bq \cdot kg^{-1}$ d.w.)	500	800	1100	100	17
Gross Beta Activity[c] ($Bq \cdot kg^{-1}$ d.w.)	1200	1700	4400	100	17
Water (filtered <0.45µm)					
Gross Alpha[c] ($Bq \cdot L^{-1}$)	0.031	0.064	0.12	0.017	45
Gross Beta[c] ($Bq \cdot L^{-1}$)	0.447	0.83	1.482	0.229	45
Total Uranium[d] ($Bq \cdot L^{-1}$)	0.037	0.065	0.093	0.023	4
Cornellà Dwells					
Flow treated per year[a] ($m3 \cdot s^{-1}$)	0.24	0.61	1.15	0.32	8
Water (filtered <0.45µm)					
Gross Alpha[c] ($Bq \cdot kg^{-1}$ d.w.)	0.053	0.091	0.145	0.022	21
Gross Beta[c] ($Bq \cdot kg^{-1}$ d.w.)	0.735	1.032	1.217	0.148	21
K[c] ($mg \cdot L^{-1}$)	24	34	40	5	20

a) ACA (2015)
b) Data for particles >0.45 μm between 2012 and 2014 (LARA 2015)
c) LARA (2015)
d) Data from 2003 to 2006 (Camacho et al., 2010)

The surface water catchment area is located in the low LR basin close to the DWTP with a median flow rate of 6.7 $m^3 \cdot s^{-1}$. Characteristics of the Llobregat river water are shown in Table 6.1. Most of the gross beta activity corresponds to ^{40}K, due to the relatively high potassium and salinity concentration of the LR because

of NORM from mining activity and geological formations of evaporite-bearing materials in the upper-middle basin of the river (Fernández-Turiel et al., 2003). The total uranium activity in the LR basin was also studied and the mean activity at the collection point was found to be 0.060 $Bq \cdot L^{-1}$(Camacho et al., 2010). The middle and low river basins are both urban and industrial and receives effluents from waste water treatment plants.

Wells are used mainly in periods of drought or on isolated days when the river flowrate is low. They are also used when episodes of river water pollution prevent water extraction or when water quality fails to reach the water company's specifications. The wells are located on the Vall Baixa Sedimentary Aquifer, in particular in the area known as Cornellà. The aquifer is recharged mainly by natural infiltration from LR (ACA 2005) and ^{40}K is the main contributor to the beta activity (Table 6.1).

Treatment at the metropolitan DWTP (Fig. 6.1) is based on physical removal of particles and elimination of dissolved compounds and is detailed as follows.

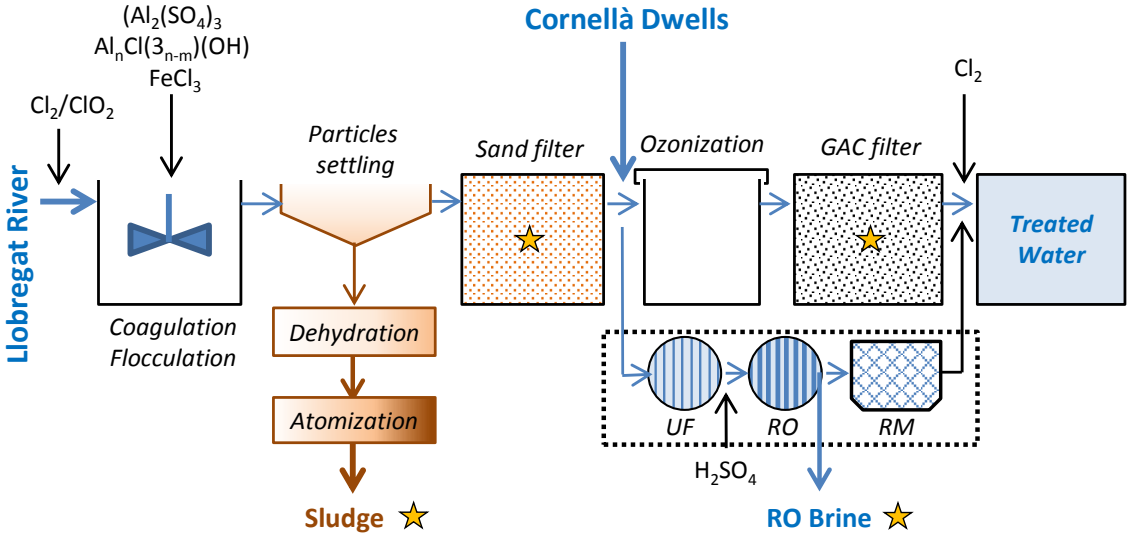

Figure 6.1: DWTP scheme and sampled by-products and materials (star). UF= Ultrafiltration, RO= Reverse Osmosis, RM= Remineralization.

Particle removal, only used for LR surface water: after chlorination and addition of coagulants, most of the particles are removed from the influent in static coned-shaped decanters where the water flows upwards. Sand bed filtration is applied after coagulation for final clarification. The sludge from decanters, after thickening, sieving, dehydrating, addition of NaOH and atomizing (500 °C) is obtained

as 150 mm dry particles. About 3500 tonnes of atomized sludge are generated each year.

Dissolved compound removal: after groundwater is taken into the plant, the flow is divided into two treatment lines. In the first one, ozonization is carried out before granular activated carbon (GAC) bed filtration (3000 m^3 of carbon installed). In order to reinforce the plant facilities a second parallel line was installed in 2009 where the water flow passes through ultrafiltration (UF) and reverse osmosis (RO) membranes which produce $6{\cdot}10^6$ m^3 RO brine per year.

6.4 Samples analysed

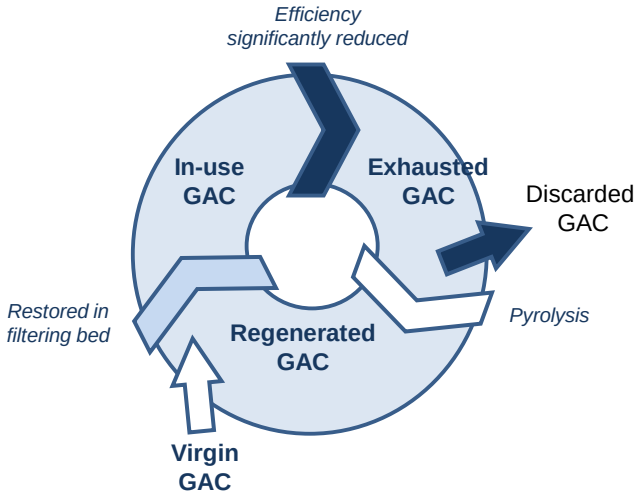

Figure 6.2: GAC cycle in the DWTP. The sampled GACs are in bold.

During the period 2007-2014 15 sludge, 4 sand, 22 GAC and 3 RO brine samples were taken at the DWTP (Table 6.2). The sludge was sampled over 2012-14, at least twice a year, for the dehydration and atomization steps as well as the data from sludge samples from the same plant reported in Montaña (2013) were taking into account for the present analysis. The filtering sands were collected once a year at three different sites of the filtering area. Furthermore, one sample of virgin sand was analyzed. GAC samples were collected at different stages during their usage cycle. Once the material reaches the plant, the adsorption capacity of the GACs is monitored by means of the iodine index (milligrams of adsorbed iodine per gram of carbon; ASTM 2014). The GAC is used until their efficiency is significantly reduced. At this stage the GAC is regenerated in industrial ovens by pyrolysis and is subsequently returned to the plant to be re-used (Fig. 6.2). After some regeneration cycles the GAC must be substituted by virgin material.

Table 6.2: Sampling data and radioniclides determined in the DWTP samples.

Sample	Date	Radionuclides analysed	
		Primordial and daughters, ^{7}Be and ^{137}Cs	^{131}I
Sludge			
Montaña (2013)			
Sludge	10/07/2007	x	
Sludge	30/10/2007	x	
Sludge	29/02/2008	x	
Sludge	06/06/2008	x	
Sludge	10/10/2008	x	
Sludge	11/12/2008	x	
Sludge	06/04/2009	x	
Campaings 2012-2014			
Dehydrated	23/10/2012	x	x
Atomized	23/10/2012	x	x
Dehydrated	30/10/2012	x	x
Atomized	30/10/2012	x	x
Dehydrated	07/02/2013	x	x
Atomized	07/02/2013	x	x
Dehydrated	02/07/2014	x	x
Atomized	02/07/2014	x	x
Sand			
Filter 1-1	22/09/2014	x	x
Filter 2-2	22/09/2014	x	x
Filter 3-1	22/09/2014	x	x
Virgin	15/10/2014	x	
GAC			
Virgin	03/06/2013	x	
Virgin	09/01/2014	x	
Virgin	09/01/2014	x	
Regenerated	06/05/2013	x	
Regenerated	13/05/2013	x	
Regenerated	14/05/2013	x	
Regenerated	28/05/2013	x	
Regenerated	03/06/2013	x	
In-use filter 1	30/10/2012	x	
In-use filter 5	30/10/2012	x	
In-use filter 14	30/10/2012	x	
In-use filter 15	30/10/2012	x	
In-use filter 5	28/01/2013	x	x
In-use filter 7	28/01/2013	x	x
In-use filter 13	28/01/2013	x	x
In-use filter 14	28/01/2013	x	x
In-use filter 18	28/01/2013	x	x
In-use filter 19	28/01/2013	x	x
Exhausted filter 1	02/07/2014	x	x
Exhausted filter 4	02/07/2014	x	x
Exhausted filter 8	02/07/2014	x	x
Exhausted filter 10	02/07/2014	x	x
RO Brine			
Sample 1	23/10/2012	x	
Sample 2	30/10/2012	x	
Sample 3	07/02/2013	x	

6.5 Results and discussion

The laboratory procedures implemented during the sample pre-treatment and the radionuclides specific activities determinations using gamma spectroscopy techniques are detailed in the *2. Materials and methods* chapter. All the experimental data represented in figures and tables in the present section can be found in the *Appendix D.1* as raw data (Tables H and I).

6.5.1 Primordial and daughters, ^{7}Be and ^{137}Cs

Specific activities in dry weight of primordial and daughters radionuclides (^{238}U decay chain; ^{238}U, ^{226}Ra and ^{210}Pb, ^{232}Th decay chain; ^{228}Ra and ^{228}Th, and also ^{40}K), cosmogenic ^{7}Be and artificial ^{137}Cs were determined in sludges (Fig. 6.3), sands, GACs and RO brines (Tables 2 and 3).

6.5.1.1 Sludge

The results in terms of activities in dry weight are shown in Fig. 6.3 as boxplots.

^{238}U decay chain: sludges showed a ^{238}U median concentration value of 47 Bq·kg^{-1} d.w. and a range of results between 33 and 88 Bq·kg^{-1} d.w. with a relative standard deviation (RSD %) of 30 %. For ^{226}Ra (RSD 17 %) the obtained median specific activity (29 Bq·kg^{-1} d.w.) was slightly lower than for ^{238}U and the results ranged within 18-35 Bq·kg^{-1} dry weight. Furthermore, variability of ^{226}Ra in the studied plant is also much lower than the RSD of 69 % found for its short-lived daughter radionuclide ^{214}Pb in the sludges from an Ebro River DWTP (Palomo et al., 2010a).^{210}Pb has shown similar results to those obtained for ^{238}U with an interval of 39-85 Bq·kg^{-1} d.w. and a mean value of 55 Bq·kg^{-1} d.w. (RSD 20 %). The results are in agreement with those reported in South East Queensland, Australia (^{238}U: 30-250 ^{226}Ra: 6-120 ^{210}Pb: 10-110 Bq·kg^{-1} dry weight; Kleinschmidt and Akber, 2008) and also with the wide range of results reported in the Fonollosa et al. (2014) review. The results indicate that ^{238}U and ^{226}Ra are not in secular equilibrium in the studied sludge, specifically the mean ^{238}U/^{226}Ra ratio of specific activities is 1.7. This is explained if we take into account the existence of ^{238}U in particulate, colloidal and dissolved phases in the Llobregat basin, the presence of significantly higher concentrations of ^{238}U rather than ^{226}Ra in the dissolved and colloidal fraction (Camacho et al., 2010) and the physicochemical interactions between these phases. The observed disequilibrium could be explained by taking into account the fact that dissolved and colloidal ^{238}U enrich other colloids and particles in the LR basin with ^{238}U (Chabaux et al., 2008). Finally, most of these colloids and particles with an extra amount of ^{238}U are removed from the treated flow during coagulation, flocculation and particle settling, and are caught in the final sludge (Baeza et al., 2006;

Gäfvert et al., 2002). On the other hand, direct precipitation of the dissolved ^{238}U as salt within the sludges is discarded as a significant enrichment pathway since the LR physicochemical properties (Table 6.1) are not favourable to this process (Baeza et al., 2006).

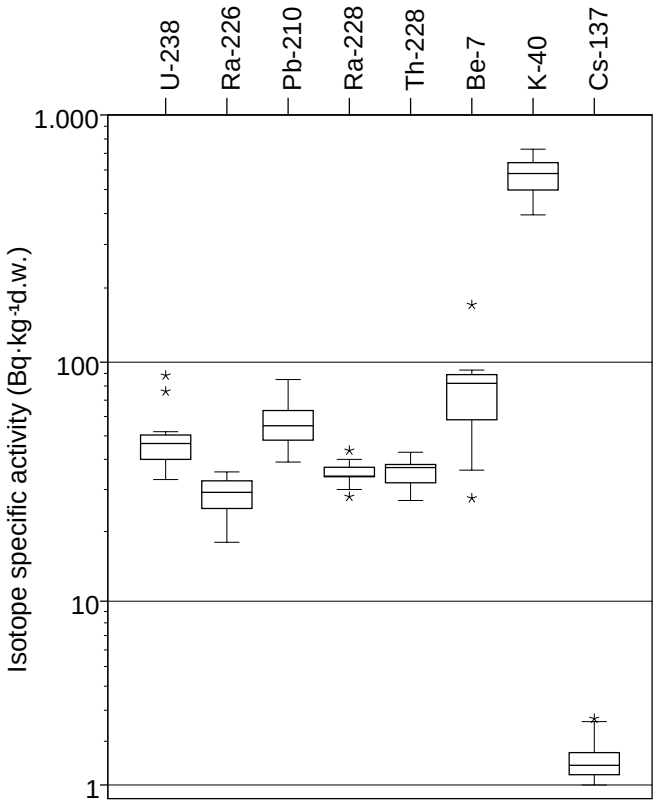

Figure 6.3: Boxplot diagram with the radionuclides specific activities detected in 15 sludges (dry weight). ^{7}Be and ^{137}Cs shown one result below the MDA not included. Extreme cases (star) correspond to values lower than Q1-1.5IQR or greater than Q3+1.5IQR.

^{210}Pb is also not in secular equilibrium with its parent isotope, since it has two possible sources: ^{210}Pb coming from the ^{226}Ra present in the sludges, and ^{210}Pb coming from atmospheric deposition phenomena in the river basin, known as unsupported ^{210}Pb$_u$ (Grossi et al., 2016; Rose et al., 2013; Saari et al., 2010). The amount of ^{210}Pb$_u$ can be estimated as follows:

$$C^{210}Pb_u = C^{210}Pb - C^{226}Ra \tag{6.1}$$

where C is the specific activity of the corresponding radionuclide. Fig. 6.4 shows that there is a high correlation between $^{210}Pb_u$(4-60 Bq·kg^{-1} d.w.) and ^{7}Be, a radionuclide of a cosmogenic origin. These results agree with those published in (Maringer,1996), which pointed out that ^{7}Be, ^{137}Cs and ^{210}Pb were transported in rivers bound to solids.

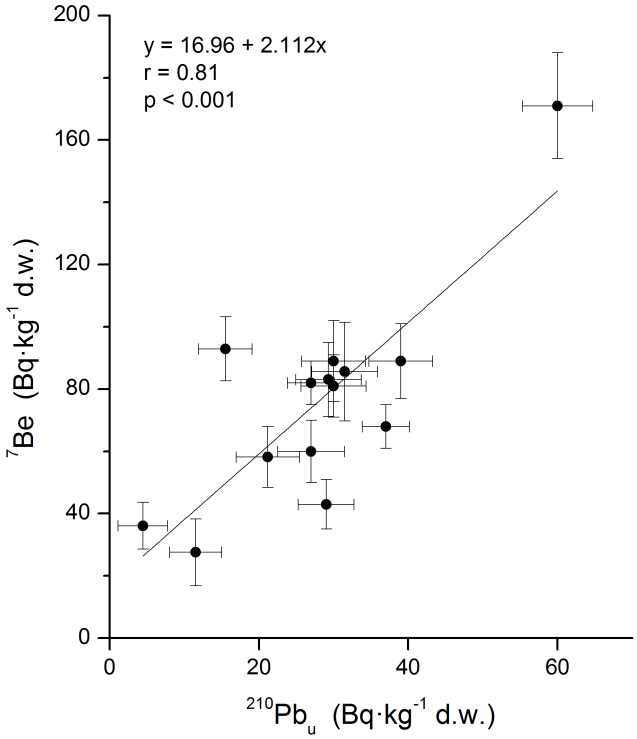

Figure 6.4: Correlation determined in sludges between ^{7}Be and $^{210}Pb_u$. The correlation data correspond to linear regression and a line was drawn to follow it.

^{232}Th decay chain: in contrast to the behaviour observed for the ^{238}U decay chain, similar median concentration values were obtained for ^{228}Ra and ^{228}Th (34 and 37 Bq·kg^{-1} d.w. and an interval of results of 28-44 and 27-43 Bq·kg^{-1} d.w. respectively) with a low RSD (11 % and 12 %, respectively). These results are different to the higher variabilities and ranges obtained in (Palomo et al., 2010a) for the short-lived ^{228}Ra and ^{228}Th decaying products, ^{228}Ac (12-212 Bq·kg^{-1} d.w.; RSD 37 %) and ^{212}Pb (4-92 Bq·kg^{-1} d.w.; RSD=42 %),respectively. The results near secular equilibrium, with a mean ^{228}Ra/^{228}Th ratio of 1.0 and low thorium

solubility for the LR pH range (Table 6.1), indicated that both radionuclides would be mainly contained in the particles removed from the inflow water into the sludge.

^{40}K, ^{7}Be and ^{137}Cs: natural ^{40}K showed the highest activity values (median value of 580 Bq·kg^{-1} d.w., range: 395-728 Bq·kg^{-1} d.w.; RSD=17 %), followed by cosmogenic ^{7}Be (mean value of 82 Bq·kg^{-1} d.w., range: 28-175 Bq·kg^{-1}; RSD=45 %). However, artificial ^{137}Cs specific activity shows the lowest median activity value of the radionuclides quantified in sludges, 1.4 Bq·kg^{-1}, with a range of 1.0-2.7 Bq·kg^{-1} d.w. and a RSD of 32 %. The high ^{40}K activity values could be explained by the geological characteristics of the basin and the potassium NORM mining activity, and were similar to the wide ranges found in previous studies on DWTP sludges. However, the ^{40}K activities found in our study showed a significantly lower range than those found by Palomo et al. (2010a) (127-1321 Bq·kg^{-1} d.w.) at an Ebro River plant (Spain) and they were one order of magnitude lower than the maximum result of 4600 Bq·kg^{-1} d.w. reported in Palomo et al. (2010b) for a Guadalhorce River plant (Spain). In the case of ^{7}Be, results are compatible with the wide range of results reported by other authors (4-353 Bq·kg^{-1} (Fonollosa et al., 2014);). The high variability of the ^{7}Be content is related to seasonal differences in the atmospheric wet and dry input fluxes in the LR basin area (Grossi et al., 2016) and sediment re-suspension phenomena (Saari et al., 2010). As regards ^{137}Cs, the presence of this radionuclide in sludge is due to solids transported in rivers (Maringer, 1996). The ^{137}Cs activity values showed a lower range of 1.0-2.7 Bq·kg^{-1} d.w. than a previous study of an Ebro River treatment plant (0.9-6.5 Bq·kg^{-1} d.w.; Palomo et al., 2010a)

6.5.1.2 Sand

The obtained results are detailed in Table 6.3. A slight increase in ^{228}Ra and ^{228}Th (^{232}Th series) activities can be observed in used sands. This result is possibly related to the progressive accumulation of particles and colloids at this treatment stage (Zevi et al., 2005). A large ^{40}K enrichment, one order of magnitude above the values observed in virgin sand, was observed. ^{40}K enrichment is probably due to the same reasons as those predicted for ^{228}Ra and ^{228}Th. However, the higher accumulation is likely to be because of the biofilm that usually covers the sand grains (Haig et al., 2011), as it assimilates both nutrients and potassium, apart from the fact that ^{40}K is the most abundant radionuclide in the raw water flow (Montaña et al., 2013b)(Table 6.1). In addition, ^{7}Be and ^{137}Cs could not be quantified above the minimum detectable activity (MDA), and no significant increase in the of ^{238}U decay chain isotopes was found.

6.5.1.3 GAC

Results for the activities found in GAC samples are given in Table 6.4 and showed as the mean ($\bar{x}$) ± standar deviation from the mean (S). An increase in the activities

Table 6.3: Specific activities ($Bq{\cdot}kg^{-1}$) of ^{238}U, ^{226}Ra, ^{210}Pb, ^{228}Ra, ^{228}Th, ^{7}Be, ^{40}K and ^{137}Cs determined in sands and RO Brine. Data below the detection limits is noted as <x.

	$Bq{\cdot}kg^{-1}$ (d.w.)			**$Bq{\cdot}L^{-1}$**	
	Virgin sand (n=1)	**Used sand (n=3)**		**RO brine (n=3)**	
	Activity ± Unc.	Min. - Max.	n > MDA	Min. - Max.	n > MDA
^{238}U Series					
^{238}U	10 ± 5	11 - 15	3	<4	-
^{226}Ra	9.6 ± 0.7	8 - 10	3	<0.4	-
^{210}Pb	<10	<11 - 15	2	<6	-
^{232}Th Series					
^{228}Ra	5 ± 1	5 - 12	3	<0.6	-
^{228}Th	6.3 ± 0.5	7 - 14	3	<0.3	-
Other					
^{7}Be	<4.5	<11	-	<2	-
^{40}K	12 ± 5	20 - 766	3	5 - 7	3
^{137}Cs	<0.3	<0.7	-	<0.2	-

Table 6.4: Iodine index(I_2 mg · GAC g^{-1}) and specific activities of ^{238}U, ^{226}Ra, ^{210}Pb, ^{228}Ra, ^{228}Th, ^{7}Be, ^{40}K and ^{137}Cs ($Bq{\cdot}kg^{-1}$ d.w.) determined in GAC.

	Virgin (n=3)		**Regenerated (n=5)**		**In-use (n=10)**		**Exhausted (n=4)**	
	$\bar{x}$ ± S	Min. - Max.	$\bar{x}$ ± S	Min. - Max.	$\bar{x}$ ± S	Min. - Max.	$\bar{x}$ ± S	Min. - Max.
Iodine Index		N.D. - 865	757 ± 29	724 - 788	665 ± 108	484 - 805	561 ± 21	532 - 581
^{238}U Series								
^{238}U		<24	63 ± 9	53 - 73	86 ± 21	60 - 121	148 ± 14	129 - 164
^{226}Ra	7 ± 3	4 - 10	11 ± 2	9 - 13	13 ± 7	4 - 29	32 ± 3	29 - 34
^{210}Pb		<20		<15		<13 - 32	24 ± 6	<19 - 31
^{232}Th Series								
^{228}Ra	7 ± 2	5 - 9	10 ± 3	7 - 14	12 ± 5	<4 - 22	17 ± 4	12 - 22
^{228}Th	5 ± 1	4 - 6	7 ± 1	6 - 8	11 ± 6	4 - 22	17 ± 2	14 - 18
Other								
^{7}Be		<32		<57		<46		<20
^{40}K	39 ± 2	<13 - 40		<18	46 ± 19	<15 - 67	26 ± 9	<15 - 34
^{137}Cs		<2		<1		<3		<1

N.D.= No data
The results < MDA are not considered to quantify the $\bar{x}$ and S
MDA in the table equals the highest obtained

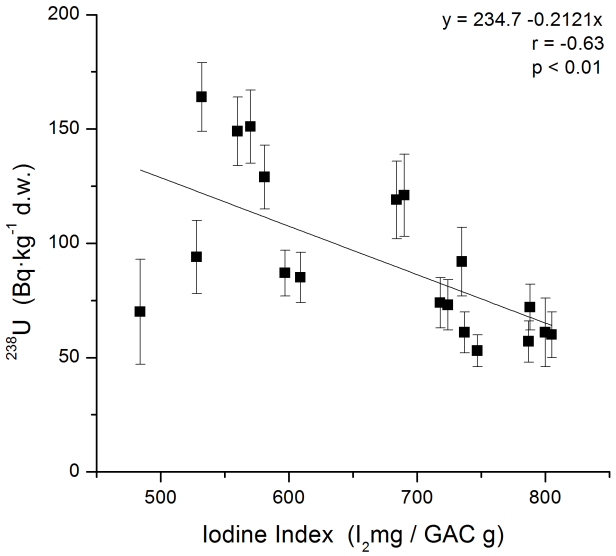

Figure 6.5: Scatter plot between the Iodine Index and the ^{238}U specific activities in regenerated, in use and exhausted GACs. Linear regression is suggested for the negative correlation.

of some isotopes belonging to the ^{238}U and the ^{232}Th decay chains can be observed, with a greater degree of enrichment for exhausted GAC, up to six times higher than the specific activities of virgin GAC. This phenomenon is more pronounced for ^{238}U with a maximum specific activity of 164 ± 15 Bq·kg^{-1} d.w. in exhausted carbons. In spite of the regeneration process, regenerated GAC showed a mean value of ^{238}U higher than virgin GAC which probably indicates that the pyrolysis process does not fully remove the ^{238}U, but reduces it significantly (mean relative reduction of 57 % among exhausted and regenerated carbons). Furthermore, a slight but significant increase of ^{226}Ra, ^{228}Ra and ^{228}Th between virgin and exhausted GAC was verified. The ^{210}Pb present in GAC may have two different origins, either the ^{210}Pb present in the water flow or the ^{210}Pb from the adsorbed ^{222}Rn (Watson and Crawford-Brown, 1991). As regards ^{40}K, in spite of its high content in raw water, no ^{40}K specific activity increase was found. It is therefore possible to state that GAC did not retain dissolved ^{40}K. Results from the present study for GAC are similar to the values obtained in Australia (Kleinschmidt and Akber, 2008) for ^{226}Ra ^{210}Pb and ^{40}K. In the case of ^{238}U, the specific activity was one order of magnitude higher than the value obtained in the Australian study, which is possibly explained by the relatively low ^{238}U concentration in the Australian raw water (1.2 mBq·kg^{-1}; Kleinschmidt and Akber, 2008) in comparison with raw water from the LR (Table 6.1). ^{238}U/^{226}Ra (4.7 ± 0.3), ^{238}U/^{228}Ra (8.9 ± 1.5) and ^{238}U/^{228}Th (8.9 ± 0.6) mean ratios ± standard deviation in exhausted GACs are significantly higher than those found in sludges (1.7 ± 0.4, 1.4 ± 0.4 and 1.4 ± 0.5). To explain this, the fact that GAC treats

both LR water and groundwater should not be taken into account because treated groundwater represents a lower proportion of the total LR raw water processed (Table 6.1). In addition, as mentioned above, the aquifers are recharged mainly by LR infiltration and this would suggest that no significant differences are expected in the dissolved fraction of both waters. Therefore, the observed activity ratios are mainly due to the fact that river particles with lower ratios have been eliminated from the water flow in the particle settling step, and therefore very little ^{226}Ra, ^{228}Ra and ^{228}Th is present in the water flow at this stage. The observed ^{238}U activity values are related to the capacity of the GAC to remove ^{238}U through diffusion, pore transport and adsorption and can be estimated to be very low (<1%) due to the LR pH range (Kütahyalı and Eral, 2004; Mellah et al., 2006; Villalobos-Rodríguez et al., 2012). Finally, the fact that the iodine index is negatively correlated with the ^{238}U concentrations found in regenerated, exhausted and in-use GACs should be highlighted (Fig. 6.5), confirming a progressive accumulation of these radionuclides, while the GAC adsorbs other compounds and becomes saturated.

6.5.1.4 RO Brine

In Table 6.4 results of the samples analyzed are shown. ^{40}K was found in all of them, with a maximum value of 7 ± 1 Bq·L^{-1}. This result follows previous research by our group, reported in (Montaña et al., 2013b), which determined a removal capacity of 90 % for beta activity in the RO step at the Llobregat DWTP by comparing the gross beta activities in raw and treated waters. Although very significant reduction of alpha activity (mainly for uranium activity) was found (Montaña et al., 2013b) for the RO step for the Llobregat DWTP, ^{238}U could not be quantified above the MDA in the studied samples since the estimated specific activity (0,5 Bq·L^{-1}) was lower than the MDA of the applied methodology (gamma spectrometry, 4 Bq·L^{-1}).

6.5.2 Medically-derived ^{131}I

Results of ^{131}I activities in dry weight obtained for sludges, sands and GACs are shown in Fig. 6.6. The highest range of specific activities corresponded to dehydrated sludges, with relatively stable ^{131}I specific activity of 29-36 Bq·kg^{-1} dry weight. In contrast, atomized sludges showed a lower range of results (<11-16 Bq·kg^{-1} d.w.). The ^{131}I relatively short half-life (8.02 days) together with the possibility of partial iodine vaporization (184 ^{o}C) at the atomization process would explain the differences found between dehydrated and the final atomized sludges. ^{131}I was also found in sand samples with a maximum value of 6.1 ± 0.5 Bq·kg^{-1} d.w., but showed the lowest interval for specific activity compared with the other studied materials. As regards GAC samples, only 4 “in use” samples and 1 “exhausted” sample had quantifiable values with a maximum value of 28 ± 8 Bq·kg^{-1} dry weight. No ^{131}I was found in the two RO brine samples analyzed (<1.0 and <1.4 Bq·kg^{-1} d.w.).

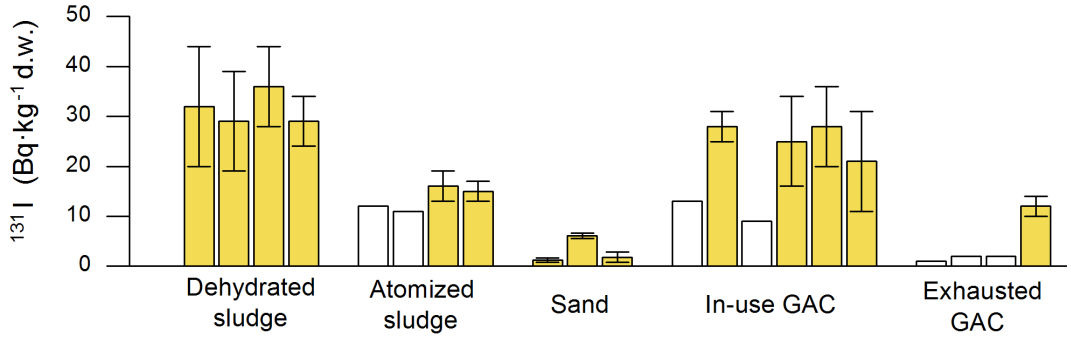

Figure 6.6: ^{131}I specific activities in dehydrated and atomized sludge sand and in-use and exhausted GACs. Non-colored bars represent the MDA.

The proposed distribution for medically-derived ^{131}I detailed in Hormann and Fischer (2014) for aquatic media is considered for discussion of the ^{131}I results: inorganic cation ($^{131}I^-$), dissolved organic and particulate. ^{131}I found in sludges was mainly associated with the ^{131}I contained in precipitated particles. The ^{131}I present in sands could be either due to the removal capacity of the sand for small particles or iodine that would be incorporated by the biofilm that usually covers sand grains. This biofilm adsorbs nutrients from the treated flow (Haig et al., 2011) and could intake dissolved organic iodine and I^-. Furthermore, as regards the ^{131}I found in GAC, it is possibly due mainly to the extremely high dissolved iodine adsorption efficiency of this material (Jeong et al., 2014; Park et al., 2015).

The presence of ^{131}I in sludge, sand and GAC could result directly from wastewater treatment plants discharges in the middle and low LR basin, upstream from the DWTP surface water catchment area. Medically-derived ^{131}I removal by wastewater treatment plants is between 1 and 56% (Fischer et al., 2009; Ham et al., 2003; Punt et al., 2007). Therefore, ^{131}I is introduced into the physicochemical dynamics of the LR through plant discharges and is thus present in colloids, particles and is also quickly diagenetically remineralized (Rose et al., 2013a).

6.5.3 Radiological risk assessment

As regards the sludge generated in a DWTP, its re-use for different applications in Spain such as additives in the cement industry (Rodríguez et al., 2010) or as ceramic bricks (Torres et al., 2012) have been considered in recent years. Therefore, the risk associated with their use in building materials has been evaluated. The Euratom 2013/59 Directive (EC 2013a) establishes reference levels for indoor gamma radiation emitted from building materials, and defines the activity concentration index (I) that should be used:

$$I = \frac{C^{226}Ra}{300\ Bq{\cdot}kg^{-1}} + \frac{C^{232}Ra}{200\ Bq{\cdot}kg^{-1}} + \frac{C^{40}K}{3{,}000\ Bq{\cdot}kg^{-1}} \tag{6.2}$$

where C is the specific activity of the corresponding radionuclide in the building material. In the case of ^{232}Th, its daughter ^{228}Ra concentration is also considered equal (EC 2013a) and used in the present study. The index relates to the gamma radiation dose, in excess of typical outdoor exposure, in a building constructed from a specified building material. Although the index applies to the building material and not to its constituents, it could be used as a preliminary conservative approach. An index value of I=1 might result in the reference level of 1 mSv·y^{-1} (indoor external exposure to gamma radiation emitted by building materials, in addition to outdoor external exposure) being exceeded. The radiological risk of the studied materials has also been assessed by comparison of the obtained concentration values with the exemption levels proposed by the IAEA (2004), and which have been adopted by the European Commission in the Euratom Directive 2013/59 (EC 2013a). Doses to individuals as a consequence of specific activities below these levels would be unlikely to exceed about 1 mSv·y^{-1}.

Table 6.5: Ranges of the specific activities found above the MDA in solid materials (sludge, sand and GAC) and its corresponding activity concentration values for exemption or clearance of materials which can be applied by default to any amount and to any type of solid material (EC 2013a). Also the activity concentration index is shown and quantified in the sludges by applying equation (6.2).

	Min.	-	Max.	Exemption level
Solid materials (Bq·kg^{-1}) d.w.				
Primordial and daughters				
^{238}U series	4	-	164	<1,000[a]
^{232}Th series	4	-	44	<1,000[a]
^{40}K	15	-	766	<10,000
Other				
^{7}Be	28	-	171	<10,000
^{131}I	1	-	36	<10,000
^{137}Cs	1	-	3	<100[a]
Sludge as a building material				
Index (I)	0.34	-	0.54	≤1

a) Assuming secular equilibrium with its daughters

The exemption values for the specific activities in moderate amounts of any type of material are not applicable in our case since moderate quantities would mean of the order of one tonne of material.

A radiological evaluation of materials from the DWTP was done of waste and also for use in recycling and re-use (used and exhausted GACs, sand and sludge, dry weight). A specific evaluation for sludge recycling as a building material was carried out because of the good properties shown by atomized DWTP sludges for use in the concrete industry (Rodríguez et al., 2010). Comparison of the obtained results with the corresponding exemption levels (Table 6.5) indicate that doses to individuals would be unlikely to exceed 1 mSv $\cdot y^{-1}$. As regards using sludge as a building material, the obtained gamma index (Table 6.5) showed that the 80% of the samples had $I \leq 0.5$, which means an external gamma dose of $\leq$0.3 mSv$\cdot y^{-1}$ while the other 20% showed I values up to 0.54, which indicates that gamma dose would be well below 1 mSv$\cdot y^{-1}$ in all cases. Therefore, the gamma index is not expected to exceed the reference value in agreement with the radionuclide concentration variabilities obtained in the present study (Fig. 6.3).

Although ^{40}K content in reverse osmosis brine does not pose a radiological risk, it is possible to state that any discharge of this effluent into the Mediterranean Sea would not mean a significant increase of the existing natural concentration. ^{40}K values (Table 6.4) are lower than the activity of 12 Bq$\cdot L^{-1}$ corresponding to the potassium average in seawater (390 mg$\cdot L^{-1}$; Castro et al., 2007).

6.6 Conclusions

The present study provides information on the radioactivity content in by-products and different filtering materials from the large-scale metropolitan DWTP-3 treating both surface and groundwater. When possible, the results have been compared with the findings of other authors.

The distributions of radionuclides in by-products and different filtering materials, as well as the study of their correlations, have provided information on the different behaviour of natural and artificial isotopes in the studied DWTP.

The highest specific activities ($Bq \cdot kg^{-1}$ d.w.) reported for sludge (727 ± 53), sand (766 ± 37) and RO brine (7 ± 2) correspond to ^{40}K. The maximum concentration in the case of exhausted GAC was found for ^{238}U (164 ± 15) while lower mean values were found in regenerated and in-use GACs and significantly lower in virgin GAC confirming accumulation during its implementation. In addition, the measurements confirmed the presence of traces of biomedical ^{131}I (<1-38 $Bq \cdot kg^{-1}$ d.w.) in sludge, sand and GAC, which indicates its presence in raw water.

Furthermore, this work has provided information on the levels and variability of the activities of different radionuclides in sludge samples. Over a period of 6 years relative standard deviations (RSDs) ≤20 % were found for ^{226}Ra, ^{210}Pb, ^{228}Ra, ^{228}Th, ^{40}K and ^{131}I. On the other hand, greater variability was observed (RSD ≥30 %) for ^{238}U, ^{7}Be, ^{137}Cs and $^{210}Pb_u$.

The radiological risk of the analysed materials was assessed by taking into account the exemption levels proposed by the European Commission and the IAEA. Although all these materials accumulated both natural and man-made biomedical radionuclides, they do not pose a radiological risk.

Chapter 7

General conclusions and future work

In agreement with the aims of the present thesis screening studies at 9 water treatment plants from the Barcelona metropolitan area (BMA) urban water cycle management network have been performed. The work covered different type of samples (waters, by-products and filtering materials) and influence parameters.

Regarding the preliminary analysis of the levels found, a total of 5 out of 7 most administrated radionuclides in nuclear medicine (NM) in the European Union were detected in the wastewater treatment plants (WWTPs). In general, the levels and detection frequencies measured in the seven WWTPs from the BMA sit well with the radiopharmaceutical administration ratios and the total administered activity patterns for each NM radionuclide in Spain. The highest values corresponded to ^{99m}Tc and ^{131}I. Furthermore ^{111}In, ^{67}Ga and ^{123}I were observed in detectable amounts. Sewage sludge and specially primary and activated sludges showed a significant accumulation of ^{99m}Tc and ^{131}I, respectively. ^{131}I was also present in the treated water sampled in the reclaimed water treatment plant (RWTP-2) and in materials from the drinking water treatment plant (DWTP-3) studied.

These results revealed the presence of medically-derived ^{131}I in the three different steps from the same urban water cycle management, which represents a novel finding revealing the high permanence of this contaminant. The present dataset also fixed the actual background levels of ^{131}I under normal operational conditions of the BMA water treatment plants and NM services. The presence of medicaly-derived radionculides in some sewage effluents of the WWTPs studied may be a source for low-level detection of these radionuclides in the BMA aquatic ecosystem.

Another relevant finding of the present work revealed that the most favourable operational conditions for total nitrogen kehjdal removal in the WWTP-2 with conventional activated sludge reactors line achieved the highest ^{131}I reduction documented until now (75 %). In future works can be a matter of interest go further in technologies able to further reduce ^{131}I in, for example, the reclaimed water for reuse, which has been found as prone to contain detectable amounts of ^{131}I and reduce radiation dose to the public.

Furthermore accumulation tendencies were defined after the study of the radionuclides levels in materials from the DWTP-2. The radionuclides associated to natural occurring radioactive materials, ^{40}K and ^{238}U, showed the highest levels in the studied materials in agreement with their presence in water from the Llobregat River basin. In the case of ^{40}K showed the highest concentrations of radionuclides analysed in sludge, sand and RO brine while ^{238}U in granular activated carbon. Cosmogenic ^{7}Be and fall-out ^{137}Cs were also found in the sludges analysed.

The cosmogenic short-lived ^{7}Be ($t_{1/2}$= 53 d) can be applied as tracer of environmental processes also in the urban water cycle. Regarding ^{7}Be and ^{210}Pb$_u$ con-

centrations correlation found in the DWTP-3 sludges was explained because they share the same behaviour in the atmosphere and in aquatic environments (attached to particles). Moreover, in WWTP-2 the presence of storm water in wastewater was associated to a significant increase of ^{7}Be and a decrease of medically-derived ^{131}I in dehydrated sludge.

After the radiological evaluation of the concentrations found in the water treatment plants from the BMA it can be concluded that the activities of the urban water cycle management do not pose a significant radiological risk neither to workers nor to the public. The management of the materials from the water treatment plants analysed do not deserve any specific consideration from existing legislation related with radiological risks.

Despite the existence of non risk background levels of ^{131}I in the BMA urban water cycle due to the presence of NM activities and patients, the concentrations of medically-derived ^{131}I in WWTPs were pointed out as the most significant.

Furthermore the study in the seven heterogeneous sized WWTPs revealed that, in the case of the largest WWTPs, levels in sludges were more stable and can be determined with a few samples. The NM radionuclides concentrations found in the BMA WWTPs have future implications for levels determinations in WWTP sewage sludge. When setting up a characterization-sampling program, a few sludge samples would be required for very large-sized WWTPs (>200,000 $m^3 \cdot d^{-1}$) to obtain an accurate enough characterization of ^{131}I levels in samples. In contrast, small-sized WWTPs (<1,000 $m^3 \cdot d^{-1}$) will require other methods such as the application of evaluation scenarios related to the excretions from a single patient.

Moreover in the present work, the contribution of the wastewater hydraulic retention time and the sewage sludge age decreasing the NM radionuclides concentrations during the treatment in WWTPs been pointed out as very significant. In the specific case of ^{131}I the hospital abatement systems for inpatients with doses above 0.8 GBq reduce one order of magnitude the background levels in wastewater.

Two novel methodologies in the fields of radiochemistry analysis and modelling have been adapted to one of the WWTPs studied from the BMA for achieving a better understanding of the dynamics of ^{131}I along WWTPs processes.

After modification of the reagents dosages radiochemical ^{131}I partitioning analysis method was tested and validated with success before its application. The experimental results in the samples taken at the WWTP-2 showed that the inorganic iodine predominates with the exception of the activated sludge reactors samples, where the precipitable fraction showed the highest percentages. However, in reclaimed water (RWTP-2) the residual dissolved fraction was revealed as the most

predominant. In the residual fraction, ^{131}I is expected to be found linked to organic molecules and in future works discriminations between the different compounds can be of scientific interest.

The model was successfully adapted to a WWTP different than the original one with conventional activate sludge reactors, confirming that can be adapted to other facilities. The partitioning analysis was also useful in the parametrization of the three different steps of the prognosis model (primary settling tanks, activated sludge reactors and secondary settling tanks). Sewage effluents ^{131}I data reported by the model match up with most of the experimental results, nevertheless, in the 18 % of the cases experimental results were overestimated. After the tests, nowadays it can be concluded that there are available information and tools to model medically-derived ^{131}I:

i) Biokentic excretion by the patient

ii) Inorganic iodine chemical behaviour wastewater

iii) Removal at WWTPs

iv) Radioecological behaviour in the aquatic environment

Therefore, a future work would be the development of model that interprete all available data in order to predict the levels of ^{131}I from the patient to the environment.

Acknowledgements

Maria Amor Duch
Antonia Camacho
Sonia Blázquez
Isabel Serrano
David Mani
Ingrid Rubio
Almudena Hierro
Ignasi Casanova

Helmut W. Fischer
Volker Hormman
Maria-Evangelia Souti
Manuel Pérez-Mayo

Ricard Devesa
Ana Garbayo
J. M. A.

... and to fundings:

... and to family and friends.

References

[Ababneh and Eyadeh, 2015] Ababneh, A. M. and Eyadeh, M. M. (2015). Coincidence summing corrections in HPGe gamma-ray spectrometry for Marinelli-beakers geometry using peak to total (P/T) calibration. *Journal of Radiation Research and Applied Sciences*, 8(3):323–327.

[ACA, 2005] ACA (2005). Fitxes de Caracterització Inicial, Pressions i Impactes de Les Masses d'Aigua Subterrànies, IMPRESS. 39 and 40.

[ACA, 2015] ACA (2015). Dades i resultats analítics històrics del programa de seguiment i control i, mesures de dades hidrològiques de nivell i cabal de rius i nivell absolut i volum embassat als embassaments. *Agència catalana de l'aigua*.

[ACA, 2018] ACA (2018). Fitxes estacions de depuració d'aigües residuals. *Agència catalana de l'aigua*.

[Achermann et al., 2018] Achermann, S., Falås, P., Joss, A., Mansfeldt, C. B., Men, Y., Vogler, B., and Fenner, K. (2018). Trends in Micropollutant Biotransformation along a Solids Retention Time Gradient. *Environmental Science & Technology*, page acs.est.8b02763.

[AGBAR, 2018] AGBAR (2018). Base de dades general de les estacions depuradores (2014-2018).

[AMB, 2014] AMB (2014). Àrea metropolitana de Barcelona public website.

[AMB, 2018] AMB (2018). Àrea metropolitana de Barcelona public website.

[APHA AWA WEF, 1998] APHA AWA WEF (1998). Standard Methods for the Examination of Water and Wastewater. page 2130D.

[APHA AWA WEF, 2005] APHA AWA WEF (2005). Standar Methods for the Examination of Water and Wastewater. pages 2510B, 5210D, 2540E, 4500–NH3 B–C,4500–P.

[APHA AWA WEF, 2012] APHA AWA WEF (2012). Standard Methods for the Examination of Water and Wastewater. pages 4500–H+,4500–Nrg.

[ASTM, 2014] ASTM (2014). Standard Test Method for Determination of Iodine Number of Activated Carbon ASTM-D4607-14. *American Society for Testing and Materials*, West Consh(ASTM International).

[Baeza et al., 2006] Baeza, A., Fernández, M., Herranz, M., Legarda, F., Miró, C., and Salas, A. (2006). Removing Uranium and Radium from a Natural Water. *Water, Air, and Soil Pollution*, 173(1-4):57–69.

[Baeza et al., 2004] Baeza, A., Miró, C., and Soleto, C. (2004). Spectrometric determination of low activities of gamma emitters in water samples. *Applied Radiation and Isotopes*, 61(2-3):203–206.

[Barci-Funel et al., 1993] Barci-Funel, G., Dalmasso, J., Magne, J., and Ardisson, G. (1993). Simultaneous detection of short-lived 201Tl, 99Tcm and 131I isotopes in sewage sludge using low energy photon spectrometry. *Science of The Total Environment*, 130-131:37–42.

[Bastian et al., 2005] Bastian, R., Bachmaier, J., Schmidt, D., Salomon, S., Jones, A., Chiu, W., Setlow, L., Wolbarst, A., Yu, C., Goodman, J., and Lenhart, T. (2005). Radioactive Materials in Biosolids. *Journal of Environment Quality*, 34(3):1152.

[Camacho et al., 2010] Camacho, A., Devesa, R., Vallés, I., Serrano, I., Soler, J., Blázquez, S., Ortega, X., and Matia, L. (2010). Distribution of uranium isotopes in surface water of the Llobregat river basin (Northeast Spain). *Journal of environmental radioactivity*, 101(12):1048–54.

[Carvalho et al., 2013] Carvalho, F. P., Oliveira, J. M., Silva, L., and Malta, M. (2013). Radioactivity of anthropogenic origin in the Tejo Estuary and need for improved waste management and environmental monitoring. *International Journal of Environmental Studies*, 70(6):952–963.

[Castro et al., 2007] Castro, P., Huber, M. E., Ober, W. C., and Garrison, C. W. (2007). *Marine Biology*. McGraw-Hill.

[Chabaux et al., 2008] Chabaux, F., Bourdon, B., and Riotte, J. (2008). U-Series Geochemistry in Weathering Profiles, River Waters and Lakes. In *U-Th Series Nuclides in Aquatic Series*, pages 49–91.

[Chang et al., 2011] Chang, B.-U., Choi, S.-W., Song, M. H., Lee, J.-S., and Kim, Y. (2011). Medically used radionuclides (131I, 99mTc) in the urban sewage system: the case of the Daejeon metropolitan city, Korea. *Radiation protection dosimetry*, 146(1-3):318–21.

[Che et al., 2017] Che, Y., Liang, P., Gong, T., Cao, X., Zhao, Y., Yang, C., and Song, C. (2017). Elucidation of major contributors involved in nitrogen removal and transcription level of nitrogen-cycling genes in activated sludge from WWTPs. *Scientific Reports*, 7(1):44728.

[Cosenza et al., 2015] Cosenza, A., Rizzo, S., Sansone Santamaria, A., and Viviani, G. (2015). Radionuclides in wastewater treatment plants: monitoring of Sicilian plants. *Water science and technology : a journal of the International Association on Water Pollution Research*, 71(2):252–8.

[CSN, 2002] CSN (2002). Límites derivados para la aplicación del reglamento de protección sanitaria contra radiaciones ionizantes (RD 783/2001) relativos a la protección del público.

[CSN, 2003] CSN (2003). Instrucción IS-05 del Consejo de Seguridad Nuclear, por la que se definen los valores de exención para nucleidos según se establece en las tablas A y B del anexo I del Real Decreto 1836-1999. IS-05.

[CSN SEPR SEFM, 2011] CSN SEPR SEFM (2011). Criterios de alta de pacientes y medidas para la protección radiológica del público después de tratamientos metabólicos con 131I. Foro sobre protección radiológica en el medio sanitario.

[CSN SEPR SEFM SEMNIM, 2014] CSN SEPR SEFM SEMNIM (2014). Proyecto DOMNES. Prospección nacional de procedimientos de diagnóstico en medicina nuclear utilizados en los centros sanitarios españoles. Estimación de dosis recibidas por los pacientes y la población.

[Dalmasso et al., 1997] Dalmasso, J., Barci-Funel, G., Magne, J., Barci, V., and Ardisson, G. (1997). Study of the transfer of the medically used radionuclides in sewage systems. *Radiochimica Acta*, 78:167–171.

[De Felice et al., 2000] De Felice, Angelini, Fazio, and Biagini (2000). Fast procedures for coincidence-summing correction in gamma-ray spectrometry. *Applied radiation and isotopes*, 52(3):745–52.

[DEMOWARE, 2017] DEMOWARE (2017). Final publishable summary report.

[Desideri et al., 2007] Desideri, D., Meli, M., Feduzi, L., Roselli, C., Rongoni, A., and Saetta, D. (2007). 238U, 234U, 226Ra, 210Po concentrations of bottled mineral waters in Italy and their dose contribution. *Journal of Environmental Radioactivity*, 94(2):86–97.

[EC, 1999] EC (1999). Management of radioactive waste arising from medical establishments in the European Union. Proceedings of a Workshop. EUR 19254.

[EC, 2013a] EC (2013a). Council Directive 2013/51/EURATOM of 22 October 2013 laying down requirements for the protection of the health of the general public with regard to radioactive substances in water intended for human consumption.

[EC, 2013b] EC (2013b). Council Directive 2013/59/Euratom of 5 December 2013 laying down basic safety standards for protection against the dangers arising from exposure to ionising radiation.

[EC, 2014] EC (2014). Medical Radiation Exposure of the European Population Part 1/2. Radiation Protection. 180.

[Fenner and Martin, 1997] Fenner, F. D. and Martin, J. E. (1997). Behavior of Na 131I and Meta (131I) Iodobenzylguanidine (MIBG) in Municipal Sewerage. *Health Physics*, 73(2):333–339.

[Fernández-Turiel et al., 2003] Fernández-Turiel, J., Gimeno, D., Rodriguez, J., Carnicero, M., and Valero, F. (2003). Spatial and Seasonal Variations of Water Quality in a Mediterranean Catchment: The Llobregat River (NE Spain). *Environmental Geochemistry and Health*, 25(4):453–474.

[Fischer et al., 2015] Fischer, H., Ulbrich, S., and Souti, M. (2015). Medical I-131 in German Rivers. *Environmental Radioactivity International Conference (ENVIRA)*.

[Fischer et al., 2014] Fischer, H. W., Igbinosa, A., and Souti, M. A. (2014). Beryllium-7 in Rainfall, River Sediment and Sewage Sludge. *3rd ICRER (Congress)*.

[Fischer et al., 2009] Fischer, H. W., Ulbrich, S., Pittauerová, D., and Hettwig, B. (2009). Medical radioisotopes in the environment - following the pathway from patient to river sediment. *Journal of environmental radioactivity*, 100(12):1079–85.

[Fonollosa et al., 2014] Fonollosa, E., Nieto, A., Peñalver, A., Aguilar, C., and Borrull, F. (2014). Presence of radionuclides in sludge from conventional drinking water treatment plants. A review. *Journal of environmental radioactivity*, 141C:24–31.

[Fréchou and Calmet, 2003] Fréchou, C. and Calmet, D. (2003). 129I in the environment of the La Hague nuclear fuel reprocessing plant—from sea to land. *Journal of Environmental Radioactivity*, 70(1-2):43–59.

[Furtado et al., 2015] Furtado, R. V., Ha, L., Clarke, S., and Sandroussi, C. (2015). Adjuvant Iodine (131) Lipiodol after Resection of Hepatocellular Carcinoma. *Journal of oncology*, 2015:746917.

[Gäfvert et al., 2002] Gäfvert, T., Ellmark, C., and Holm, E. (2002). Removal of radionuclides at a waterworks. *Journal of Environmental Radioactivity*, 63(2):105–115.

[Garcia-Orellana et al., 2009] Garcia-Orellana, J., Pates, J., Masqué, P., Bruach, J., and Sanchez-Cabeza, J. (2009). Distribution of artificial radionuclides in deep sediments of the Mediterranean Sea. *Science of The Total Environment*, 407(2):887–898.

[Gilmore, 2008] Gilmore, G. R. (2008). Practical gamma-ray spectrometry. 2nd ed.

[Grande and Risica, 2015] Grande, S. and Risica, S. (2015). Radionuclides in drinking water: the recent legislative requirements of the European Union. *Journal of Radiological Protection*, 35(1):1–19.

[Grossi et al., 2016] Grossi, C., Ballester, J., Serrano, I., Galmarini, S., Camacho, A., Curcoll, R., Morguí, J., Rodò, X., and Duch, M. (2016). Influence of long-range atmospheric transport pathways and climate teleconnection patterns on the variability of surface 210Pb and 7Be concentrations in southwestern Europe. *Journal of Environmental Radioactivity*, 165:103–114.

[Haig et al., 2011] Haig, S. J., Collins, G., Davies, R. L., Dorea, C. C., and Quince, C. (2011). Biological aspects of slow sand filtration: past, present and future. *Water Science & Technology: Water Supply*, 11(4):468.

[Ham et al., 2003] Ham, G., Crockett, G., and Mand-Wilkins, B. (2003). Partitioning of radionuclides with sewage sludge and transfer along terrestrial foodchain pathways from sludge-amended land-a review of data. NRPB-W32.

[Hormann and Fischer, 2017] Hormann, V. and Fischer, H. (2017). The physico-chemical distribution of 131I in a municipal wastewater treatment plant. *Journal of Environmental Radioactivity*, (178-179):55–62.

[Hormann and Fischer, 2014] Hormann, V. and Fischer, H. W. (2014). Estimation of Speciation and Distribution of 131I in urban and natural Environments. *3rd ICRER (Congress)*.

[Hormann and Fischer, 2018] Hormann, V. and Fischer, H. W. (2018). A Simple Compartment Model for the Dynamical Behavior of Medically Derived 131I in a Municipal Wastewater Treatment Plant. *Environmental Science & Technology*, 52(16):9235–9242.

[Hou et al., 2009] Hou, X., Hansen, V., Aldahan, A., Possnert, G., Lind, O. C., and Lujaniene, G. (2009). A review on speciation of iodine-129 in the environmental and biological samples. *Analytica chimica acta*, 632(2):181–96.

[IAEA, 2004] IAEA (2004). Application of the Concepts of Exclusion, Exemption and Clearance. *International Atomic Energy Agency*, (IAEA Safety Standards Series):RS–G–1.7.

[IAEA, 2009] IAEA (2009). Release of Patients After Radionuclide Therapy. *Safety Reports Series*, 63.

[IAEA, 2014] IAEA (2014). Radiation Protection and Safety of Radiation Sources: International Basic Safety Standards. No. GSR Pa(Publication 1578).

[ISO, 2002] ISO (2002). Water quality. Determination of the chemical oxygen demand index (ST-COD). Small-scale sealed-tube method. (ISO 15705).

[ISO IEC, 2017] ISO IEC (2017). ISO/IEC 17025:2017. General requirements for the competence of testing and calibration laboratories. *International Organization for Standardization and International Electrotechnical Commission*.

[Jeong et al., 2014] Jeong, G., Lee, K., Kim, B., Lee, S., Lee, J., and Koo, A. (2014). Study on Removal of Artificial Radionuclide (I-131) in Water. *Journal of Korean Society of Environmental Engineers*, 36(11):747–752.

[Jiménez, 2010] Jiménez, F. (2010). Determinación y seguimiento de I131 Po210 y otros radionucleidos en diferentes entornos laborales. *PhD Thesis*.

[Karamanis et al., 2008] Karamanis, D., Stamoulis, K., Ioannides, K., and Patiris, D. (2008). Spatial and seasonal trends of natural radioactivity and heavy metals in river waters of Epirus, Macedonia and Thessalia. *Desalination*, 224(1-3):250–260.

[Kirkpatrick et al., 2013] Kirkpatrick, J. M., Venkataraman, R., and Young, B. M. (2013). Minimum detectable activity, systematic uncertainties, and the ISO 11929 standard. *Journal of Radioanalytical and Nuclear Chemistry*, 296(2):1005–1010.

[Kitto et al., 2006] Kitto, M. E., Fielman, E. M., Hartt, G. M., Gillen, E. A., Semkow, T. M., Parekh, P. P., and Bari, A. (2006). Long-term monitoring of radioactivity in surface air and deposition in New York state. *Health Physics*, 90(1):31–37.

[Kleinschmidt and Akber, 2008] Kleinschmidt, R. and Akber, R. (2008). Naturally occurring radionuclides in materials derived from urban water treatment plants in southeast Queensland, Australia. *Journal of environmental radioactivity*, 99(4):607–20.

[Knoll, 2010] Knoll, G. (2010). Radiation dectection and measurement. 4th ed.

[Korun et al., 2019] Korun, M., Siri, S., Collins, S., Duch, M., Karfopoulos, K., Gomes, R., Laubenstein, M., Fornaciari-Iljadica, M. C., Pibida, L., Delgado, J., Camacho, A., Ali-Santoro, M., Boshkova, T., Diaz-Perez, R., Mitsios, I., Peyres, V., Potiriadis, C., Silva, R., Gudelis, A., Jevremovic, A., Long, S., Vukanac, I., Seslak, B., Vodenik, B., Durasavic, M., Mulas, D., Kandic, A., Elvira, V., Margineanu, R., Pantelica, A., Hurtado, S., Idoeta, R., Zorko, B., Anagnostakis, M., Verheyen, L., Nikolic, J., Wiedner, H., and Gurau, H. (2019). Determining the probability of locating peaks using computerized peak-location methods in gamma-ray spectra as a function of the relative peak-area uncertainty. *Applied Radiation and Isotopes*.

[Krawczyk et al., 2013] Krawczyk, E., Piñero-García, F., and Ferro-García, M. (2013). Discharges of nuclear medicine radioisotopes in Spanish hospitals. *Journal of Environmental Radioactivity*, 116:93–98.

[Kütahyalı and Eral, 2004] Kütahyalı, C. and Eral, M. (2004). Selective adsorption of uranium from aqueous solutions using activated carbon prepared from charcoal by chemical activation. *Separation and Purification Technology*, 40(2):109–114.

[LARA, 2015] LARA (2015). Progama de col·laboració per a la determinació i control dels continguts radioactius de les aigües. *Laboratori d'anàlisi de radioactivitat*, (Resums de les activitats 2007-2014).

[Lee et al., 2016] Lee, S. Y., Lee, J. Y., Min, J. H., Kim, S. S., Baik, M. H., Chung, S. Y., Lee, M., and Lee, Y. (2016). Microbial copper reduction method to scavenge anthropogenic radioiodine. 6.

[Lee et al., 2018] Lee, U., Kim, M. J., and Kim, H. R. (2018). Radioactive iodine analysis in environmental samples around nuclear facilities and sewage treatment plants. *Nuclear Engineering and Technology*, 50(8):1355–1363.

[Leggett, 2010] Leggett, R. W. (2010). A Physiological Systems Model for Iodine for Use in Radiation Protection. *Radiation Research*, 174(4):496–516.

[Li et al., 2014] Li, D., Kaplan, D. I., Knox, A. S., Crapse, K. P., and Diprete, D. P. (2014). Aqueous 99Tc, 129I and 137Cs removal from contaminated groundwater and sediments using highly effective low-cost sorbents. *Journal of Environmental Radioactivity*, 136:56–63.

[LNHB, 2016] LNHB (2016). *Monographie BIPM-5 - Table of Radionuclides. ISBN: 978-92-822-2264-5*, volume 8.

[Lu et al., 2013] Lu, H., Dai, R., Liu, Y., Song, A., and Liu, X. (2013). The effects of anaerobic fermentation on dehydrated sludge. *Water Science and Technology*, 67(11):2630–2636.

[Maringer, 1996] Maringer, F. (1996). The partitioning of natural radionuclides in a large alpine river. *Environment International*, 22:323–331.

[Maringer et al., 2015] Maringer, F. J., Seidel, C., Baumgartner, A., and Stietka, M. (2015). Radioactivity in the Danube.

[McGowan et al., 2014] McGowan, D. R., Pratt, B. E., Hinton, P. J., Peet, D. J., and Crawley, M. T. (2014). Iodine-131 monitoring in sewage plant outflow. *Journal of radiological protection : official journal of the Society for Radiological Protection*, 34(1):1–14.

[Montaña, 2013] Montaña, M. (2013). *Optimization of alpha emitter's determination in water. Behaviour of radionuclides in wastewater treatment plants.* PhD thesis, Universitat Politècnica de Catalunya.

[Montaña et al., 2013a] Montaña, M., Camacho, A., Devesa, R., Vallés, I., Céspedes, R., Serrano, I., Blàzquez, S., and Barjola, V. (2013a). The presence of radionuclides in wastewater treatment plants in Spain and their effect on human health. *Journal of Cleaner Production*, 60:77–82.

[Montaña et al., 2013b] Montaña, M., Camacho, A., Serrano, I., Devesa, R., Matia, L., and Vallés, I. (2013b). Removal of radionuclides in drinking water by membrane treatment using ultrafiltration, reverse osmosis and electrodialysis reversal. *Journal of environmental radioactivity*, 125:86–92.

[Mora et al., 2016] Mora, J. C., Baeza, A., Robles, B., and Sanz, J. (2016). Assessment for the management of NORM wastes in conventional hazardous and nonhazardous waste landfills. *Journal of Hazardous Materials*, 310:161–169.

[Mulas et al., 2016] Mulas, D., Garcia-Orellana, J., Casacuberta, N., Hierro, A., Moreno, V., and Masqué, P. (2016). Dose assessment to workers in a dicalcium phosphate production plant. *Journal of Environmental Radioactivity*, 165:182–190.

[Nakamura et al., 2005] Nakamura, A., Hayabuchi, N., Osaki, T., and Osaki, S. (2005). Output of radiopharmaceutlcal nuclides of known injected doses from a municipal sewage treatment system. *Health Physics*, 88(2):163–168.

[Palomo et al., 2010a] Palomo, M., Peñalver, A., Aguilar, C., and Borrull, F. (2010a). Presence of Naturally Occurring Radioactive Materials in sludge samples from several Spanish water treatment plants. *Journal of Hazardous Materials*, 181(1-3):716–721.

[Palomo et al., 2010b] Palomo, M., Peñalver, A., Aguilar, C., and Borrull, F. (2010b). Radioactivity evaluation of Ebro river water and sludge treated in a potable water treatment plant located in the South of Catalonia (Spain). *Applied radiation and isotopes*, 68(3):474–80.

[Park et al., 2015] Park, H.-K., Son, H.-J., Yeom, H.-S., Kim, Y.-J., Choi, J.-T., and Ryu, D.-C. (2015). Evaluation of Adsorption Characteristics of Radioactive Iodine (I-131) for Various Materials of Granular Activated Carbon (GAC). *Journal of Environmental Science International*, 24(9):1123–1129.

[Petrucci and Traino, 2015] Petrucci, C. and Traino, A. C. (2015). Focus on the legislative approach to short half life radioactive hospital waste releasing. *Physica medica : PM : an international journal devoted to the applications of physics to*

medicine and biology : official journal of the Italian Association of Biomedical Physics (AIFB), 31(7):726–32.

[Poluianov et al., 2016] Poluianov, S. V., Kovaltsov, G. A., Mishev, A. L., and Usoskin, I. G. (2016). Production of cosmogenic isotopes 7Be, 10Be, 14C, 22Na, and 36Cl in the atmosphere: Altitudinal profiles of yield functions. *Journal of Geophysical Research: Atmospheres*, 121(13):8125–8136.

[Prăvălie, 2014] Prăvălie, R. (2014). Nuclear weapons tests and environmental consequences: a global perspective. *Ambio*, 43(6):729–44.

[Punt et al., 2007] Punt, A., Wood, M., and Rose, D. (2007). Radionuclide discharges to sewer. A field investigation. *Environmental Agency Science Report*.

[Rädlinger and Heumann, 2000] Rädlinger, G. and Heumann, K. G. (2000). Transformation of Iodide in Natural and Wastewater Systems by Fixation on Humic Substances.

[RD 1620/2007,] RD 1620/2007. Real Decreto 1620/2007, de 7 de diciembre, por el que se establece el régimen jurídico de la reutilización de las aguas depuradas.

[Rodríguez et al., 2018] Rodríguez, A., Corbacho, J. A., Dickson, N., Tovar, E., and Baeza, A. (2018). Performance analysis of different methods to determine 131I in water samples for environmental monitoring. *Journal of Radioanalytical and Nuclear Chemistry*, pages 1–8.

[Rodríguez et al., 2010] Rodríguez, N. H., Ramírez, S. M., Varela, M. T. B., Guillem, M., Puig, J., Larrotcha, E., and Flores, J. (2010). Re-use of drinking water treatment plant (DWTP) sludge: Characterization and technological behaviour of cement mortars with atomized sludge additions. 40(5):778–786.

[Rose et al., 2015] Rose, P. S., Smith, J. P., Aller, R. C., Cochran, J. K., Swanson, R. L., and Coffin, R. B. (2015). Medically-Derived (131)I as a Tool for Investigating the Fate of Wastewater Nitrogen in Aquatic Environments. *Environmental science & technology*, 49(17):10312–9.

[Rose et al., 2013] Rose, P. S., Smith, J. P., Cochran, J. K., Aller, R. C., and Swanson, R. L. (2013). Behavior of medically-derived 131I in the tidal Potomac River. *The Science of the total environment*, 452-453:87–97.

[Rose and Swanson, 2013] Rose, P. S. and Swanson, R. L. (2013). Iodine-131 in sewage sludge from a small water pollution control plant serving a thyroid cancer treatment facility. *Health physics*, 105(2):115–20.

[Rose et al., 2012] Rose, P. S., Swanson, R. L., and Cochran, J. K. (2012). Medically-derived 131I in municipal sewage effluent. *Water research*, 46(17):5663–71.

[Saari et al., 2010] Saari, H.-K., Schmidt, S., Castaing, P., Blanc, G., Sautour, B., Masson, O., and Cochran, J. K. (2010). The particulate 7Be/210Pbxs and 234Th/210Pbxs activity ratios as tracers for tidal-to-seasonal particle dynamics in the Gironde estuary (France): implications for the budget of particle-associated contaminants. *The Science of the total environment*, 408(20):4784–94.

[Smith et al., 2003] Smith, K. P., Arnish, J. J., Williams, G. P., and Blunt, D. L. (2003). Assessment of the Disposal of Radioactive Petroleum Industry Waste in Nonhazardous Landfills Using Risk-Based Modeling. *Environmental Science & Technology*, 37(10):2060–2066.

[Souti et al., 2014] Souti, M., Hormann, V., Toma, E., and Fischer, H. (2014). I-131 Extraction from Fresh water and Sewage plant effluent. *3rd ICRER (Congress)*.

[Steinhauser, 2014] Steinhauser, G. (2014). Fukushima's forgotten radionuclides: a review of the understudied radioactive emissions. *Environmental science & technology*, 48(9):4649–63.

[Sundell-Bergman et al., 2008] Sundell-Bergman, S., de la Cruz, I., Avila, R., and Hasselblad, S. (2008). A new approach to assessment and management of the impact from medical liquid radioactive waste. *Journal of Environmental Radioactivity*, 99(10):1572–1577.

[Tomás Zerquera et al., 2017] Tomás Zerquera, J., Mora, J., Robles, B., Tomás Zerquera, J., Mora, J. C., and Robles, B. (2017). Probabilistic Prognosis of Environmental Radioactivity Concentrations due to Radioisotopes Discharged to Water Bodies from Nuclear Power Plants. *Toxics*, 5(4):32.

[Torres et al., 2012] Torres, P., Hernández, D., and Paredes, D. (2012). Uso productivo de lodos de plantas de tratamiento de agua potable en la fabricación de ladrillos cerámicos. *Revista Ingenieria de Construccion*, 27(3):145–154.

[UNE, 2006] UNE (2006). Water quality. Determination of suspended solids. Method by filtration through glass fibre filters. (UNE-EN 872).

[UNSCEAR, 2000] UNSCEAR (2000). Sources and effects of ionizing radiation. Volume: I.

[Villalobos-Rodríguez et al., 2012] Villalobos-Rodríguez, R., Montero-Cabrera, M. E., Esparza-Ponce, H. E., Herrera-Peraza, E. F., and Ballinas-Casarrubias, M. L. (2012). Uranium removal from water using cellulose triacetate membranes added with activated carbon. *Applied radiation and isotopes : including data, instrumentation and methods for use in agriculture, industry and medicine*, 70(5):872–81.

[Wafelman et al., 1997] Wafelman, A., Hoefnagel, C., Maessen, H., Maes, R., and Beijnen, J. (1997). Renal excretion of iodine-131 labelled meta-iodobenzylguanidine and metabolites after therapeutic doses in patients suffering from different neural crest-derived tumours. *European Journal of Nuclear Medicine*, 24(5):544–552.

[Watson and Crawford-Brown, 1991] Watson, J. and Crawford-Brown, D. (1991). Use of activated carbon to remove radon from drinking water. *Departament of envioronmental science and Enginnering. University of North Carolina*, UNC-WRRI-9.

[Webber et al., 2007] Webber, W. R., Higbie, P. R., and McCracken, K. G. (2007). Production of the cosmogenic isotopes 3H, 7Be, 10Be, and 36Cl in the Earth's atmosphere by solar and galactic cosmic rays. *Journal of Geophysical Research: Space Physics*, 112(A10):n/a–n/a.

[WHO, 2017] WHO (2017). Potable reuse. Gudiance for producing safe driniking-water.

[Yeong et al., 2014] Yeong, C.-H., Cheng, M.-h., and Ng, K.-H. (2014). Therapeutic radionuclides in nuclear medicine: current and future prospects. *Journal of Zhejiang University. Science. B*, 15(10):845–63.

[Zannoni et al., 2019] Zannoni, D., Cantaluppi, C., Ceccotto, F., Giacetti, W., and Lovisetto, B. (2019). Human and environmental factors affecting the activity of 131I and 137Cs in urban wastewater: A case study. *Journal of Environmental Radioactivity*, 198:135–146.

[Zevi et al., 2005] Zevi, Y., Dathe, A., McCarthy, J. F., Richards, B. K., and Steenhuis, T. S. (2005). Distribution of colloid particles onto interfaces in partially saturated sand. *Environmental science & technology*, 39(18):7055–64.

Appendix

A Scientific contribution

A.1 Publications associated to the thesis

Scientific articles

Mulas, D., Camacho, A., Serrano, I., Montes, S., Devesa, R., Duch, M.A., (2017). **Natural and artificial radionuclides in sludge, sand, granular activated carbon and reverse osmosis brine from a metropolitan drinking water treatment plant.** J. Environ. Radioact. 177, 233-240. doi:10.1016/j.jenvrad.2017.07.001

Mulas, D., Camacho, A., Garbayo, A., Devesa, R., Duch, M.A., (2019). **Medically-derived radionuclides levels in seven heterogeneous urban wastewater treatment plants: The role of operating conditions and catchment area.** Sci. Total Environ. 663, 818-829. doi:10.1016/J.Scitotenv.2019.01.349

Mulas, D., Camacho, A., Hierro, A., Garbayo, A., Devesa, R., Duch, M.A., (2020). **Levels and chemical behaviour of ^{131}I in a large-sized WWTP with conventional activated sludge reactors.** In progress.

Congress presentations

IX Jornadas sobre Calidad en el Control de la Radiactividad Ambiental. D. Mulas. *Caracterización radiológica de los materiales filtrantes y subproductos de una planta potabilizadora metropolitan (Oral communication).* Sitges (Spain). 15-17/06/2016.

5º Congreso conjunto SEFM-SEPR. D. Mulas, A. Camacho, I. Serrano, J. M. Agulló, R. Devesa, M. A. Duch. *Radionúclidos de uso médico en estaciones depuradoras del Área Metropolitana de Barcelona (Oral communication).* Girona (Spain). 13-15/06/2017.

4th International Coneference on Radioecology and Environmental Radioactivity. D. Mulas, A.Camacho, I. Serrano, A. Garbayo, J. M. Agulló, R. Devesa, M. A. Duch. *Presence of medically-derived radionuclides in the urban water cycle (Poster).* Berlin (Germany). 3-8/09/2017.

X Jornadas sobre Calidad en el Control de la Radiactividad Ambiental. D. Mulas. *Validación y estudio de la distribución del ^{131}I (precipitable, inorgánica disuelta, residual) en muestras líquidas procedentes de una EDAR (Oral communication).* Bilbao (Spain). 19-22/6/2018.

2nd International Conference on risk assessment of pharmaceuticals in the environment. D. Mulas, A. Camacho, R. Devesa, M.A. Duch. *Nuclear medicine activities and presence of radionuclides in the Barcelona metropolitan area urban water cycle (Poster).* Barcelona (Spain). 28–29 /11 /2019.

Internal reports

Laboratori d'anàlisi de radioactivitat (INTE-UPC). Progama de col·laboració per a la determinació i control dels continguts radioactius de les aigües. AGBAR. Resum anual. 2014.

Laboratori d'anàlisi de radioactivitat (INTE-UPC). Progama de col·laboració per a la determinació i control dels continguts radioactius de les aigües. AGBAR. Resum anual. 2015.

Laboratori d'anàlisi de radioactivitat (INTE-UPC). Progama de col·laboració per a la determinació i control dels continguts radioactius de les aigües. AGBAR. Resum anual. 2016.

Laboratori d'anàlisi de radioactivitat (INTE-UPC). Progama de col·laboració per a la determinació i control dels continguts radioactius de les aigües. AGBAR. Resum anual. 2017.

Laboratori d'anàlisi de radioactivitat (INTE-UPC). Progama de col·laboració per a la determinació i control dels continguts radioactius de les aigües. AGBAR. Resum anual. 2018.

A.2 Other publications

Scientific articles

Mulas, D., Garcia-Orellana, J., Casacuberta, N., Hierro, A., Moreno, V., and Masqué, P. (2016). **Dose assessment to workers in a dicalcium phosphate production plant.** Journal of Environmental Radioactivity, 165:182-190. doi:10.1016/j.jenvrad.2016.09.018

Korun, M., Siri, S., Collins, S., Duch, M., Karfopoulos, K., Gomes, R., Laubenstein, M., Fornaciari-Iljadica, M. C., Pibida, L., Delgado, J., Camacho, A., Ali-Santoro, M., Boshkova, T., Diaz-Perez, R., Mitsios, I., Peyres, V., Potiriadis, C., Silva, R., Gudelis, A., Jevremovic, A., Long, S., Vukanac, I., Seslak, B., Vodenik, B., Durasavic, M., Mulas, D., Kandic, A., Elvira, V., Margineanu, R., Pantelica, A., Hurtado, S., Idoeta, R., Zorko, B., Anagnostakis, M., Verheyen, L., Nikolic, J., Wiedner, H., and Gurau, H. (2020). **Determining the probability of locating peaks using computerized peak-location methods in gamma-ray spectra as a function of the relative peak-area uncertainty.** Applied Radiation and Isotopes, 155:x-x. doi:10.1016/j.apradiso.2019.108920

Congress presentations

4º Congreso conjunto SEFM-SEPR. D. Mulas, A.Camacho, I. Serrano , X. Prat, R. Devesa, S. Blázquez, M.A. Duch. *Evolution of radioactivity removal at a Besòs Aquifer Drinking Water Treatment Plant (DWTP).* Valencia (Spain). 22 - 26/06/2015.

ENVIRA 2015. A. Camacho, D. Mulas, I. Serrano , R. Cardeñoso, R. Devesa, S. Blázquez, M.A. Duch. *Long-term radiological characterization of waters at one Catalan drinking water treatment plant.* Thessaloniki (Grècia). 21 - 25/09/15.

B List of tables

C List of figures

D General dataset

D.1 Radionuclides concentratons in samples

Table A: Specific activities in inflow wastewater and sewage effluent from the 7 WWTPs.

	Sampling		Bq·L^{-1}				
	Start	**End**	^{131}**I**	^{99m}**Tc**	^{111}**In**	^{67}**Ga**	^{123}**I**
Inflow wastewater							
WWTP-1	06/05/2014	07/05/2014	1.39 ± 0.19	50.4 ± 2.7	<MDA	<MDA	<MDA
WWTP-1	30/09/2014	01/10/2014	0.79 ± 0.10	26.0 ± 1.7	<MDA	<MDA	0.64 ± 0.44
WWTP-1	24/02/2015	25/02/2015	1.52 ± 0.17	32 ± 20	<MDA	<MDA	<MDA
WWTP-1	20/10/2015	21/10/2015	4.43 ± 0.29	47.4 ± 3.1	0.28 ± 0.13	<MDA	<MDA
WWTP-2	07/07/2015	08/07/2015	1.54 ± 0.27	6.5 ± 1.2	<MDA	<MDA	<MDA
WWTP-3	15/11/2016	16/11/2016	0.34 ± 0.15	13.7 ± 4.6	<MDA	<MDA	<MDA
WWTP-4	29/11/2016	29/11/2016	0.32 ± 0.16	<MDA	0.26 ± 0.16	<MDA	<MDA
WWTP-5	21/03/2017	22/03/2017	<MDA	8.0 ± 2.2	<MDA	<MDA	<MDA
WWTP-6	18/07/2016	19/07/2016	<MDA	<MDA	<MDA	<MDA	<MDA
WWTP-7	31/01/2017	01/02/2017	<MDA	<MDA	<MDA	<MDA	<MDA
Sewage effluent							
WWTP-1	06/05/2014	07/05/2014	2.12 ± 0.17	5.3 ± 1.3	0.178 ± 0.093	<MDA	<MDA
WWTP-1	30/09/2014	01/10/2014	0.58 ± 0.12	4.97 ± 0.65	<MDA	<MDA	<MDA
WWTP-1	24/02/2015	25/02/2015	1.16 ± 0.21	<MDA	<MDA	<MDA	<MDA
WWTP-1	20/10/2015	21/10/2015	1.21 ± 0.16	6.5 ± 1.3	0.196 ± 0.052	<MDA	<MDA
WWTP-2a	07/07/2015	08/07/2015	1.70 ± 0.23	<MDA	<MDA	<MDA	<MDA
WWTP-2b	07/07/2015	08/07/2015	3.38 ± 0.23	<MDA	<MDA	<MDA	<MDA
WWTP-3	15/11/2016	16/11/2016	0.23 ± 0.11	<MDA	<MDA	<MDA	<MDA
WWTP-4	29/11/2016	29/11/2016	0.29 ± 0.11	<MDA	0.261 ± 0.059	<MDA	<MDA
WWTP-5 IFAS	21/03/2017	22/03/2017	<MDA	<MDA	<MDA	<MDA	<MDA
WWTP-5 MBR	21/03/2017	22/03/2017	<MDA	<MDA	<MDA	<MDA	<MDA
WWTP-6	18/07/2016	19/07/2016	<MDA	<MDA	<MDA	<MDA	<MDA
WWTP-7	31/01/2017	01/02/2017	<MDA	<MDA	<MDA	<MDA	<MDA

Table B: Specific activities in the 3 different types of sewage sludge sampled at the 7 WWTPs.

	Sampling date	Bq·kg^{-1} d.w.				
		^{131}I	^{99m}Tc	^{111}In	^{67}Ga	^{123}I
Primary sludge						
WWTP-1	07/05/2014	260 ± 16	7,330 ± 360	19.2 ± 7.1	141 ± 37	49 ± 25
WWTP-1	01/10/2014	508 ± 25	2,880 ± 240	13.5 ± 3.6	78 ± 39	<MDA
WWTP-1	25/02/2015	434 ± 17	7,980 ± 280	29.0 ± 2.5	23.0 ± 8.3	19.4 ± 6.1
WWTP-1	21/10/2015	410 ± 17	9,170 ± 350	48.2 ± 4.7	30.6 ± 9.3	<MDA
WWTP-1	05/09/2016	254 ± 11	<MDA	<MDA	<MDA	<MDA
WWTP-1	06/09/2016	131.9 ± 7.3	<MDA	3.2 ± 2.2	<MDA	<MDA
WWTP-1	07/09/2016	236 ± 15	6.830 ± 250	<MDA	<MDA	15.0 ± 9.0
WWTP-1	08/09/2016	325 ± 17	9,530 ± 340	<MDA	25 ± 12	19.4 ± 8.4
WWTP-1	09/09/2016	233 ± 17	6,410 ± 240	16.6 ± 4.1	<MDA	57 ± 13
WWTP-2	08/07/2015	502 ± 24	3,350 ± 160	155.1 ± 11.2	92 ± 41	58 ± 18
WWTP-2	07/10/2015	227 ± 10	889 ± 41	36.0 ± 3.9	86 ± 11	<MDA
WWTP-3	16/11/2016	30 ± 10	2,230 ± 120	<MDA	206 ± 36	<MDA
WWTP-3	29/03/2017	<MDA	1,211 ± 70	<MDA	110 ± 44	<MDA
WWTP-4	14/10/2015	70.7 ± 6.9	<MDA	<MDA	<MDA	<MDA
WWTP-4	30/11/2016	93 ± 14	<MDA	13.0 ± 5.7	<MDA	<MDA
WWTP-5	22/03/2017	28.9 ± 5.5	1,322 ± 74	<MDA	<MDA	<MDA
WWTP-5	18/03/2015	138.8 ± 6.9	609 ± 31	<MDA	<MDA	<MDA
Activated sludge						
WWTP-1	07/05/2014	2,383 ± 72	3,930 ± 160	15.7 ± 6.4	59 ± 25	55 ± 30
WWTP-1	01/10/2014	395 ± 22	5,190 ± 310	<MDA	70 ± 46	<MDA
WWTP-1	25/02/2015	2,890 ± 110	3,950 ± 180	63.4 ± 11.1	<MDA	<MDA
WWTP-1	21/10/2015	2,609 ± 92	5,450 ± 280	74.9 ± 8.1	<MDA	<MDA
WWTP-1	05/09/2016	2,109 ± 78	<MDA	<MDA	<MDA	<MDA
WWTP-1	06/09/2016	1,953 ± 73	<MDA	<MDA	<MDA	<MDA
WWTP-1	07/09/2016	2,022 ± 78	353 ± 32	<MDA	<MDA	<MDA
WWTP-1	08/09/2016	1,529 ± 57	335 ± 22	<MDA	<MDA	<MDA
WWTP-1	09/09/2016	2,459 ± 88	4,490 ± 180	27 ± 5.7	<MDA	80 ± 12
WWTP-2	08/07/2015	1,124 ± 47	230 ± 210	38.2 ± 10	<MDA	<MDA
WWTP-2	07/10/2015	991 ± 38	268 ± 36	18.0 ± 5.0	<MDA	<MDA
WWTP-3	16/11/2016	923 ± 35	90 ± 49	16.0 ± 3.1	<MDA	<MDA
WWTP-3	29/03/2017	305 ± 16	<MDA	<MDA	<MDA	<MDA
WWTP-4	14/10/2015	517 ± 28	<MDA	<MDA	<MDA	<MDA
WWTP-4	30/11/2016	709 ± 39	<MDA	<MDA	<MDA	<MDA
WWTP-5 IFAS	08/02/2017	145.7 ± 6.6	321 ± 20	41.4 ± 3.3	<MDA	<MDA
WWTP-5 IFAS	22/03/2017	930 ± 35	297 ± 38	27.4 ± 4.7	<MDA	<MDA
WWTP-5 MBR	08/02/2017	27.5 ± 3.3	447 ± 35	5.8 ± 3.1	<MDA	<MDA
WWTP-5 MBR	23/03/2017	275 ± 15	185 ± 13	<MDA	<MDA	<MDA
WWTP-6	18/07/2016	19.9 ± 7.0	<MDA	<MDA	<MDA	<MDA
WWTP-6	08/02/2017	<MDA	<MDA	<MDA	<MDA	<MDA
WWTP-7	16/11/2016	1,579 ± 62	<MDA	<MDA	<MDA	<MDA
WWP-7	01/02/2017	<MDA	<MDA	<MDA	<MDA	<MDA
Dehydrated sludge						
WWTP-1	01/10/2014	660 ± 93	3,190 ± 200	16.9 ± 3.6	83 ± 18	31 ± 15
WWTP-1	25/02/2015	1,069 ± 32	4,080 ± 180	33.3 ± 3.0	18 ± 10	<MDA
WWTP-1	21/10/2015	924 ± 28	6,420 ± 280	52 ± 3.6	31.3 ± 5.9	<MDA
WWTP-1	05/09/2016	981 ± 29	<MDA	13.6 ± 2.5	17.9 ± 5.5	<MDA
WWTP-1	05/09/2016	1,016 ± 31	<MDA	8.2 ± 2.3	16 ± 13	<MDA
WWTP-1	07/09/2016	595 ± 18	2,683 ± 76	8.1 ± 1.7	19.2 ± 7.9	6.0 ± 4.1
WWTP-1	08/09/2016	487 ± 15	3,830 ± 100	5.4 ± 1.4	11.2 ± 4.0	10.6 ± 3.9
WWTP-1	09/09/2016	822 ± 23	5,190 ± 140	18.1 ± 2.1	<MDA	55.6 ± 6.4
WWTP-2	08/07/2015	145.5 ± 7.4	<MDA	13.7 ± 2.9	<MDA	<MDA
WWTP-2	07/10/2015	92.2 ± 4.3	70.2 ± 5.0	8.4 ± 1.7	16 ± 11	<MDA
WWTP-4	14/10/2015	83 ± 3.7	<MDA	<MDA	6.3 ± 3.9	<MDA
WWTP-4	30/11/2016	51.3 ± 5.6	<MDA	<MDA	<MDA	<MDA
WWTP-5	18/03/2015	67.2 ± 8.9	<MDA	<MDA	<MDA	<MDA
WWTP-5	22/03/2017	41.1 ± 5.5	<MDA	<MDA	<MDA	<MDA

Table C: ^{131}I activity measured in the tests carried out for the ^{131}I partitioning method validation.

Sample code	Reference solution	^{131}I Bq determined			
		Total	**AEI**	**BEI**	**RI**
$NaHCO_3$ 2mM water samples					
D1	I-2	3.86 ± 0.27	-	3.01 ± 0.28	ND
D2	I-2	3.60 ± 0.25	-	2.08 ± 0.33	ND
D3	I-2	3.84 ± 0.27	-	3.35 ± 0.34	ND
D4	I-2	3.83 ± 0.27	-	3.84 ± 0.33	ND
D5	I-1	67.1 ± 2.0	-	67.1 ± 2.7	1.07 ± 0.31
WWTP samples					
IW8	I-2	27.6 ± 1.9	ND	0.68 ± 0.11	ND
IW9	I-2	28.1 ± 2.0	ND	28.3 ± 1.4	ND
IW1	I-1	66.9 ± 2.0	1.22 ± 0.10	64.8 ± 2.7	1.46 ± 0.46
IW2	I-1	67.2 ± 2.0	1.210 ± 0.060	69.0 ± 2.7	0.61 ± 0.22
PE1	I-2	17.1 ± 1.2	ND	15.60 ± 0.84	ND
PE2	I-2	17.2 ± 1.2	ND	16.2 ± 1.0	ND
PE3	I-2	17.2 ± 1.2	ND	17.28 ± 0.80	ND
SE8	I-2	28.0 ± 2.0	ND	13.1 ± 1.0	ND
SE9	I-2	28.1 ± 2.0	ND	26.3 ± 1.6	ND
SE1	I-1	66.6 ± 2.0	0.985 ± 0.074	66.7 ± 2.4	0.58 ± 0.19
SE2	I-1	67.1 ± 2.0	1.315 ± 0.088	66.7 ± 2.5	0.74 ± 0.24

Activities in samples traced with I-1 have been determined at 12/02/2018 9:00 and with I-2 at 05/06/2018 9:00 respectively

Table D: Specific activities in WWTP-2 and RWTP-2.

Sampling		$Bq \cdot L^{-1}$				
Start	**End**	^{131}**I**	^{99m}**Tc**	^{111}**In**	^{67}**Ga**	^{123}**I**
General recirculation						
03/10/2018		1.03 ± 0.13	3.31 ± 0.30	<MDA	<MDA	<MDA
24/10/2018		17.82 ± 0.70	17.28 ± 1.16	0.37 ± 0.12	<MDA	<MDA
06/11/2018	07/11/2018	2.45 ± 0.17	<MDA	<MDA	<MDA	<MDA
13/11/2018	14/11/2018	0.78 ± 0.17	<MDA	<MDA	<MDA	<MDA
28/11/2018	27/11/2018	1.71 ± 0.50	<MDA	<MDA	<MDA	<MDA
Primary inflow						
07/07/2015	08/07/2015	1.53 ± 0.27	6.5 ± 1.2	<MDA	<MDA	<MDA
14/02/2016	15/02/2016	0.39 ± 0.15	<MDA	<MDA	<MDA	<MDA
15/02/2016	16/2/2016	0.99 ± 0.20	6.25 ± 0.67	<MDA	<MDA	<MDA
16/02/2016	17/2/2016	2.54 ± 0.30	10.8 ± 1.5	0.321 ± 0.093	<MDA	<MDA
17/02/2016	18/02/2016	1.67 ± 0.26	10.4 ± 1.8	<MDA	<MDA	<MDA
18/02/2016	19/02/2016	3.09 ± 0.19	<MDA	0.19 ± 0.11	<MDA	<MDA
06/03/2016	07/03/2016	0.89 ± 0.18	<MDA	<MDA	<MDA	<MDA
07/03/2016	08/03/2016	0.78 ± 0.21	8.6 ± 1.3	<MDA	<MDA	<MDA
08/03/2016	09/03/2016	0.85 ± 0.19	4.97 ± 0.96	<MDA	<MDA	<MDA
09/03/2016	10/3/2016	3.84 ± 0.34	8.1 ± 0.92	<MDA	<MDA	<MDA
10/03/2016	11/3/2016	1.03 ± 0.28	6.1 ± 1.9	<MDA	<MDA	<MDA
11/03/2016	120/3/2016	0.74 ± 0.23	5.9 ± 1.4	<MDA	<MDA	<MDA
12/03/2016	13/3/2016	0.69 ± 0.20	<MDA	<MDA	<MDA	<MDA
13/03/2016	14/3/2016	<MDA	<MDA	<MDA	<MDA	<MDA
24/05/2016	25/05/2016	0.74 ± 0.20	7.2 ± 1.5	<MDA	<MDA	<MDA
31/05/2016	01/06/2016	3.78 ± 0.37	11.9 ± 2.5	<MDA	<MDA	<MDA
07/06/2016	08/06/2016	1.04 ± 0.24	3.0 ± 1.5	<MDA	<MDA	<MDA
14/06/2016	15/06/2016	0.50 ± 0.22	8.1 ± 2.8	<MDA	<MDA	<MDA
21/06/2016	22/06/2016	0.37 ± 0.22	10.1 ± 1.7	0.32 ± 0.11	<MDA	<MDA
28/06/2016	29/06/2016	0.85 ± 0.23	3.3 ± 1.7	<MDA	<MDA	<MDA
05/07/2016	06/07/2016	1.24 ± 0.25	6.1 ± 1.9	<MDA	<MDA	<MDA
12/07/2016	13/07/2016	1.72 ± 0.24	9.3 ± 1.6	<MDA	<MDA	<MDA
19/07/2016	20/07/2016	0.59 ± 0.24	3.7 ± 1.7	<MDA	<MDA	<MDA
15/05/2018	16/05/2018	1.34 ± 0.20	5.3 ± 2.6	<MDA	<MDA	<MDA
07/06/2018		1.36 ± 0.36	8.13 ± 0.61	<MDA	<MDA	0.44 ± 0.29
28/11/2018	29/11/2018	1.48 ± 0.33	17.0 ± 2.2	<MDA	<MDA	<MDA
Primary effluent						
28/06/2017		1.47 ± 0.24	<MDA	<MDA	<MDA	<MDA
30/08/2017		6.64 ± 0.38	<MDA	<MDA	<MDA	<MDA
13/12/2017		0.77 ± 0.28	1.01 ± 0.61	<MDA	<MDA	<MDA
15/05/2018	16/05/2018	1.34 ± 0.27	<MDA	<MDA	<MDA	<MDA
30/05/2018		0.93 ± 0.16	3.39 ± 0.44	<MDA	<MDA	<MDA
07/06/2018		1.05 ± 0.32	5.86 ± 0.79	<MDA	<MDA	0.74 ± 0.41
12/11/2018		0.24 ± 0.16	<MDA	<MDA	<MDA	<MDA
Reactors line A						
31/10/2017		3.78 ± 0.16	1.98 ± 0.57	<MDA	<MDA	<MDA
Reactors line B						
18/10/2017		3.89 ± 0.18	3.39 ± 0.32	<MDA	<MDA	<MDA
Reclaimed water						
14/07/2016		0.209 ± 0.035	<MDA	<MDA	<MDA	<MDA
21/07/2016		0.43 ± 0.17	<MDA	<MDA	<MDA	<MDA
02/11/2016		0.57 ± 0.13	<MDA	<MDA	<MDA	<MDA
16/11/2016		0.89 ± 0.18	<MDA	<MDA	<MDA	<MDA
01/02/2017		<MDA	<MDA	<MDA	<MDA	<MDA
30/03/2017		0.221 ± 0.021	<MDA	<MDA	<MDA	<MDA
07/06/2017		0.616 ± 0.090	<MDA	<MDA	<MDA	<MDA
14/06/2017		0.50 ± 0.12	<MDA	<MDA	<MDA	<MDA
19/07/2017		0.51 ± 0.12	<MDA	<MDA	<MDA	<MDA
03/10/2018		0.77 ± 0.10	<MDA	<MDA	<MDA	<MDA
06/11/2018		0.238 ± 0.086	<MDA	<MDA	<MDA	<MDA

Table E: Specific activities in sewage effluents A and B from WWTP-2.

Sampling		Bq·L^{-1}				
Start	**End**	^{131}**I**	^{99m}**Tc**	^{111}**In**	^{67}**Ga**	^{123}**I**
Sewage effluent A						
13/05/2014	14/05/2014	0.44 ± 0.12	<MDA	<MDA	0.61 ± 0.23	<MDA
8/10/2014	8/10/2015	0.34 ± 0.12	<MDA	<MDA	<MDA	<MDA
03/03/2015	04/03/2015	0.222 ± 0.079	<MDA	<MDA	<MDA	<MDA
07/07/2015	08/07/2015	1.70 ± 0.23	<MDA	<MDA	<MDA	<MDA
06/10/2015	07/10/2015	3.00 ± 0.40	<MDA	<MDA	<MDA	<MDA
14/02/2016	15/2/2016	<MDA	<MDA	<MDA	<MDA	<MDA
15/02/2016	16/02/2016	<MDA	<MDA	<MDA	<MDA	<MDA
16/02/2016	17/02/2016	0.30 ± 0.13	<MDA	<MDA	<MDA	<MDA
17/02/2016	18/02/2016	0.48 ± 0.16	<MDA	<MDA	<MDA	<MDA
18/02/2016	19/02/2016	0.590 ± 0.075	<MDA	0.128 ± 0.032	<MDA	<MDA
06/03/2016	07/03/2016	0.34 ± 0.12	<MDA	<MDA	<MDA	<MDA
07/03/2016	8/3/2016	0.24 ± 0.13	<MDA	<MDA	<MDA	<MDA
08/03/2016	9/3/2016	0.18 ± 0.11	<MDA	<MDA	<MDA	<MDA
09/03/2016	10/3/2016	0.20 ± 0.12	<MDA	<MDA	<MDA	<MDA
10/03/2016	11/03/2016	0.39 ± 0.12	<MDA	<MDA	0.73 ± 0.36	<MDA
11/03/2016	120/3/2016	0.191 ± 0.066	<MDA	<MDA	<MDA	<MDA
12/03/2016	13/3/2016	0.43 ± 0.15	<MDA	<MDA	<MDA	<MDA
13/03/2016	14/3/2016	0.216 ± 0.085	<MDA	<MDA	<MDA	<MDA
24/05/2016	25/05/2016	0.69 ± 0.15	<MDA	<MDA	<MDA	<MDA
31/05/2016	01/06/2016	6.78 ± 0.34	<MDA	<MDA	<MDA	<MDA
07/06/2016	08/06/2016	0.59 ± 0.13	<MDA	<MDA	<MDA	<MDA
14/06/2016	15/06/2016	0.58 ± 0.11	<MDA	<MDA	<MDA	<MDA
21/06/2016	22/06/2016	0.24 ± 0.12	<MDA	0.265 ± 0.041	<MDA	<MDA
28/06/2016	29/06/2016	0.41 ± 0.12	<MDA	<MDA	<MDA	<MDA
05/07/2016	06/07/2016	0.55 ± 0.12	<MDA	<MDA	<MDA	<MDA
12/07/2016	13/07/2016	0.24 ± 0.12	10.9 ± 5.3	<MDA	<MDA	<MDA
19/07/2016	20/07/2016	0.74 ± 0.14	<MDA	<MDA	<MDA	<MDA
22/11/2017		0.432 ± 0.062	<MDA	<MDA	<MDA	<MDA
25/07/2018		2.50 ± 0.21	<MDA	<MDA	<MDA	<MDA
12/03/2018		0.62 ± 0.30	<MDA	<MDA	<MDA	<MDA
20/03/2018		0.53 ± 0.22	0.69 ± 0.35	<MDA	<MDA	<MDA
12/11/2018		0.24 ± 0.15	<MDA	<MDA	<MDA	<MDA
Sewage effluent B						
07/07/2015	08/07/2015	3.39 ± 0.23	<MDA	<MDA	<MDA	<MDA
06/10/2015	07/10/2015	4.89 ± 0.28	<MDA	<MDA	<MDA	<MDA
14/02/2016	15/02/2016	0.69 ± 0.18	<MDA	<MDA	<MDA	<MDA
15/02/2016	16/2/2016	0.22 ± 0.20	<MDA	<MDA	<MDA	<MDA
16/02/2016	172/2016	1.23 ± 0.25	<MDA	<MDA	<MDA	<MDA
17/02/2016	18/02/2016	1.48 ± 0.23	<MDA	0.136 ± 0.082	<MDA	<MDA
18/02/2016	19/2/2016	2.01 ± 0.13	<MDA	<MDA	<MDA	<MDA
06/03/2016	7/3/2016	1.38 ± 0.19	<MDA	<MDA	<MDA	<MDA
07/03/2016	8/3/2016	0.41 ± 0.18	<MDA	<MDA	<MDA	<MDA
08/03/2016	9/3/2016	0.61 ± 0.19	<MDA	<MDA	<MDA	<MDA
09/03/2016	10/3/2016	1.16 ± 0.20	<MDA	<MDA	<MDA	<MDA
10/03/2016	11/03/2016	1.28 ± 0.18	<MDA	<MDA	<MDA	<MDA
11/03/2016	120/3/2016	0.64 ± 0.22	<MDA	<MDA	<MDA	<MDA
12/03/2016	13/3/2016	1.05 ± 0.20	<MDA	<MDA	<MDA	<MDA
13/03/2016	14/03/2016	1.02 ± 0.24	<MDA	<MDA	<MDA	<MDA
24/05/2016	25/05/2016	1.64 ± 0.20	<MDA	<MDA	<MDA	<MDA
31/05/2016	01/06/2016	11.57 ± 0.57	<MDA	<MDA	<MDA	<MDA
07/06/2016	08/06/2016	0.78 ± 0.19	<MDA	<MDA	<MDA	<MDA
14/06/2016	15/06/2016	0.60 ± 0.23	<MDA	<MDA	<MDA	<MDA
21/06/2016	22/06/2016	0.31 ± 0.15	<MDA	0.328 ± 0.090	<MDA	<MDA
28/06/2016	29/06/2016	1.24 ± 0.20	<MDA	0.24 ± 0.16	<MDA	<MDA
05/07/2016	06/07/2016	0.70 ± 0.18	<MDA	<MDA	<MDA	<MDA
12/07/2016	13/07/2016	0.65 ± 0.18	<MDA	<MDA	<MDA	<MDA
19/07/2016	20/07/2016	1.32 ± 0.15	<MDA	<MDA	<MDA	<MDA
09/11/2017		1.70 ± 0.14	<MDA	<MDA	<MDA	<MDA
25/07/2018		3.62 ± 0.53	<MDA	<MDA	<MDA	<MDA
07/06/2018		1.06 ± 0.30	<MDA	<MDA	<MDA	<MDA

Table F: Specific activities in sewage sludges from WWTP-2.

Sampling	Bq·L^{-1}				
date	^{131}I	^{99m}Tc	^{111}In	^{67}Ga	^{123}I
Primary sludge					
14/05/14	430 ± 15	3478 ± 169	39 ± 3	65 ± 7	<MDA
8/10/2014	170 ± 19	256 ± 64	<MDA 0	<MDA	<MDA
4/03/2015	190 ± 9	1181 ± 99	60 ± 4	<MDA	26 ± 20
8/7/2015	502 ± 24	3345 ± 159	155 ± 11	92 ± 41	58 ± 18
7/10/2015	227 ± 10	889 ± 41	36 ± 4	86 ± 11	<MDA
15/02/2016	276 ± 17	<MDA	19 ± 7	<MDA	<MDA
16/02/2016	308 ± 20	1485 ± 75	40 ± 9	<MDA	<MDA
17/02/2016	319 ± 20	974 ± 54	53 ± 10	<MDA	<MDA
18/02/2016	331 ± 21	1495 ± 75	54 ± 10	<MDA	<MDA
19/02/2016	313 ± 21	947 ± 56	105 ± 10	39 ± 19	12 ± 19
Activated sludge					
14/05/14	674 ± 27	80 ± 42	<MDA	<MDA	<MDA
8/10/2014	723 ± 34	567 ± 95	15 ± 5	45 ± 23	<MDA
4/03/2015	980 ± 85	220 ± 20	21 ± 4	<MDA	<MDA
8/7/2015	1124 ± 47	227 ± 214	38 ± 10	15 ± 48	<MDA
7/10/2015	991 ± 38	268 ± 36	18 ± 5	13 ± 20	<MDA
Dehydrated sludge					
8/10/2014	105 ± 4	<MDA	7 ± 1	8 ± 2	<MDA
4/03/15	139 ± 6	<MDA	8 ± 1	<MDA	<MDA
8/7/2015	145 ± 7	<MDA	14 ± 3	<MDA	<MDA
7/10/2015	92 ± 4	70 ± 5	8 ± 2	16 ± 11	<MDA
19/02/2016	318 ± 15	16 ± 7	10 ± 3	<MDA	<MDA

Table G: ^{131}I partitioning methodology results in samples taken at WWTP-2.

Sampling			**Bq·L^{-1}**			
Code	**Start**	**End**	**AEI**	**Non-precipitable**	**BEI**	**RI**
General recirculation						
GR1	03/10/2018		0.2323 ± 0.025	0.79 ± 0.13		
GR2	24/10/2018		10.91 ± 0.40	6.91 ± 0.80		
GR3	06/11/2018	07/11/2018	0.409 ± 0.050	2.04 ± 0.18		
GR4	13/11/2018	14/11/2018	0.229 ± 0.029	0.55 ± 0.17		
GR5	28/11/2018	29/11/2018	0.434 ± 0.056	1.16 ± 0.13	1.001 ± 0.068	0.16 ± 0.11
Primary inflow						
PI1	15/05/2018	16/05/2018	0.324 ± 0.042	1.01 ± 0.20		
PI2	28/11/2018	29/11/2018	0.125 ± 0.027	1.118 ± 0.097	0.971 ± 0.046	0.148 ± 0.086
Primary effluent						
PE1	30/08/2017		0.1443 ± 0.0099	6.50 ± 0.38		
PE2	13/12/2017		0.0406 ± 0.0087	0.89 ± 0.16		
PE3	15/05/2018	16/05/2018	0.0676 ± 0.0139	1.27 ± 0.27		
PE4	30/05/2018		0.0484 ± 0.0065	0.84 ± 0.18	0.716 ± 0.064	0.12 ± 0.16
Reactors						
Reactor A	31/10/2017		2.82 ± 0.11	0.96 ± 0.19		
Reactor B	18/10/2017		2.014 ± 0.0780	1.88 ± 0.20		
Sewage effluent A						
EA1	22/11/2017		0.0234 ± 0.0019	0.409 ± 0.062		
EA2	25/07/2018		0.0736 ± 0.0099	2.29 ± 0.15	2.175 ± 0.098	0.11 ± 0.11
Sewage effluent B						
EB1	09/11/2017		0.0130 ± 0.0013	1.70 ± 0.14		
EB2	25/07/2018		0.0396 ± 0.0070	3.87 ± 0.15	3.60 ± 0.15	<0.26
Reclaimed water						
RW1	03/10/2018		0.0072 ± 0.0024	0.55 ± 0.11	0.170 ± 0.027	0.38 ± 0.11
RW2	06/11/2018		0.0015 ± 0.0020	0.237 ± 0.086		

Table H: ^{238}U and ^{232}Th decay chain radionuclides specific activities in samples form the DWTP-2.

Samples	Sampling date	Radionuclides specific activities				
		^{238}U	^{226}Ra	^{210}Pb	^{228}Ra	^{228}Th
Sludges (Bq·kg^{-1} d.w.)						
Montaña (2013)						
Sludge	10/07/2007	60 ± 11	29 ± 5	54 ± 14	34 ± 3	38 ± 5
Sludge	30/10/2007	47 ± 10	32 ± 5	64 ± 14	38 ± 3	43 ± 6
Sludge	29/02/2008	76 ± 11	36 ± 6	65 ± 14	44 ± 3	35 ± 5
Sludge	06/06/2008	34 ± 10	29 ± 2	45 ± 11	34 ± 3	38 ± 2
Sludge	10/10/2008	47 ± 11	33 ± 5	54 ± 13	40 ± 3	38 ± 5
Sludge	11/12/2008	50 ± 9	35 ± 2	39 ± 9	34 ± 3	30 ± 1
Sludge	06/04/2009	88 ± 11	33 ± 2	45 ± 10	37 ± 3	32 ± 1
Campaings 2012-2014						
Dehydrated	23/10/2012	40 ± 13	21 ± 4	48 ± 16	36 ± 3	36 ± 5
Atomized	23/10/2012	49 ± 12	25 ± 4	85 ± 18	35 ± 4	39 ± 6
Dehydrated	30/10/2012	33 ± 11	29 ± 2	58 ± 12	34 ± 4	39 ± 2
Atomized	30/10/2012	36 ± 8	24 ± 1	51 ± 9	28 ± 3	32 ± 1
Dehydrated	07/02/2013	43 ± 9	18 ± 1	55 ± 9	33 ± 3	27 ± 1
Atomized	07/02/2013	52 ± 9	32 ± 5	62 ± 14	32 ± 3	29 ± 4
Dehydrated	02/07/2014	52 ± 10	31 ± 5	61 ± 13	34 ± 3	38 ± 5
Atomized	02/07/2014	42 ± 10	28 ± 5	67 ± 13	30 ± 3	37 ± 5
Sands (Bq·kg^{-1}d.w.)						
Filter 1-1	22/09/2014	11 ± 6	9.5 ± 0.8	<11	5 ± 1	6.7 ± 0.5
Filter 2-2	22/09/2014	12 ± 7	8 ± 1	14 ± 7	10 ± 2	9 ± 1
Filter 3-1	22/09/2014	15 ± 8	8 ± 1	15 ± 8	12 ± 2	14 ± 2
Virgin	15/10/2014	10 ± 5	9.6 ± 0.7	<10	5 ± 1	6.3 ± 0.5
GACs (Bq·kg^{-1} d.w.)						
Virgin	03/06/2013	<13	4 ± 1	<11	5 ± 2	4 ± 1
Virgin	09/01/2014	<18	10 ± 3	<15	9 ± 4	6 ± 2
Virgin	09/01/2014	<24	8 ± 3	<20	8 ± 3	5 ± 2
Regenerated	06/05/2013	57 ± 9	10 ± 2	<11	10 ± 3	7 ± 2
Regenerated	13/05/2013	61 ± 9	13 ± 2	<11	8 ± 2	8 ± 2
Regenerated	14/05/2013	53 ± 7	10 ± 1	<10	7 ± 2	6 ± 1
Regenerated	28/05/2013	73 ± 11	11 ± 2	<12	9 ± 3	8 ± 2
Regenerated	03/06/2013	72 ± 10	9 ± 2	<15	14 ± 3	8 ± 2
In-use filter 1	30/10/2012	87 ± 10	11 ± 2	21 ± 11	8 ± 2	8 ± 2
In-use filter 5	30/10/2012	85 ± 11	17 ± 2	<14	10 ± 3	11 ± 1
In-use filter 14	30/10/2012	60 ± 10	5 ± 2	<13	<4 ±	4 ± 1
In-use filter 15	30/10/2012	74 ± 11	4 ± 2	<17	<5 ±	4 ± 1
In-use filter 5	28/01/2013	119 ± 17	29 ± 5	<18	22 ± 5	18 ± 4
In-use filter 7	28/01/2013	61 ± 15	9 ± 3	<19	8 ± 5	12 ± 3
In-use filter 13	28/01/2013	94 ± 16	17 ± 3	32 ± 17	10 ± 5	13 ± 3
In-use filter 14	28/01/2013	92 ± 15	11 ± 3	<20	11 ± 4	11 ± 3
In-use filter 18	28/01/2013	121 ± 18	11 ± 3	<21	11 ± 5	10 ± 2
In-use filter 19	28/01/2013	70 ± 23	18 ± 4	<17	14 ± 7	22 ± 2
Exhausted filter 1	02/07/2014	149 ± 15	34 ± 5	22 ± 12	19 ± 3	18 ± 3
Exhausted filter 4	02/07/2014	164 ± 15	34 ± 5	26 ± 12	22 ± 3	17 ± 3
Exhausted filter 8	02/07/2014	129 ± 14	29 ± 5	<19	12 ± 3	14 ± 2
Exhausted filter 10	02/07/2014	151 ± 16	30 ± 5	20 ± 13	16 ± 3	18 ± 3
RO Brine (Bq·L^{-1})						
Sample 1	23/10/2012	<4	<0.4	<6	<0.5	<0.3
Sample 2	30/10/2012	<3	<0.3	<3	<0.6	<0.3
Sample 3	07/02/2013	<4	<0.4	<6	<0.6	<0.3

Table I: ^{40}K, ^{7}Be, ^{137}Cs and ^{131}I radionuclides specific activities and iodine index in samples form the DWTP-2.

Samples	Sampling date	Radionuclides specific activities				Iodine index
		^{40}K	^{7}Be	^{137}Cs	^{131}I	
Sludges (Bq·kg^{-1} d.w.)						
Montaña (2013)						
Sludge	10/07/2007	634 ± 48	<74	1.8 ± 0.6	ND	
Sludge	30/10/2007	728 ± 53	86 ± 16	1.6 ± 0.5	ND	
Sludge	29/02/2008	580 ± 43	83 ± 12	1.9 ± 0.3	ND	
Sludge	06/06/2008	645 ± 26	93 ± 10	2.6 ± 0.6	ND	
Sludge	10/10/2008	666 ± 49	58 ± 10	2.7 ± 0.5	ND	
Sludge	11/12/2008	478 ± 20	36 ± 8	1.5 ± 0.3	ND	
Sludge	06/04/2009	457 ± 21	28 ± 11	1.2 ± 0.6	ND	
Campaings 2012-2014						
Dehydrated	23/10/2012	563 ± 44	60 ± 10	1.4 ± 0.6	32 ± 12	
Atomized	23/10/2012	597 ± 45	171 ± 17	1.7 ± 0.5	<12	
Dehydrated	30/10/2012	563 ± 27	43 ± 8	1.4 ± 0.6	29 ± 10	
Atomized	30/10/2012	498 ± 21	82 ± 7	1.1 ± 0.5	<11	
Dehydrated	07/02/2013	395 ± 18	68 ± 7	1.1 ± 0.5	36 ± 8	
Atomized	07/02/2013	436 ± 33	81 ± 10	<2 ±	16 ± 3	
Dehydrated	02/07/2014	642 ± 47	89 ± 13	1.0 ± 0.6	29 ± 5	
Atomized	02/07/2014	621 ± 46	89 ± 12	1.4 ± 0.5	15 ± 2	
Sands (Bq·kg^{-1}d.w.)						
Filter 1-1	22/09/2014	20 ± 5	<6	<0.5	1.2 ± 0.4	
Filter 2-2	22/09/2014	263 ± 15	<8	<0.6	4.9 ± 0.4	
Filter 3-1	22/09/2014	766 ± 37	<11	<0.7	1.7 ± 0.9	
Virgin	15/10/2014	12 ± 5	<4.5	<0.3	ND	
GACs (Bq·kg^{-1}d.w.)						
Virgin	03/06/2013	<13	<32	<1	ND	865
Virgin	09/01/2014	37 ± 14	<20	<2	ND	ND
Virgin	09/01/2014	40 ± 17	<24	<2	ND	ND
Regenerated	06/05/2013	<13	<57	<1	ND	787
Regenerated	13/05/2013	15 ±	<47	<1	ND	737
Regenerated	14/05/2013	<11	<49	<1	ND	747
Regenerated	28/05/2013	17 ± 9	<39	<1	ND	724
Regenerated	03/06/2013	<18	<20	<1	ND	788
In-use filter 1	30/10/2012	<15	<12	<1	ND	597
In-use filter 5	30/10/2012	<16	<15	<1	ND	609
In-use filter 14	30/10/2012	<15	<15	<1	ND	805
In-use filter 15	30/10/2012	<19	<17	<1	ND	718
In-use filter 5	28/01/2013	37 ± 18	<23	<2	<13	684
In-use filter 7	28/01/2013	<29	<23	<2	28 ± 3	800
In-use filter 13	28/01/2013	33 ± 17	<15	<2	<9	528
In-use filter 14	28/01/2013	<26	<25	<2	25 ± 9	735
In-use filter 18	28/01/2013	<30	<46	<2	28 ± 8	690
In-use filter 19	28/01/2013	67 ± 30	<42	<3	21 ± 10	484
Exhausted filter 1	02/07/2014	<15	<13	<1	<1	560
Exhausted filter 4	02/07/2014	34 ± 11	<14	<1	<2	532
Exhausted filter 8	02/07/2014	27 ± 10	<18	<1	<2	581
Exhausted filter 10	02/07/2014	17 ± 11	<20	<1	12 ± 2	570
RO Brine (Bq·L^{-1})						
Sample 1	23/10/2012	7 ± 2	<2	<0.2	<1	
Sample 2	30/10/2012	5 ± 1	<2	<0.2	<1	
Sample 3	07/02/2013	7 ± 2	<2	<0.1	ND	

D.2 ^{131}I sewage effluent results for WWTP-2 modeling

Table J: Simulation results for February 2016 dataset at sewage effluent A (1/3).

Sewage effluent A								
Simulation	**Kr (h^{-1})**			λ_{ini}			**Uncertainty**	
time (h)	**0.120**	**0.140**	**0.160**	**0.006**	**0.010**	**0.024**	+	-
February 2016 dataset								
201	0.174	0.175	0.176				0.175	0.175
202	0.174	0.175	0.176				0.175	0.175
203	0.174	0.175	0.176				0.175	0.175
204	0.174	0.175	0.176				0.175	0.175
205	0.174	0.174	0.175				0.174	0.174
206	0.173	0.174	0.175				0.174	0.174
207	0.173	0.174	0.175				0.174	0.173
208	0.172	0.173	0.174				0.173	0.173
209	0.172	0.172	0.173				0.173	0.172
210	0.171	0.172	0.172				0.173	0.170
211	0.171	0.171	0.171				0.173	0.169
212	0.170	0.170	0.170				0.173	0.167
213	0.170	0.169	0.169				0.173	0.165
214	0.169	0.168	0.168				0.173	0.163
215	0.169	0.168	0.167				0.174	0.161
216	0.168	0.167	0.166				0.174	0.159
217	0.168	0.166	0.165				0.175	0.157
218	0.167	0.165	0.163				0.176	0.155
219	0.167	0.164	0.162				0.176	0.152
220	0.166	0.164	0.161				0.177	0.150
221	0.166	0.163	0.160				0.178	0.148
222	0.165	0.162	0.159				0.178	0.146
223	0.165	0.161	0.158				0.179	0.143
224	0.164	0.160	0.157				0.179	0.141
225	0.164	0.159	0.155				0.180	0.139
226	0.163	0.158	0.154				0.180	0.136
227	0.162	0.157	0.153				0.180	0.134
228	0.162	0.156	0.152				0.181	0.132
229	0.161	0.155	0.150				0.181	0.130
230	0.160	0.154	0.149				0.181	0.127
231	0.160	0.153	0.148				0.181	0.125
232	0.159	0.152	0.147				0.182	0.123
233	0.159	0.152	0.146				0.183	0.122
234	0.160	0.152	0.146				0.184	0.120
235	0.161	0.153	0.146				0.186	0.120
236	0.163	0.155	0.147				0.189	0.120
237	0.165	0.157	0.149				0.193	0.120
238	0.168	0.159	0.151				0.197	0.121
239	0.172	0.162	0.154				0.202	0.123
240	0.176	0.166	0.157				0.207	0.125

Table K: Simulation results for February 2016 dataset at sewage effluent A (2/3).

Sewage effluent A								
Simulation	**Kr (h^{-1})**			λ_{ini}			**Uncertainty**	
time (h)	**0.120**	**0.140**	**0.160**	**0.006**	**0.010**	**0.024**	+	-
February 2016 dataset								
241	0.180	0.170	0.161				0.212	0.127
242	0.185	0.174	0.165				0.218	0.130
243	0.190	0.179	0.169				0.224	0.133
244	0.195	0.183	0.173				0.229	0.137
245	0.200	0.187	0.177				0.234	0.140
246	0.205	0.192	0.181				0.240	0.144
247	0.210	0.196	0.185				0.245	0.148
248	0.215	0.201	0.189				0.251	0.151
249	0.219	0.205	0.193				0.255	0.155
250	0.224	0.209	0.197				0.260	0.159
251	0.229	0.214	0.201				0.265	0.162
252	0.233	0.218	0.204				0.269	0.166
253	0.237	0.222	0.208				0.274	0.169
254	0.242	0.226	0.212				0.278	0.173
255	0.247	0.230	0.216				0.283	0.177
256	0.252	0.234	0.220				0.287	0.181
257	0.257	0.240	0.224				0.293	0.186
258	0.264	0.245	0.230				0.299	0.192
259	0.271	0.253	0.237				0.307	0.198
260	0.280	0.261	0.245				0.316	0.206
261	0.291	0.271	0.254				0.327	0.215
262	0.303	0.282	0.264				0.339	0.226
263	0.315	0.294	0.275				0.351	0.236
264	0.328	0.306	0.287				0.364	0.248
265	0.342	0.318	0.298				0.377	0.259
266	0.356	0.331	0.311				0.391	0.272
267	0.371	0.345	0.323				0.406	0.284
268	0.387	0.360	0.337				0.422	0.298
269	0.403	0.375	0.351				0.438	0.312
270	0.420	0.390	0.365				0.454	0.327
271	0.437	0.406	0.380				0.470	0.341
272	0.453	0.421	0.394				0.487	0.356
273	0.469	0.435	0.407				0.501	0.369
274	0.483	0.449	0.419				0.516	0.382
275	0.497	0.461	0.431				0.529	0.393
276	0.510	0.474	0.442				0.542	0.405
277	0.523	0.485	0.453				0.554	0.416
278	0.535	0.496	0.463				0.566	0.427
279	0.548	0.508	0.473				0.578	0.437
280	0.560	0.518	0.483				0.589	0.447
281	0.571	0.528	0.492				0.600	0.457
282	0.581	0.538	0.500				0.610	0.465
283	0.592	0.547	0.509				0.620	0.474
284	0.603	0.557	0.518				0.630	0.483
285	0.615	0.567	0.527				0.642	0.493
286	0.625	0.577	0.536				0.652	0.502
287	0.635	0.586	0.544				0.661	0.510
288	0.644	0.593	0.551				0.670	0.517
289	0.651	0.600	0.556				0.677	0.523
290	0.658	0.605	0.561				0.683	0.527

Table L: Simulation results for February 2016 dataset at sewage effluent A (3/3).

Sewage effluent A								
Simulation	**Kr (h^{-1})**			λ_{ini}			**Uncertainty**	
time (h)	**0.005**	**0.010**	**0.015**	**0.006**	**0.010**	**0.024**	+	-
February 2016 dataset								
291	0.663	0.610	0.565				0.688	0.531
292	0.667	0.613	0.567				0.691	0.534
293	0.669	0.614	0.568				0.694	0.535
294	0.671	0.615	0.569				0.695	0.536
295	0.671	0.615	0.568				0.695	0.536
296	0.671	0.615	0.567				0.695	0.535
297	0.670	0.613	0.566				0.693	0.533
298	0.668	0.611	0.563				0.691	0.531
299	0.666	0.608	0.560				0.688	0.528
300	0.662	0.604	0.556				0.684	0.524
301	0.658	0.600	0.551				0.679	0.520
302	0.653	0.595	0.546				0.674	0.515
303	0.647	0.589	0.541				0.668	0.510
304	0.642	0.584	0.536				0.663	0.506
305	0.638	0.580	0.532				0.658	0.502
306	0.635	0.577	0.530				0.655	0.500
307	0.633	0.576	0.528				0.653	0.499
308	0.633	0.576	0.528				0.652	0.499
309	0.634	0.577	0.529				0.653	0.500
310	0.636	0.579	0.532				0.655	0.503
311	0.640	0.583	0.536				0.658	0.508
312	0.645	0.588	0.541				0.663	0.513
313	0.651	0.594	0.547				0.668	0.520
314	0.658	0.601	0.554				0.675	0.527
315	0.666	0.609	0.561				0.682	0.536
316	0.675	0.617	0.570				0.690	0.545
317	0.685	0.627	0.579				0.699	0.555
318	0.696	0.638	0.589				0.709	0.567
319	0.708	0.649	0.600				0.720	0.578
320	0.720	0.661	0.611				0.731	0.591

Table M: Simulation results for March 2016 dataset at sewage effluent A (1/4).

Sewage effluent A								
Simulation	**Kr (h^{-1})**			λ_{ini}			**Uncertainty**	
time (h)	**0.120**	**0.140**	**0.160**	**0.006**	**0.010**	**0.024**	+	-
March 2016 dataset								
201	0.338	0.326	0.315	0.338	0.355	0.357	0.326	0.326
202	0.338	0.326	0.315	0.338	0.355	0.357	0.326	0.326
203	0.338	0.326	0.315	0.338	0.355	0.357	0.326	0.326
204	0.338	0.325	0.315	0.338	0.355	0.357	0.325	0.325
205	0.338	0.325	0.315	0.338	0.355	0.357	0.325	0.325
206	0.337	0.324	0.314	0.337	0.354	0.356	0.324	0.324
207	0.336	0.323	0.313	0.336	0.353	0.355	0.324	0.323
208	0.335	0.322	0.312	0.335	0.352	0.354	0.323	0.322
209	0.335	0.321	0.311	0.335	0.350	0.352	0.322	0.321
210	0.334	0.320	0.310	0.334	0.349	0.350	0.321	0.319
211	0.333	0.319	0.309	0.333	0.347	0.349	0.321	0.318
212	0.332	0.318	0.307	0.332	0.346	0.347	0.320	0.316
213	0.331	0.317	0.306	0.331	0.344	0.345	0.320	0.314
214	0.330	0.316	0.305	0.330	0.343	0.343	0.320	0.313
215	0.329	0.315	0.304	0.329	0.341	0.340	0.320	0.311
216	0.328	0.314	0.303	0.328	0.339	0.338	0.320	0.309
217	0.328	0.313	0.301	0.328	0.337	0.335	0.320	0.307
218	0.327	0.312	0.300	0.327	0.335	0.333	0.320	0.304
219	0.326	0.311	0.299	0.326	0.333	0.330	0.320	0.302
220	0.325	0.310	0.298	0.325	0.332	0.327	0.320	0.300
221	0.325	0.309	0.297	0.325	0.330	0.325	0.321	0.298
222	0.324	0.308	0.295	0.324	0.328	0.322	0.321	0.295
223	0.323	0.307	0.294	0.323	0.326	0.319	0.321	0.293
224	0.322	0.306	0.293	0.322	0.324	0.317	0.321	0.291
225	0.321	0.305	0.292	0.321	0.322	0.314	0.321	0.289
226	0.320	0.304	0.290	0.320	0.320	0.311	0.321	0.286
227	0.319	0.302	0.288	0.319	0.318	0.308	0.321	0.284
228	0.318	0.301	0.287	0.318	0.315	0.305	0.320	0.281
229	0.317	0.299	0.285	0.317	0.312	0.301	0.320	0.278
230	0.315	0.297	0.282	0.315	0.309	0.297	0.319	0.275
231	0.313	0.295	0.280	0.313	0.306	0.293	0.318	0.271
232	0.311	0.293	0.278	0.311	0.303	0.289	0.318	0.268
233	0.310	0.291	0.275	0.310	0.300	0.285	0.317	0.264
234	0.308	0.289	0.273	0.308	0.297	0.282	0.317	0.261
235	0.307	0.287	0.272	0.307	0.294	0.278	0.317	0.258
236	0.306	0.286	0.270	0.306	0.292	0.275	0.317	0.255
237	0.305	0.285	0.269	0.305	0.290	0.272	0.317	0.253
238	0.304	0.284	0.267	0.304	0.288	0.269	0.318	0.250
239	0.303	0.283	0.266	0.303	0.286	0.267	0.318	0.247
240	0.302	0.282	0.265	0.302	0.284	0.264	0.319	0.245
241	0.302	0.281	0.264	0.302	0.283	0.261	0.320	0.243
242	0.301	0.280	0.263	0.301	0.281	0.259	0.321	0.240
243	0.301	0.280	0.262	0.301	0.279	0.257	0.321	0.238
244	0.300	0.279	0.261	0.300	0.278	0.255	0.322	0.236
245	0.299	0.278	0.260	0.299	0.276	0.253	0.322	0.234
246	0.298	0.277	0.260	0.298	0.275	0.251	0.322	0.232
247	0.298	0.276	0.259	0.298	0.273	0.249	0.323	0.230
248	0.297	0.275	0.258	0.297	0.272	0.247	0.323	0.228
249	0.296	0.274	0.256	0.296	0.271	0.245	0.322	0.226
250	0.295	0.273	0.255	0.295	0.269	0.244	0.322	0.224

Table N: Simulation results for March 2016 dataset at sewage effluent A 2/4).

Sewage effluent A								
Simulation	**Kr (h^{-1})**			λ_{ini}			**Uncertainty**	
time (h)	**0.120**	**0.140**	**0.160**	**0.006**	**0.010**	**0.024**	+	-
March 2016 dataset								
251	0.293	0.272	0.254	0.293	0.267	0.242	0.321	0.222
252	0.292	0.270	0.252	0.292	0.266	0.240	0.320	0.220
253	0.290	0.269	0.251	0.290	0.264	0.238	0.319	0.218
254	0.289	0.267	0.249	0.289	0.262	0.236	0.318	0.215
255	0.287	0.265	0.247	0.287	0.260	0.234	0.317	0.213
256	0.285	0.264	0.246	0.285	0.258	0.233	0.316	0.212
257	0.284	0.263	0.245	0.284	0.257	0.231	0.315	0.210
258	0.283	0.262	0.244	0.283	0.256	0.230	0.315	0.209
259	0.283	0.261	0.244	0.283	0.256	0.230	0.314	0.208
260	0.282	0.261	0.243	0.282	0.255	0.229	0.315	0.207
261	0.282	0.261	0.243	0.282	0.255	0.229	0.315	0.207
262	0.282	0.261	0.244	0.282	0.255	0.229	0.316	0.206
263	0.283	0.261	0.244	0.283	0.255	0.229	0.316	0.206
264	0.283	0.261	0.244	0.283	0.255	0.229	0.317	0.206
265	0.283	0.262	0.245	0.283	0.255	0.229	0.318	0.206
266	0.283	0.262	0.245	0.283	0.256	0.229	0.319	0.206
267	0.284	0.263	0.245	0.284	0.256	0.229	0.319	0.206
268	0.284	0.263	0.246	0.284	0.256	0.229	0.320	0.206
269	0.284	0.263	0.246	0.284	0.257	0.229	0.321	0.206
270	0.285	0.264	0.246	0.285	0.257	0.229	0.321	0.206
271	0.285	0.264	0.247	0.285	0.257	0.229	0.321	0.206
272	0.285	0.264	0.247	0.285	0.257	0.229	0.322	0.206
273	0.285	0.264	0.247	0.285	0.257	0.229	0.322	0.206
274	0.285	0.264	0.247	0.285	0.257	0.229	0.322	0.206
275	0.285	0.264	0.247	0.285	0.257	0.229	0.321	0.206
276	0.285	0.264	0.246	0.285	0.257	0.229	0.321	0.206
277	0.285	0.264	0.246	0.285	0.256	0.229	0.321	0.206
278	0.285	0.264	0.247	0.285	0.257	0.229	0.321	0.207
279	0.287	0.265	0.248	0.287	0.258	0.230	0.322	0.209
280	0.290	0.268	0.251	0.290	0.261	0.232	0.325	0.212
281	0.295	0.273	0.256	0.295	0.266	0.236	0.330	0.217
282	0.302	0.280	0.263	0.302	0.272	0.242	0.338	0.223
283	0.312	0.290	0.272	0.312	0.281	0.249	0.347	0.232
284	0.324	0.301	0.283	0.324	0.292	0.258	0.359	0.243
285	0.338	0.315	0.296	0.338	0.305	0.269	0.374	0.256
286	0.354	0.330	0.311	0.354	0.319	0.282	0.390	0.271
287	0.372	0.347	0.327	0.372	0.336	0.295	0.408	0.287
288	0.391	0.366	0.345	0.391	0.353	0.310	0.427	0.304
289	0.412	0.386	0.364	0.412	0.372	0.326	0.448	0.323
290	0.434	0.407	0.383	0.434	0.392	0.343	0.470	0.343
291	0.458	0.429	0.405	0.458	0.413	0.361	0.494	0.364
292	0.482	0.452	0.426	0.482	0.435	0.379	0.518	0.386
293	0.506	0.475	0.448	0.506	0.457	0.398	0.542	0.408
294	0.531	0.497	0.469	0.531	0.478	0.416	0.565	0.429
295	0.554	0.519	0.490	0.554	0.499	0.434	0.589	0.450
296	0.577	0.541	0.510	0.577	0.519	0.451	0.611	0.470
297	0.599	0.561	0.529	0.599	0.539	0.467	0.632	0.490
298	0.621	0.581	0.548	0.621	0.558	0.483	0.654	0.509
299	0.643	0.602	0.566	0.643	0.577	0.500	0.675	0.528
300	0.665	0.622	0.585	0.665	0.597	0.516	0.696	0.548

Table O: Simulation results for March 2016 dataset at sewage effluent A (3/4).

Sewage effluent A								
Simulation	**Kr (h^{-1})**			λ_{ini}			**Uncertainty**	
time (h)	**0.120**	**0.140**	**0.160**	**0.006**	**0.010**	**0.024**	+	-
March 2016 dataset								
301	0.688	0.643	0.605	0.688	0.617	0.533	0.719	0.568
302	0.712	0.665	0.625	0.712	0.638	0.551	0.741	0.589
303	0.734	0.685	0.643	0.734	0.657	0.567	0.762	0.609
304	0.755	0.704	0.660	0.755	0.675	0.582	0.782	0.626
305	0.773	0.720	0.675	0.773	0.690	0.595	0.799	0.642
306	0.790	0.735	0.688	0.790	0.704	0.607	0.815	0.656
307	0.805	0.748	0.700	0.805	0.717	0.618	0.829	0.668
308	0.819	0.761	0.711	0.819	0.729	0.628	0.842	0.679
309	0.833	0.773	0.722	0.833	0.740	0.638	0.856	0.690
310	0.847	0.786	0.734	0.847	0.753	0.648	0.870	0.702
311	0.860	0.797	0.743	0.860	0.763	0.657	0.882	0.712
312	0.870	0.805	0.750	0.870	0.771	0.664	0.891	0.719
313	0.878	0.812	0.756	0.878	0.777	0.670	0.899	0.725
314	0.883	0.815	0.758	0.883	0.781	0.673	0.903	0.728
315	0.885	0.817	0.759	0.885	0.782	0.674	0.905	0.728
316	0.885	0.816	0.757	0.885	0.781	0.673	0.905	0.727
317	0.883	0.812	0.752	0.883	0.777	0.670	0.901	0.722
318	0.878	0.806	0.746	0.878	0.772	0.665	0.896	0.716
319	0.871	0.799	0.739	0.871	0.765	0.660	0.889	0.709
320	0.863	0.791	0.730	0.863	0.757	0.653	0.881	0.700
321	0.854	0.781	0.720	0.854	0.748	0.645	0.871	0.691
322	0.842	0.770	0.709	0.842	0.737	0.636	0.860	0.679
323	0.830	0.757	0.696	0.830	0.725	0.626	0.847	0.667
324	0.814	0.742	0.682	0.814	0.711	0.614	0.832	0.652
325	0.797	0.724	0.665	0.797	0.694	0.600	0.814	0.635
326	0.776	0.705	0.646	0.776	0.676	0.584	0.794	0.616
327	0.756	0.685	0.627	0.756	0.657	0.568	0.773	0.597
328	0.736	0.666	0.609	0.736	0.639	0.553	0.754	0.578
329	0.716	0.647	0.591	0.716	0.621	0.538	0.734	0.560
330	0.696	0.629	0.574	0.696	0.604	0.523	0.716	0.542
331	0.677	0.611	0.558	0.677	0.587	0.509	0.698	0.525
332	0.658	0.593	0.541	0.658	0.570	0.495	0.679	0.507
333	0.638	0.575	0.524	0.638	0.552	0.480	0.660	0.489
334	0.617	0.555	0.506	0.617	0.534	0.464	0.641	0.470
335	0.596	0.536	0.488	0.596	0.515	0.449	0.621	0.451
336	0.576	0.518	0.471	0.576	0.498	0.434	0.602	0.433
337	0.555	0.499	0.454	0.555	0.480	0.419	0.583	0.415
338	0.536	0.482	0.438	0.536	0.463	0.405	0.565	0.398
339	0.517	0.464	0.423	0.517	0.447	0.391	0.548	0.381
340	0.499	0.449	0.408	0.499	0.432	0.378	0.531	0.366
341	0.483	0.434	0.395	0.483	0.418	0.366	0.516	0.352
342	0.468	0.421	0.383	0.468	0.406	0.356	0.502	0.339
343	0.455	0.409	0.372	0.455	0.394	0.346	0.490	0.327
344	0.442	0.397	0.362	0.442	0.383	0.337	0.478	0.317
345	0.431	0.387	0.353	0.431	0.374	0.329	0.467	0.307
346	0.420	0.377	0.344	0.420	0.364	0.321	0.457	0.298
347	0.409	0.368	0.336	0.409	0.356	0.313	0.447	0.289
348	0.399	0.359	0.328	0.399	0.347	0.306	0.438	0.281
349	0.389	0.351	0.321	0.389	0.339	0.299	0.429	0.273
350	0.380	0.343	0.313	0.380	0.331	0.293	0.420	0.266

Table P: Simulation results for March 2016 dataset at sewage effluent A (4/4).

Sewage effluent A								
Simulation	**Kr (h^{-1})**			λ_{ini}			**Uncertainty**	
time (h)	**0.120**	**0.140**	**0.160**	**0.006**	**0.010**	**0.024**	+	-
March 2016 dataset								
351	0.372	0.335	0.307	0.372	0.324	0.287	0.411	0.259
352	0.364	0.329	0.301	0.364	0.318	0.281	0.404	0.253
353	0.357	0.323	0.296	0.357	0.312	0.277	0.398	0.248
354	0.351	0.318	0.291	0.351	0.307	0.273	0.392	0.243
355	0.346	0.313	0.287	0.346	0.303	0.269	0.387	0.239
356	0.341	0.309	0.284	0.341	0.299	0.265	0.382	0.235
357	0.336	0.304	0.280	0.336	0.295	0.262	0.378	0.231
358	0.331	0.300	0.277	0.331	0.291	0.258	0.373	0.227
359	0.326	0.296	0.273	0.326	0.287	0.255	0.369	0.224
360	0.322	0.293	0.270	0.322	0.284	0.252	0.365	0.221
361	0.317	0.289	0.267	0.317	0.280	0.249	0.361	0.217
362	0.313	0.286	0.265	0.313	0.277	0.247	0.358	0.215
363	0.310	0.283	0.262	0.310	0.274	0.244	0.354	0.212
364	0.306	0.280	0.260	0.306	0.271	0.242	0.351	0.209
365	0.303	0.277	0.257	0.303	0.269	0.240	0.348	0.207
366	0.300	0.275	0.255	0.300	0.267	0.238	0.345	0.205
367	0.297	0.273	0.253	0.297	0.264	0.236	0.343	0.203
368	0.295	0.271	0.252	0.295	0.262	0.234	0.340	0.201
369	0.292	0.269	0.250	0.292	0.261	0.233	0.338	0.199
370	0.290	0.267	0.249	0.290	0.259	0.231	0.336	0.198
371	0.288	0.265	0.247	0.288	0.257	0.230	0.334	0.197
372	0.286	0.264	0.246	0.286	0.256	0.228	0.332	0.195
373	0.284	0.262	0.245	0.284	0.254	0.227	0.330	0.194
374	0.282	0.261	0.243	0.282	0.253	0.226	0.328	0.193
375	0.281	0.259	0.242	0.281	0.251	0.224	0.326	0.191
376	0.279	0.257	0.240	0.279	0.250	0.223	0.324	0.190
377	0.277	0.255	0.238	0.277	0.248	0.221	0.322	0.189
378	0.274	0.253	0.237	0.274	0.246	0.220	0.320	0.187
379	0.272	0.251	0.235	0.272	0.244	0.218	0.318	0.185
380	0.270	0.249	0.233	0.270	0.242	0.216	0.315	0.183
381	0.267	0.247	0.230	0.267	0.239	0.214	0.313	0.181
382	0.264	0.244	0.228	0.264	0.237	0.212	0.311	0.179
383	0.261	0.242	0.226	0.261	0.235	0.210	0.309	0.176
384	0.258	0.239	0.223	0.258	0.232	0.208	0.306	0.173
385	0.255	0.236	0.220	0.255	0.229	0.205	0.304	0.170
386	0.251	0.232	0.217	0.251	0.226	0.203	0.301	0.167
387	0.247	0.229	0.214	0.247	0.222	0.200	0.298	0.163
388	0.243	0.225	0.211	0.243	0.219	0.197	0.295	0.159
389	0.239	0.221	0.207	0.239	0.215	0.194	0.293	0.156
390	0.235	0.217	0.203	0.235	0.212	0.190	0.290	0.152
391	0.231	0.213	0.200	0.231	0.208	0.187	0.287	0.147
392	0.226	0.209	0.196	0.226	0.204	0.184	0.284	0.143

Table Q: Simulation results for February 2016 dataset at sewage effluent B 1/3).

Sewage effluent B								
Simulation	**Kr (h^{-1})**			λ_{ini}			**Uncertainty**	
time (h)	**0.005**	**0.010**	**0.015**	**0.006**	**0.010**	**0.024**	+	-
February 2016 dataset								
201	0.772	0.764	0.759				0.772	0.772
202	0.772	0.764	0.759				0.772	0.772
203	0.772	0.764	0.759				0.772	0.772
204	0.771	0.764	0.758				0.771	0.771
205	0.771	0.763	0.758				0.771	0.771
206	0.769	0.762	0.756				0.770	0.769
207	0.767	0.759	0.753				0.768	0.767
208	0.764	0.755	0.749				0.765	0.762
209	0.759	0.750	0.743				0.761	0.756
210	0.752	0.743	0.736				0.756	0.748
211	0.744	0.734	0.727				0.750	0.738
212	0.735	0.725	0.717				0.743	0.727
213	0.724	0.714	0.705				0.735	0.714
214	0.713	0.701	0.692				0.727	0.699
215	0.700	0.688	0.678				0.718	0.683
216	0.687	0.675	0.664				0.708	0.666
217	0.673	0.660	0.649				0.699	0.648
218	0.659	0.645	0.634				0.688	0.630
219	0.644	0.630	0.618				0.678	0.611
220	0.630	0.615	0.603				0.668	0.592
221	0.615	0.600	0.587				0.658	0.573
222	0.601	0.585	0.572				0.647	0.554
223	0.587	0.571	0.557				0.638	0.537
224	0.574	0.557	0.543				0.628	0.519
225	0.562	0.545	0.530				0.620	0.503
226	0.549	0.532	0.517				0.611	0.487
227	0.537	0.520	0.505				0.603	0.472
228	0.524	0.507	0.491				0.594	0.455
229	0.512	0.494	0.479				0.586	0.439
230	0.501	0.483	0.467				0.579	0.423
231	0.490	0.471	0.455				0.571	0.408
232	0.480	0.461	0.445				0.565	0.394
233	0.471	0.453	0.436				0.561	0.382
234	0.465	0.446	0.430				0.558	0.372
235	0.461	0.442	0.426				0.558	0.365
236	0.460	0.440	0.424				0.560	0.360
237	0.461	0.441	0.424				0.564	0.358
238	0.464	0.444	0.427				0.571	0.358
239	0.470	0.450	0.432				0.580	0.360
240	0.478	0.457	0.439				0.590	0.365
241	0.487	0.466	0.448				0.603	0.371
242	0.498	0.476	0.458				0.617	0.379
243	0.510	0.488	0.469				0.632	0.389
244	0.522	0.499	0.480				0.646	0.398
245	0.534	0.511	0.492				0.661	0.408
246	0.547	0.523	0.503				0.675	0.418
247	0.559	0.535	0.515				0.690	0.429
248	0.571	0.547	0.526				0.704	0.439
249	0.583	0.558	0.537				0.717	0.449
250	0.595	0.569	0.548				0.731	0.459

Table R: Simulation results for February 2016 dataset at sewage effluent B 2/3).

Sewage effluent B								
Simulation	**Kr (h^{-1})**			λ_{ini}			**Uncertainty**	
time (h)	**0.005**	**0.010**	**0.015**	**0.006**	**0.010**	**0.024**	+	-
February 2016 dataset								
251	0.607	0.581	0.559				0.745	0.469
252	0.621	0.594	0.571				0.761	0.481
253	0.634	0.607	0.583				0.776	0.492
254	0.647	0.620	0.595				0.791	0.504
255	0.662	0.633	0.608				0.808	0.517
256	0.678	0.648	0.622				0.825	0.531
257	0.696	0.664	0.637				0.845	0.547
258	0.715	0.682	0.654				0.866	0.564
259	0.737	0.702	0.673				0.890	0.583
260	0.760	0.725	0.693				0.916	0.605
261	0.788	0.750	0.718				0.946	0.630
262	0.818	0.779	0.745				0.979	0.658
263	0.852	0.810	0.774				1.014	0.689
264	0.886	0.842	0.805				1.051	0.720
265	0.923	0.877	0.838				1.091	0.754
266	0.961	0.914	0.873				1.132	0.790
267	1.002	0.953	0.909				1.176	0.828
268	1.047	0.995	0.950				1.223	0.870
269	1.092	1.038	0.991				1.272	0.912
270	1.136	1.080	1.031				1.319	0.953
271	1.178	1.120	1.069				1.364	0.992
272	1.219	1.159	1.107				1.408	1.030
273	1.257	1.196	1.142				1.449	1.066
274	1.295	1.232	1.176				1.490	1.101
275	1.333	1.268	1.211				1.530	1.137
276	1.374	1.307	1.248				1.574	1.175
277	1.414	1.344	1.283				1.616	1.212
278	1.453	1.381	1.318				1.658	1.248
279	1.494	1.420	1.354				1.702	1.286
280	1.533	1.456	1.388				1.744	1.323
281	1.571	1.490	1.419				1.784	1.357
282	1.604	1.521	1.447				1.820	1.389
283	1.634	1.547	1.471				1.851	1.416
284	1.658	1.569	1.490				1.878	1.439
285	1.680	1.588	1.506				1.901	1.458
286	1.696	1.602	1.518				1.919	1.474
287	1.710	1.613	1.527				1.933	1.486
288	1.720	1.621	1.534				1.945	1.495
289	1.727	1.626	1.537				1.952	1.501
290	1.730	1.627	1.537				1.956	1.504
291	1.729	1.625	1.533				1.956	1.503
292	1.726	1.620	1.528				1.953	1.499
293	1.720	1.614	1.520				1.947	1.494
294	1.713	1.605	1.511				1.940	1.486
295	1.705	1.597	1.502				1.931	1.478
296	1.696	1.588	1.493				1.922	1.470
297	1.687	1.578	1.484				1.913	1.461
298	1.678	1.569	1.474				1.903	1.452
299	1.668	1.559	1.464				1.893	1.442

Table S: Simulation results for February 2016 dataset at sewage effluent B 3/3).

Sewage effluent B								
Simulation	**Kr (h^{-1})**			λ_{ini}			**Uncertainty**	
time (h)	**0.005**	**0.010**	**0.015**	**0.006**	**0.010**	**0.024**	+	-
February 2016 dataset								
300	1.657	1.548	1.454				1.882	1.431
301	1.646	1.537	1.443				1.870	1.421
302	1.634	1.526	1.432				1.859	1.410
303	1.623	1.515	1.421				1.847	1.399
304	1.614	1.505	1.412				1.837	1.390
305	1.606	1.498	1.404				1.829	1.384
306	1.602	1.493	1.400				1.823	1.380
307	1.601	1.493	1.399				1.822	1.381
308	1.605	1.496	1.403				1.824	1.385
309	1.613	1.504	1.410				1.831	1.395
310	1.625	1.516	1.422				1.842	1.408
311	1.641	1.531	1.437				1.856	1.426
312	1.660	1.550	1.455				1.874	1.447
313	1.684	1.573	1.477				1.895	1.472
314	1.710	1.598	1.502				1.919	1.500
315	1.738	1.626	1.529				1.946	1.531
316	1.770	1.656	1.559				1.975	1.564
317	1.803	1.688	1.590				2.006	1.599
318	1.837	1.722	1.623				2.039	1.636
319	1.870	1.754	1.654				2.070	1.671
320	1.904	1.787	1.686				2.102	1.706

Table T: Simulation results for March 2016 dataset at sewage effluent B (1/4).

Sewage effluent B								
Simulation	**Kr (h^{-1})**			λ_{ini}			**Uncertainty**	
time (h)	**0.005**	**0.010**	**0.015**	**0.006**	**0.010**	**0.024**	+	-
March 2016 dataset								
201	1.359	1.382	1.404	1.359	1.381	1.334	1.359	1.359
202	1.359	1.382	1.405	1.359	1.382	1.334	1.359	1.359
203	1.359	1.382	1.404	1.359	1.381	1.334	1.359	1.359
204	1.358	1.382	1.404	1.358	1.381	1.334	1.358	1.358
205	1.358	1.381	1.403	1.358	1.381	1.334	1.358	1.358
206	1.357	1.379	1.401	1.357	1.379	1.332	1.357	1.356
207	1.354	1.377	1.398	1.354	1.377	1.330	1.355	1.354
208	1.351	1.373	1.393	1.351	1.374	1.327	1.352	1.350
209	1.346	1.367	1.387	1.346	1.369	1.322	1.348	1.345
210	1.341	1.360	1.379	1.341	1.363	1.316	1.343	1.339
211	1.333	1.351	1.368	1.333	1.355	1.308	1.336	1.330
212	1.325	1.341	1.356	1.325	1.346	1.299	1.329	1.320
213	1.315	1.329	1.343	1.315	1.335	1.288	1.321	1.308
214	1.303	1.315	1.327	1.303	1.323	1.275	1.311	1.295
215	1.291	1.301	1.311	1.291	1.309	1.261	1.301	1.280
216	1.277	1.285	1.293	1.277	1.295	1.246	1.291	1.264
217	1.263	1.268	1.274	1.263	1.279	1.230	1.279	1.246
218	1.247	1.250	1.254	1.247	1.263	1.213	1.267	1.228
219	1.231	1.231	1.232	1.231	1.245	1.195	1.254	1.208
220	1.213	1.210	1.209	1.213	1.226	1.174	1.240	1.186
221	1.194	1.189	1.184	1.194	1.205	1.153	1.225	1.162
222	1.175	1.166	1.159	1.175	1.185	1.131	1.211	1.139
223	1.155	1.144	1.134	1.155	1.164	1.109	1.196	1.115
224	1.136	1.122	1.109	1.136	1.142	1.087	1.180	1.091
225	1.120	1.103	1.089	1.120	1.125	1.069	1.168	1.071
226	1.104	1.086	1.070	1.104	1.109	1.052	1.157	1.052
227	1.091	1.070	1.053	1.091	1.094	1.036	1.146	1.035
228	1.077	1.055	1.035	1.077	1.079	1.020	1.136	1.018
229	1.062	1.038	1.017	1.062	1.063	1.003	1.125	0.999
230	1.046	1.020	0.997	1.046	1.046	0.985	1.113	0.979
231	1.030	1.002	0.977	1.030	1.028	0.967	1.101	0.959
232	1.014	0.983	0.957	1.014	1.010	0.948	1.089	0.938
233	0.997	0.965	0.937	0.997	0.992	0.928	1.077	0.917
234	0.981	0.947	0.918	0.981	0.975	0.910	1.066	0.897
235	0.965	0.930	0.899	0.965	0.958	0.892	1.054	0.877
236	0.950	0.913	0.881	0.950	0.942	0.875	1.043	0.857
237	0.936	0.897	0.864	0.936	0.926	0.858	1.033	0.839
238	0.922	0.882	0.848	0.922	0.911	0.843	1.023	0.821
239	0.909	0.868	0.833	0.909	0.897	0.828	1.014	0.804
240	0.896	0.855	0.819	0.896	0.883	0.814	1.005	0.788
241	0.884	0.842	0.806	0.884	0.871	0.801	0.996	0.772
242	0.872	0.830	0.793	0.872	0.858	0.788	0.988	0.757
243	0.861	0.817	0.781	0.861	0.845	0.775	0.980	0.742
244	0.850	0.806	0.769	0.850	0.834	0.763	0.972	0.727
245	0.839	0.795	0.758	0.839	0.823	0.751	0.965	0.714
246	0.830	0.785	0.748	0.830	0.813	0.741	0.958	0.702
247	0.821	0.777	0.739	0.821	0.803	0.732	0.952	0.690
248	0.813	0.769	0.732	0.813	0.795	0.724	0.946	0.680
249	0.807	0.762	0.725	0.807	0.788	0.717	0.942	0.671
250	0.800	0.756	0.719	0.800	0.782	0.710	0.937	0.663

Table U: Simulation results for February 2016 dataset at sewage effluent B (2/4).

Sewage effluent B								
Simulation	**Kr (h^{-1})**			λ_{ini}			**Uncertainty**	
time (h)	**0.005**	**0.010**	**0.015**	**0.006**	**0.010**	**0.024**	+	-
March 2016 dataset								
300	1.740	1.665	1.600	1.740	1.664	1.437	2.047	1.612
301	1.799	1.722	1.654	1.799	1.721	1.485	2.115	1.673
302	1.865	1.784	1.713	1.865	1.783	1.538	2.189	1.741
303	1.930	1.845	1.770	1.930	1.845	1.590	2.264	1.808
304	1.993	1.903	1.824	1.993	1.905	1.641	2.336	1.873
305	2.052	1.958	1.875	2.052	1.961	1.689	2.404	1.933
306	2.102	2.003	1.916	2.102	2.009	1.729	2.461	1.984
307	2.146	2.042	1.951	2.146	2.050	1.765	2.512	2.029
308	2.181	2.073	1.977	2.181	2.084	1.793	2.552	2.064
309	2.205	2.093	1.994	2.205	2.107	1.813	2.582	2.089
310	2.221	2.104	2.002	2.221	2.122	1.826	2.600	2.103
311	2.228	2.108	2.002	2.228	2.128	1.832	2.609	2.109
312	2.226	2.103	1.995	2.226	2.127	1.831	2.608	2.106
313	2.217	2.091	1.981	2.217	2.119	1.824	2.599	2.095
314	2.201	2.073	1.960	2.201	2.103	1.811	2.582	2.076
315	2.178	2.048	1.933	2.178	2.082	1.793	2.557	2.050
316	2.149	2.017	1.901	2.149	2.054	1.769	2.525	2.018
317	2.114	1.981	1.864	2.114	2.021	1.741	2.487	1.979
318	2.076	1.942	1.825	2.076	1.985	1.711	2.445	1.938
319	2.036	1.902	1.785	2.036	1.947	1.679	2.401	1.894
320	1.996	1.861	1.744	1.996	1.909	1.647	2.357	1.850
321	1.958	1.823	1.707	1.958	1.872	1.616	2.314	1.809
322	1.919	1.785	1.669	1.919	1.835	1.585	2.271	1.767
323	1.883	1.750	1.634	1.883	1.801	1.556	2.231	1.728
324	1.845	1.712	1.598	1.845	1.765	1.525	2.189	1.686
325	1.804	1.672	1.559	1.804	1.726	1.492	2.144	1.642
326	1.758	1.628	1.516	1.758	1.682	1.455	2.092	1.592
327	1.710	1.581	1.471	1.710	1.637	1.417	2.039	1.540
328	1.660	1.533	1.425	1.660	1.589	1.376	1.983	1.486
329	1.609	1.484	1.378	1.609	1.541	1.335	1.926	1.432
330	1.561	1.438	1.334	1.561	1.495	1.297	1.873	1.380
331	1.512	1.391	1.289	1.512	1.448	1.257	1.818	1.328
332	1.465	1.347	1.247	1.465	1.404	1.220	1.766	1.278
333	1.420	1.304	1.207	1.420	1.361	1.184	1.716	1.231
334	1.378	1.264	1.169	1.378	1.321	1.149	1.668	1.186
335	1.337	1.226	1.133	1.337	1.282	1.116	1.623	1.143
336	1.299	1.190	1.100	1.299	1.246	1.086	1.580	1.103
337	1.262	1.156	1.067	1.262	1.211	1.056	1.539	1.065
338	1.227	1.123	1.037	1.227	1.177	1.028	1.499	1.029
339	1.194	1.092	1.008	1.194	1.145	1.001	1.461	0.994
340	1.163	1.063	0.982	1.163	1.116	0.976	1.427	0.963
341	1.134	1.036	0.957	1.134	1.089	0.952	1.394	0.933
342	1.107	1.012	0.934	1.107	1.063	0.931	1.364	0.906
343	1.083	0.990	0.913	1.083	1.040	0.911	1.337	0.882
344	1.061	0.969	0.895	1.061	1.019	0.894	1.312	0.860
345	1.042	0.952	0.879	1.042	1.001	0.878	1.290	0.841
346	1.024	0.936	0.864	1.024	0.984	0.864	1.270	0.823
347	1.008	0.921	0.851	1.008	0.969	0.851	1.252	0.807
348	0.992	0.907	0.838	0.992	0.953	0.838	1.233	0.791
349	0.975	0.892	0.824	0.975	0.938	0.824	1.215	0.775

Table V: Simulation results for March 2016 dataset at sewage effluent B (3/4).

Sewage effluent B								
Simulation	**Kr (h^{-1})**			λ_{ini}			**Uncertainty**	
time (h)	**0.005**	**0.010**	**0.015**	**0.006**	**0.010**	**0.024**	+	-
March 2016 dataset								
300	1.740	1.665	1.600	1.740	1.664	1.437	2.047	1.612
301	1.799	1.722	1.654	1.799	1.721	1.485	2.115	1.673
302	1.865	1.784	1.713	1.865	1.783	1.538	2.189	1.741
303	1.930	1.845	1.770	1.930	1.845	1.590	2.264	1.808
304	1.993	1.903	1.824	1.993	1.905	1.641	2.336	1.873
305	2.052	1.958	1.875	2.052	1.961	1.689	2.404	1.933
306	2.102	2.003	1.916	2.102	2.009	1.729	2.461	1.984
307	2.146	2.042	1.951	2.146	2.050	1.765	2.512	2.029
308	2.181	2.073	1.977	2.181	2.084	1.793	2.552	2.064
309	2.205	2.093	1.994	2.205	2.107	1.813	2.582	2.089
310	2.221	2.104	2.002	2.221	2.122	1.826	2.600	2.103
311	2.228	2.108	2.002	2.228	2.128	1.832	2.609	2.109
312	2.226	2.103	1.995	2.226	2.127	1.831	2.608	2.106
313	2.217	2.091	1.981	2.217	2.119	1.824	2.599	2.095
314	2.201	2.073	1.960	2.201	2.103	1.811	2.582	2.076
315	2.178	2.048	1.933	2.178	2.082	1.793	2.557	2.050
316	2.149	2.017	1.901	2.149	2.054	1.769	2.525	2.018
317	2.114	1.981	1.864	2.114	2.021	1.741	2.487	1.979
318	2.076	1.942	1.825	2.076	1.985	1.711	2.445	1.938
319	2.036	1.902	1.785	2.036	1.947	1.679	2.401	1.894
320	1.996	1.861	1.744	1.996	1.909	1.647	2.357	1.850
321	1.958	1.823	1.707	1.958	1.872	1.616	2.314	1.809
322	1.919	1.785	1.669	1.919	1.835	1.585	2.271	1.767
323	1.883	1.750	1.634	1.883	1.801	1.556	2.231	1.728
324	1.845	1.712	1.598	1.845	1.765	1.525	2.189	1.686
325	1.804	1.672	1.559	1.804	1.726	1.492	2.144	1.642
326	1.758	1.628	1.516	1.758	1.682	1.455	2.092	1.592
327	1.710	1.581	1.471	1.710	1.637	1.417	2.039	1.540
328	1.660	1.533	1.425	1.660	1.589	1.376	1.983	1.486
329	1.609	1.484	1.378	1.609	1.541	1.335	1.926	1.432
330	1.561	1.438	1.334	1.561	1.495	1.297	1.873	1.380
331	1.512	1.391	1.289	1.512	1.448	1.257	1.818	1.328
332	1.465	1.347	1.247	1.465	1.404	1.220	1.766	1.278
333	1.420	1.304	1.207	1.420	1.361	1.184	1.716	1.231
334	1.378	1.264	1.169	1.378	1.321	1.149	1.668	1.186
335	1.337	1.226	1.133	1.337	1.282	1.116	1.623	1.143
336	1.299	1.190	1.100	1.299	1.246	1.086	1.580	1.103
337	1.262	1.156	1.067	1.262	1.211	1.056	1.539	1.065
338	1.227	1.123	1.037	1.227	1.177	1.028	1.499	1.029
339	1.194	1.092	1.008	1.194	1.145	1.001	1.461	0.994
340	1.163	1.063	0.982	1.163	1.116	0.976	1.427	0.963
341	1.134	1.036	0.957	1.134	1.089	0.952	1.394	0.933
342	1.107	1.012	0.934	1.107	1.063	0.931	1.364	0.906
343	1.083	0.990	0.913	1.083	1.040	0.911	1.337	0.882
344	1.061	0.969	0.895	1.061	1.019	0.894	1.312	0.860
345	1.042	0.952	0.879	1.042	1.001	0.878	1.290	0.841
346	1.024	0.936	0.864	1.024	0.984	0.864	1.270	0.823
347	1.008	0.921	0.851	1.008	0.969	0.851	1.252	0.807
348	0.992	0.907	0.838	0.992	0.953	0.838	1.233	0.791
349	0.975	0.892	0.824	0.975	0.938	0.824	1.215	0.775

Table W: Simulation results for February 2016 dataset at sewage effluent B 4/4).

Sewage effluent B								
Simulation	**Kr (h^{-1})**			λ_{ini}			**Uncertainty**	
time (h)	**0.005**	**0.010**	**0.015**	**0.006**	**0.010**	**0.024**	+	-
March 2016 dataset								
350	0.957	0.875	0.809	0.957	0.920	0.810	1.194	0.757
351	0.939	0.859	0.795	0.939	0.903	0.795	1.173	0.739
352	0.921	0.843	0.780	0.921	0.886	0.780	1.153	0.721
353	0.902	0.826	0.765	0.902	0.868	0.765	1.132	0.704
354	0.885	0.811	0.751	0.885	0.852	0.751	1.112	0.687
355	0.868	0.795	0.737	0.868	0.836	0.737	1.092	0.671
356	0.852	0.781	0.724	0.852	0.820	0.724	1.074	0.655
357	0.837	0.767	0.712	0.837	0.805	0.712	1.056	0.640
358	0.822	0.754	0.700	0.822	0.792	0.700	1.039	0.626
359	0.808	0.742	0.689	0.808	0.779	0.689	1.023	0.613
360	0.795	0.730	0.679	0.795	0.766	0.678	1.008	0.601
361	0.783	0.719	0.669	0.783	0.755	0.668	0.994	0.590
362	0.772	0.709	0.660	0.772	0.744	0.659	0.981	0.580
363	0.761	0.700	0.652	0.761	0.734	0.651	0.969	0.570
364	0.752	0.691	0.644	0.752	0.724	0.642	0.957	0.561
365	0.742	0.683	0.637	0.742	0.716	0.635	0.946	0.552
366	0.734	0.676	0.630	0.734	0.708	0.628	0.936	0.545
367	0.726	0.669	0.624	0.726	0.700	0.622	0.927	0.538
368	0.719	0.663	0.619	0.719	0.694	0.616	0.919	0.532
369	0.714	0.658	0.615	0.714	0.688	0.611	0.912	0.527
370	0.708	0.654	0.611	0.708	0.683	0.607	0.905	0.522
371	0.704	0.650	0.607	0.704	0.679	0.603	0.899	0.518
372	0.699	0.646	0.604	0.699	0.674	0.599	0.894	0.514
373	0.694	0.641	0.600	0.694	0.669	0.595	0.888	0.509
374	0.688	0.637	0.596	0.688	0.664	0.591	0.881	0.504
375	0.683	0.632	0.592	0.683	0.659	0.586	0.875	0.499
376	0.677	0.627	0.588	0.677	0.653	0.581	0.867	0.494
377	0.670	0.621	0.582	0.670	0.646	0.575	0.860	0.488
378	0.663	0.614	0.577	0.663	0.640	0.570	0.852	0.481
379	0.655	0.607	0.570	0.655	0.632	0.563	0.844	0.474
380	0.647	0.600	0.563	0.647	0.624	0.556	0.835	0.466
381	0.637	0.591	0.555	0.637	0.615	0.549	0.827	0.457
382	0.627	0.582	0.547	0.627	0.606	0.541	0.817	0.447
383	0.617	0.573	0.538	0.617	0.596	0.532	0.808	0.437
384	0.606	0.562	0.528	0.606	0.586	0.523	0.798	0.426
385	0.595	0.552	0.518	0.595	0.575	0.514	0.788	0.415
386	0.583	0.541	0.508	0.583	0.563	0.504	0.778	0.403
387	0.570	0.529	0.497	0.570	0.552	0.494	0.768	0.390
388	0.556	0.516	0.484	0.556	0.538	0.482	0.756	0.375
389	0.542	0.503	0.472	0.542	0.525	0.471	0.745	0.361
390	0.528	0.490	0.460	0.528	0.511	0.460	0.733	0.347
391	0.515	0.477	0.447	0.515	0.498	0.448	0.722	0.332
392	0.501	0.464	0.436	0.501	0.486	0.437	0.712	0.319